


FOREWORD

The material contained in this publication, FHWA-RD-89-227, is a supplement to the material contained in Publication No. FHWA-RD-89-226, "Truck Characteristics for Use in Highway Design and Operation."

This publication, FHWA-RD-89-227, documents in detail the investigation of six aspects of the study. These six areas are: braking distances, horizontal curve design to reduce truck rollovers, offtracking, performance on grades, intersection sight distance, and the cost-effectiveness methodology used to assess the economic justification for changes in highway design and operational criteria to accommodate trucks.

The material in this publication will mainly be of interest to other researchers. Therefore, copies are not being distributed. A limited number of copies for, official use, are available from the Federal Highway Administration, RD&T Report Center, HRD-11, 6300 Georgetown Pike, McLean, Virginia 22101-2296. Copies for the public are available from the National Technical Information Service (NTIS), Department of Commerce, 5285 Port Royal Road, Springfield, Virginia 22161. A small charge will be imposed by NTIS.



R. J. Betsold, Director
Office of Safety and Traffic
Operations Research and Development

NOTICE

This document is disseminated under the sponsorship of the Department of Transportation in the interest of information exchange. The United States Government assumes no liability for the contents or use thereof.

The contents of this report reflect the views of the Contractor, who is responsible for the accuracy of the data presented herein. The contents do not necessarily reflect the official policy of the Department of Transportation.

This report does not constitute a standard, specification, or regulation.

The United States Government does not endorse products or manufacturers. Trade or manufacturers' names appear herein only because they are considered essential to the objective of this document.

1. Report No. FHWA-RD-89-227		2. Government Accession No.		3. Recipient's Catalog No.	
4. Title and Subtitle TRUCK CHARACTERISTICS FOR USE IN HIGHWAY DESIGN AND OPERATION Volume II: Appendixes				5. Report Date August 1990	
				6. Performing Organization Code	
7. Author(s) D. W. Harwood, J. M. Mason, W. D. Glauz, B. T. Kulakowski, and K. Fitzpatrick				8. Performing Organization Report No. 8932-S	
9. Performing Organization Name and Address Midwest Research Institute 425 Volker Boulevard Kansas City, Missouri 64110				10. Work Unit No. (TRAIS) 3A4A3072	
				11. Contract or Grant No. DTFH61-87-C-00088	
				13. Type of Report and Period Covered Final Report August 1987-November 1989	
12. Sponsoring Agency Name and Address Office of Safety and Traffic Operations R&D Federal Highway Administration 6300 Georgetown Pike McLean, Virginia 22101-2296				14. Sponsoring Agency Code	
15. Supplementary Notes FHWA Contract Manager: J. True (HSR-20)					
16. Abstract <p>Highway geometric design and traffic operations are based in part on consideration of vehicle characteristics. However, many of the current highway design and operational criteria are based on passenger car characteristics, even though truck characteristics may be more critical. The study of which this report is part involved a review of existing data on truck characteristics and the use of those data to assess the appropriate geometric design and traffic operational criteria to accommodate trucks. The appendixes presented in this volume document detailed investigation of six aspects of design and operational criteria for trucks. These are: (1) truck braking distances, (2) horizontal curve design to reduce truck roll-overs, (3) truck offtracking, (4) truck performance on grades, (5) intersection sight distance requirements for trucks, and (6) cost-effectiveness methodology for assessing the need to change current criteria to accommodate trucks.</p> <p>Volume I of the report (FHWA-RD-89-226) presents the main findings of the study including recommended changes in highway geometric design and operational criteria to accommodate trucks.</p>					
17. Key Words Trucks Geometric Design Traffic Operations Sight Distance Intersections Horizontal Curves			18. Distribution Statement No restrictions. This document is available to the public through the National Technical Information Service, Springfield, Virginia 22161		
19. Security Classif. (of this report) UNCLASSIFIED		20. Security Classif. (of this page) UNCLASSIFIED		21. No. of Pages 230	22. Price

SI* (MODERN METRIC) CONVERSION FACTORS

APPROXIMATE CONVERSIONS TO SI UNITS

Symbol	When You Know	Multiply By	To Find	Symbol
LENGTH				
in	inches	25.4	millimetres	mm
ft	feet	0.305	metres	m
yd	yards	0.914	metres	m
mi	miles	1.61	kilometres	km
AREA				
in ²	square inches	645.2	millimetres squared	mm ²
ft ²	square feet	0.093	metres squared	m ²
yd ²	square yards	0.836	metres squared	m ²
ac	acres	0.405	hectares	ha
mi ²	square miles	2.59	kilometres squared	km ²
VOLUME				
fl oz	fluid ounces	29.57	millilitres	mL
gal	gallons	3.785	litres	L
ft ³	cubic feet	0.028	metres cubed	m ³
yd ³	cubic yards	0.765	metres cubed	m ³

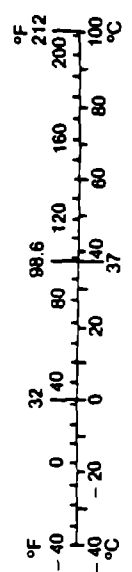
NOTE: Volumes greater than 1000 L shall be shown in m³.

MASS				
oz	ounces	28.35	grams	g
lb	pounds	0.454	kilograms	Kg
T	short tons (2000 lb)	0.907	megagrams	Mg

TEMPERATURE (exact)		
°F	Fahrenheit temperature	$5(F-32)/9$
°C	Celsius temperature	temperature

APPROXIMATE CONVERSIONS FROM SI UNITS

Symbol	When You Know	Multiply By	To Find	Symbol
LENGTH				
mm	millimetres	0.039	inches	in
m	metres	3.28	feet	ft
m	metres	1.09	yards	yd
km	kilometres	0.621	miles	mi
AREA				
mm ²	millimetres squared	0.0016	square inches	in ²
m ²	metres squared	10.764	square feet	ft ²
ha	hectares	2.47	acres	ac
km ²	kilometres squared	0.386	square miles	mi ²
VOLUME				
mL	millilitres	0.034	fluid ounces	fl oz
L	litres	0.264	gallons	gal
m ³	metres cubed	35.315	cubic feet	ft ³
m ³	metres cubed	1.308	cubic yards	yd ³
MASS				
g	grams	0.035	ounces	oz
kg	kilograms	2.205	pounds	lb
Mg	megagrams	1.102	short tons (2000 lb)	T
TEMPERATURE (exact)				
°C	Celsius temperature	$1.8C + 32$	Fahrenheit temperature	°F



(Revised April 1989)

* SI is the symbol for the International System of Measurement

TABLE OF CONTENTS

Volume I

	<u>Page</u>
I. INTRODUCTION.....	1
A. Research Objectives and Scope.....	2
B. Organization and Scope of This Report.....	3
II. TRUCK CHARACTERISTICS.....	5
A. Truck Dimensions.....	5
B. Braking Distance.....	10
C. Driver Eye Height.....	22
D. Truck Acceleration Characteristics.....	25
E. Speed-Maintenance Capabilities on Grades.....	32
F. Turning Radius and Offtracking.....	38
G. Suspension Characteristics.....	39
H. Rollover Threshold.....	49
III. HIGHWAY DESIGN AND OPERATIONAL CRITERIA.....	55
A. Stopping Sight Distance.....	55
B. Passing and No-Passing Zones on Two-Lane Highways.....	72
C. Decision Sight Distance.....	90
D. Intersection Sight Distance.....	99
E. Intersection and Channelization Geometrics.....	143
F. Railroad-Highway Grade Crossing Sight Distance.....	156
G. Crest Vertical Curve Length.....	173
H. Sag Vertical Curve Length.....	174
I. Critical Length of Grade.....	178
J. Lane Width.....	182
K. Horizontal Curve Radius and Superelevation.....	184
L. Pavement Widening on Horizontal Curves.....	202
M. Cross-Slope Breaks.....	210
N. Roadside Slopes.....	212
O. Vehicle Change Interval.....	213
P. Sign Placement.....	220
IV. CONCLUSIONS AND RECOMMENDATIONS.....	229
A. Design Vehicles.....	229
B. Stopping Sight Distance.....	229
C. Passing and No-Passing Zones on Two-Lane Highways.....	230

TABLE OF CONTENTS (Continued)

	<u>Page</u>
D. Decision Sight Distance.....	231
E. Intersection Sight Distance.....	231
F. Intersection and Channelization Geometrics.....	232
G. Railroad-Highway Grade Crossing Sight Distance.....	232
H. Crest Vertical Curve Length.....	233
I. Sag Vertical Curve Length.....	233
J. Critical Length of Grade.....	233
K. Lane Width.....	233
L. Horizontal Curve Radius and Superelevation.....	233
M. Pavement Widening on Horizontal Curves.....	234
N. Cross-Slope Breaks.....	234
O. Roadside Slopes.....	234
P. Vehicle Change Interval.....	235
Q. Sign Placement.....	235
REFERENCES.....	236

TABLE OF CONTENTS (Continued)

Volume II

		<u>Page</u>
APPENDIX A	TRUCK BRAKING DISTANCES.....	1
	A. Tire-Pavement Friction in Braking Maneuvers.....	1
	B. Locked Wheel Braking vs. Controlled Braking.....	2
	C. Pavement and Truck Characteristics Affecting Braking Distance.....	5
	D. Recent Research on Truck Braking Distance.....	12
	E. Braking Distance for Use in Highway Design Criteria.....	14
APPENDIX B	HORIZONTAL CURVE DESIGN TO REDUCE TRUCK ROLLOVERS.....	20
	A. Background.....	20
	B. Computer Simulation of Truck Dynamics on Horizontal Curves.....	21
	C. Effect of Truck Characteristics on Rollover Threshold.....	25
APPENDIX C	TRUCK OFFTRACKING.....	70
	A. Background.....	70
	B. Low-Speed Offtracking.....	75
	C. Model for Low-Speed and High-Speed Offtracking Including Superelevation Effects.....	87
	D. Derivation of Offtracking Model.....	90
	E. Sensitivity of Offtracking to Truck Characteristics.....	97
APPENDIX D	TRUCK PERFORMANCE ON GRADES.....	102
	A. Background.....	102
	B. Literature Review.....	104
	C. Computation of Weight-Power Ratio From Observed Speeds of Trucks.....	108
	D. Reanalysis of Gillespie Data.....	113

TABLE OF CONTENTS (Continued)

	<u>Page</u>
APPENDIX E	INTERSECTION SIGHT DISTANCE..... 114
A.	Overall Study Methodology..... 115
B.	Data Collection..... 116
C.	Data Reduction..... 124
D.	Data Analysis..... 133
E.	Summary of Findings..... 159
F.	Alternative Intersection Sight Distance Criteria..... 162
G.	Recommended Data Collection for Future Intersection Sight Distance Studies..... 176
APPENDIX F	COST-EFFECTIVENESS METHODOLOGY..... 180
A.	Overview of Cost-Effectiveness Methodology..... 180
B.	Examples of Cost-Effectiveness Analysis for Stopping Sight Distance..... 188
REFERENCES.....	205

LIST OF FIGURES

Volume I

<u>Figure</u>		<u>Page</u>
1	Variation of braking and cornering friction coefficients with percent slip.....	12
2	Tractor-trailer dynamics with locked wheels.....	14
3	Truck braking distances on a poor, wet road.....	21
4	Truck deceleration rates on a poor, wet road.....	21
5	Field observations of time for tractor-trailer trucks to clear intersection after starting from a stop.....	27
6	Observed time versus distance curves for initial acceleration from a stop by tractor-trailer trucks.....	28
7	Comparison of time for a tractor-trailer truck to clear an intersection starting from a stop based on Gillespie and Hutton data.....	29
8	Speed versus distance curves for truck acceleration from a stop.....	31
9	Observed time versus distance curves for acceleration to high speed from a stop by a tractor-trailer truck.....	33
10	Observed speed versus time curves for acceleration by trucks with various weight-to-power ratios.....	33
11	Comparison of weight-to-power ratios estimated by St. John to those observed by Messer.....	36
12	Trend in weight-to-power ratios of trucks from 1949 to 1984....	37
13	Swept path width and offtracking of a truck negotiating a 90° intersection turn.....	40
14	Diagram of walking-beam suspension.....	42
15	Diagram of four-spring suspension.....	42
16	Diagram of roll by trailer body illustrating location of roll center.....	47
17	Loading data and resulting rollover thresholds for example tractor-semitrailers at full load.....	50
18	Influence of axle load variations on rollover threshold.....	51
19	Percent of single-truck accidents in which rollover occurs as a function of rollover threshold.....	54
20	Example sight obstruction envelope on horizontal curves for condition where the stopping sight distance is less than the length of the curve.....	62
21	Comparison of stopping sight distance requirements for trucks to current AASHTO criteria.....	65
22	Required passing sight distance for passenger cars and trucks in comparison to current criteria.....	85
23	Required passing zone length to complete a pass at or near the highway design speed.....	85
24	Comparison of estimated decision sight distance for trucks with AASHTO criteria.....	97
25	Design considerations for intersection sight distance.....	100

LIST OF FIGURES (Continued)

<u>Figure</u>		<u>Page</u>
26	Intersection sight distance cases for STOP-controlled intersections.....	103
27	Comparison of case I intersection sight distance for 70- and 75-ft (21- and 23-m) trucks to existing AASHTO criteria.....	113
28	Comparison of case III-A intersection sight distance for 70- and 75-ft (21- and 23-m) trucks to existing AASHTO criteria..	117
29	Distances considered in case III-B intersection sight distance criteria.....	119
30	Intersection sight distance requirements for clearing a vehicle in the near lane.....	122
31	Intersection sight distance curves for major-road vehicle traveling at design speed without decelerating.....	126
32	Intersection sight distance curves for deceleration by major-road vehicle from design speed to average running speed.....	131
33	Intersection sight distance curves.....	136
34	Intersection sight distance curves for present study.....	137
35	Offtracking plot for STAA single 48-ft (14.6-m) semitrailer truck with conventional tractor.....	150
36	Offtracking plot for long single 53-ft (16.2-m) semitrailer truck with conventional tractor.....	151
37	Offtracking plot for STAA double-trailer truck with cab-over-engine tractor.....	152
38	Offtracking plot for STAA double-trailer truck with cab-behind engine tractor.....	153
39	Dimensions considered in railroad-highway grade crossing sight distance.....	157
40	Sensitivity of sight distance along the highway to vehicle speeds.....	167
41	Sensitivity of sight distance along the railroad tracks for a moving vehicle to train speed for a vehicle speed of 40 mi/h (64 km/h).....	169
42	Sensitivity of sight distance along the railroad tracks to train speed for a stopped vehicle.....	172
43	AASHTO criteria for superelevation rates of horizontal curves as a function of radius and maximum superelevation rate.....	187
44	Example of variation in side friction demand between wheels of a truck on a horizontal curve.....	189
45	Nominal lateral accelerations of trucks based on their observed speeds on selected horizontal curves in the Chicago area.....	190
46	Required vehicle change intervals at signalized intersections for passenger cars and trucks.....	219
47	AASHTO criteria for passenger car deceleration rates at intersections.....	223

LIST OF FIGURES (Continued)

Volume II

<u>Figure</u>		<u>Page</u>
1	Variation of braking and cornering friction coefficients with percent slip.....	3
2	Tractor-trailer dynamics with locked wheels.....	4
3	Truck braking distances on a poor, wet road.....	13
4	Truck deceleration rates on a poor, wet road.....	13
5	NHTSA test results for stable stopping distance from 60 mi/h (97 km/h) on dry road.....	15
6	Overturning and resisting moments about the longitudinal axis of a truck on a superelevated curve.....	22
7	Effect of gross vehicle weight on rollover threshold, single-semitrailer truck, superelevated curve.....	38
8	Effect of gross vehicle weight on rollover threshold, single-semitrailer truck, flat road.....	38
9	Effect of gross vehicle weight on rollover threshold, double-trailer truck, superelevated curve.....	39
10	Effect of gross vehicle weight on rollover threshold, double-trailer truck, flat road.....	39
11	Effect of suspension stiffness on rollover threshold, single-semitrailer truck, superelevated curve.....	41
12	Effect of suspension stiffness on rollover threshold, double-trailer truck, flat road.....	41
13	Effect of suspension stiffness on rollover threshold, single-semitrailer truck, flat road.....	42
14	Effect of longitudinal weight distribution on rollover threshold, single-semitrailer truck, superelevated curve.....	43
15	Effect of longitudinal weight distribution on rollover threshold, single-semitrailer truck, flat road.....	43
16	Effect of cornering stiffness on rollover threshold, single-semitrailer truck.....	45
17	Comparison of roll angles for simulation runs with different driver lag times (case D40).....	46
18	Comparison of lateral accelerations for simulation runs with different driver lag times (case D40).....	47
19	Dimensions used in calculation of pavement elevation at any point on a spiral transition curve.....	50
20	Lateral acceleration versus distance, single-semitrailer truck, case A, Type I transition area.....	61
21	Roll angle versus distance, single-semitrailer truck, case A, Type I transition area.....	62
22	Lateral acceleration versus distance, single-semitrailer truck, case A, Type II transition area.....	63
23	Roll angle versus distance, single-semitrailer truck, case A, Type II transition area.....	64

LIST OF FIGURES (Continued)

<u>Figure</u>		<u>Page</u>
24	Lateral acceleration versus distance, single-semitrailer truck, case A, Type III transition area.....	65
25	Roll angle versus distance, single-semitrailer truck, case A, Type III transition area.....	66
26	Swept path width and offtracking of a truck negotiating a 90-degree intersection turn.....	71
27	Example of output provided by Caltrans truck offtracking model.....	76
28	Offtracking plot for single 37-ft (11.2-m) semitrailer truck with conventional tractor (WB-50).....	78
29	Offtracking plot for single 45-ft (23.7-m) semitrailer truck with conventional tractor.....	79
30	Offtracking plot for STAA single 48-ft (14.6-m) semitrailer truck with conventional tractor.....	80
31	Offtracking plot for STAA single 48-ft (14.6-m) semitrailer truck with long tractor.....	81
32	Offtracking plot for long single 53-ft (16.2-m) semitrailer truck with conventional tractor.....	82
33	Offtracking plot for STAA double-trailer truck with cab-over-engine tractor.....	83
34	Offtracking plot for STAA double-trailer truck with cab-behind-engine tractor.....	84
35	Offtracking plot for STAA single 48-ft (16.2-m) semitrailer truck with long tractor on long radius turns.....	86
36	Forces and moments on trailer.....	91
37	Tire/pavement forces with superelevation.....	92
38	Slip and steer angles.....	93
39	Trailer roll with superelevation.....	94
40	Trend in weight-to-power ratios of trucks from 1949 to 1984....	103
41	Comparison of weight-to-power ratios estimated by St. John to those observed by Messer.....	105
42	Effect of percent grade on tractor-trailer crawl speeds.....	106
43	Truck speed change per unit distance as a function of speed....	107
44	Forces acting on a vehicle as a function of speed.....	108
45	Gap and minimum separation dimensions considered in intersection sight distance criteria.....	117
46	Typical setup for video collection plan.....	120
47	Typical setup for tapeswitch data collection plan.....	122
48	Site plan for Route 26 and Central Valley Asphalt intersection.....	126
49	Site plan for Route 64 and Truck Stop 64 intersection.....	127
50	Site plan for Trindle Road and Railroad Avenue intersection.....	128
51	Typical gap acceptance plots for Greenshield, Raff, and logit methods.....	135

LIST OF FIGURES (Continued)

<u>Figure</u>		<u>Page</u>
52	Gap acceptance analysis by Greenshield method for a typical data set.....	136
53	Gap acceptance analysis by Raff method for a typical data set.....	137
54	Gap acceptance analysis using logit model for a typical data set.....	139
55	Cumulative distribution of average acceleration rate for left turns by four-axle trucks at the Central Valley Asphalt intersection.....	147
56	Cumulative distribution of average acceleration rate for right turns by four-axle trucks at the Central Valley Asphalt intersection.....	147
57	Cumulative distribution of average acceleration rate for right turns by five-axle trucks at the Truck Stop 64 intersection.....	148
58	Cumulative distribution of average acceleration rate for right turns by five-axle trucks at the Trindle and Railroad intersection.....	148
59	Cumulative distribution of deceleration rates for major road vehicles impeded by turning maneuvers by five-axle trucks.....	152
60	Cumulative distribution of speed reductions for major road vehicles impeded by turning maneuvers by five-axle trucks....	152
61	Speed vs. distance plot to determine minimum separation for a typical vehicle.....	157
62	Intersection sight distance curves from Green Book.....	163
63	Intersection sight distance curves for present study.....	164
64	Speed vs. distance curves for right turns by five-axle trucks at the Trindle and Railroad intersections.....	169
65	Distance considered in case II-C criteria for intersection sight distance.....	171
66	Typical cross sections for cost-effectiveness analysis.....	183

LIST OF TABLES

Volume I

<u>Table</u>		<u>Page</u>
1	Design and operational criteria based on vehicle characteristics.....	2
2	AASHTO design vehicle dimensions.....	6
3	Recommended dimensions for longer design vehicles.....	8
4	Detailed axle spacings for longer design vehicles.....	9
5	Braking distances for trucks with and without automatic limiting values for front-axle brakes.....	18
6	Truck deceleration rates and braking distances for use in highway design.....	23
7	Average driver eye heights for trucks.....	24
8	Clearance time (s) for low-speed acceleration by a tractor-semitrailer.....	27
9	Minimum and maximum clearance times (s) for 65-ft tractor-trailer truck.....	30
10	Average acceleration capabilities of trucks from specified speed to 40 mi/h (64 km/h).....	34
11	Average weights and power values for trucks.....	36
12	Dimensions and turning radii of current AASHTO design vehicles.....	38
13	Typical range of vertical stiffness per axle for truck suspension.....	43
14	Typical range of damping for truck suspension.....	43
15	Typical range of inter-axle load transfer for truck suspension.....	45
16	Typical range of roll center heights for truck suspensions.....	45
17	Typical range of roll stiffness for truck suspensions.....	47
18	Typical range of roll steer coefficients for truck suspensions.....	48
19	Typical range of compliance steer coefficients for truck suspensions.....	48
20	AASHTO criteria for stopping sight distance.....	57
21	Minimum vertical curve lengths (ft) needed to provide AASHTO stopping sight distance.....	58
22	Evolution of AASHTO stopping sight distance policy.....	60
23	Stopping sight distance requirements for trucks in comparison to current AASHTO criteria.....	64
24	Candidate stopping sight distance criteria for trucks.....	66
25	Minimum vertical curve lengths (ft) to provide stopping sight distance for trucks.....	67
26	Minimum percent reduction in truck accidents on crest vertical curves required for cost effectiveness of improved stopping sight distance on rural two-lane highways.....	69
27	Minimum percent reduction in truck accidents on crest vertical curves required for cost effectiveness of improved stopping sight distance on rural freeways.....	70

LIST OF TABLES (Continued)

<u>Table</u>		<u>Page</u>
28	AASHTO passing sight distance requirements including field data used in their derivation.....	74
29	MUTCD minimum passing sight distance warrants for no-passing zones.....	76
30	Derivation of MUTCD passing sight distance warrants (based on 1940 AASHTO policy).....	77
31	Alternative criteria for minimum length of passing zones on two-lane highways.....	80
32	Speed differentials between passing and passed vehicles for particular design speeds.....	82
33	Sight distance requirements for passing by passenger cars based on Glennon model.....	82
34	Sight distance requirements for passing by trucks based on revised Glennon model.....	83
35	Minimum vertical curve length (ft) to maintain required passing sight distance.....	86
36	Passing zone length required to complete a pass for various passing scenarios.....	88
37	AASHTO criteria for decision sight distance.....	91
38	Required minimum vertical curve length (ft) to provide maximum AASHTO decision sight distance for passenger cars.....	91
39	Revised criteria for decision sight distance (maneuver time increased by 21 percent to allow for trucks).....	95
40	Revised criteria for decision sight distance (maneuver time increased by 100 percent to allow for trucks).....	96
41	Required minimum vertical curve length (ft) to provide maximum decision sight distance for trucks.....	98
42	AASHTO adjustment factor for the effect of crossroad grade on accelerating time at intersections.....	105
43	AASHTO criteria for sight distance along the crossroad for an at-grade ramp terminal.....	106
44	Summary of truck characteristics for intersection sight distance (ISD).....	109
45	Sensitivity analysis of case I intersection sight distance (ISD) for trucks.....	112
46	Percent increase in case II intersection sight distance (ISD) for trucks over AASHTO criteria.....	115
47	Sensitivity analysis of case III-A intersection sight distance (ISD) for trucks.....	116
48	Curve B-1 intersection sight distance values.....	121
49	Curve B-2a & Ca sight distance values.....	125
50	Curve B-2b & Cb sight distance values.....	130

LIST OF TABLES (Continued)

<u>Table</u>		<u>Page</u>
51	Time gaps accepted from field data.....	133
52	Acceleration rates from field data.....	133
53	Deceleration rates and speed reductions for major road vehicles impeded by right turns by 5-axle trucks.....	134
54	Minimum separation times and distances.....	134
55	Additional area of clear sight triangle and clearing costs to provide case II sight distance for trucks at rural inter- sections.....	141
56	Minimum percent reduction in truck accidents at rural inter- sections required for cost-effectiveness of providing larger clear sight triangles.....	142
57	Width, wheelbase, and turning radii of AASHTO design vehicles..	143
58	Design vehicle dimensions used in Texas study.....	146
59	Minimum turning radii of design vehicles in Texas study.....	147
60	Minimum designs and channelization guidelines for turning roadways.....	149
61	Additional pavement construction costs to accommodate design vehicles larger than in AASHTO WB-50 truck at urban intersections.....	155
62	Summary of parameters for railroad-highway grade crossing sight distance.....	162
63	Summary of parameters varied in sensitivity analysis for railroad-highway grade crossing sight distance.....	164
64	Sensitivity analysis for sight distance along a highway (D_H) at railroad-highway grade crossing.....	166
65	Sensitivity analysis for sight distance to and along tracks (D_T) for a moving vehicle at railroad-highway grade crossings.....	168
66	Sensitivity analysis for sight distance along track for a stopped vehicle at railroad-highway grade crossings.....	171
67	Minimum sag vertical curve lengths (ft) for passenger cars and trucks.....	176
68	AASHTO criteria for maximum degree of curve and minimum radius for horizontal curves on rural highways and high- speed urban streets.....	186
69	Margins of safety against skidding on horizontal curves.....	192
70	Margins of safety against rollover on horizontal curves.....	195
71	Vehicle speed at impending skidding or rollover on horizontal curves.....	199
72	Lateral acceleration developed by overdriving design speed for horizontal curves designed to AASHTO minimum radii.....	200
73	Guidelines for ramp design speed as related to highway design design speed.....	202

LIST OF TABLES (Continued)

<u>Table</u>		<u>Page</u>
74	AASHTO criteria for pavement widening on horizontal curves.....	203
75	Minimum lane width required to accommodate truck offtracking on horizontal curves.....	208
76	Recommended passenger car performance criteria for determin- ing vehicle change interval.....	216
77	Sensitivity of vehicle change interval (s) to differences between passenger cars and trucks.....	218
78	MUTCD criteria for advance warning sign placement distance (based on MUTCD table II-1).....	222
79	AASHTO criteria for comfortable passenger car deceleration rates (derived from AASHTO Green Book figure II-13).....	225
80	Revised criteria for advance warning sign placement distances adequate for trucks.....	226
81	Minimum percent reduction in truck accidents required for cost effectiveness of sign relocation to implement revised advance warning sign distances.....	228

LIST OF TABLES (Continued)

Volume II

<u>Table</u>		<u>Page</u>
1	Test results for effect of brake adjustment on braking distance.....	9
2	Effect of brake lining temperature on braking distance.....	9
3	Braking distances for trucks with and without automatic limiting valves for front-axle brakes.....	10
4	Summary of NHTSA braking test results conducted for the current study.....	16
5	Truck deceleration rates and braking distances for use in highway design.....	18
6	Rollover thresholds for three truck types.....	25
7	Phase-4 model input parameters STAA single with 48-ft (14.6-m) trailer, S21 loading.....	26
8	Phase-4 model input parameters for STAA single with 53-ft (16.2-m) trailer, S21 loading.....	29
9	Phase-4 model input parameters for STAA double with COE tractor, D21 loading.....	32
10	Horizontal curve geometrics for Type I transition area (2/3 - 1/3 rule).....	51
11	Horizontal curve geometrics for Type II transition area (full superelevation on tangent).....	52
12	Horizontal curve geometrics for Type III transition area (spiral).....	53
13	Results of computer simulation for Type I transition area (2//3 - 1/3 rule).....	54
14	Results of computer simulation for Type II transition area (full superelevation on tangent).....	55
15	Results of computer simulation for Type III transition area (spiral).....	56
16	Comparison of computer simulation results for Type I and II transition areas.....	58
17	Comparison of computer simulation results for Type I and III transition areas.....	59
18	AASHTO design speed and critical speed values calculated from the computer simulation results.....	68
19	Acceleration overshoot values for the simulated cases.....	68
20	AASHTO design vehicle dimensions.....	72
21	Recommended dimensions for longer design vehicles.....	73
22	Detailed axle spacing for longer design vehicles.....	74
23	Offtracking for selected combinations of turn radius and turn angle.....	85
24	Assumed characteristics for loaded and empty trucks used in offtracking sensitivity analyses.....	98
25	Typical values of parameters for offtracking model.....	98
26	Components of total offtracking on a 500-ft (150-m) radius curve.....	99

LIST OF TABLES (Continued)

<u>Table</u>		<u>Page</u>
27	Average weights and power values for trucks.....	105
28	Distributions of weight-to-power ratios (lb/hp) from reanalysis of Gillespie data.....	113
29	Selected intersection characteristics for ISD study sites.....	119
30	Amount of data collected.....	125
31	Number of vehicles reduced for gap analysis.....	130
32	Number of vehicles for acceleration analysis.....	132
33	Number of vehicles for deceleration analysis.....	133
34	Results of gap acceptance analysis, critical gap (s) for left turn maneuvers.....	140
35	Results of gap acceptance analysis, critical gap (s) for right turn maneuvers.....	140
36	Findings from similar studies.....	142
37	Distance gaps for trucks at the Trindle and Railroad intersection.....	144
38	Example calculation for acceleration rate.....	145
39	Acceleration rates calculated from field data.....	149
40	Acceleration rates reported in the literature.....	149
41	Speed reductions for major road vehicles impeded by five-axle trucks turning right.....	153
42	Deceleration rates and maximum speed reductions for left turns.....	154
43	Deceleration rates (mi/h/s) from the Green Book.....	155
44	Deceleration rates from the Transportation and Traffic Engineering Handbook.....	156
45	Minimum separation times and distances for right turns by five-axle trucks.....	158
46	Time gaps accepted from field data.....	160
47	Acceleration rates from field data.....	160
48	Deceleration rates and speed reductions for major road vehicles impeded by right turns by five-axle trucks.....	161
49	Minimum separation times and distances.....	161
50	Basic sight distance model and parameter values used to derive each intersection sight distance curve.....	165
51	Basic sight distance model and parameter values used to derive each stopping sight distance curve.....	166
52	Speed reductions from pilot field study used to derive ISD criteria.....	167
53	ISD criteria for reduced speeds by major-road vehicles (ISD- RS_T) from field data.....	170
54	Acceleration distance and time for right turns by five-axle trucks at the Trindle and Railroad intersections.....	173
55	Distribution of crest vertical curves by algebraic difference in grade.....	184
56	Expected accident rates and severity distributions based on California data.....	185

LIST OF TABLES (Continued)

<u>Table</u>		<u>Page</u>
57	Candidate stopping sight distance criteria for trucks in comparison to AASHTO criteria.....	188
58	Assumed conditions--example 1.....	189
59	Computation of average construction cost per vertical curve--example 1.....	190
60	Computation of minimum percent accident reduction required for cost effectiveness--example 1.....	191
61	Assumed conditions--example 2.....	195
62	Computation of average construction cost per vertical curve--example 2.....	196
63	Computation of minimum percent accident reduction required for cost effectiveness--example 2.....	197
64	Assumed conditions--example 3.....	198
65	Computation of average construction cost per vertical curve--example 3.....	199
66	Computation of minimum percent accident reduction required for cost effectiveness--example 3.....	200
67	Assumed conditions--example 4.....	201
68	Computation of average construction cost per vertical curve--example 4.....	202
69	Computation of minimum percent accident reduction required for cost effectiveness--example 4.....	203

APPENDIX A
TRUCK BRAKING DISTANCES

This appendix presents the fundamental principles of truck braking performance and the development of the best available theoretical and empirical estimates of the distances required for trucks to brake to a stop from specified speeds. The results presented here are used in volume I in the evaluation of stopping sight distance and other design criteria to accommodate trucks.

Braking distance is defined in the American Association of State Highway and Transportation Officials (AASHTO) Green Book as "the distance required to stop the vehicle from the instant brake application begins."¹ It is used in the determination of many highway design and operational criteria, including stopping sight distance, intersection sight distance, vehicle change intervals for traffic signals, and advance warning sign placement distances. Currently, all of these design and operational criteria are based on passenger car braking distances and do not consider the longer braking distances required for trucks. The process of bringing a truck to a stop requires a complex interaction between the driver, the brake system, the truck tires, the dimensions and loading characteristics of the truck, and the pavement surface characteristics. Because truck braking is much more complex than passenger car braking, it is necessary to discuss the role of each of these characteristics in truck braking distances.

A. Tire-Pavement Friction in Braking Maneuvers

Vehicles are brought to a stop by brakes that retard the rotation of the wheels and allow tire-pavement friction forces to decelerate the vehicle. An understanding of the forces involved in tire-pavement friction is, therefore, critical to the understanding of braking distances.

The coefficient of braking friction (f_y) is defined as the ratio of the braking force (F_y) generated at the tire-pavement interface to the vertical load (F_z) carried by the tire. In other words:

$$f_y = \frac{F_y}{F_z} \quad (1)$$

On a horizontal curve, tire-pavement friction also supplies a cornering force to keep the vehicle from skidding off the road. The coefficient of cornering friction (f_x) is the ratio of the cornering force (F_x) generated at the tire-pavement interface to the vertical load (F_z) carried by the tire. In other words:

$$f_x = \frac{F_x}{F_z} \quad (2)$$

Figure 1 illustrates that both braking and cornering friction vary as a function of percent slip, which is the percent decrease in the angular velocity of a wheel relative to the pavement surface as a vehicle undergoes braking. A freely rolling wheel is operating at zero percent slip. A locked wheel is operating at 100 percent slip with the tire sliding across the pavement. Figure 1 shows that the coefficient of braking friction increases rapidly with percent slip to a peak value that typically occurs between 10 and 15 percent slip. The coefficient of braking friction then decreases as percent slip increases, reaching a level known as the coefficient of sliding friction at 100 percent slip.

The coefficient of cornering friction has its maximum value near zero percent slip and decreases to a minimum at 100 percent slip. Thus, when a braking vehicle locks its wheels, it may lose its steering capability due to a lack of cornering friction.

B. Locked Wheel Braking vs. Controlled Braking

The discussion of figure 1 implies that braking maneuvers can be performed in two general modes: locked wheel braking and controlled braking. Locked wheel braking occurs when the brakes grip the wheels tightly enough to cause them to stop rotating, or "lock," before the vehicle has come to a stop. Braking in this mode causes the vehicle to slide over the pavement surface on its tires. Locked wheel braking uses sliding friction (100 percent slip) represented by the right end of the graph in figure 1, rather than rolling or peak friction. The sliding coefficient of friction takes advantage of most of the friction available from the pavement surface, but is generally less than the peak available friction. On dry pavements, the peak coefficient of friction is relatively high and there is very little decrease in friction at 100 percent slip. On wet pavements, the peak coefficient of friction is lower and the decrease in friction at 100 percent slip is generally greater.

The braking distance required for a vehicle to make a locked wheel stop can be determined from the following relationship:

$$BD = \frac{V^2}{30f_s} \quad (3)$$

where: BD = braking distance (ft)

V = initial speed (mi/h)

f_s = coefficient of sliding friction

The coefficient of sliding friction in equation (3) is mathematically equivalent to the deceleration rate used by the vehicle expressed as a fraction of the acceleration of gravity (g), equal to 32.2 ft/s² (9.8 m/s²). The coefficient of friction and, thus, the deceleration rate may vary as a function of speed during the stop, so f_s in equation (3) should be understood as the average coefficient of friction or deceleration rate during the stop.

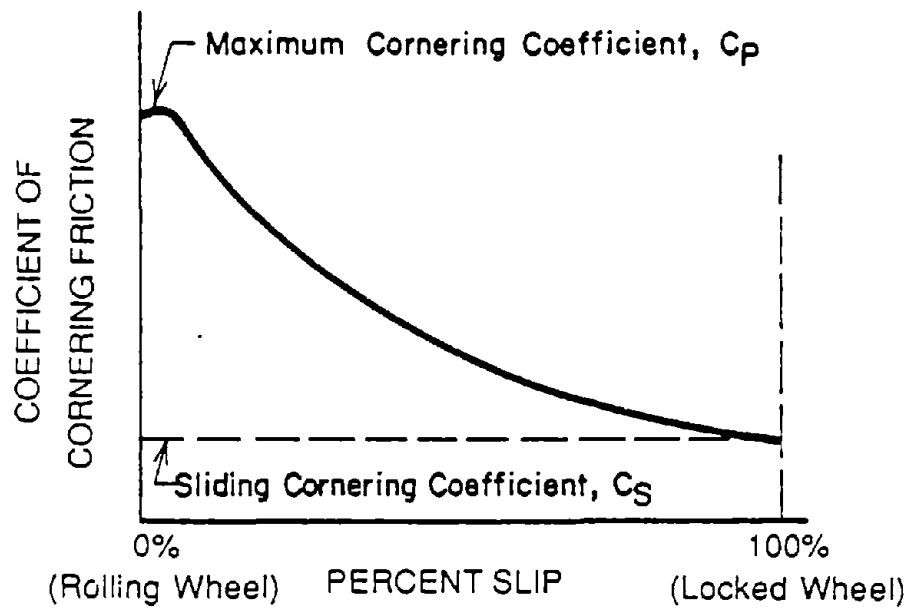
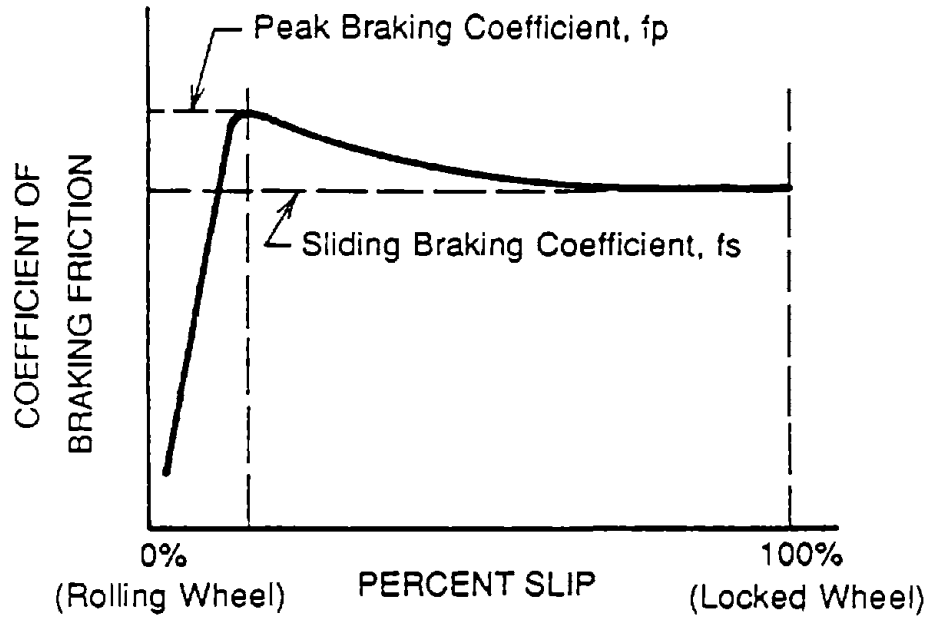


Figure 1. Variation of braking and cornering friction coefficients with percent slip.

Controlled braking is the application of the brakes in such a way that the wheels continue to roll without locking up while the vehicle is decelerating. Drivers generally achieve controlled braking by "modulating" the brake pedal to vary the braking force and to avoid locking the wheels. Controlled braking distances are governed by the rolling coefficient of friction which, for a typical truck and driver, occurs at a value of percent slip to the left of the peak available friction shown in figure 1. Due to the steep slope of the braking friction curve to the left of the peak and due to braking techniques used by drivers to avoid wheel lock up, the average rolling friction utilized by trucks is generally less than the sliding friction coefficient. Therefore, controlled braking distances are usually longer than locked wheel braking distances.

Locked wheel braking is commonly used by passenger car drivers during emergency situations. Passenger cars can often stop in a stable manner, even with the front wheels locked. In this situation the driver loses steering control, and the vehicle generally slides straight ahead. On a tangent section of road this is perhaps acceptable behavior, although on a horizontal curve the vehicle may leave its lane, and possibly the roadway. Trucks, by contrast, have much more difficulty stopping in the locked-wheel mode. Figure 2 illustrates the dynamics of a tractor-trailer truck if its wheels are locked during emergency braking.² The behavior depends upon which axle locks first -- they usually do not all lock up together. When the steering wheels (front axle) are locked, steering control is eliminated, but the truck maintains rotational stability and it "plows" straight ahead. If the rear wheels of the tractor are locked, that axle(s) slides and the tractor rotates or spins, resulting in a "jackknife" loss of control. If the trailer wheels are locked, those axles will slide and the trailer will rotate out from behind the tractor which also leads to loss of control. Although a skilled driver can recover from the trailer swing through quick reaction, the jackknife situation is not correctable. None of these locked-wheel stopping scenarios for trucks are considered safe. Therefore, it is essential that trucks stop in a controlled braking mode and that highway design and operational criteria recognize the longer distances required for trucks to make a controlled stop.

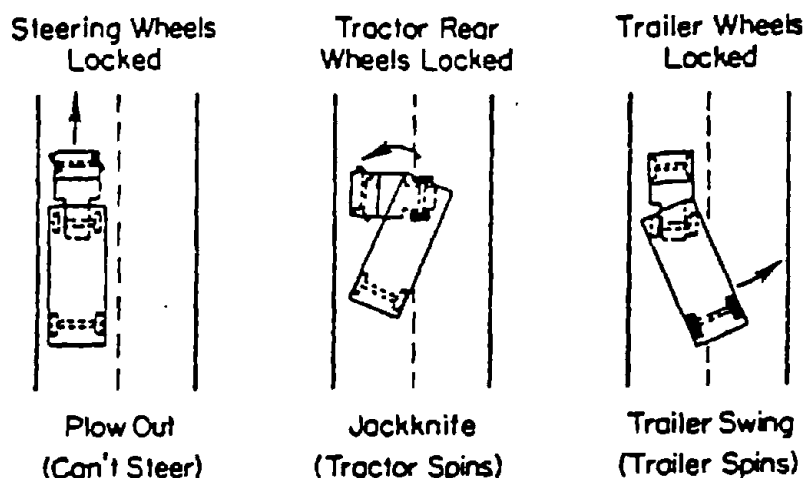


Figure 2. Tractor-trailer dynamics with locked wheels.²

The braking distance for a vehicle to make a controlled stop can be determined from the following relationship:

$$BD = \frac{V^2}{30f_r} \quad (4)$$

where: f_r = coefficient of rolling friction

As in the case of sliding friction, the coefficient of rolling friction (f_r) in equation (4) represents the average coefficient of friction or average deceleration rate during the entire controlled stop.

C. Pavement and Truck Characteristics Affecting Braking Distance

In order to stop without the risk of loss of control, trucks must use controlled braking rather than locked wheel braking. The deceleration rates used by trucks in making a controlled stop are represented by f_r in equation (4). The following discussion reviews the individual pavement and truck characteristics that affect the value of f_r and, thus, the braking distance of a truck.

1. Pavement Properties

The shape of the braking friction curve in figure 1 is a function of both pavement and tire properties. Highway agencies generally measure pavement friction by means of locked-wheel skid tests with a standard tire. These tests determine a value equivalent to f_s in equation (3). The results of these tests are often multiplied by 100 and referred to as skid numbers rather than coefficients of friction. Although skid numbers are usually determined at 40 mi/h (64 km/h), a procedure is available to determine the skid number at any speed from the skid number at 40 mi/h (64 km/h).^{3,4,5} The peak coefficient of friction (f_p) can be estimated from the sliding coefficient of friction by the following relationship:³

$$f_p = 1.45 f_s \quad (5)$$

Equation (5) represents the average relationship for truck tires between peak and sliding friction; this relationship can vary markedly between pavements and for the same pavement under wet and dry conditions. Pavements generally have much lower coefficients of friction under wet conditions than under dry conditions, so highway design criteria are generally based on wet conditions.

Estimates of braking distance in a recent evaluation of stopping sight distance requirements in NCHRP Report 270 used an assumed pavement skid number at 40 mi/h (64 km/h) (SN_{40}) of 28.³ The AASHTO Green Book criteria for stopping sight distance are based on a pavement with SN_{40} equal to 32.

Road roughness can increase braking distance.⁶ Tests found a 15 percent increase in braking distance for a rough surface with amplitude of 1 in (2.5 cm) and a frequency near the resonance frequency of the truck suspension.

2. Tire Properties

Truck tires are designed primarily for wear resistance. For this reason, they tend to have somewhat lower wet friction coefficients than passenger car tires. It is generally estimated that truck tires have coefficients of friction that are about 70 percent of those of passenger car tires.³ However, passenger car tires generally have coefficients of friction that are about 120 percent of the friction coefficients of the standard tires used in skid testing. Thus, the peak coefficient of friction can be estimated from skid test results with the following relationship:

$$f_p = (1.20)(0.70)(1.45) f_s = 0.0122 SN_{40} \quad (6)$$

The coefficient of friction for truck tires decreases as the tires wear and their tread depth decreases. New truck tires have tread depths of 15/32 in (1.2 cm) for ribbed tires and 31/32 in (2.4 cm) for lug type tires. NCHRP Report 270 assumes, based on the literature, that the tread wear of truck tires has very little effect on their frictional properties until the tread depth falls below 12/32 in (0.9 cm).^{3,7} Tire tread depth has little effect on the coefficient of friction on pavements with high macrotexture, but the coefficient of friction does decrease substantially with tread depth in smooth, poorly textured pavements.⁸ The following relationship was used in NCHRP Report 270 to estimate the reduction in friction coefficient of tires as their tread depth decreases:³

$$TF = 1 - \frac{\Delta f_p (1 - x/n)}{f_p} \quad (7)$$

where: TF = adjustment factor for tire tread depth

Δf_p = difference in coefficient of friction between new and bald (completely worn) tires

x = remaining tread depth (in) (use 12/32 if $x \geq 12/32$)

n = minimum tread depth with coefficient of friction equivalent to a new tire (assumed: 12/32 in or 0.9 cm)

Equation (7) is apparently based on studies of passenger car tires, but no equivalent relationship for truck tires is currently available.

Data on the coefficients of friction for various types of truck tires are available from references 8, 9, 10, and 11. Both references 8 and 9 indicate that the friction coefficients of truck tires decrease slightly with increasing axle load. Tire inflation pressure has very little effect on peak friction coefficient (f_p), but increasing the inflation pressure from 68 to 102 lb/in² (47 to 70 kPa) results in a very small loss (less than 10 percent) in the sliding friction coefficient (f_s).¹¹

3. Braking Efficiency

Current truck braking systems are limited in their ability to take advantage of all of the friction available at the tire-pavement interface. Fancher has estimated that the braking efficiency for single-unit trucks is between 55 and 59 percent of the peak available friction.¹² Fancher and NCHRP Report 270 assume that this same level of braking efficiency is applicable to tractor-trailer trucks.^{3,12} A primary reason for this relatively low level of braking efficiency is that most controlled braking takes place at a value of percent slip less than the peak level. Several other vehicle-related factors that contribute to low braking efficiencies are reviewed in this section. Factors, such as antilock brake systems, that might lead to future increases in braking efficiency are also discussed.

By way of introduction, the operation of air brakes -- the most common braking system for trucks -- is reviewed. Air brake systems use compressed air to transmit and amplify the driver's input from the brake pedal to the brakes on individual wheels. The use of air as an amplifying medium results in a slight delay in the system response due to the compressibility of air. (In contrast, hydraulic braking systems provide an almost immediate response). Once the brake pedal is released, the air in the system is expelled to the atmosphere and is replaced by air from a compressor on board the truck. Therefore, air brakes are not "pumped," as might be done in making a controlled stop with hydraulic brakes. Pumping of air brakes will result in the rapid depletion of the compressed air supply which in turn results in a total loss of braking ability. Rather, for an air brake system, the pressure within the system is adjusted by slightly depressing or slightly releasing the brake pedal to apply more or less braking force. This braking practice is called "modulating" the brakes. As discussed earlier in this section, "modulating" the brakes requires some experience on the part of the driver to obtain the maximum braking effect from the system without causing the wheels to lock.

Loading configuration: Braking tests for tractor-trailer combinations have generally found that loaded trucks have the shortest braking distances. Empty trucks generally have longer braking distances and bobtail tractors (with no trailer attached) have the longest braking distances. Some comparative braking distances for these loading configurations are presented in the review of braking test results later in this section. These differences occur primarily because the truck braking system is designed to be balanced for the loaded condition and is, therefore, out of balance for the empty and bobtail conditions.

Technology improvements to braking systems may minimize the effects of loading conditions in future years. For example, some tractors are already equipped with a sensor in the "gladhand" brake line connection that detects whether or not a trailer is attached and adjusts the brakes on the drive axle of the tractor accordingly. Future trucks may have microprocessor controlled braking systems with load sensors on each axle to adjust the braking system accordingly. At present, conservative estimates of braking distance should be based on an empty tractor-trailer truck.

Brake adjustment: Poor adjustment of air brakes has been found to substantially decrease braking efficiency and, thus, increase braking distance. A 1977 survey by the California Highway Patrol found that 68 percent of trucks surveyed had at least one brake out of adjustment, and 19 percent had 40 percent or more of the brakes out of adjustment and were placed out of service. A follow up survey in 1981, after an increase in enforcement efforts in California, found a reduction to about 44 percent of trucks with one or more brakes out of adjustment, and 12 percent with 40 percent or more out of adjustment. Another survey in 1981, conducted in Maryland, found 69 percent of trucks with one or more brakes out of adjustment, and 28 percent with 40 percent or more out of adjustment. Thus, trucks with brakes out of adjustment are fairly common.^{13,14}

A 1982 study by the the National Highway Traffic Safety Administration (NHTSA) investigated the effects of air brake adjustment on truck braking performance.^{13,14} Trucks were tested with all of their brakes adjusted for optimum performance. Then the brakes were readjusted such that they were nearly out of adjustment, but were just within the allowable limits. The results of these tests, presented in table 1, indicate that braking distances can increase up to 30 percent due to brake maladjustment.

Brake lining temperature: The NHTSA study mentioned above also determined the effect of brake lining temperature on braking efficiency and braking distance.^{13,14} Tests were conducted at various brake lining temperatures with the three-axle single-unit truck with a 10 percent overload described in table 1. Table 2 presents the test results at the different temperatures, both for fully adjusted brakes and for brakes readjusted to the limit of the specifications.

Table 2 shows that brake lining temperature compounds the effects of brake maladjustment. For maladjusted brakes, the relatively hot brake lining temperature of 400 °F (200 °C) resulted in a 54 percent increase in braking distance over the relatively cool brake lining temperature of 150 °F. Brake lining temperatures as high as 400 °F (200 °C) are not unusual in normal operation and can go considerably higher in city or mountain driving. Fully adjusted brakes were found to be less sensitive to temperature than maladjusted brakes. The increase in stopping distance from 150 °F to 400 °F (65 °C to 200 °C) was found to be only 15 percent for fully adjusted brakes.

Table 1. Test results for effect of brake adjustment on braking distance.^{13,14}

Vehicle	Weight (lb)	Speed (mi/h)	Brake temp. (°F)	Average braking distance (ft)		
				Optimally adjusted	Adjusted to limit	Percent increase
Single-unit truck with two axles	27,500	55	< 200	219	283	29
Tractor-semitrailer (3S2)	80,500	60	< 200	256	319	25
Single-unit truck with three axles (10% overload)	55,000	60	< 200	342	458	34

Note: 1 lb = 0.454 kg
 1 mi = 1.61 km
 1 ft = 0.305 m

Table 2. Effect of brake lining temperature on braking distance.^{13,14}

Vehicle: Single-unit truck with three axles
 Weight : 55,000 lb (10% overload)
 Speed : 60 mi/h
 Average stopping distance (ft):

	Brake lining temp. (°F)			
	150	200	300	400
Fully adjusted brakes:	342	351	366	393
Adjusted to limit:	458	519	625	692

Note: 1 lb = 0.454 kg
 1 mi = 1.61 km
 1 ft = 0.305 m

Disconnection of front-axle brakes: For many years, truckers in the United States have disconnected the front-axle brakes of their trucks. Although this practice is now illegal, it became widespread because of concern by drivers that they might lose control of the truck if the front-axle brakes were locked in an emergency situation. Figure 2 illustrates that while locked front-axle brakes may lead to the inability to steer, this is potentially much less hazardous than locking the brakes on other axles of the truck. Tests by

NHTSA have shown that trucks with disconnected front brakes require 20 to 25 percent greater braking distance.¹⁵ Enforcement activities to assure that front brakes are not disconnected have been increased.

Automatic limiting valves for front-axle brakes: A new component added to braking systems that has gained popularity among truck drivers in recent years is an automatic limiting valve for the front-axle brakes. The purpose of the automatic limiting valve is to limit the amount of braking achievable on the front axle. According to NHTSA, approximately two-thirds of post-1980 combination unit trucks are equipped with automatic limiting valves.² The advantage of an automatic limiting valve is that it reduces the possibility of wheel lock on the steering axle, which means the driver retains steering control during heavy application of the brakes, even if other wheels might lock. The main disadvantage is that, similar to disconnection of the front-axle brakes, an automatic limiting valve reduces the braking capability of the truck, which lengthens the braking distance. Table 3 presents data for controlled stops by trucks with and without automatic limiting valves.² In all cases, the shorter braking distance in each range shown in table 3 is the braking distance without an automatic limiting valve. The increase in braking distance resulting from use of an automatic limiting valve ranges from 8 to 29 percent.

Table 3. Braking distances for trucks with and without automatic limiting valves for front-axle brakes.²

60 mi/h, empty, straight-line stop	
Single-unit truck with three axles	440 to 355 ft
Bobtail tractor with three axles	418 to 324 ft
50 mi/h, empty, 500 ft radius curve, wet asphalt	
Single-unit truck with three axles	268 to 233 ft
Tractor-semitrailer (2S1)	260 to 224 ft
Bobtail tractor with two axles	308 to 249 ft
Auto transport truck (stinger)	251 to 181 ft
18 mi/h, loaded, 500 ft radius curve, ice	
Tractor-semitrailer (3S2)	273 to 253 ft
Tractor-semitrailer (2S1)	213 to 179 ft

Note: 1 mi = 1.61 km
1 ft = 0.305 m

Antilock brake systems: During the mid 1970s, regulations for truck braking distances were adopted, which resulted in the introduction of antilock brake systems on trucks. Shortly afterwards, the restrictions were removed by court order and, due to a lack of consumer interest, trucks equipped with antilock brakes were no longer commercially available from domestic truck manufacturers. Since that time, with technological advancements and improved design, antilock braking systems have gained acceptance in Europe and are slowly being reintroduced into the United States, primarily through imported passenger cars. It is possible that antilock brake systems for trucks will become common in the United States (or may be required by regulation) within 5 to 10 years. Thus, the improvements in truck braking distances that might result from antilock brake systems need be considered in the development of highway design criteria for future application.

The purpose of antilock brakes is to take full advantage of the available tire-pavement friction capabilities without locking the wheels and losing vehicle control. Antilock brake systems try to achieve and maintain the peak coefficient of tire-pavement friction shown in figure 1, thereby maximizing the braking effort.

Antilock brake systems operate by monitoring each wheel for impending lock up. When wheel lock up occurs or is anticipated, the system releases brake pressure on the wheel. When the wheel begins to roll freely again, the system reapplies braking pressure. The system constantly monitors each wheel and readjusts the brake pressure until the wheel torque is no longer sufficient to lock the wheel. Present antilock brake systems are controlled by on-board microprocessors.

A recent NHTSA study of the performance of a commercially available antilock brake system on a two-axle single-unit truck found a 15 percent reduction in braking distance for a straight line stop from 60 mi/h (97 km/h) on a wet polished concrete pavement surface with an SN_{10} of approximately 30 (very similar to the surface used by the AASHTO Green Book in the specification of stopping sight distance standards).¹⁶ Tests on other pavement surfaces and in other types of maneuvers found decreases in braking distance up to 42 percent with the antilock brake system. Furthermore, in addition to improving the braking efficiency by operating closer to the peak braking friction coefficient, antilock brake systems should also minimize the increase in braking distance due to driver inexperience (see discussion in the following section).

4. Driver Control Efficiency

Most truck drivers have had little or no practice in emergency braking situations. This lack of expertise in modulating the brakes results in braking distances that are longer than the vehicle capability. NCHRP Report 270 examined the effect of driver efficiency on braking distance using both experienced test drivers and professional truck drivers without test track experience.³ The study found that the driver efficiencies ranged from 62 to 100 percent of the vehicle capability. The braking performance of the drivers tended to improve during the testing period as the drivers gained experience

in modulating the brakes. Truck driver training programs stress the importance of controlled braking in emergency situations, but do not typically include practice in actual controlled braking under test-track or highway conditions. Because so many drivers on the road lack experience in emergency braking, the authors recommended the use of a driver efficiency of 62 percent in stopping sight distance design criteria. However, it should be recognized that this is a very conservative choice. Experienced drivers can operate at efficiencies approaching 100 percent. Furthermore, in the future, antilock brake systems could eliminate the concern over driver efficiency by providing computer-controlled modulation of the brakes to achieve minimum braking distance.

D. Recent Research on Truck Braking Distance

There are two main sources of data on truck braking distances in recent published literature: the University of Michigan Transportation Research Institute (UMTRI) (see references 3 and 12) and the NHTSA Vehicle Research and Test Center (VRTC) (see references 13, 14, 15, 16, 17, 18, 19, and 20).

NCHRP Report 270 has suggested a model to predict braking distance as a function of pavement surface characteristics, tire characteristics, vehicle braking performance, and driver control efficiency.³ Parametrically, the model expresses the coefficient of rolling friction, f_r , as:

$$f_r = f_p \times TF \times BE \times CE \quad (8)$$

where: f_p = peak braking friction coefficient available given the pavement surface characteristics

TF = adjustment factor for tire tread depth (see equation (6))

BE = adjustment factor for braking efficiency (the efficiency of the braking system in using the available friction, typically 0.55 to 0.59 for conventional braking systems)

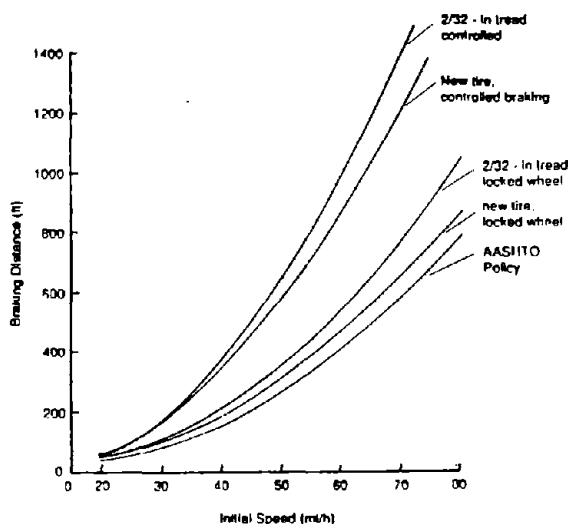
CE = adjustment factor for driver control efficiency (the efficiency of the driver or in modulating the brakes to obtain optimum braking performance, typically 0.62 to 1.00 for conventional braking systems)

The factors that influence each term of equation (8) have been addressed in the preceding discussion.

A paper by Fancher, derived from NCHRP Report 270, used the model in Equation (8) to predict truck braking distances.^{3,12} Figure 3 shows the braking distances for trucks under controlled and locked wheel stops with new and worn tires (2/32-in [0.2 cm] tread depth) in comparison to the braking distances assumed in the AASHTO Green Book. Figure 3 shows that the braking distances predicted by Fancher are substantially longer than the distances for

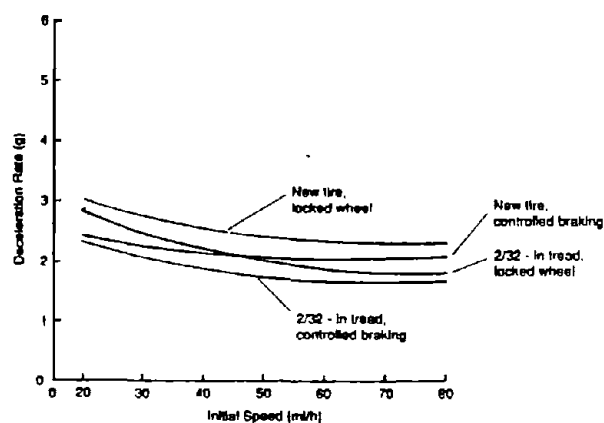
locked wheel braking by a passenger car assumed by AASHTO. The figure is based on a pavement with SN_{40} of 28 and the best performance driver who uses 100 percent of the vehicle braking capability. A less experienced driver would require even longer stopping distances.

Figure 4 illustrates the deceleration rates (i.e., values of f_r) used to develop figure 3. Figure 4 shows that the deceleration rates for controlled stops on a wet pavement by the best performance driver are generally between 0.20 and 0.25 g, and are relatively insensitive to vehicle speed.¹² In contrast, appendix B of NCHRP Report 270 shows deceleration rates as high as 0.5 g in controlled stops on a wet pavement by experienced drivers.³ These tests were performed on a pavement that apparently has a very high peak friction coefficient even when wet. The data in figures 3 and 4 were derived theoretically from the model given in equation (8).



Note: 1 ft = 0.305 m
1 mi = 1.61 km

Figure 3. Truck braking distances on a poor, wet road.¹²



Note: 1 mi = 1.61 km

Figure 4. Truck deceleration rates on a poor, wet road.¹²

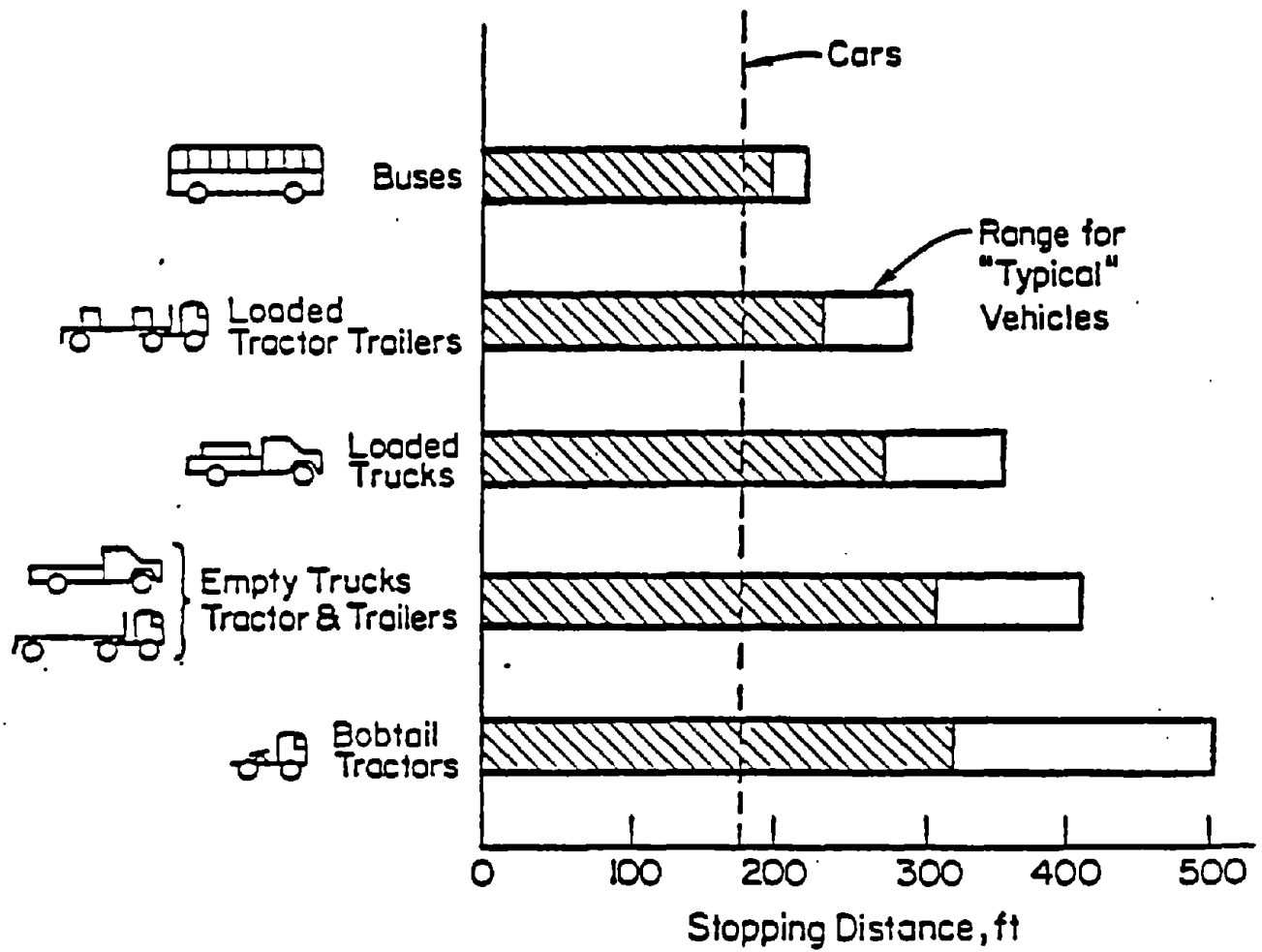
In contrast, the NHTSA Vehicle Research and Test Center (VRTC) in East Liberty, Ohio, has conducted full-scale braking tests for a variety of truck and braking system configurations. Figure 5 summarizes the NHTSA braking distance test results for controlled stops from 60 mi/h (97 km/h) by several vehicle types on a dry pavement.¹⁸ All of the vehicles tested were equipped with air brakes except the passenger car, which was used as a reference. Of the trucks, stopping distances are shortest for loaded tractor-trailers, because their braking systems are designed for this situation. Braking distances are longer for empty trucks, because of the imbalance in the brake torque capabilities on the various axles relative to their loads. The longest observed braking distances are for bobtail tractors.

Longer braking distances than those shown in figure 5 would be expected on wet pavement. Because the recent NHTSA tests have been conducted at a variety of speeds, for a variety of pavement types, and for a variety of maneuver types (straight line stop, curved path, lane changing, etc.) formal comparisons with the theoretical UMTRI braking estimates shown in figures 3 and 4 are difficult. Therefore, NHTSA conducted a limited set of braking tests for use in this study for straight-line stops under consistent pavement conditions. The results of these tests are presented in table 4. All of the tests consisted of straight-line stops on a wet, polished concrete surface with SN_{40} of about 30 (i.e., very close to the AASHTO design coefficient of friction of 0.32 at 40 mi/h [64 km/h]). A number of vehicle types were tested, including a passenger car, a pickup truck, a single-unit truck, a school bus, a tractor-semitrailer truck, a double-trailer truck, and a bobtail tractor. The trucks were tested in an empty (unloaded) condition with radial tires in good condition. The reported results represent the shortest braking distance in a sequence of six tests. The use of the shortest braking distance minimizes the influence of driver factors on the test results and represents the best available estimate of the vehicle braking capability (i.e., 100 percent driver control efficiency).

E. Braking Distance for Use in Highway Design Criteria

The available literature does not provide a clear indication of which braking distances should be used in highway design criteria. Many of the factors that influence braking distances, such as pavement characteristics and driver efficiencies, vary widely. For purposes of the evaluation of current highway design and operational criteria in this report, three braking scenarios have been derived for consideration in the development of design criteria for trucks. These three scenarios are: tractor-trailer truck with a conventional brake system and the worst-performance driver, tractor-trailer truck with a conventional brake system and the best-performance driver, and a tractor-trailer truck with an antilock brake system. Deceleration rates and braking distances for these three scenarios are shown in table 5. These data are based on the results obtained by Fancher shown in figures 3 and 4, with a minor change in the assumption concerning pavement surface properties (from SN_{40} of 28 assumed by Fancher to SN_{40} of 32 assumed by the AASHTO Green Book).¹² All of the braking distances in table 5 are appropriate for an empty truck with relatively good radial tires (at least 12/32 in [0.9 cm] of tread depth).

The data for the worst performance driver in table 5 are based on an assumed 62 percent driver control efficiency (CE in equation (8)), which represents a very conservative, worst case condition. The data for the best performance driver are based on a driver control efficiency of 100 percent, and, thus, represent the full capability of conventional brake systems. Most truck drivers on the road today have control efficiencies that fall between these two extremes. The data for an antilock brake system are based on the NHTSA data in table 4 and represent a 20 to 30 percent improvement over the best performance driver. This may, in fact, be a conservative estimate of the improvement that could be obtained from future antilock brake systems.



Note: 1 ft = 0.305 m

Figure 5. NHTSA test results for stable stopping distance from 60 mi/h (97 km/h) on dry road.¹⁸

Table 4. Summary of NHTSA braking test results conducted for the current study.

<u>Vehicle type</u>	<u>Vehicle make and model</u>	<u>Test conditions</u>	<u>Braking distance (ft)</u>		<u>Deceleration rate (g)</u>	
			<u>30 mi/h</u>	<u>40 mi/h</u>	<u>30 mi/h</u>	<u>40 mi/h</u>
Passenger car	Buick Electra	No ABS	66	138	0.45	0.39
Passenger car	Buick Electra	w/ ABS	71	124	0.42	0.43
Pickup truck	Ford F150	No ABS	72	109	0.42	0.49
Single-unit truck	IH 1954	No ABS	102	180	0.29	0.30
School bus	IH 66 passenger	No ABS	100	194	0.30	0.27
Tractor-semitrailer truck (2S1)	Ford/Great Dane (27 ft)	No ABS or ALV	167	339	0.18	0.16
Tractor-semitrailer truck (2S1)	Ford/Great Dane (27 ft)	w/ALV	209	403	0.14	0.13
Tractor-semitrailer truck (3S2)	IH/Fontaine (42 ft)	No ABS or ALV	167	352	0.18	0.15
Tractor-semitrailer truck (3S2)	IH/Fontaine (42 ft)	w/ALV	187	384	0.16	0.14
Tractor-semitrailer truck (3S2)	Freightliner/Fontaine (42 ft)	No ABS or ALV	167	337	0.18	0.16
Tractor-semitrailer truck (3S2)	Freightliner/Fontaine (42 ft)	w/ALV	198	363	0.15	0.15
Tractor-semitrailer truck (3S2)	Freightliner/Fontaine (42 ft)	w/ABS	100	188	0.30	0.28
Tractor-semitrailer truck (3S2)	Freightliner/Trailmobile (40 ft)	No ABS or ALV	148	282	0.20	0.19
Tractor-semitrailer truck (3S2)	Freightliner/Trailmobile (40 ft)	w/ALV	147	302	0.20	0.18

Table 4. Summary of NHTSA braking test results conducted for the current study (continued).

Vehicle type	Vehicle make and model	Test conditions	Braking distance (ft)		Deceleration rate (g)	
			30 mi/h	40 mi/h	30 mi/h	40 mi/h
Double-trailer truck (2SIF2)	Peterbilt/Great Dane (27 ft)	No ABS or ALV	115	225	0.26	0.24
Double-trailer truck (2SIF2)	Peterbilt/Great Dane (27 ft)	w/ALV	142	283	0.21	0.19
Bobtail tractor (2-axle)	Ford	No ABS or ALV	178	336	0.17	0.16
Bobtail tractor (2-axle)	Ford	w/ALV	296	474	0.10	0.11
Bobtail tractor (2-axle)	Peterbilt	No ABS or ALV	159	268	0.19	0.20
Bobtail tractor (2-axle)	Peterbilt	w/ALV	190	347	0.16	0.15
Bobtail tractor (3-axle)	Freightliner	No ABS or ALV	167	287	0.18	0.19
Bobtail tractor (3-axle)	Freightliner	w/ALV	195	317	0.15	0.17
Bobtail tractor (3-axle)	Freightliner	w/ABS	90	176	0.33	0.30

Note: ABS = Antilock brake system

ALV = Automatic limiting value for front-axle brakes

1 ft = 0.305 m

1 mi = 1.61 km

Table 5. Truck deceleration rates and braking distances for use in highway design.^a

Vehicle speed (mi/h)	Deceleration rate (g)			Braking distance (ft)			
	AASHTO policy	Worst-performance driver ^b	Best-performance driver ^c	AASHTO policy	Worst-performance driver ^b	Best-performance driver ^c	Antilock brake system
20	0.40	0.17	0.28	33	77	48	37
30	0.35	0.16	0.26	86	186	115	88
40	0.32	0.16	0.25	167	344	213	172
50	0.30	0.16	0.25	278	538	333	267
60	0.29	0.16	0.26	414	744	462	375
70	0.28	0.16	0.26	583	1,013	628	510

^a Based on empty tractor-trailer truck on a wet pavement with $SN_{4.0} = 32$.

^b Based on driver control efficiency of 0.62.

^c Based on driver control efficiency of 1.00.

Note: 1 ft = 0.305 m

It is important to note that the estimates of deceleration rate and braking distances in table 5 for trucks equipped with antilock brake systems are very similar to the AASHTO criteria for passenger cars, which are also shown in the table.

APPENDIX B

HORIZONTAL CURVE DESIGN TO REDUCE TRUCK ROLLOVERS

Studies such as "Impact of Specific Geometric Features on Truck Operations and Safety at Interchanges" have shown that rollover is one of the major factors contributing to truck accidents.²¹ The roll performance of trucks on horizontal curves is determined by truck dynamics and by the curve geometry as well as by the way in which these two components of this complex system interact under dynamic highway conditions. This appendix reports the results of a study undertaken to investigate the effect of variations in truck characteristics on rollover thresholds and the effect of variations in horizontal curve design criteria on the rollover performance of trucks. The study was based on review and analysis of published literature and computer simulation of truck dynamics. The results of the study have been used in volume I to assess the need for changes in horizontal curve design criteria to accommodate trucks.

A. Background

Horizontal curves are designed in accordance with the standard curve formula:¹

$$R_{\min} = \frac{V_d^2}{15(e_{\max} + f_{\max})} \quad (9)$$

where: R_{\min} = minimum radius of curvature (ft)
 V_d = design speed (mi/h)
 e_{\max} = maximum pavement cross-slope (superelevation) (ft/ft)
 f_{\max} = maximum tolerable lateral acceleration (g)

Curves with radii larger than R_{\min} can be designed with superelevation less than e_{\max} .

The net lateral acceleration on any horizontal curve at any speed can be estimated in a simple variation of the standard curve formula as:

$$a_{\text{net}} = \frac{V^2}{15 R} - e \quad (10)$$

where: a_{net} = net lateral acceleration (g)
 V = vehicle speed (mi/h)

R = radius of vehicle path (ft)

e = superelevation (ft/ft)

The rollover threshold of a truck expressed in units of the acceleration of gravity must exceed the value of a_{net} in equation (10) or the vehicle will roll over. The available coefficient of tire-pavement friction must exceed the value of a_{net} in equation (10) or the vehicle will skid.

While equation (10) provides nominal estimates of lateral acceleration for vehicles on horizontal curves, it is only applicable to steady-state conditions; real-world accelerations may vary from the nominal value because of driver characteristics or dynamic variations in the vehicle path. Computer simulation provides a tool to investigate the actual vehicle dynamics in horizontal curves, as well as to estimate the rollover threshold of particular trucks. The following discussion describes the most appropriate computer simulation model for truck dynamics.

B. Computer Simulation of Truck Dynamics on Horizontal Curves

A vehicle on a horizontal curve is subjected to three moments about its longitudinal axis: the primary overturning moment, M_y , due to vehicle lateral acceleration; the lateral displacement moment, M_d , due to lateral displacement of the vehicle center of gravity; and the restoring moment, M_r , due to net force generated by the left and right sides of the vehicle suspension. On a level surface, the primary overturning moment and the lateral displacement moment tend to increase the truck roll angle (the resistive action is generated by the restoring suspension moment). When a road surface is superelevated, as illustrated in figure 6, the lateral displacement moment opposes the primary overturning moment for small truck roll angles and then changes sign and begins contributing to truck roll when the roll angle becomes greater than the angle of the road superelevation. Because truck rolling is a dynamic process, it depends not only on the curve radius and superelevation, but also on the design of the transition between the normal crown section and the superelevated curve.

The three moments that act on the truck during turning and affect rollover characteristics depend primarily on the following parameters:

- Gross vehicle weight.
- Longitudinal weight distribution.
- Roll center height.
- Center of gravity height.
- Suspension stiffness.
- Road geometry.

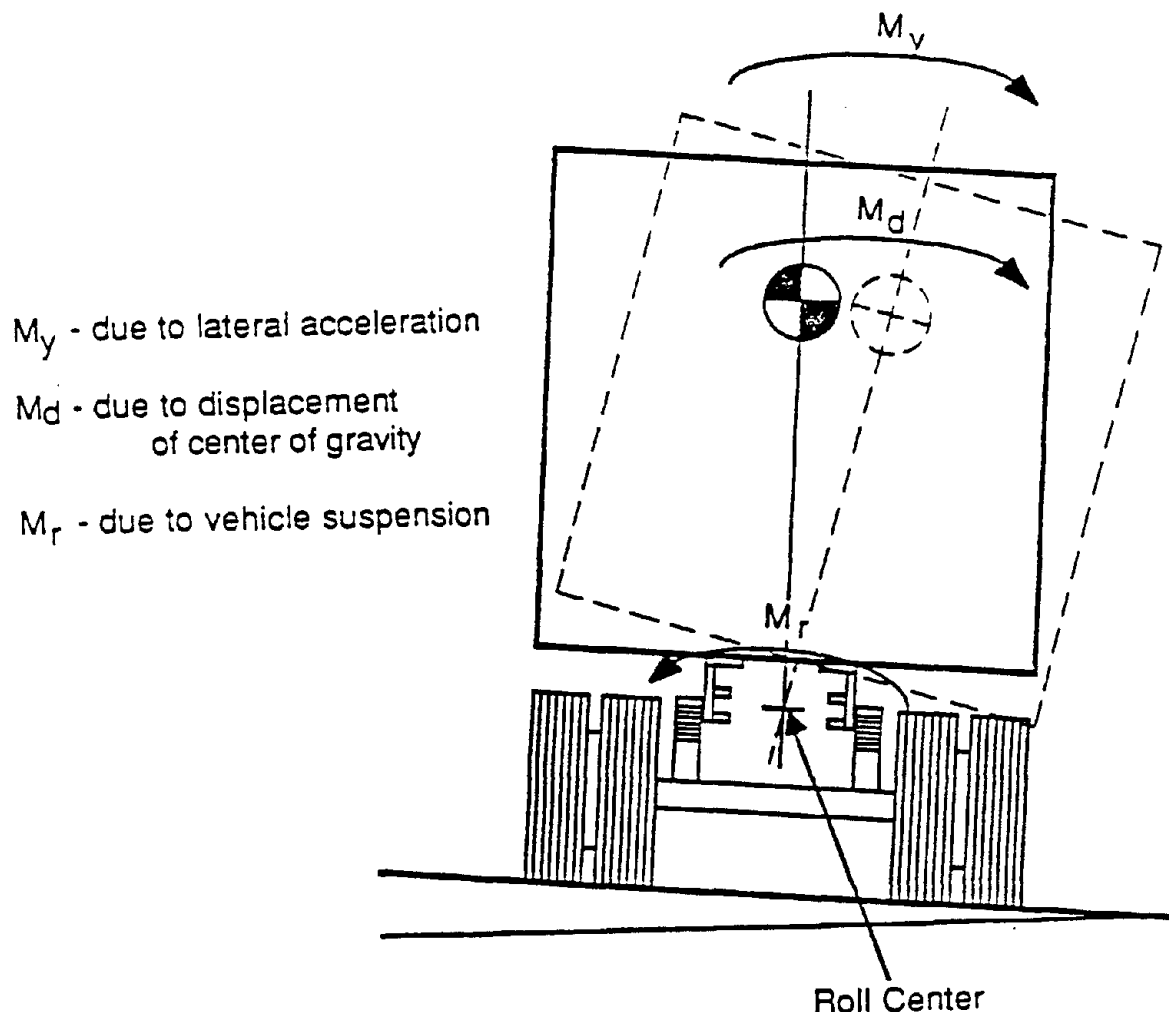


Figure 6. Overturning and resisting moments about the longitudinal axis of a truck on a superelevated curve.

The first four parameters represent truck characteristics; the last parameter represents highway characteristics. All of these parameters interact dynamically during truck rolling. To accomplish the objective of this study, computer simulation was used to determine the effects of both truck and road characteristics on truck rollover.

The investigation of truck rollover performance on horizontal curves was performed with the Phase-4 simulation model developed for FHWA and the Motor Vehicle Manufacturers Association.²² The Phase-4 model is the most complete available vehicle dynamics model that can simulate articulated trucks.

The Phase-4 program is an elaborate heavy truck computer simulation model. It can simulate various heavy truck configurations, including straight trucks, bobtail tractors, and tractors with one, two, or three trailers, in steering and braking maneuvers. Trucks can be simulated with or without payloads.

The Phase-4 model is very complex and can perform a wide variety of vehicle evaluations. For example, the program can evaluate the effects of payload placement and weight variations; the effects of various tire, axle, and suspension systems; braking system effectiveness; understeering; oversteering; and threshold values of yaw, roll, and pitch.

The Phase-4 model is a large program consisting of 30 subroutines (approximately 8,000 lines of FORTRAN code). The structure of the program allows the subroutines to interact, rarely returning to the main calling program after the simulation begins. This decreases the run time, but the logic becomes very difficult to trace. This also makes it difficult if the user wants to change or add to the existing program structure. The Phase-4 program did not require extensive modifications for this study. However, a subroutine to process user-specified road geometry had to be developed.

Several computer truck simulation models were recently compared: the Linear Yaw Plane Model, the TBS Model, the Yaw/Roll Model, and the Phase-4 model. In this comparison study, two tractor-trailer configurations were simulated for a steady-state turning maneuver and a lane change maneuver. The results were then compared to actual test results. According to this study, Phase-4 best predicts lateral acceleration for steady-state turning.²³

UMTRI has conducted extensive tests that verified the results obtained in Phase-4 including comparison of several maneuvers simulated with Phase-4 to actual test data. A complete discussion and presentation of the verification findings can be found in the user's manual for the Phase-4 model.²²

The Phase-4 model is built around a series of differential equations, which are derived from Newtonian mechanics and are solved through numerical integration. The numerical integration routine used in the original Phase-4 model has been replaced with a routine using the Runge-Kutta algorithm with an adjustable time step for greater computational efficiency. The tires and suspension systems are modeled with spring and damper systems, which may or may not be linear depending on which options the user chooses. The fifth-wheel and pintle hook connections are modeled with a spring dashpot system, which gives the model a roll compliance at the hitch that is similar to actual situations.

The Phase-4 model uses extensive input information. Input data for each unit of the vehicle (i.e., each tractor, trailer, or dolly) are entered separately. The following types of input parameters can be specified:

- Vehicle frame parameters.
- Front suspension and axle.
- Front tires.
- Rear suspension and axle.
- Rear tires.

- Payload.
- Front and rear brake parameters (if braking is used).

A different payload can be placed on each unit of the vehicle. Payloads can vary in size, shape, and weight, as represented by each payload's moment of inertia.

The only unrealistic feature of the Phase-4 model for evaluation of horizontal curves is that it is incapable of applying drive force to the wheels of the truck. Thus, the truck coasts around the curve and decelerates slightly due to tire/pavement friction. This is not a critical limitation of the model for evaluation of horizontal curves, since model runs typically last only a few seconds and the speed reduction through the length of the curve is less than 1 ft/s (0.3 m/s).

The Phase-4 model is capable of simulating vehicle dynamics along any predefined path specified in three-dimensional (x,y,z) coordinates. However, the original Phase-4 program was readily adaptable only to level surfaces or to simple, constant radius curves with constant superelevation. To accomplish the main objective of this study, a new subroutine had to be developed to allow users to specify horizontal curves of more complex geometry.

The Phase-4 model uses a linear tire model, and the roll angles are assumed to be small. The assumption that the angles are small is reasonable because large roll angles indicate that the truck is rolling over and the accuracy of the tire model is irrelevant after the truck has begun to roll over.

The simulation output consists of two major sections. The first section is an echo of the input values, which can be very helpful in ensuring that the correct values were read. The second output section consists of eight types of pages for each unit of the vehicle configuration. These output pages present information that describes the following:

- Sprung mass positions.
- Sprung mass velocities.
- Sprung mass acceleration.
- Tire forces.
- Brake summary.
- Lateral acceleration.
- Unsprung mass data.
- Temperature data.

Each type of output data is provided at user-specified time increments.

The output format produced by the Phase-4 model is very cumbersome. To obtain output in other forms so that plots can be generated or variables can be viewed readily, extra output files were created in the revised version of the Phase-4 model. For example, one of these output files contains information that will allow the user to view or plot the change of vehicle roll angle or lateral acceleration with time.

C. Effect of Truck Characteristics on Rollover Threshold

The Phase-4 model was used to determine the rollover thresholds of three of the design vehicles identified during the research:

- STAA single with 48-ft (14.6-m) semitrailer and conventional tractor.
- Long single with 53-ft (16.2-m) semitrailer.
- STAA double with two 28-ft (8.5-m) trailers and cab-over-engine tractor.

The rollover thresholds for the three vehicles were found on a flat, simple curve with 500-ft (150-m) radius and a curve with maximum superelevation of 0.06 and are presented in table 6. Detailed vehicle and load parameters for the first three vehicles used in the simulation are presented in tables 7, 8, and 9.

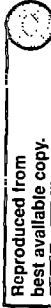
Table 6. Rollover thresholds for three truck types.

<u>Truck type</u>	<u>Rollover threshold (g)</u>	<u>Speed at rollover (mi/h)</u>
STAA 48-ft single	0.36	50.5
STAA 53-ft single	0.38	51.8
STAA COE double	0.45	53.9

An investigation of the effect of truck characteristics on rollover threshold was conducted using one selected type of truck, the STAA single with 48-ft (14.6-m) semitrailer and conventional tractor. The Phase-4 model was used to determine these rollover thresholds. A truck was simulated traveling through a horizontal curve at a given speed and the roll angle and lateral acceleration were monitored. If the vehicle did not roll over at this speed, the simulation was repeated with a slightly increased speed. This process was repeated until the vehicle rolled over. The maximum lateral acceleration of that simulation was then determined to be the rollover threshold for that particular vehicle case. The results of these simulations to determine rollover threshold are presented in the following sections.

1. Effect of Center of Gravity Height

It is well known that trucks have a lower rollover threshold than automobiles partially due to their higher center of gravity (CG). More specifically, the rollover threshold is directly related to the height difference between the CG and the roll center of the vehicle suspension. As this difference in height increases, the vehicle's rollover threshold decreases.



Reproduced from
best available copy.

Table 7. Phase 4-model input parameters for STAA single with 48-ft (14.6-m) trailer, S21 loading.

TRACTOR PARAMETERS

WHEELBASE - DISTANCE FROM FRONT AXLE TO CENTER OF REAR SUSPENSION (IN) 240.00
 BASE VEHICLE CURB WEIGHT ON FRONT SUSPENSION (LB) 6959.00
 BASE VEHICLE CURB WEIGHT ON REAR SUSPENSION (LB) 6879.00
 SPRING MASS CG HEIGHT (IN. ABOVE GROUND) 40.00
 SPRING MASS ROLL MOMENT OF INERTIA (IN-LB-SEC**2) 30139.00
 SPRING MASS PITCH MOMENT OF INERTIA (IN-LB-SEC**7) 400980.00
 SPRING MASS YAW MOMENT OF INERTIA (IN-LB-SEC**2) 400980.00
 PAYLOAD WEIGHT (LB) 0.00
 *** ZERO ENTRY INDICATES NO PAYLOAD ***
 *** FIVE PAYLOAD DESCRIPTION PARAMETERS ARE NOT ENTERED ***
 FIFTH WHEEL LOCATION (IN. AHEAD OF REAR SUSP. CENTER) 0.00
 FIFTH WHEEL HEIGHT ABOVE GROUND (IN) 48.00
 TRACTOR FRAME STIFFNESS (IN-LB/DEG) 50000.00
 TRACTOR FRAME TORSIONAL AXIS HEIGHT ABOVE GROUND (IN) 36.00

TRACTOR FRONT SUSPENSION AND AXLE PARAMETERS

SUSPENSION SPRING RATE (LB/IN/SIDE/AXLE) 1132.00
 SUSPENSION VISCOUS DAMPING (LB-SEC/IN/SIDE/AXLE) 15.00
 COULOMB FRICTION (LB/SIDE/AXLE) 150.00
 AXLE ROLL MOMENT OF INERTIA (IN-LB-SEC**2) 3719.00
 ROLL CENTER HEIGHT (IN. ABOVE GROUND) 23.00
 ROLL STEER COEFFICIENT (DEG. STEER/DEG. ROLL) 0.00
 AUXILIARY ROLL STIFFNESS (IN-LB/DEG/AXLE) 1500.00
 LATERAL DISTANCE BETWEEN SUSPENSION SPRINGS (IN) 32.00
 TRACK WIDTH (IN) 80.00
 UNSPRUNG WEIGHT (LB) 1200.00

TRACTOR FRONT TIRES AND WHEELS

CORNERING STIFFNESS (LB/DEG/TIRE) 676.00
 LONGITUDINAL STIFFNESS (LB/SLIP/TIRE) 35400.00
 CAMBER STIFFNESS (LB/DEG/TIRE) 0.00
 ALIGNING MOMENT (IN-LB/DEG/TIRE) 1200.00
 TIRE SPRING RATE (LB/IN/TIRE) 4500.00
 TIRE LOADED RADIUS (IN) 19.50
 POLAR MOMENT OF INERTIA (IN-LB-SEC**2/WHEEL) 103.00

LEFT SIDE RIGHT SIDE

1132.00 1132.00
 15.00 15.00
 150.00 150.00
 3719.00
 23.00
 0.00
 1500.00
 32.00
 80.00
 1200.00

LEFT SIDE RIGHT SIDE

676.00 676.00
 35400.00 35400.00
 0.00 0.00
 1200.00 1200.00
 4500.00 4500.00
 19.50 19.50
 103.00 103.00

Table 7. Phase-4 model input parameters for STAA single with 48-ft (14.6-m) trailer, S21 loading (continued).

	LEADING TANDEM AXLE		TRAILING TANDEM AXLE	
	LEFT SIDE	RIGHT SIDE	LEFT SIDE	RIGHT SIDE
TRACTOR REAR SUSPENSION AND AXLE PARAMETERS				
SUSPENSION KEY - 0 INDICATES SINGLE AXLE, 1 INDICATES FOUR SPRING, 2 WALKING BEAM				2
TANDEM AXLE SEPARATION (IN BETWEEN LEADING AND TRAILING AXLES)	51.10			
STATIC LOAD TRANSFER (PERCENT LOAD ON LEAD AXLE)	50.00			
DYNAMIC LOAD TRANSFER (% BRAKE TORQUE REACTED AS TANDEM AXLE LOAD TRANSFER)	0.00			
SUSPENSION SPRING RATE (LB/IN/SIDE/AXLE)	7200.00	7200.00	7200.00	7200.00
SUSPENSION VISCOUS DAMPING (LB-SEC/IN/SIDE/AXLE)	15.00	15.00	15.00	15.00
COULOMB FRICTION (LB/SIDE/AXLE)	500.00	500.00	500.00	500.00
AXLE ROLL MOMENT OF INERTIA (IN-LB-SEC**2)				
ROLL CENTER HEIGHT (IN. ABOVE GROUND)	4458.00			4458.00
ROLL STIFFER COEFFICIENT (DEG. STEER/DEG. ROLL)	29.00			29.00
AUXILIARY ROLL STIFFNESS (IN-LB/DEG/AXLE)	0.00			0.00
LATERAL DISTANCE BETWEEN SUSPENSION SPRINGS (IN)	6000.00			6000.00
TRACK WIDTH (IN)	38.00			38.00
UNSPRUNG WEIGHT (LB)	72.63			72.63
	2300.00			2300.00
TRACTOR REAR TIRES AND WHEELS				
DUAL TIRE SEPARATION (IN)			13.00	13.00
CORNERING STIFFNESS (LB/DEG/TIRE)	676.00		676.00	676.00
LONGITUDINAL STIFFNESS (LB/SLIP/TIRE)	35400.00		35400.00	35400.00
CAMBER STIFFNESS (LB/DEG/TIRE)	0.00		0.00	0.00
ALIGNING MOMENT (IN-LB/DEG/TIRE)	1200.00		1200.00	1200.00
TIRE SPRING RATE (LB/IN/TIRE)	4500.00		4500.00	4500.00
TIRE LOADED RADIUS (IN)	19.50		19.50	19.50
POLAR MOMENT OF INERTIA (IN-LB-SEC**2/WHEEL)	103.00		103.00	103.00

Table 7. Phase-4 model input parameters for STAA single with 48-ft (14.6-m) trailer, S21 loading (continued).

TRAILER NO. 1 PARAMETERS

WHEELBASE - DISTANCE FROM KINGPIN TO CENTER OF REAR SUSPENSION (IN) 486.00
 BASE VEHICLE KINGPIN STATIC LOAD (LB) 5217.00
 BASE VEHICLE CURB WEIGHT ON REAR SUSPENSION (LB) 9562.00
 SPRUNG MASS CG HEIGHT (IN. ABOVE GROUND) 71.00
 SPRUNG MASS ROLL MOMENT OF INERTIA (IN-LB-SEC**2) 90000.00
 SPRUNG MASS PITCH MOMENT OF INERTIA (IN-LB-SFC**2) 1128867.00
 SPRUNG MASS YAW MOMENT OF INERTIA (IN-LB-SEC**2) 1128867.00
 PAYLOAD WEIGHT (LB) 52363.00
 PAYLOAD DISTANCE AHEAD OF REAR SUSPENSION CENTER (IN) 246.02
 PAYLOAD CG HEIGHT (IN. ABOVE GROUND) 90.00
 PAYLOAD ROLL MOMENT OF INERTIA (IN-LB-SEC**2) 151074.00
 PAYLOAD PITCH MOMENT OF INERTIA (IN-LB-SEC**2) 3425490.00
 PAYLOAD YAW MOMENT OF INERTIA (IN-LB-SEC**2) 3465907.00

TRAILER NO. 1 REAR SUSPENSION AND AXLE PARAMETERS

	LEADING TANDEM AXLE		TRAILING TANDEM AXLE	
	LEFT SIDE	RIGHT SIDE	LEFT SIDE	RIGHT SIDE

SUSPENSION KEY - 0 INDICATES SINGLE AXLE, 1 INDICATES FOUR SPRING, 2 WALKING DEAM 2

TANDEM AXLE SEPARATION (IN BETWEEN LEADING AND TRAILING AXLES) 48.00
 STATIC LOAD TRANSFER (PERCENT LOAD ON LEAD AXLE) 50.00
 DYNAMIC LOAD TRANSFER (% BRAKE TORQUE REACTED AS TANDEM AXLE LOAD TRANSFER) 0.00
 SUSPENSION SPRING RATE (LB/IN/SIDE/AXLE) 7500.00 7500.00 7500.00 7500.00
 SUSPENSION VISCOUS DAMPING (LB-SEC/IN/SIDE/AXLE) 15.00 15.00 15.00 15.00
 COULOMB FRICTION (LB/SIDE/AXLE) 1000.00 1000.00 1000.00 1000.00

AXLE ROLL MOMENT OF INERTIA (IN-LB-SFC**2) 4100.00 4100.00
 ROLL CENTER HEIGHT (IN. ABOVE GROUND) 29.00 29.00
 ROLL STEER COEFFICIENT (DEG. STEER/DEG. ROLL) 0.00 0.00
 AUXILIARY ROLL STIFFNESS (IN-LB/DEG/AXLE) 10000.00 10000.00
 LATERAL DISTANCE BETWEEN SUSPENSION SPRINGS (IN) 44.00 44.00
 TRACK WIDTH (IN) 78.00 78.00
 UNSPRUNG WEIGHT (LB) 1500.00 1500.00

TRAILER NO. 1 REAR TIRES AND WHEELS

	LEFT SIDE	RIGHT SIDE

DUAL TIRE SEPARATION (IN) 13.00 13.00
 CORNERING STIFFNESS (LB/DEG/TIRE) 676.00 676.00
 LONGITUDINAL STIFFNESS (LB/SLIP/TIRE) 35400.00 35400.00
 CAMBER STIFFNESS (LB/DEG/TIRE) 0.00 0.00
 ALIGNING MOMENT (IN-LB/DEG/TIRE) 1200.00 1200.00
 TIRE SPRING RATE (LB/IN/TIRE) 5000.00 5000.00
 TIRE LOADED RADIUS (IN) 19.50 19.50
 POLAR MOMENT OF INERTIA (IN-LB-SEC**2/WHEEL) 103.00 103.00

Table 8. Phase-4 model input parameters for STAA single with 53-ft (16.2-m) trailer, S21 loading.

TRACTOR PARAMETERS

WHEELBASE - DISTANCE FROM FRONT AXLE TO CENTER OF REAR SUSPENSION (IN) 240.00
 BASE VEHICLE CURB WEIGHT ON FRONT SUSPENSION (LB) 6959.00
 BASE VEHICLE CURB WEIGHT ON REAR SUSPENSION (LB) 6879.00
 SPRUNG MASS CG HEIGHT (IN. ABOVE GROUND) 40.00
 SPRUNG MASS ROLL MOMENT OF INERTIA (IN-LB-SEC**2) 30129.00
 SPRUNG MASS FITCH MOMENT OF INERTIA (IN-LB-SEC**2) 400500.00
 SPRUNG MASS YAW MOMENT. OF INERTIA (IN-LB-SEC**2) 460980.00
 PAYLOAD WEIGHT (LB) 0.00

*** ZERO ENTRY INDICATES NO PAYLOAD ***

*** FIVE PAYLOAD DESCRIPTION PARAMETERS ARE NOT ENTERED ***

FIFTH WHEEL LOCATION (IN. AHEAD OF REAR SUSP. CENTER) 0.00
 FIFTH WHEEL HEIGHT ABOVE GROUND (IN) 42.00
 TRACTOR FRAME STIFFNESS (IN-LB/DEG) 50000.00
 TRACTOR FRAME TORSIONAL AXIS HEIGHT ABOVE GROUND (IN) 36.00

TRACTOR FRONT SUSPENSION AND AXLE PARAMETERS

SUSPENSION SPRING RATE (LB/IN/SIDE/AXLE) 1132.00
 SUSPENSION VISCOUS DAMPING (LB-SEC/IN/SIDE/AXLE) 15.00
 COULOMB FRICTION (LB/SIDE/AXLE) 150.00

AXLE ROLL MOMENT OF INERTIA (IN-LB-SEC**2) 3719.00
 ROLL CENTER HEIGHT (IN. ABOVE GROUND) 23.00
 ROLL STEER COEFFICIENT (DEG. STEER/DEG. ROLL) 0.00
 AUXILIARY ROLL STIFFNESS (IN-LB/DEG/AXLE) 1500.00
 LATERAL DISTANCE BETWEEN SUSPENSION SPRINGS (IN) 32.00
 TRACK WIDTH (IN) 80.00
 UNSPRUNG WEIGHT (LB) 1200.00

LEFT SIDE 1132.00
 15.00
 150.00

RIGHT SIDE 1132.00
 15.00
 150.00

TRACTOR FRONT TIRES AND WHEELS

CORNERING STIFFNESS (LB/DEG/TIRE) 676.00
 LONGITUDINAL STIFFNESS (LB/SLIP/TIRE) 35400.00
 CAMBER STIFFNESS (LB/DEG/TIRE) 0.00
 ALIGNING MOMENT (IN-LB/DEG/TIRE) 1200.00
 TIRE SPRING RATE (LB/IN/TIRE) 4500.00
 TIRE LOADED RADIUS (IN) 19.50
 POLAR MOMENT OF INERTIA (IN-LB-SEC**2/WHEEL) 103.00

LEFT SIDE 676.00
 35400.00
 0.00
 1200.00
 4500.00
 19.50
 103.00

RIGHT SIDE 676.00
 35400.00
 0.00
 1200.00
 4500.00
 19.50
 103.00

Table 8. Phase-4 model input parameters for STAA single with 53-ft (16.2-m) trailer, S21 loading (continued).

TRACTOR REAR SUSPENSION AND AXLE PARAMETERS		LEADING TANDEM AXLE		TRAILING TANDEM AXLE	
		LEFT SIDE	RIGHT SIDE	LEFT SIDE	RIGHT SIDE
SUSPENSION KEY - 0 INDICATES SINGLE AXLE, 1 INDICATES FOUR SPRING, 2 WALKING BEAM					
TANDEM AXLE SEPARATION (IN BETWEEN LEADING AND TRAILING AXLES)					
			11.10		
STATIC LOAD TRANSFER (PERCENT LOAD ON LEAD AXLE)					
			50.00		
DYNAMIC LOAD TRANSFER (% BRAKE TORQUE REACTED AS TANDEM AXLE LOAD TRANSFER)					
		7200.00	7200.00	7200.00	7200.00
SUSPENSION SPRING RATE (LB/IN/SIDE/AXLE)		15.00	15.00	15.00	15.00
SUSPENSION VISCOUS DAMPING (LB-SEC/IN/SIDE/AXLE)		500.00	500.00	500.00	500.00
COULOMB FRICTION (LB/SIDE/AXLE)					
AXLE ROLL MOMENT OF INERTIA (IN-LB-SEC**2)		4458.00		4458.00	
ROLL CENTER HEIGHT (IN, ABOVE GROUND)		29.00		29.00	
ROLL STEER COEFFICIENT (DEG. STEER/DEG. ROLL)		0.00		0.00	
AUXILIARY ROLL STIFFNESS (IN-LB/DEG/AXLE)		6000.00		6000.00	
LATERAL DISTANCE BETWEEN SUSPENSION SPRINGS (IN)		38.00		38.00	
TRACK WIDTH (IN)		72.63		72.63	
UNSPRUNG WEIGHT (LB)		2300.00		2300.00	
TRACTOR REAR TIRES AND WHEELS					
DUAL TIRE SEPARATION (IN)		13.00		13.00	
CORNERING STIFFNESS (LB/DEG/TIRE)		676.00		676.00	
LONGITUDINAL STIFFNESS (LB/SLIP/TIRE)		35400.00		35400.00	
CAMBER STIFFNESS (LB/DEG/TIRE)		0.00		0.00	
ALIGNING MOMENT (IN-LB/DEG/TIRE)		1200.00		1200.00	
TIRE SPRING RATE (LB/IN/TIRE)		4500.00		4500.00	
TIRE LOADED RADIUS (IN)		19.50		19.50	
POLAR MOMENT OF INERTIA (IN-LB-SEC**2/WHEEL)		103.00		103.00	

Table 8. Phase-4 model input parameters for STAA single with 53-ft (16.2-m) trailer, S21 loading (continued).

TRAILER NO. 1 PARAMETERS

WHEELBASE - DISTANCE FROM KINGPIN TO CENTER OF REAR SUSPENSION (IN) 540.00
 BASE VEHICLE KINGPIN STATIC LOAD (LB) 5785.00
 BASE VEHICLE CURB WEIGHT ON REAR SUSPENSION (LB) 9454.00
 SPRUNG MASS CG HEIGHT (IN, ABOVE GROUND) 71.00
 SPRUNG MASS ROLL MOMENT OF INERTIA (IN-LB-SEC**2) 89347.00
 SPRUNG MASS PITCH MOMENT OF INERTIA (IN-LB-SEC**2) 1809428.00
 SPRUNG MASS YAW MOMENT OF INERTIA (IN-LB-SEC**2) 1809428.00
 PAYLOAD WEIGHT (LB) 50926.00
 PAYLOAD DISTANCE AHEAD OF REAR SUSPENSION CENTER (IN) 264.00
 PAYLOAD CG HEIGHT (IN, ABOVE GROUND) 40.00
 PAYLOAD ROLL MOMENT OF INERTIA (IN-LB-SEC**2) 180130.00
 PAYLOAD PITCH MOMENT OF INERTIA (IN-LB-SEC**2) 4429580.00
 PAYLOAD YAW MOMENT OF INERTIA (IN-LB-SEC**2) 4429120.00

TRAILER NO. 1 REAR SUSPENSION AND AXLE PARAMETERS

	LEADING TANDEM AXLE		TRAILING TANDEM AXLE	
	LEFT SIDE	RIGHT SIDE	LEFT SIDE	RIGHT SIDE
SUSPENSION KEY - 0 INDICATES SINGLE AXLE, 1 INDICATES FOUR SPRING, 2 WALKING BEAM				2
TANDEM AXLE SEPARATION (IN BETWEEN LEADING AND TRAILING AXLES)	42.00			
STATIC LOAD TRANSFER (PERCENT LOAD ON LEAD AXLE)	50.00			
DYNAMIC LOAD TRANSFER (% BRAKE TORQUE REACTED AS TANDEM AXLE LOAD TRANSFER)	0.00			
SUSPENSION SPRING RATE (LB/IN/SIDE/AXLE)	7500.00	7500.00	7500.00	7500.00
SUSPENSION VISCOUS DAMPING (LB-SEC/IN/SIDE/AXLE)	15.00	15.00	15.00	15.00
COULOMB FRICTION (LB/SIDE/AXLE)	1000.00	1000.00	1000.00	1000.00

SUSPENSION KEY - 0 INDICATES SINGLE AXLE, 1 INDICATES FOUR SPRING, 2 WALKING BEAM

TANDEM AXLE SEPARATION (IN BETWEEN LEADING AND TRAILING AXLES) 42.00
 STATIC LOAD TRANSFER (PERCENT LOAD ON LEAD AXLE) 50.00
 DYNAMIC LOAD TRANSFER (% BRAKE TORQUE REACTED AS TANDEM AXLE LOAD TRANSFER) 0.00
 SUSPENSION SPRING RATE (LB/IN/SIDE/AXLE) 7500.00 7500.00 7500.00 7500.00
 SUSPENSION VISCOUS DAMPING (LB-SEC/IN/SIDE/AXLE) 15.00 15.00 15.00 15.00
 COULOMB FRICTION (LB/SIDE/AXLE) 1000.00 1000.00 1000.00 1000.00

TRAILER NO. 1 REAR TIRES AND WHEELS

	LEFT SIDE	RIGHT SIDE
AXLE ROLL MOMENT OF INERTIA (IN-LP-SEC**2)	4100.00	4100.00
ROLL CENTER HEIGHT (IN, ABOVE GROUND)	29.00	29.00
ROLL STEER COEFFICIENT (DEG. STEER/DEG. ROLL)	0.00	0.00
AUXILIARY ROLL STIFFNESS (IN-LB/DEG/AXLE)	10000.00	10000.00
LATERAL DISTANCE BETWEEN SUSPENSION SPRINGS (IN)	44.00	44.00
TRACK WIDTH (IN)	78.00	78.00
UNSPRUNG WEIGHT (LB)	1500.00	1500.00

DUAL TIRE SEPARATION (IN) 13.00
 CORNERING STIFFNESS (LB/DEG/TIRE) 676.00
 LONGITUDINAL STIFFNESS (LB/SLIP/TIRE) 35400.00
 CAMBER STIFFNESS (LB/DEG/TIRE) 0.00
 ALIGNING MOMENT (IN-LB/DEG/TIRE) 1200.00
 TIRE SPRING RATE (LB/IN/TIRE) 5000.00
 TIRE LOADED RADIUS (IN) 19.50
 POLAR MOMENT OF INERTIA (IN-LB-SEC**2/WHEEL) 103.00

Table 9. Phase-4 model input parameters for STAA double with COE tractor, D21 loading.

TRACTOR PARAMETERS

WHEELBASE - DISTANCE FROM FRONT AXLE TO CENTER OF REAR SUSPENSION (IN) 126.00
 BASE VEHICLE CURB WEIGHT ON FRONT SUSPENSION (LB) 6860.00
 BASE VEHICLE CURB WEIGHT ON REAR SUSPENSION (LB) 4132.00
 SPRUNG MASS CG HEIGHT (IN, ABOVE GROUND) 48.00
 SPRUNG MASS ROLL MOMENT OF INERTIA (IN-LB-SEC**2) 33942.00
 SPRUNG MASS FITCH MOMENT OF INERTIA (IN-LB-SEC**2) 89723.00
 SPRUNG MASS YAW MOMENT OF INERTIA (IN-LB-SEC**2) 20925.00
 PAYLOAD WEIGHT (LB) 0.00

*** ZERO ENTRY INDICATES NO PAYLOAD ***

*** FIVE PAYLOAD DESCRIPTION PARAMETERS ARE NOT ENTERED ***

FIFTH WHEEL LOCATION (IN, AHEAD OF REAR SUSP. CENTER)

FIFTH WHEEL HEIGHT ABOVE GROUND (IN)

TRACTOR FRAME STIFFNESS (IN-LB/DEG)

TRACTOR FRAME TORSIONAL AXIS HEIGHT ABOVE GROUND (IN)

TRACTOR FRONT SUSPENSION AND AXLE PARAMETERS

SUSPENSION SPRING RATE (LB/IN/SIDE/AXLE) 1132.00
 SUSPENSION VISCOUS DAMPING (LB-SEC/IN/SIDE/AXLE) 15.00
 COULOMBE FRICTION (LB/SIDE/AXLE) 150.00

AXLE ROLL MOMENT OF INERTIA (IN-LB-SEC**2) 3719.00
 ROLL CENTER HEIGHT (IN, ABOVE GROUND) 23.00
 ROLL STEER COEFFICIENT (DEG. STEER/DEG. ROLL) 0.00
 AUXILIARY ROLL STIFFNESS (IN-LB/DEG/AXLE) 1500.00
 LATERAL DISTANCE BETWEEN SUSPENSION SPRINGS (IN) 32.00
 TRACK WIDTH (IN) 80.00
 UNSPRUNG WEIGHT (LB) 1200.00

TRACTOR FRONT TIRES AND WHEELS

CORNERING STIFFNESS (LB/DEG/TIRE) 676.00
 LONGITUDINAL STIFFNESS (LB/SLIP/TIRE) 35400.00
 CAMBER STIFFNESS (LB/DEG/TIRE) 0.00
 ALIGNING MOMENT (IN-LB/DEG/TIRE) 1200.00
 TIRE SPRING RATE (LB/IN/TIRE) 4500.00
 TIRE LOADED RADIUS (IN) 19.50
 POLAR MOMENT OF INERTIA (IN-LB-SEC**2/WHEEL) 103.00

LEFT SIDE ----- RIGHT SIDE -----

1132.00 1132.00
 15.00 15.00
 150.00 150.00

3719.00
 23.00
 0.00
 1500.00
 32.00
 80.00
 1200.00

LEFT SIDE ----- RIGHT SIDE -----

676.00 676.00
 35400.00 35400.00
 0.00 0.00
 1200.00 1200.00
 4500.00 4500.00
 19.50 19.50
 103.00 103.00

Table 9. Phase-4 model input parameters for STAA double with COE tractor, D21 loading (continued).

TRACTOR REAR SUSPENSION AND AXLE PARAMETERS	LEFT SIDE	RIGHT SIDE
SUSPENSION KEY - 0 INDICATES SINGLE AXLE, 1 INDICATES FOUR SPRING, 2 WALKING BEAM	0	
SUSPENSION SPRING RATE (LB/IN/SIDE/AXLE)	5500.00	5500.00
SUSPENSION VISCOUS DAMPING (LE-SEC/IN/SIDE/AXLE)	15.00	15.00
COULOMB FRICTION (LE/SIDE/AXLE)	500.00	500.00
AXLE ROLL MOMENT OF INERTIA (IN-LB-SEC**2)	4458.00	
ROLL CENTER HEIGHT (IN, ABOVE GROUND)	38.00	
ROLL STEER COEFFICIENT (DEG. STEER/DEG. ROLL)	0.00	
AUXILIARY ROLL STIFFNESS (IN-LB/DEG/AXLE)	6000.00	
LATERAL DISTANCE BETWEEN SUSPENSION SPRINGS (IN)	38.00	
TRACK WIDTH (IN)	72.00	
UNSPRUNG WEIGHT (LB)	2300.00	
TRACTOR REAR TIRES AND WHEELS		
DUAL TIRE SEPARATION (IN)	13.00	13.00
CORNERING STIFFNESS (LE/DEG/TIRE)	676.00	676.00
LONGITUDINAL STIFFNESS (LB/SLIP/TIRE)	35400.00	35400.00
CAMBER STIFFNESS (LE/DEG/TIRE)	0.00	0.00
ALIGNING MOMENT (IN-LB/DEG/TIRE)	1200.00	1200.00
TIRE SPRING RATE (LB/IN/TIRE)	4500.00	4500.00
TIRE LOADED RADIUS (IN)	19.00	19.00
POLAR MOMENT OF INERTIA (IN-LB-SEC**2/WHEEL)	103.00	103.00

Table 9. Phase-4 model input parameters for STAA double with COE tractor, D21 loading (continued).

TRAILER NO. 1 PARAMETERS

WHEELEASE - DISTANCE FROM KINGPIN TO CENTER OF REAR SUSPENSION (IN)	270.00		
BASE VEHICLE KINGPIN STATIC LOAD (LB)	2665.00		
BASE VEHICLE CURB WEIGHT ON REAR SUSPENSION (LB)	4088.00		
SPRUNG MASS CG HEIGHT (IN. ABOVE GROUND)	66.00		
SPRUNG MASS ROLL MOMENT OF INERTIA (IN-LB-SEC**2)	32324.00		
SPRUNG MASS FITCH MOMENT OF INERTIA (IN-LB-SEC**2)	475519.00		
SPRUNG MASS YAW MOMENT OF INERTIA (IN-LB-SEC**2)	475519.00		
PAYLOAD WEIGHT (LB)	27255.00		
PAYLOAD DISTANCE AHEAD OF REAR SUSPENSION CENTER (IN)	136.96		
PAYLOAD CG HEIGHT (IN. ABOVE GROUND)	90.00		
PAYLOAD ROLL MOMENT OF INERTIA (IN-LB-SEC**2)	78635.00		
PAYLOAD FITCH MOMENT OF INERTIA (IN-LB-SEC**2)	579752.00		
PAYLOAD YAW MOMENT OF INERTIA (IN-LB-SEC**2)	609700.00		
LOCATION OF FINILE HOOK (IN BEHIND REAR SUSP. CENTER)	28.00		
HEIGHT OF FINILE HOOK (IN ABOVE GROUND)	44.00		

TRAILER NO. 1 REAR SUSPENSION AND AXLE PARAMETERS

SUSPENSION KEY - 0 INDICATES SINGLE AXLE, 1 INDICATES FOUR SPRING, 2 WALKING BEAH	0		
SUSPENSION SPRING RATE (LB/IN/SIDE/AXLE)	6750.00	LEFT SIDE	6750.00
SUSPENSION VISCOUS DAMPING (LB-SEC/IN/SIDE/AXLE)	15.00		15.00
COULOMBS FRICTION (LE/SIDE/AXLE)	1000.00		1000.00
AXLE ROLL MOMENT OF INERTIA (IN-LB-SEC**2)	4100.00		
ROLL CENTER HEIGHT (IN. ABOVE GROUND)	29.00		
ROLL STEER COEFFICIENT (DEG. STEER/DEG. ROLL)	0.00		
AUXILIARY ROLL STIFFNESS (IN-LB/DEG/AXLE)	10000.00		
LATERAL DISTANCE BETWEEN SUSPENSION SPRINGS (IN)	44.00		
TRACK WIDTH (IN)	78.00		
UNSPRUNG WEIGHT (LB)	1500.00		

TRAILER NO. 1 REAR TIRES AND WHEELS

DUAL TIRE SEPARATION (IN)	13.00	LEFT SIDE	13.00	RIGHT SIDE
CORNERING STIFFNESS (LB/DEG/TIRE)	676.00		676.00	
LONGITUDINAL STIFFNESS (LB/SLIP/TIRE)	35400.00		35400.00	
CAMBER STIFFNESS (LB/DEG/TIRE)	0.00		0.00	
ALIGNING MOMENT (IN-LB/DEG/TIRE)	1200.00		1200.00	
TIRE SPRING RATE (LP/IN/TIRE)	4500.00		4500.00	
TIRE LOADED RADIUS (IN)	19.50		19.50	
POLAR MOMENT OF INERTIA (IN-LB-SEC**2/WHEEL)	103.00		103.00	

Table 9. Phase-4 model input parameters for STAA double with COE tractor, D21 loading (continued).

TRAILER NO. 2 PARAMETERS

DOLLY KEY: 1 = CONVERTER DOLLY, 2 = FIXED DOLLY	1
DISTANCE FROM DOLLY SUSPENSION TO PINTLE HOOK (IN)	72.00
TURNABLE LOCATION (IN AHEAD OF SUSP. CENTER)	0.00
TURNTABLE HEIGHT ABOVE GROUND (IN)	44.00
WHEELBASE - DISTANCE FROM CENTER OF FRONT SUSP. TO CENTER OF REAR SUSP. (IN)	270.00
BASE VEHICLE CURVE WEIGHT ON FRONT SUSPENSION (LB)	2660.00
BASE VEHICLE CURVE WEIGHT ON REAR SUSPENSION (LB)	4088.00
SPRUNG MASS CG HEIGHT (IN. ABOVE GROUND)	60.00
SPRUNG MASS ROLL MOMENT OF INERTIA (IN-LB-SEC**2)	52524.00
SPRUNG MASS PITCH MOMENT OF INERTIA (IN-LB-SEC**2)	475319.00
SPRUNG MASS YAW MOMENT OF INERTIA (IN-LB-SEC**2)	475319.00
PAYLOAD WEIGHT (LB)	28247.00
PAYLOAD DISTANCE AHEAD OF REAR SUSPENSION CENTER (IN)	143.69
PAYLOAD CG HEIGHT (IN. ABOVE GROUND)	90.00
PAYLOAD ROLL MOMENT OF INERTIA (IN-LB-SEC**2)	81497.00
PAYLOAD PITCH MOMENT OF INERTIA (IN-LB-SEC**2)	600895.00
PAYLOAD YAW MOMENT OF INERTIA (IN-LB-SEC**2)	622564.00

TRAILER NO. 2 FRONT SUSPENSION AND AXLE PARAMETERS

SUSPENSION KEY - 0 INDICATES SINGLE AXLE, 1 INDICATES FOUR SPRING, 2 WALKING BEAM	0		
SUSPENSION SPRING RATE (LE/IN/SIDE/AXLE)	6750.00		6750.00
SUSPENSION VISCOUS DAMPING (LB-SEC/IN/SIDE/AXLE)	15.00		15.00
COULOMB FRICTION (LE/SIDE/AXLE)	1000.00		1000.00
AXLE ROLL MOMENT OF INERTIA (IN-LB-SEC**2)		4100.00	
ROLL CENTER HEIGHT (IN. ABOVE GROUND)		29.00	
ROLL STEER COEFFICIENT (DEG. STEER/DEG. ROLL)		0.00	
AUXILIARY ROLL STIFFNESS (IN-LB/DEG/AXLE)		10000.00	
LATERAL DISTANCE BETWEEN SUSPENSION SPRINGS (IN)		44.00	
TRACK WIDTH (IN)		78.00	
UNSPRUNG WEIGHT (LB)		1500.00	

TRAILER NO. 2 FRONT TIRES AND WHEELS

DUAL TIRE SEPARATION (IN)	13.00		13.00
CORNERING STIFFNESS (LE/DEG/TIRE)	676.00		676.00
LONGITUDINAL STIFFNESS (LB/SLIP/TIRE)	35400.00		35400.00
CAMBER STIFFNESS (LE/DEG/TIRE)	0.00		0.00
ALIGNING MOMENT (IN-LB/DEG/TIRE)	1200.00		1200.00
TIRE SPRING RATE (LE/IN/TIRE)	4500.00		4500.00
TIRE LOADED RADIUS (IN)	19.50		19.50
POLAR MOMENT OF INERTIA (IN-LB-SEC**2/WHEEL)	103.00		103.00

Table 9. Phase-4 model1 input parameters for STAA double with COE tractor, D21 loading (continued).

TRAILER NO. 2 REAR SUSPENSION AND AXLE PARAMETERS	LEFT SIDE	RIGHT SIDE
SUSPENSION KEY - 0 INDICATES SINGLE AXLE. 1 INDICATES FOUR SPRING. 2 WALKING BEAM	0	
SUSPENSION SPRING RATE (LB/IN/SIDE/AXLE)	6750.00	6750.00
SUSPENSION VISCOUS DAMPING (LB-SEC/IN/SIDE/AXLE)	15.00	15.00
COULOMB FRICTION (LB/SIDE/AXLE)	1000.00	1000.00
AXLE ROLL MOMENT OF INERTIA (IN-LB-SEC**2)	4100.00	
ROLL CENTER HEIGHT (IN. ABOVE GROUND)	29.00	
ROLL STEER COEFFICIENT (DEG. STEER/DEG. ROLL)	0.00	
AUXILIARY ROLL STIFFNESS (IN-LB/DEG/AXLE)	10000.00	
LATERAL DISTANCE BETWEEN SUSPENSION SPRINGS (IN)	44.00	
TRACK WIDTH (IN)	78.00	
UNSPRUNG HEIGHT (LB)	1500.00	
TRAILER NO. 2 REAR TIRES AND WHEELS	LEFT SIDE	RIGHT SIDE
DUAL TIRE SEPARATION (IN)	13.00	13.00
CORNERING STIFFNESS (LB/DEG/TIRE)	676.00	676.00
LONGITUDINAL STIFFNESS (LB/SLIP/TIRE)	35400.00	35400.00
CAMBER STIFFNESS (LB/DEG/TIRE)	0.00	0.00
ALIGNING MOMENT (IN-LB/DEG/TIRE)	1200.00	1200.00
TIRE SPRING RATE (LB/IN/TIRE)	4500.00	4500.00
TIRE LOADED RADIUS (IN)	19.50	19.50
FOLAR MOMENT OF INERTIA (IN-LB-SEC**2/WHEEL)	103.00	103.00

A recent study has presented examples of typical loadings found in the trucking industry.²⁴ Center of gravity heights range from 70 to 110 in (178 to 279 cm). A very common CG height is found in the "LTL" (less-than-truckload) freight load. This loading case creates a payload that has a 95-in (241-cm) CG height and a gross vehicle weight of 73,000 lb (33,200 kg). Although large CG heights are undesirable from a rollover aspect, they are still very common.

Rollover thresholds were determined for 48-ft (14.6-m) single-semitrailer and the double-trailer truck configurations with various payload CG heights. These results are presented in figures 7 through 10. The values presented in figures 7 and 9 are for a vehicle traveling on the curve with superelevation of 0.06; in figures 8 and 10, the values are for the same vehicle traveling on a flat road.

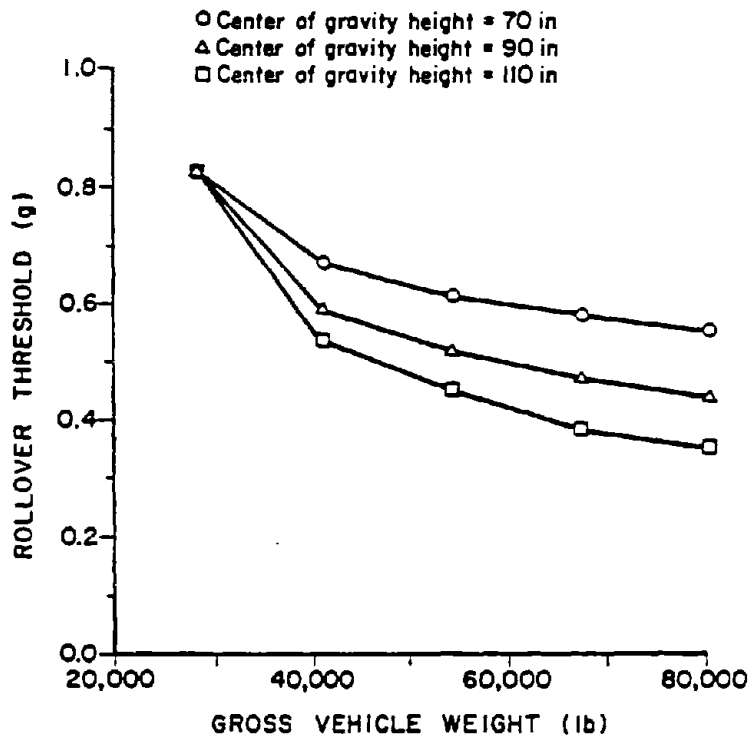
An increase in CG height decreases the rollover threshold. However, as the payload weight decreases, the effect of CG height becomes less pronounced because lighter payload will contribute less of a moment for a given lateral shift. Therefore, an increased CG height will have less of an effect on the rollover threshold for lighter payloads. Also, as the payload weight decreases, the vehicle's composite CG height nears that of an unloaded vehicle. For fully loaded trucks, both singles and doubles, the rollover threshold decreases by 0.005 g for each 1 in (2.5 cm) of increase in CG height. Figures 7 through 10 also show that rollover thresholds for fully loaded single-trailer trucks are lower than for fully loaded doubles by approximately 0.06 g.

Superelevation increases the rollover threshold values for each case by a lateral acceleration in units of the acceleration of gravity that is numerically equal to the superelevation. Thus, the superelevation of 0.06 increased the rollover threshold for each case by approximately 0.06 g for each vehicle.

2. Effect of Gross Vehicle Weight

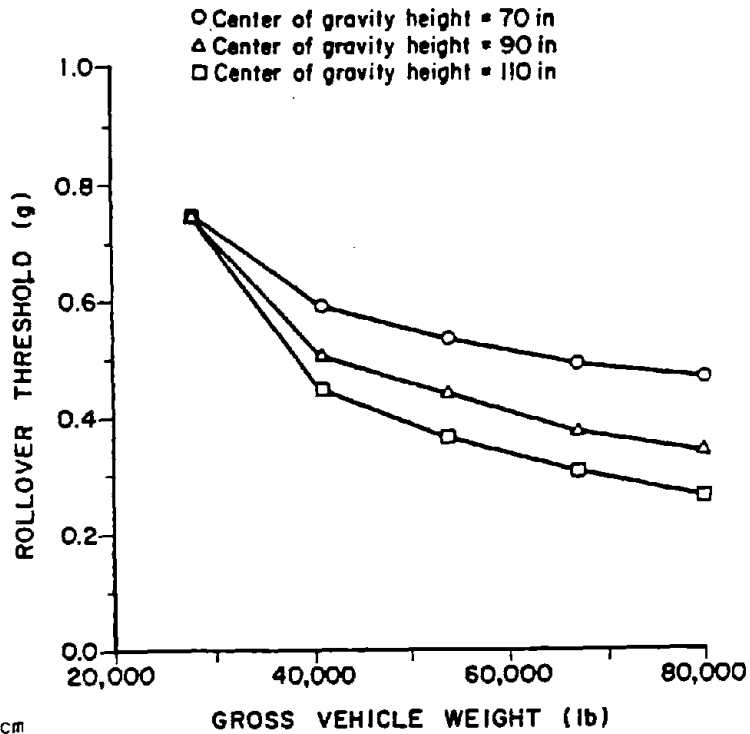
The moment created as the CG shifts laterally is equal to the product of the lateral displacement and the CG's weight. Therefore, the vehicle's gross weight plays an important part in determining its rollover threshold.

The effects of gross vehicle weight for the 48-ft (14.6 m) single-semitrailer and the double-trailer truck configurations are presented in figures 7 through 10. The gross vehicle weight ranges from that of an empty vehicle to a maximum of 80,000 lb (36,400 kg). At a gross weight of 80,000 lb (36,000 kg), the axles were loaded as a typical vehicle on the road might be loaded. For the single-trailer configuration, the axle loads were 34,000 lb (15,500 kg) per tandem axle. For the double-trailer configuration, the axle loads were 17,500 lb (8,000 kg) per axle. The loads on the steering axles were 12,000 and 10,000 lb (5,400 and 4,500 kg) in the singles and doubles configurations, respectively. It was assumed that as the gross vehicle weight decreases, the payload CG location remains the same (i.e., the cargo density decreases).



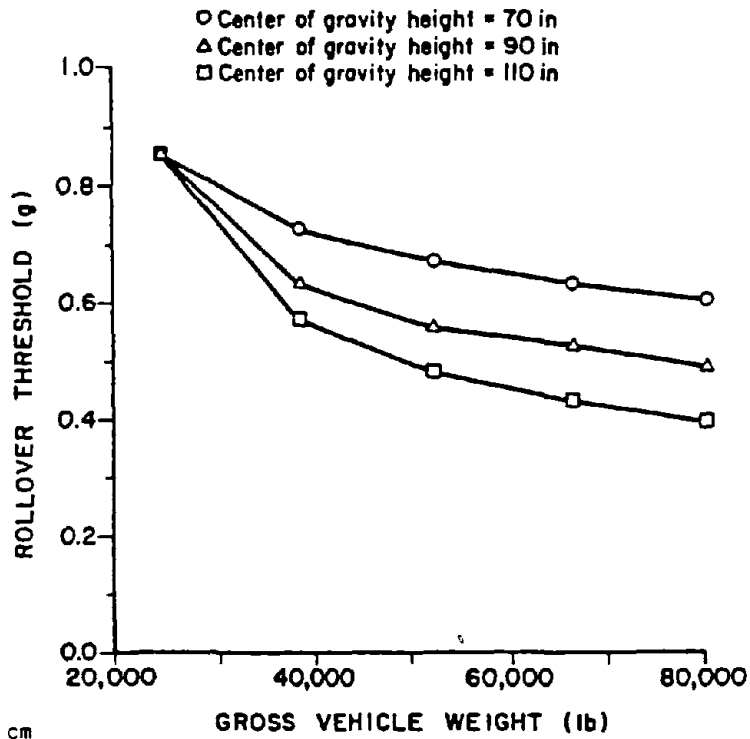
Note: 1 in = 2.54 cm
 1 lb = 0.454 kg

Figure 7. Effect of gross vehicle weight on rollover threshold, single-semitrailer truck, superelevated curve.



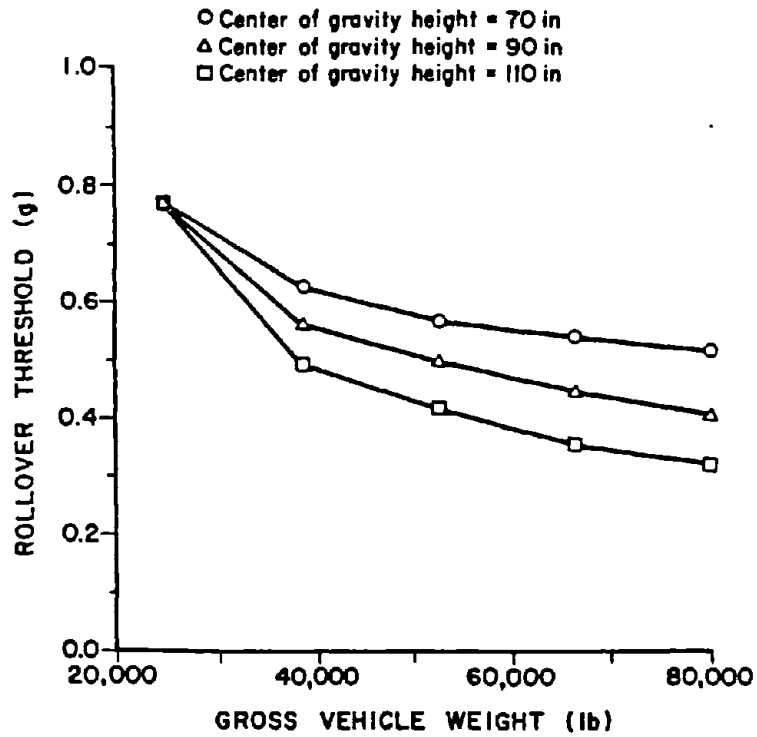
Note: 1 in = 2.54 cm
 1 lb = 0.454 kg

Figure 8. Effect of gross vehicle weight on rollover threshold, single-semitrailer truck, flat road.



Note: 1 in = 2.54 cm
1 lb = 0.454 kg

Figure 9. Effect of gross vehicle weight on rollover threshold, double-trailer truck, superelevated curve.



Note: 1 in = 2.54 cm
1 lb = 0.454 kg

Figure 10. Effect of gross vehicle weight on rollover threshold, double-trailer truck, flat road.

Although this is not a completely realistic assumption, it is not inconceivable and it illustrates more clearly the effect of gross vehicle weight.

The results indicate that truck rollover thresholds generally decrease as gross weight increases.

3. Effect of Suspension Stiffness

For a given lateral acceleration, the extent of the vehicle roll depends on various vehicle and payload parameters. One of these vehicle parameters is the suspension's vertical stiffness. As the vehicle rolls, the suspension creates a moment about the roll center. This moment acts to resist the roll motion. Therefore, with a given lateral acceleration, a stiff suspension allows a smaller roll angle than a softer suspension. On the vehicles evaluated in this study, the auxiliary stiffness can produce at least 140 and 170 percent more rollover resistance than that produced by the suspension's vertical stiffness of the typical singles and doubles configurations.

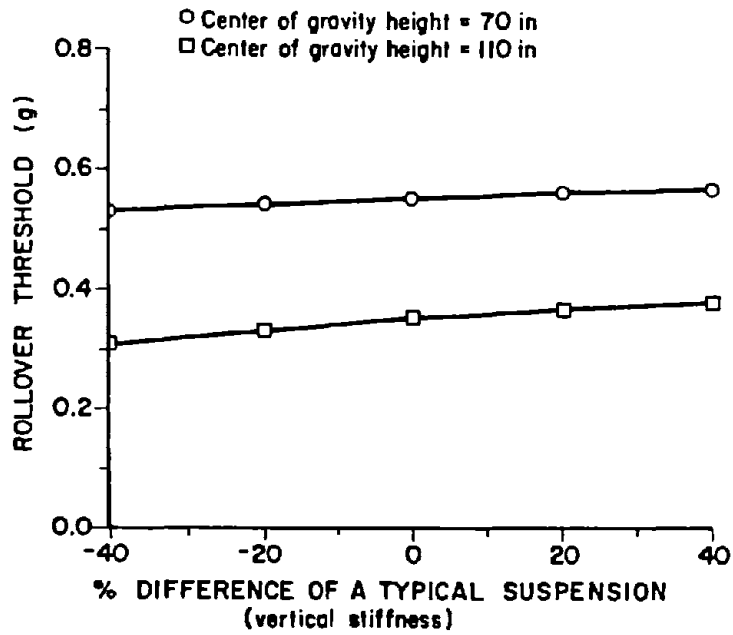
To study the effects of a suspension's vertical stiffness on the rollover threshold, the payload was held constant while the suspension stiffness was varied. For the singles and doubles configurations, the typical suspension's vertical stiffness was increased and decreased by up to 40 percent. The steering suspensions remained the same because the range of variation of vertical stiffness on steering axles is known to be very small.¹⁰

The suspension effects were evaluated for two cases with fully loaded (80,000 lb or 36,400 kg) singles and doubles: the first case with a 70-in (178-cm) CG height and the second case with a 110-in (279-cm) CG height. Figures 11, 12, and 13 illustrate the effects of vertical suspension stiffness on the rollover threshold for these cases. The only difference between the superelevated curve and the flat road is a 0.06-g increase of the rollover threshold.

The rollover threshold only changed slightly as the suspension stiffness was varied because much of a truck's roll resistance comes from its auxiliary roll stiffness. Auxiliary roll stiffness is created by various suspension mechanisms such as antisway bars and resistance to twisting of the suspension's leaf springs.

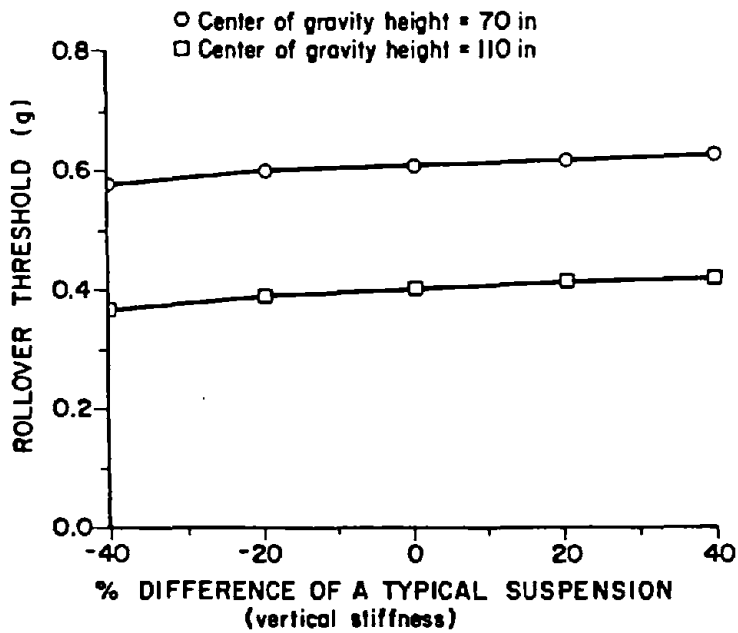
The greatest difference in rollover threshold for the range of vertical stiffness investigated was found when the CG height was 110 in (279 cm): 0.07 g (19 percent) and 0.05 g (13 percent) for the singles and doubles configurations, respectively.

A stiffening of suspensions is desirable to increase rollover thresholds. However, drivers dislike stiffer suspensions because of their poor ride quality, particularly when the vehicle is unloaded. This problem is even worse for a tractor that is not pulling a trailer.



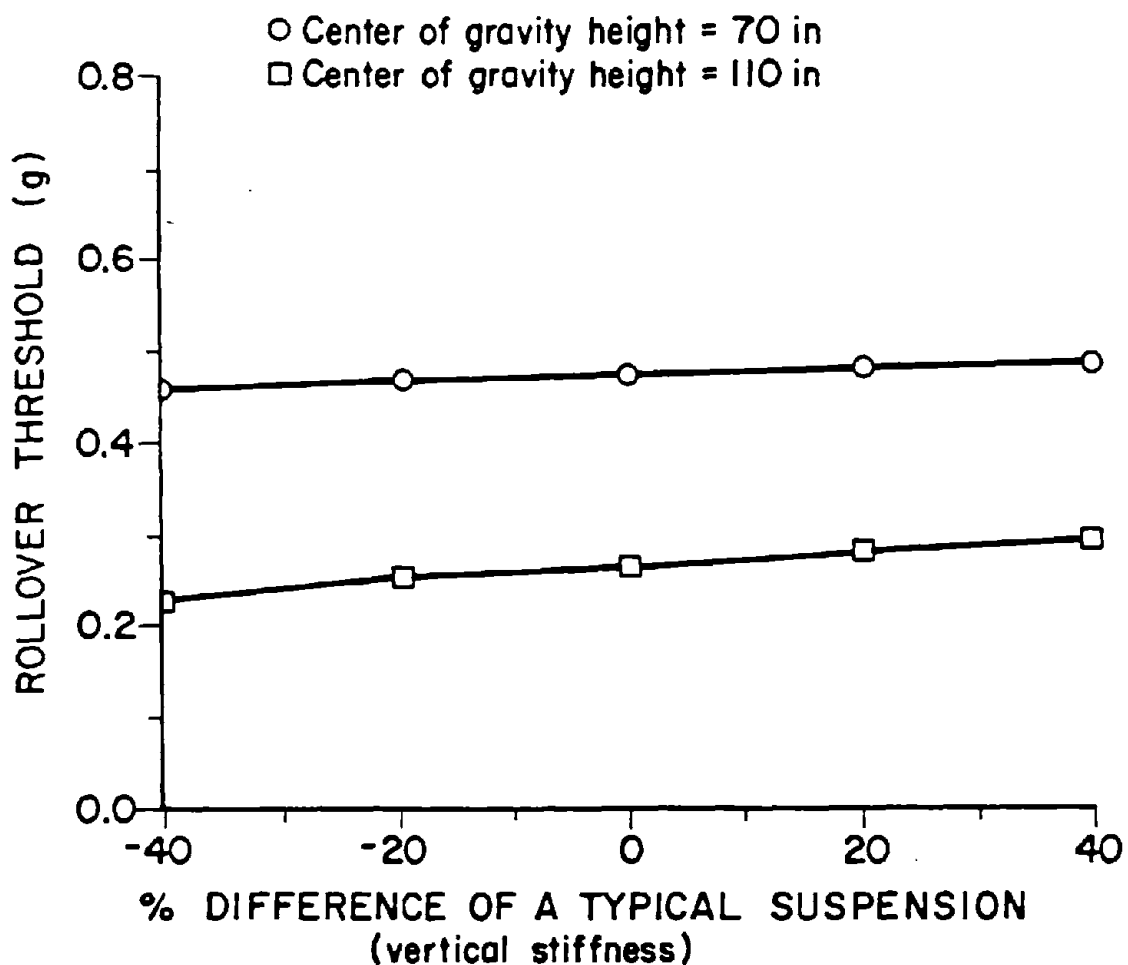
Note: 1 in = 2.54 cm

Figure 11. Effect of suspension stiffness on rollover threshold, single-semitrailer truck, superelevated curve.



Note: 1 in = 2.54 cm

Figure 12. Effect of suspension stiffness on rollover threshold, double-trailer truck, flat road.



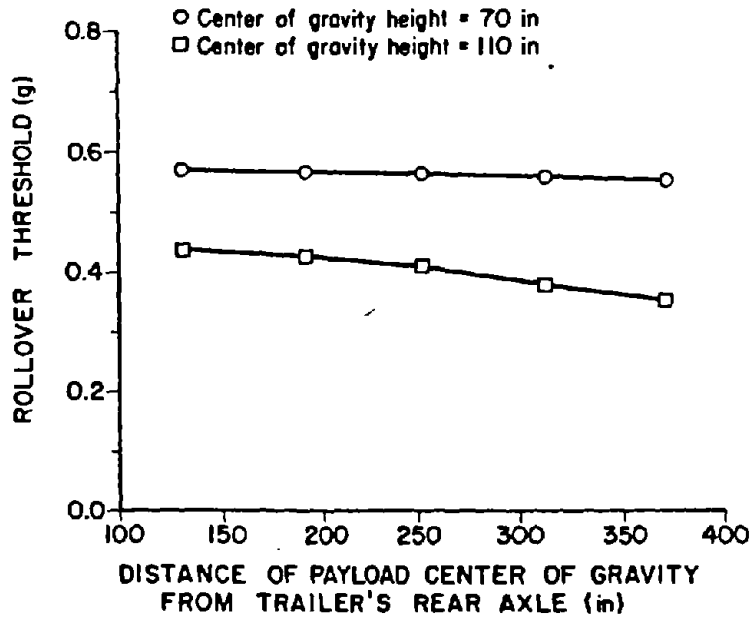
Note: 1 in = 2.54 cm

Figure 13. Effect of suspension stiffness on rollover threshold, single-semitrailer truck, flat road

4. Effect of Longitudinal Weight Distribution

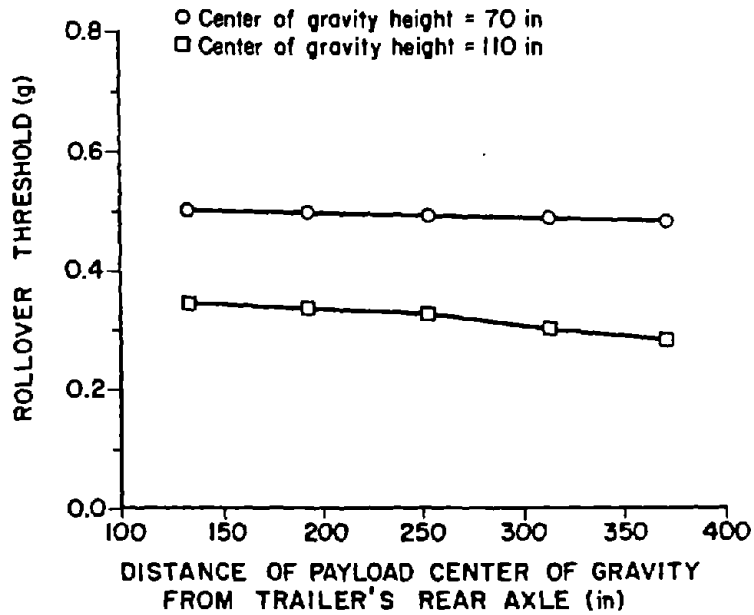
Longitudinal weight distribution affects a truck rollover threshold in two ways. First, by moving the payload's CG forward on the trailer, the tractor's rear axles take up more of the load. This is undesirable since the tractor's rear suspension is softer than the trailer's rear suspension. As previously shown, a softer suspension will decrease the rollover threshold. Second, tractors are not as wide as trailers, which means that an increase in the load on the tractor's rear axle suspension for the same rolling moment and, therefore, decrease the rollover threshold.

Figures 14 and 15 illustrate the effects of longitudinal weight distribution on the rollover threshold of a single-trailer truck.



Note: 1 in = 2.54 cm

Figure 14. Effect of longitudinal weight distribution on rollover threshold, single-semitrailer truck, superelevated curve.



Note: 1 in = 2.54 cm

Figure 15. Effect of longitudinal weight distribution on rollover threshold, single-semitrailer truck, flat road.

To realistically evaluate longitudinal payload placement, a representative payload weight had to be chosen. The payload had to be such that when it was in its rearmost position, the load on the trailer's rear suspension was at its limit of 34,000 lb (15,500 kg). Also, when the payload was moved to its frontmost position, the load on the tractor's rear axles was at its limit of 34,000 lb (15,500 kg). These conditions resulted in a payload of 34,909 lb (15,868 kg) and a gross vehicle weight of 62,546 lb (28,430 kg).

As the payload is moved longitudinally, rollover threshold changes slightly because in the computer model, the tractor's rear axle suspension is only 4 percent less stiff than the trailer's rear axle. However, with many vehicles used by the trucking industry, the difference in suspension stiffness may be much greater.

Moving the payload forward decreased the rollover threshold. The largest decrease in rollover threshold due to longitudinal placement occurred on for single-trailer trucks with a CG height of 110 in (279 cm). This reduction was 0.08 g (19 percent) for a 20-ft (6.1-m) longitudinal movement. It should be noted, however, that another potential problem -- yaw instability -- may arise when the payload is moved toward the rear of the vehicle. Yaw stability is improved by increasing the load on the front axles.²⁵ Yaw instability can lead to problems such as "jackknifing" or "trailer swing."

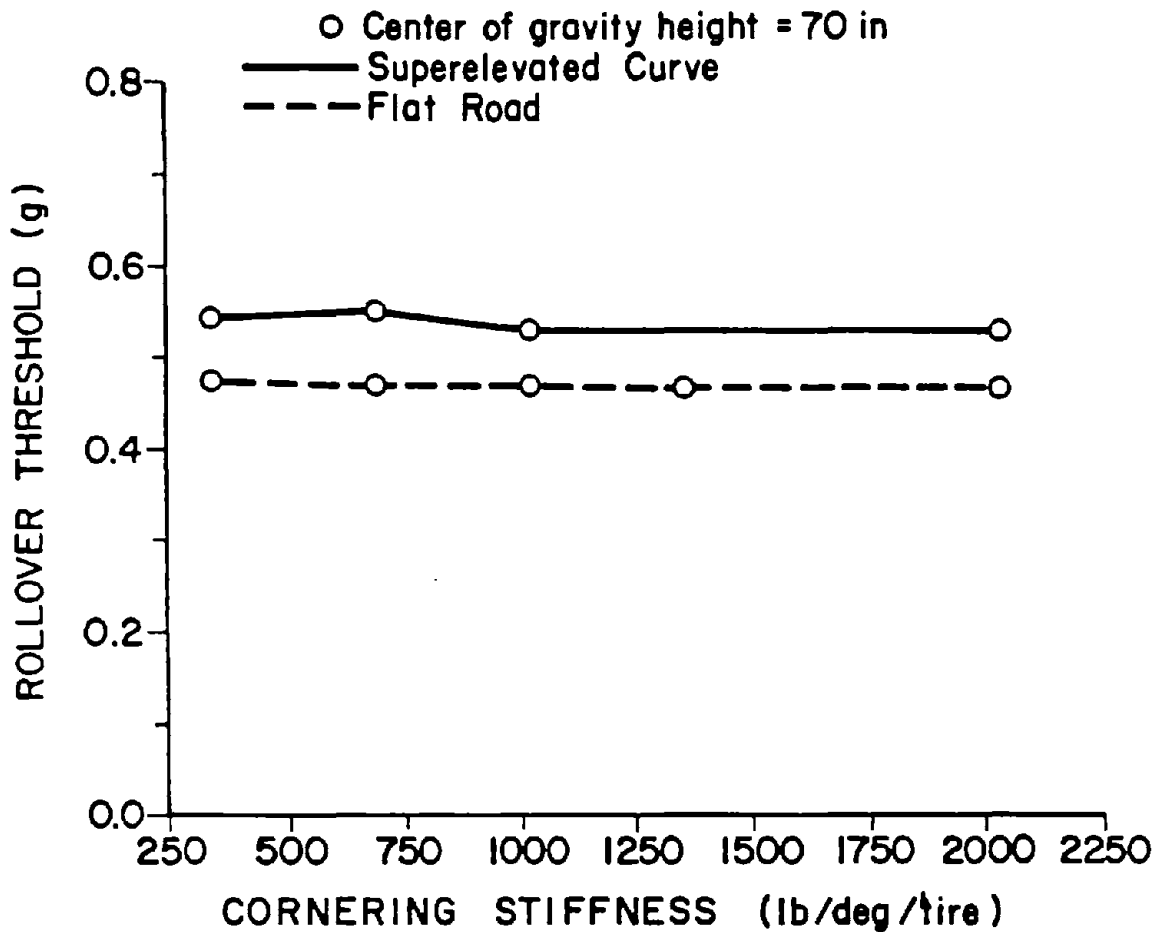
5. Effect of Tire Cornering Stiffness

Cornering stiffness is defined as the initial slope of the curve of tire lateral force versus slip angle. Slip angle is the angle between the tire's direction of travel and the direction in which the tire is pointed.

The effect of cornering stiffness for both a flat curve and a curve with a superelevation of 0.06 is shown in figure 16. The cornering stiffness values used were those of a new, typical, and worn tire.¹⁰ A value three times greater than that of a typical tire was also used. The vehicle was a fully loaded single-trailer truck with a CG height of 70 in (178 cm). Because little or no lateral tire sliding occurs in the simulated cases, the cornering stiffness has almost no effect on the rollover threshold.

6. Effect of Driver Path Follower Model on Lateral Acceleration and Roll Angle

The Phase-4 model uses a simulated driver model that controls the steering angle to follow a user-defined path given to the program in x-y form. The two parameters that are used to adjust the driver model are a preview interval and a driver lag time. The preview interval is the time interval corresponding to the distance that the driver can see in front of the vehicle. The lag time is the time delay until the driver reacts after seeing something. The driver model for all of the simulation runs used a preview interval of 1.5 s and a lag time of .001 s. This model produced realistic results for a driver who is good at path following since the truck maintained a fairly smooth path while wandering 1 or 2 ft (0.3 to 0.6 m) either way in the lane. A good driver was desired for these simulations so that valid comparisons between the



Note: 1 in = 2.54 cm
 1 lb = 0.454 kg

Figure 16. Effect of cornering stiffness on rollover threshold, single-semitrailer truck.

different curve types could be made. To investigate the sensitivity of the simulation results to the driver path follower model, a run was made in which the driver model was changed to use a driver lag time of 0.3 s rather than 0.001 s used for the baseline case. Plots of the output of this run for roll angle and lateral acceleration in comparison to the baseline case are given in figures 17 and 18. In this simulation, the driver lag was increased to

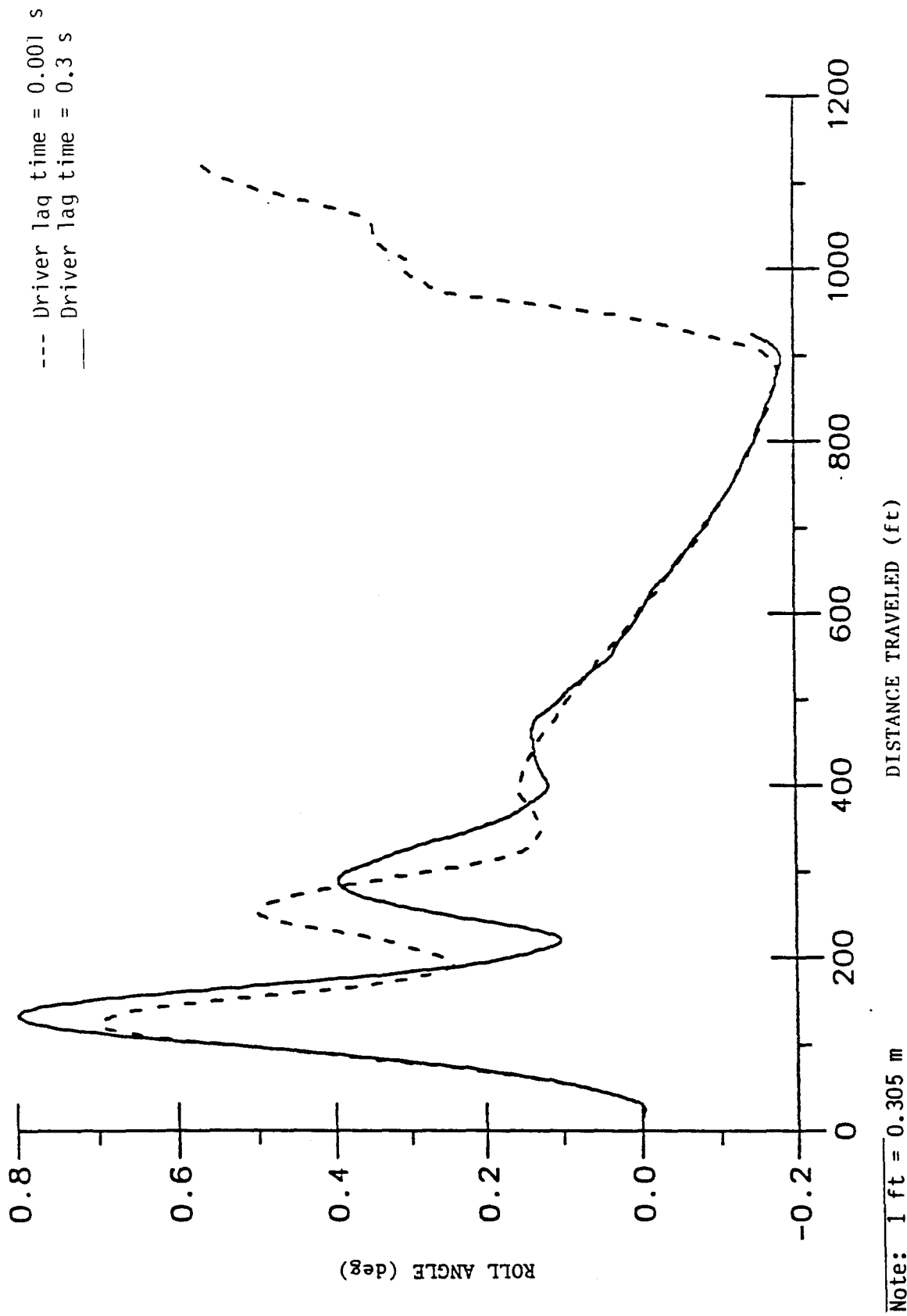


Figure 17. Comparison of roll angles for simulation runs with different driver lag times (case D40).

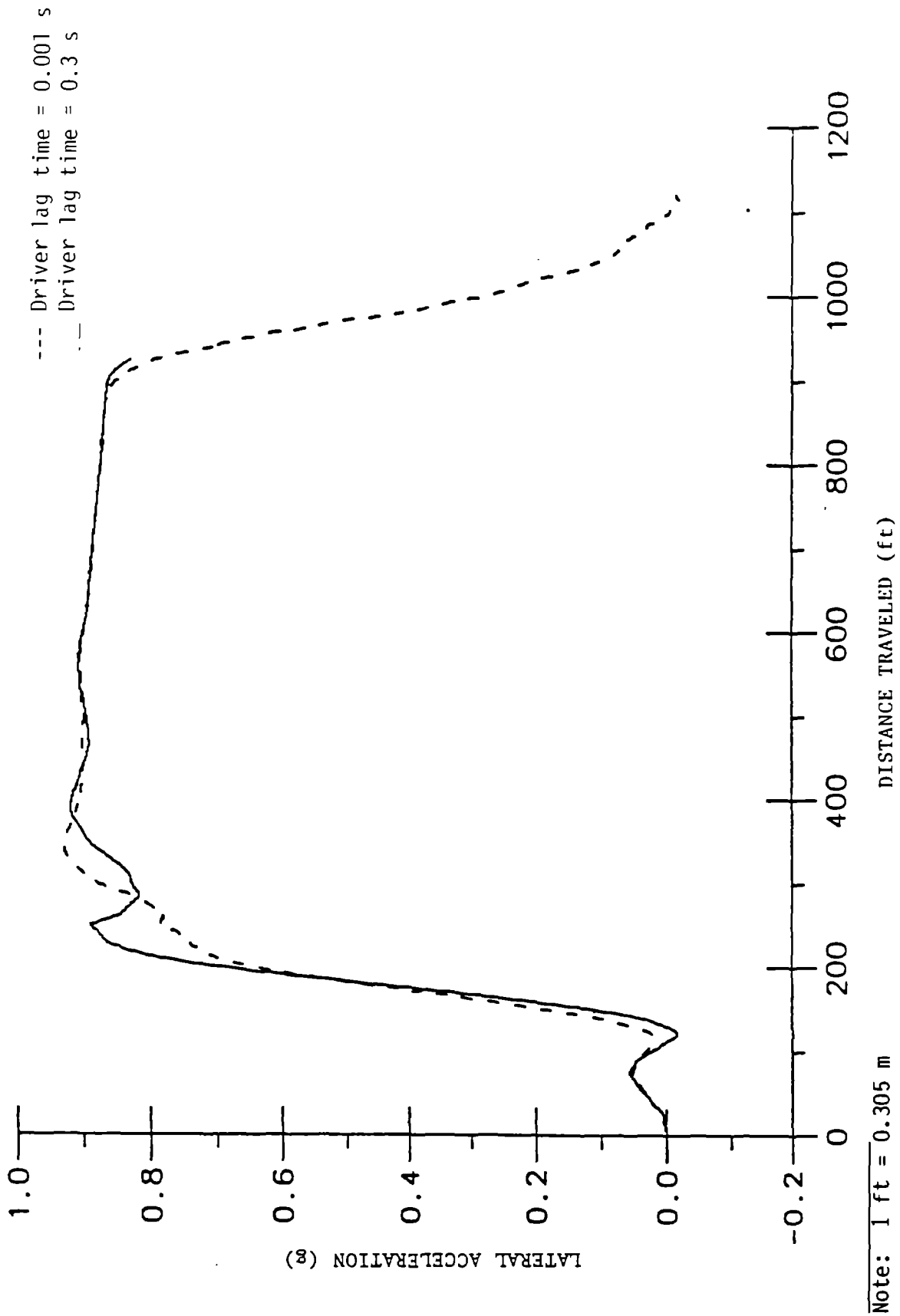


Figure 18. Comparison of lateral accelerations for simulation runs with different driver lag times (case D40).

0.3 sec, which made the system slightly more unstable. The roll angle plot shows that the driver is making steering corrections in this case. The lateral acceleration plot is not quite as smooth although the maximum value is actually slightly lower than for the baseline case.

7. Effect of Superelevation Transition Geometrics on Truck Rollover

Types of Transitions Studied: The effect of superelevation transition geometrics was evaluated for three types of transitions:

- Superelevation transition following 2/3 - 1/3 rule (Type I).
- Development of full superelevation on the tangent (Type II).
- Spiral transition curve (Type III).

The first two types both involve circular curves with direct tangent-to-curve transitions and no intervening transition curve. The horizontal curves for case I, designed in accordance with the 2/3 - 1/3 rule, which is specified as a desirable practice in the AASHTO Green Book, allow 2/3 of the superelevation to be developed on the tangent and the last 1/3 of the superelevation to be developed on the first portion of the curve itself. In a Type II transition, all of the superelevation is developed on the tangent so that the entire circular curve has constant superelevation. A Type III transition incorporates a short spiral transition curve between the tangent and circular curve at both the beginning and end of the curve. Superelevation development takes place completely within the spiral transition curve so that the entire circular curve has constant superelevation.

The curve and transition geometry are defined for the computer program in a new subroutine that calculates the elevation and gradient of the road surface at any point specified by the program. This is a simple matter for the Type I and Type II designs because they are simple curves and as such can be described by closed-form trigonometric relations. The radius of the curve at any point is known, and it is a simple matter to calculate the distance between the desired point and the centerline of the road. The elevation of the road at the desired point is then this distance multiplied by the superelevation at that point. The gradient of the road at the desired point can be found using a divided difference scheme. The Type III spiral transition design is not straightforward because the describing equations are not in a closed form; therefore, the radius at any particular point is not easily determined.

The (x,y) coordinates of the spiral, shown in figure 19, are given by the following equations:

$$x = l_s \left(1 - \frac{\theta^2}{10} + \frac{\theta^4}{216} - \frac{\theta^6}{9,360} \right) \quad (11)$$

$$y = l_s \left(\frac{\theta}{3} - \frac{\theta^3}{42} + \frac{\theta^5}{1,320} - \frac{\theta^7}{75,600} \right) \quad (12)$$

where: θ = angle from T.S. (tangent to spiral transition) to any point on the spiral

l_s = spiral length from T.S. to point (x,y)

x = longitudinal distance from T.S.

y = lateral distance from T.S.

The elevation of any point the spiral roadway can be determined using a minimization technique. Referring to figure 19, which is a plan view of a spiral transition curve, point A is the point where the elevation and gradients are desired. The elevation of A is the superelevation of the road at that point multiplied by distance D. Distance D, however, is the length of the shortest line that passes through A and intersects line C, which is the centerline of the road. The (x,y) coordinates of any point on line C are known from equations (11) and (12) as a power series of the angle θ , and the elevation of any point on line C is known from the centerline profile of the road. Distance D is found by using a modified Newton method to minimize the length of the line passing through A and intersecting line C, which also produces the angle θ , which is used to determine the superelevation at that point. The gradients are found by repeating this process for additional points and using a divided difference.

Situations Investigated: A total of 36 cases were investigated, with curve radii ranging from 432 to 1,528 ft (131 to 466 m) and superelevations ranging from 0.04 to 0.10. These correspond to curves designed to AASHTO minimum radii for design speeds from 40 to 60 mi/h (64 to 97 km/h) and for maximum superelevation rates (e_{max}) from 0.04 to 0.10. In all cases, the superelevation was developed along the runoff and runout lengths as a linear function of distance. The curve geometry and truck speed data for each of the three types of spiral transition designs that were evaluated are presented in tables 10, 11, and 12. Cases A through L in tables 10, 11, and 12 represent the 12 combinations of horizontal curve design speed, maximum superelevation rate, and truck speed that were simulated.

Ideal road conditions were assumed for the simulations, i.e., the pavement surface was assumed to be smooth with high friction. Since the objective of this study was to investigate roll characteristics, it was assumed that the available lateral pavement friction was never exceeded, which is reasonable for a loaded truck on a dry road.

The truck type used in this investigation was the STAA single with 48-ft (14.6-m) trailer and conventional tractor. The parameters for this truck type are those listed in table 7. The rollover threshold of this truck on a flat curve is 0.36 g.

Results: The results of the computer simulation runs are summarized in tables 13, 14, and 15. Table 13 summarizes the results for the Type I transition area (the 2/3 - 1/3 rule), which was considered the baseline case.

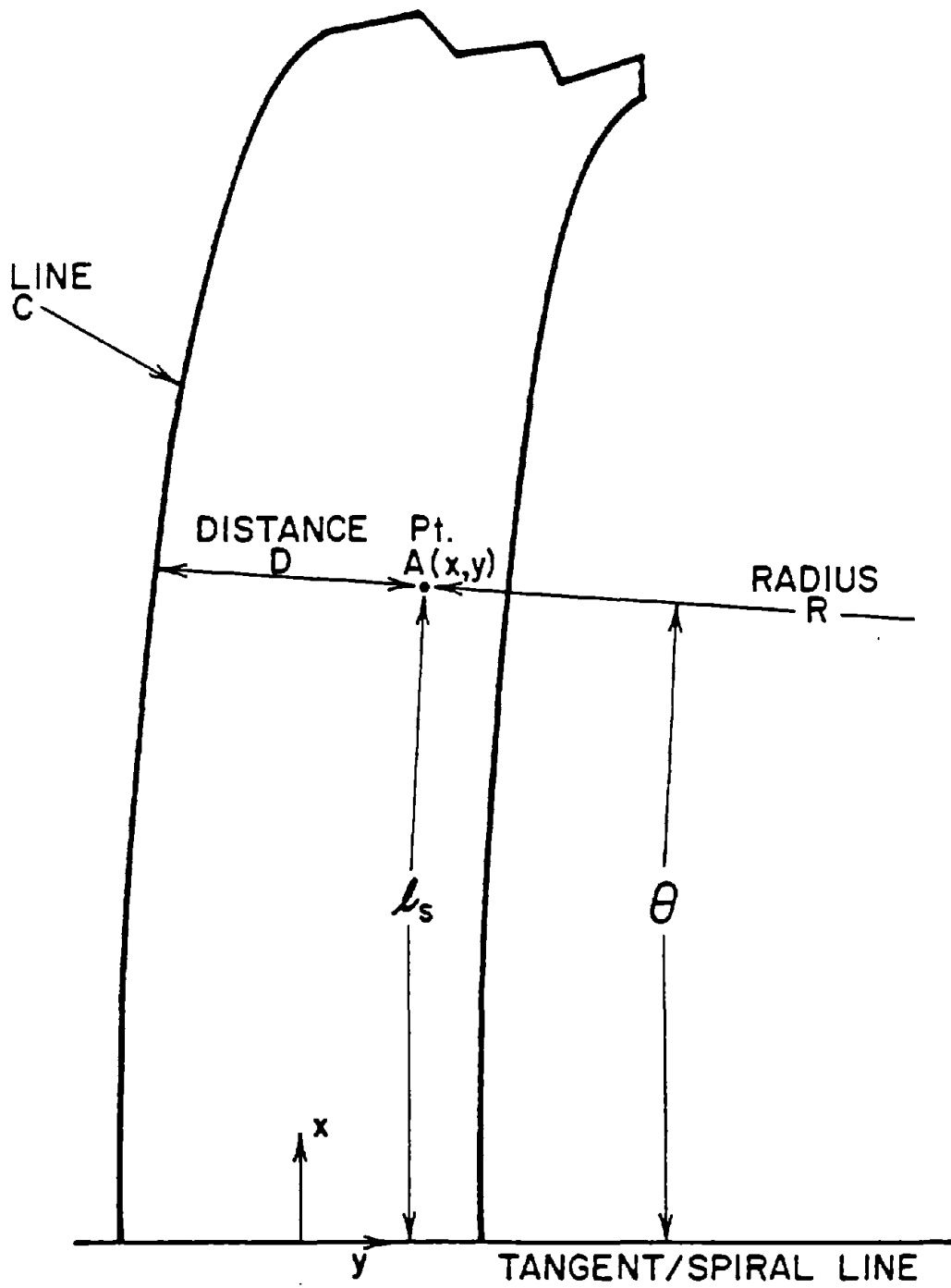


Figure 19. Dimensions used in calculation of pavement elevation at any point on a spiral transition curve.

Table 10. Horizontal curve geometrics for Type I transition area (2/3 - 1/3 rule).

Case	Design speed (mi/h)	Vehicle speed for computer runs (mi/h)	R (ft)	e _{max} (ft/ft)	Length of super. runoff (ft)	L ^a (ft)	Stations of key points on curve (ft)					
							PC	EOR	BOR	PI	SR	RNC
A	40	40,50,60	573	0.04	125	900.07	1+43.33	1+85.00	10+01.73	10+43.40	11+26.73	11+76.73
B	50	50,60	955	0.04	150	1,500.11	1+60.00	2+10.00	16+10.11	16+60.11	17+60.11	18+10.11
C	60	60	1,528	0.04	175	2,400.18	1+76.67	2+35.00	25+18.51	25+76.84	26+93.51	27+43.51
D	40	40,50,60	509	0.06	125	799.54	1+43.33	1+85.00	9+01.20	9+42.87	10+26.20	10+76.20
E	50	50,60	849	0.06	150	1,333.61	1+60.00	2+10.00	14+43.61	14+93.61	14+93.61	16+43.61
F	60	60	1,348	0.06	175	2,117.43	1+76.67	2+35.00	22+35.77	22+94.10	24+10.77	24+60.77
G	40	40,50,60	468	0.08	170	735.13	1+73.33	2+30.00	8+51.80	9+08.47	10+21.80	10+71.80
H	50	50,60	764	0.08	190	1,200.09	1+86.67	2+50.00	13+23.42	13+86.75	15+13.42	15+63.42
I	60	60	1,206	0.08	215	1,894.38	2+03.33	2+75.00	20+26.05	20+97.71	22+41.05	22+91.05
J	40	40,50,60	432	0.10	210	678.58	2+00.00	2+70.00	8+08.58	8+78.58	10+18.58	10+68.58
K	50	50,60	694	0.10	240	1,090.13	2+20.00	3+00.00	12+30.13	13+10.13	14+70.13	15+20.13
L	60	60	1,091	0.10	270	1,713.74	2+40.00	3+30.00	18+63.74	19+53.74	21+33.74	21+83.74

^a Length of curve corresponds to central angle (W) of 90 degrees.

L = Length of curve

PC = Point of curvature

EOR = End of runoff (beyond PC)

BOR = Beginning of runoff (before PI)

PT = Point of tangency

SR = Start of runoff

RNC = Return to normal crown

Note: 1 mi = 1.61 km

1 ft = 0.305 m

Table 11. Horizontal curve geometrics for Type II transition area
(full superelevation on tangent).

Case	Design speed (mi/h)	Vehicle speeds for computer runs (mi/h)	R (ft)	e _{max} (ft/ft)	Length of super. runoff (ft)	L ^a	Stations of key points on curve (ft)			
							PC ^b	PT ^c	SR	RNC
A	40	40,50,60	573	0.04	125	900.07	1+85.00	10+85.07	12+10.07	12+60.07
B	50	50,60	955	0.04	150	1,500.11	2+10.00	17+10.11	18+60.11	19+10.11
C	60	60	1,528	0.04	175	2,400.18	2+35.00	26+35.18	28+10.18	28+60.18
D	40	40,50,60	509	0.06	125	799.54	1+85.00	9+84.54	11+09.54	11+59.54
E	50	50,60	849	0.06	150	1,333.61	2+10.00	15+43.61	16+93.61	17+43.61
F	60	60	1,348	0.06	175	2,117.43	2+35.00	23+52.43	25+27.43	25+77.43
G	40	40,50,60	468	0.08	170	735.13	2+30.00	9+65.13	11+35.13	11+85.13
H	50	50,60	764	0.08	190	1,200.09	2+50.00	14+50.09	16+40.09	16+90.09
I	60	60	1,206	0.08	215	1,894.38	2+75.00	21+69.38	23+84.38	24+34.38
J	40	40,50,60	432	0.10	210	678.58	2+70.00	9+48.58	11+58.58	12+08.58
K	50	50,60	694	0.10	240	1,090.13	3+00.00	13+90.13	16+30.13	16+80.13
L	60	60	1,091	0.10	270	1,713.74	3+30.00	20+43.74	23+13.74	23+63.74

^a Length of curve corresponds to central angle (W) of 90 degrees.

^b Superelevation runoff ends at PC.

^c Superelevation runoff starts at PT.

L = Length of curve

PC = Point of curvature

PT = Point of tangency

SR = Start of runoff

RNC = Return to normal crown

Note: 1 mi = 1.61 km

1 ft = 0.305 m

Table 12. Horizontal curve geometrics for Type III transition area (spiral).

Case	Design speed (mi/h)	Vehicle speeds for computer runs (mi/h)	R (ft)	e _{max} (ft/ft)	L _S (ft)	W _S (deg)	L ^a	Stations of key points on curve (ft)				
								IS	SC	CS	ST	RNC
A	40	40,50,60	573	0.04	125	6.25	775.07	0+60.00	1+85.00	9+60.07	10+85.07	11+35.07
B	50	50,60	955	0.04	150	4.50	1,350.11	0+60.00	2+10.00	15+60.11	17+10.11	17+60.11
C	60	60	1,528	0.04	175	3.28	2,225.18	0+60.00	2+35.00	24+60.18	26+35.18	26+85.18
D	40	40,50,60	509	0.06	125	7.04	674.54	0+60.00	1+85.00	8+59.54	9+84.54	10+34.54
E	50	50,60	849	0.06	150	5.06	1,183.61	0+60.00	2+10.00	13+93.61	15+43.61	15+93.61
F	60	60	1,348	0.06	175	3.72	1,942.43	0+60.00	2+35.00	21+77.43	23+52.43	24+02.43
G	40	40,50,60	468	0.08	170	10.41	565.13	0+60.00	2+30.00	7+95.13	9+65.13	10+15.13
H	50	50,60	764	0.08	190	7.12	1,010.09	0+60.00	2+50.00	12+60.09	14+50.09	15+00.09
I	60	60	1,206	0.08	215	5.11	1,679.38	0+60.00	2+75.00	19+54.38	21+69.38	22+19.38
J	40	40,50,60	432	0.10	210	13.93	468.58	0+60.00	2+70.00	7+38.58	9+48.58	9+98.58
K	50	50,60	694	0.10	240	9.91	850.13	0+60.00	3+00.00	11+50.13	13+90.13	14+40.13
L	60	60	1,091	0.10	270	7.09	1,443.74	0+60.00	3+30.00	17+73.74	20+43.74	20+93.74

^a Length of curve corresponds to central angle (W) of 90 degrees.

- L = Length of curve
 - L_S = Length of spiral
 - W_S = Central angle of spiral
 - TS = Tangent-to-spiral point
 - SC = Spiral-to-curve point
 - CS = Curve-to-spiral point
 - ST = Spiral-to-tangent point
 - RNC = Return to normal crown
- Note: 1 mi = 1.61 km
1 ft = 0.305 m

Table 13. Results of computer simulation for Type I transition area (2/3 - 1/3 rule).

Case	Design speed (mi/h)	Radius (ft)	Super-elevation (ft/ft)	Vehicle speed (mi/h)	Nominal lateral acceleration (g)	Maximum lateral acceleration (g)	Roll stability margin ^a (g)	Location of maximum lateral acceleration (ft)	Maximum roll angle (deg)
A	40	573	0.04	40	0.186	0.204	0.196	3+47.8	-0.949
A	40	573	0.04	50	0.291	0.315	0.085	3+39.9	-3.814
A	40	573	0.04	60	0.419	0.437	-0.037	3+44.2	^b
B	50	955	0.04	50	0.175	0.189	0.211	3+63.8	-0.651
B	50	955	0.04	60	0.251	0.282	0.118	3+76.9	-3.044
C	60	1,528	0.04	60	0.157	0.175	0.225	3+97.7	-0.323
D	40	509	0.06	40	0.210	0.232	0.188	3+42.5	0.373
D	40	509	0.06	50	0.327	0.354	0.066	3+71.5	-2.813
D	40	509	0.06	60	0.472	0.473	-0.053	3+39.4	^b
E	50	849	0.06	50	0.196	0.214	0.206	3+94.1	0.772
E	50	849	0.06	60	0.283	0.312	0.108	3+86.4	-1.778
F	60	1,348	0.06	60	0.178	0.194	0.226	4+40.3	1.217
G	40	468	0.08	40	0.228	0.252	0.188	3+86.8	1.839
G	40	468	0.08	50	0.356	0.382	0.058	3+91.1	-1.566
G	40	468	0.08	60	0.513	0.509	-0.069	3+64.6	^b
H	50	764	0.08	50	0.218	0.237	0.203	4+34.3	2.202
H	50	764	0.08	60	0.314	0.343	0.097	4+23.6	-0.547
I	60	1,206	0.08	60	0.199	0.215	0.225	4+69.0	2.717
J	40	432	0.10	40	0.247	0.273	0.187	4+32.8	3.209
J	40	432	0.10	50	0.386	0.411	0.049	4+55.3	-0.429
J	40	432	0.10	60	0.556	0.553	-0.093	3+75.4	^b
K	50	694	0.10	50	0.240	0.257	0.203	4+81.8	3.632
K	50	694	0.10	60	0.346	0.372	0.088	4+64.8	0.724
L	60	1,091	0.10	60	0.220	0.233	0.227	5+02.8	4.284

^a Based on truck with rollover threshold of 0.36 g.

^b Indicates rollover occurred.

Note: 1 mi = 1.61 km
1 ft = 0.305 m

Table 14. Results of computer simulation for Type II transition area (full superelevation on tangent).

Case	Design speed (mi/h)	Radius (ft)	Super-elevation (ft/ft)	Vehicle speed (mi/h)	Nominal lateral acceleration (g)	Maximum lateral acceleration (g)	Roll stability margin ^a (g)	Location of maximum lateral acceleration (ft)	Maximum roll angle (deg)
A	40	573	0.04	40	0.186	0.204	0.196	3+52.0	-0.938
A	40	573	0.04	50	0.291	0.321	0.079	3+71.9	-3.964
A	40	573	0.04	60	0.419	0.435	-0.035	3+81.3	^b
B	50	955	0.04	50	0.175	0.195	0.205	4+03.6	-0.770
B	50	955	0.04	60	0.251	0.289	0.111	4+21.1	-3.232
C	60	1,528	0.04	60	0.157	0.182	0.218	4+47.0	-0.507
D	40	509	0.06	40	0.210	0.232	0.188	3+52.9	0.399
D	40	509	0.06	50	0.327	0.364	0.056	3+76.9	-2.988
D	40	509	0.06	60	0.472	0.477	-0.057	3+64.0	^b
E	50	849	0.06	50	0.196	0.222	0.198	4+02.4	0.584
E	50	849	0.06	60	0.283	0.326	0.094	4+28.4	-2.093
F	60	1,348	0.06	60	0.178	0.207	0.213	4+58.1	0.903
G	40	468	0.08	40	0.228	0.252	0.188	3+93.2	1.922
G	40	468	0.08	50	0.356	0.397	0.043	4+02.2	-1.806
G	40	468	0.08	60	0.513	0.515	-0.075	4+01.5	^b
H	50	764	0.08	50	0.218	0.247	0.193	4+42.6	1.993
H	50	764	0.08	60	0.314	0.363	0.077	4+69.5	-1.000
I	60	1,206	0.08	60	0.199	0.233	0.207	4+99.0	2.306
J	40	432	0.10	40	0.247	0.273	0.187	4+37.5	3.346
J	40	432	0.10	50	0.386	0.429	0.031	4+59.2	-0.628
J	40	432	0.10	60	0.556	0.557	-0.097	4+30.1	^b
K	50	694	0.10	50	0.240	0.27	0.190	4+90.1	3.440
K	50	694	0.10	60	0.346	0.399	0.061	5+17.6	0.107
L	60	1,091	0.10	60	0.220	0.257	0.203	5+58.5	3.736

^a Based on truck with rollover threshold of 0.36 g.

^b Indicates rollover occurred.

Note: 1 mi = 1.61 km

1 ft = 0.305 m

Table 15. Results of computer simulation for Type III transition area (spiral).

Case	Design speed (mi/h)	Radius (ft)	Super-elevation (ft/ft)	Vehicle speed (mi/h)	Nominal lateral acceleration (g)	Maximum lateral acceleration (g)	Roll stability margin ^a (g)	Location of maximum lateral acceleration (ft)	Maximum roll angle (deg)
A	40	573	0.04	40	0.186	0.203	0.197	3+46.7	-0.933
A	40	573	0.04	50	0.291	0.308	0.092	3+59.1	-3.652
A	40	573	0.04	60	0.419	0.435	-0.035	3+45.8	^b
B	50	955	0.04	50	0.175	0.185	0.215	3+99.5	-0.546
B	50	955	0.04	60	0.251	0.270	0.130	3+73.4	-2.726
C	60	1,528	0.04	60	0.157	0.166	0.234	4+06.4	-0.085
D	40	509	0.06	40	0.210	0.231	0.189	3+46.3	-0.048
D	40	509	0.06	50	0.327	0.349	0.071	3+73.2	-2.700
D	40	509	0.06	60	0.472	0.470	-0.050	3+33.8	^b
E	50	849	0.06	50	0.196	0.211	0.209	4+01.6	0.454
E	50	849	0.06	60	0.283	0.300	0.120	4+19.8	-1.478
F	60	1,348	0.06	60	0.178	0.189	0.231	4+56.5	0.899
G	40	468	0.08	40	0.228	0.251	0.189	3+90.9	0.559
G	40	468	0.08	50	0.356	0.378	0.062	4+18.0	-1.607
G	40	468	0.08	60	0.513	0.509	-0.069	3+57.3	^b
H	50	764	0.08	50	0.218	0.235	0.205	4+44.9	0.953
H	50	764	0.08	60	0.314	0.330	0.110	4+66.5	-0.312
I	60	1,206	0.08	60	0.199	0.211	0.229	5+34.6	1.288
J	40	432	0.10	40	0.247	0.273	0.187	4+32.0	0.878
J	40	432	0.10	50	0.386	0.410	0.050	4+61.6	-0.670
J	40	432	0.10	60	0.556	0.546	-0.086	3+80.8	^b
K	50	694	0.10	50	0.240	0.258	0.202	4+94.0	1.248
K	50	694	0.10	60	0.346	0.362	0.098	5+28.7	0.468
L	60	1,091	0.10	60	0.220	0.233	0.227	5+72.0	4.154

^a Based on truck with rollover threshold of 0.36 g.

^b Indicates rollover occurred.

Note: 1 mi = 1.61 km

1 ft = 0.305 m

Tables 14 and 15 show the results for the Type II and III transition areas, respectively. Tables 16 and 17 compare the results for the Type I baseline to the simulation results for the Type II and III transition areas, respectively.

The effective maximum lateral acceleration, a'_{\max} , not offset by superelevation was calculated using the following equation:

$$a'_{\max} = a_{\max} - e(x_a) \quad (13)$$

where: a'_{\max} = effective maximum lateral acceleration (g) not offset by superelevation

a_{\max} = lateral acceleration at any point along the superelevation transition (g)

$e(x)$ = superelevation at distance x from the beginning of the transition curve

x_a = location of the point where the maximum lateral acceleration occurs, i.e., $a(x_a) = a_{\max}$

The roll stability margin, RSM, is defined by the following equation:

$$\text{RSM} = \rho_0 - a_{\max} + e(x_a) \quad (14)$$

where: ρ_0 = truck rollover threshold on a flat curve ($\rho_0 = 0.36$)

Equation (14) can also be presented in the following form:

$$\text{RSM} = \rho_0 - a'_{\max} \quad (15)$$

The roll stability margin is a measure of the additional lateral acceleration that the truck could undergo without rolling over. A positive value of RSM indicates that the truck could undergo additional lateral acceleration without rolling over. A negative value of RSM indicates that the truck should roll over; in fact, a rollover did occur in every instance in which it was predicted by a negative value of RSM in the simulation results shown in tables 13, 14, and 15. The calculated values of RSM in tables 13, 14, and 15 are applicable to a truck with a rollover threshold of 0.36 g. This rollover threshold is low by historical standards, which assumed that most trucks had rollover thresholds of at least 0.40 g, but it is substantially higher than the minimum rollover threshold of 0.30 g found recently for some truck configurations. A sensitivity analysis of the effect on horizontal curve design criteria of variations in the rollover threshold is found in volume I of this report.

Table 16. Comparison of computer simulation results for Type I and II transition areas.

Case	Roll stability margin (g)			Location of point of maximum lateral acceleration			Maximum roll angle (deg)		
	Type I	Type II	Δ	Type I	Type II	Δ	Type I	Type II	Δ
A	0.196	0.196	0.000	3+47.8	3+52.0	4.2	-0.949	-0.938	-0.011
A	0.085	0.079	0.006	3+39.9	3+71.9	32.0	-3.814	-3.964	0.150
A	-0.037	-0.035	-0.002	3+44.2	3+81.3	37.1	-	-	-
B	0.211	0.205	0.006	3+63.8	4+03.6	39.8	-0.651	-0.770	0.119
B	0.118	0.111	0.007	3+76.9	4+21.1	44.2	-3.044	-3.232	0.188
C	0.225	0.218	0.007	3+97.7	4+47.0	49.3	-0.323	-0.507	0.184
D	0.188	0.188	0.000	3+42.5	3+52.9	10.4	0.373	0.399	0.026
D	0.066	0.056	0.010	3+71.5	3+76.9	5.4	-2.813	-2.988	0.175
D	-0.053	-0.057	0.004	3+39.4	3+64.0	24.6	-	-	-
E	0.206	0.198	0.008	3+94.1	4+02.4	8.3	0.772	0.584	-0.188
E	0.108	0.094	0.014	3+86.4	4+28.4	42.0	-1.778	-2.093	0.315
F	0.226	0.213	0.013	4+40.3	4+58.1	17.8	1.217	0.903	-0.314
G	0.188	0.188	0.000	3+86.8	3+93.2	6.4	1.839	1.922	-0.083
G	0.058	0.043	0.015	3+91.1	4+20.2	29.1	-1.566	-1.806	0.240
G	-0.069	-0.075	0.006	3+64.6	4+01.5	36.9	-	-	-
H	0.203	0.193	0.010	4+34.3	4+42.6	8.3	2.202	1.993	-0.209
H	0.097	0.077	0.020	4+23.6	4+69.5	45.9	-0.547	-1.000	0.453
I	0.225	0.207	0.018	4+69.0	4+99.0	30.0	2.717	2.306	-0.411
J	0.187	0.187	0.000	4+32.8	4+37.5	4.7	3.209	3.346	0.137
J	0.049	0.031	0.018	4+55.3	4+59.2	3.9	-0.429	-0.628	0.199
J	-0.093	-0.097	0.004	3+75.4	4+30.1	54.7	-	-	-
K	0.203	0.190	0.013	4+81.8	4+90.1	8.3	3.632	3.440	-0.192
K	0.088	0.061	0.027	4+64.8	5+17.6	52.8	0.724	0.107	-0.617
L	0.227	0.203	0.024	5+02.8	5+48.5	45.7	4.284	3.736	-0.548

Table 17. Comparison of computer simulation results for Type I and III transition areas.

Case	Roll stability margin (g)			Location of point of maximum lateral acceleration			Maximum roll angle (deg)		
	Type I	Type III	Δ	Type I	Type III	Δ	Type I	Type III	Δ
A	0.196	0.197	-0.001	3+47.8	3+46.7	-1.1	-0.949	-0.933	-0.016
A	0.085	0.092	-0.007	3+39.9	3+59.1	29.2	-3.814	-3.652	-0.162
A	-0.037	-0.035	-0.002	3+44.2	3+45.8	1.6	-	-	-
B	0.211	0.215	-0.004	3+63.8	3+99.5	35.7	-0.651	-0.546	-0.105
B	0.118	0.130	-0.012	3+76.9	3+73.4	-3.5	-3.044	-2.726	-0.318
C	0.225	0.234	-0.009	3+97.0	4+06.4	8.7	-0.323	-0.085	-0.238
D	0.188	0.189	-0.001	3+42.0	3+46.3	3.8	0.373	-0.048	0.325
D	0.066	0.071	-0.005	3+71.5	3+73.2	1.7	-2.813	-2.700	-0.113
D	-0.053	-0.050	-0.003	3+39.4	3+33.8	-5.6	-	-	-
E	0.206	0.029	-0.003	3+94.1	4+01.6	7.5	0.772	0.454	-0.318
E	0.108	0.120	-0.012	3+86.4	4+19.8	33.4	-1.778	-1.478	-0.300
F	0.226	0.231	-0.005	4+40.3	4+56.5	16.2	1.217	0.899	0.318
G	0.188	0.189	-0.001	3+86.8	3+90.9	4.1	1.839	0.559	1.280
G	0.058	0.062	-0.004	3+91.1	4+18.0	26.9	-1.566	-1.607	0.041
G	-0.069	-0.066	-0.003	3+64.6	3+57.0	-7.3	-	-	-
H	0.203	0.205	-0.002	4+34.3	4+44.9	10.6	2.202	0.953	1.249
H	0.097	0.110	-0.013	4+23.6	4+66.5	42.9	-0.547	-0.312	-0.235
I	0.225	0.229	-0.004	4+69.0	5+34.6	65.6	2.717	1.288	1.429
J	0.187	0.187	0.000	4+32.0	4+32.0	-0.8	3.209	0.878	2.311
J	0.049	0.050	-0.001	4+55.0	4+61.6	6.3	-0.429	-0.670	0.241
J	-0.093	-0.086	-0.007	3+75.0	3+80.8	5.4	-	-	-
K	0.203	0.202	0.001	4+81.0	4+94.0	12.2	3.632	1.248	2.384
K	0.088	0.098	-0.010	4+64.0	5+28.7	63.9	0.724	0.468	0.256
L	0.227	0.227	0.000	5+02.0	5+72.0	69.2	4.284	4.154	0.130

A maximum roll angle is actually the "most negative" or, strictly speaking, the smallest roll angle, because a negative roll angle means that the truck is leaning out of the turn. Sample plots of lateral acceleration versus distance and roll angle versus distance for case A with the three transition designs are shown in figures 20 through 25. All of these results are for the STAA single-semitrailer truck with 48-ft (14.6-m) trailer documented in table 11. The roll angles and lateral accelerations in the plots are all in reference to an inertial coordinate system, i.e., the roll angle on a superelevated road is the true roll angle of the truck relative to the flat initial starting plane, not to the road itself. To find the roll angle relative to the superelevated road, the angle of the superelevation must be subtracted from the plotted vehicle roll angle. The superelevation angles are:

- 0.04 superelevation -- 2.3°.
- 0.06 superelevation -- 3.4°.
- 0.08 superelevation -- 4.6°.
- 0.10 superelevation -- 5.7°.

A positive roll angle means the vehicle is leaning into the turn; a negative angle means the vehicle is leaning out of the turn. The lateral acceleration plotted is in the inertial horizontal plane. On a flat road, lateral acceleration contributes only to the vehicle rolling moment and lateral tire load; on a superelevated road, it contributes in a lesser degree to the rolling moment and lateral tire load as it also adds to the normal tire load.

In addition to the roll stability margin defined by equation (14), another parameter--a critical speed--is introduced to provide a quantitative measure of truck roll performance. Critical speed, v_{crit} , for a specified truck negotiating a horizontal curve of specified geometry is defined as the minimum steady speed at which the truck would roll over on the curve. In other words, the roll stability margin for a truck negotiating a curve at the critical speed is equal to zero. Using equation (14), the truck maximum lateral acceleration at the critical speed is such that:

$$p_0 = a_{max}(v_{crit}) + e(x_a) = 0 \quad (16)$$

For steady-state turning, the lateral acceleration is expressed by:

$$a_{ss} = \frac{v^2}{15 R} \quad (17)$$

where: v = steady-state speed (mi/h)

R = curve radius (ft)

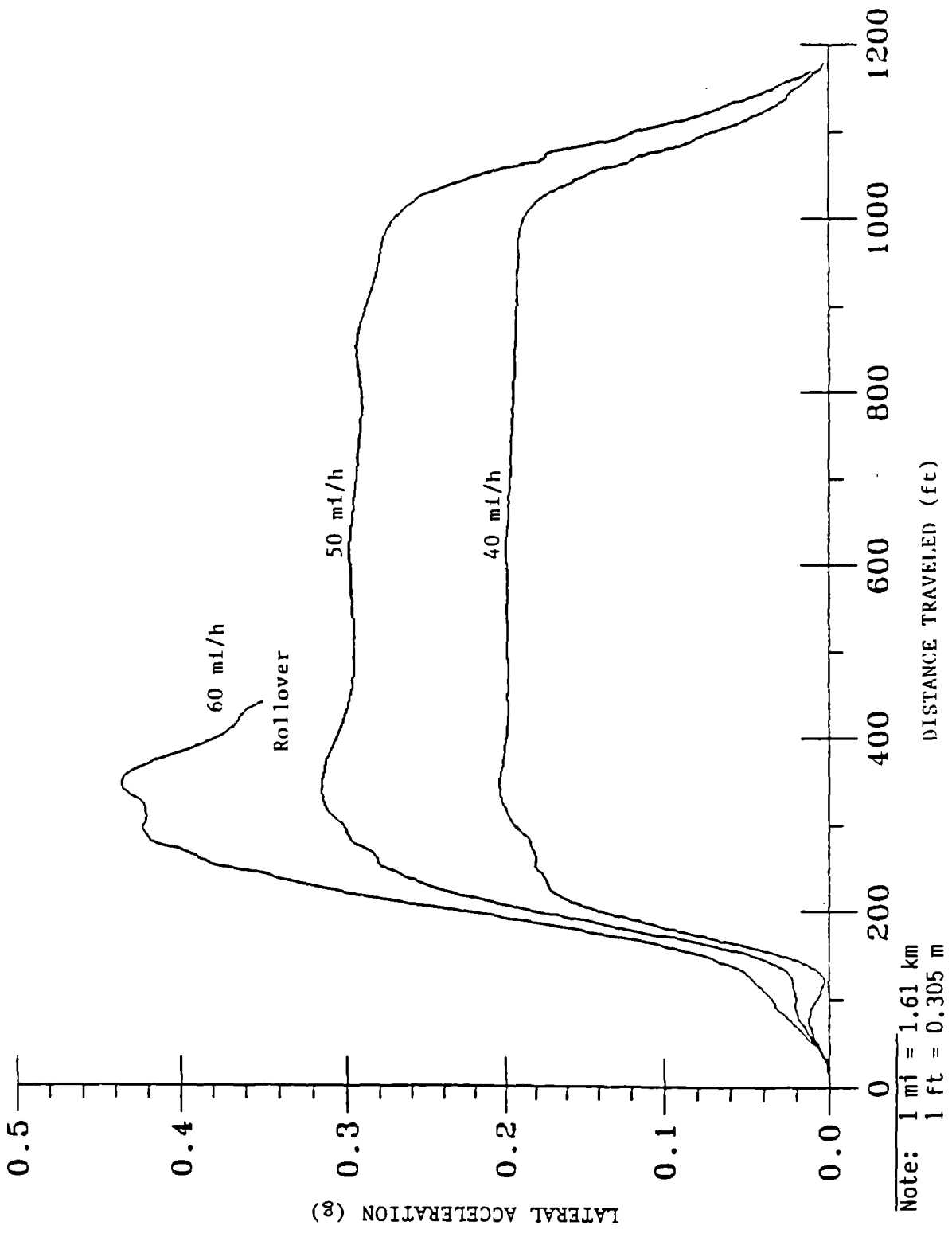


Figure 20. Lateral acceleration versus distance, single-semitrailer truck, case A, Type I transition area.

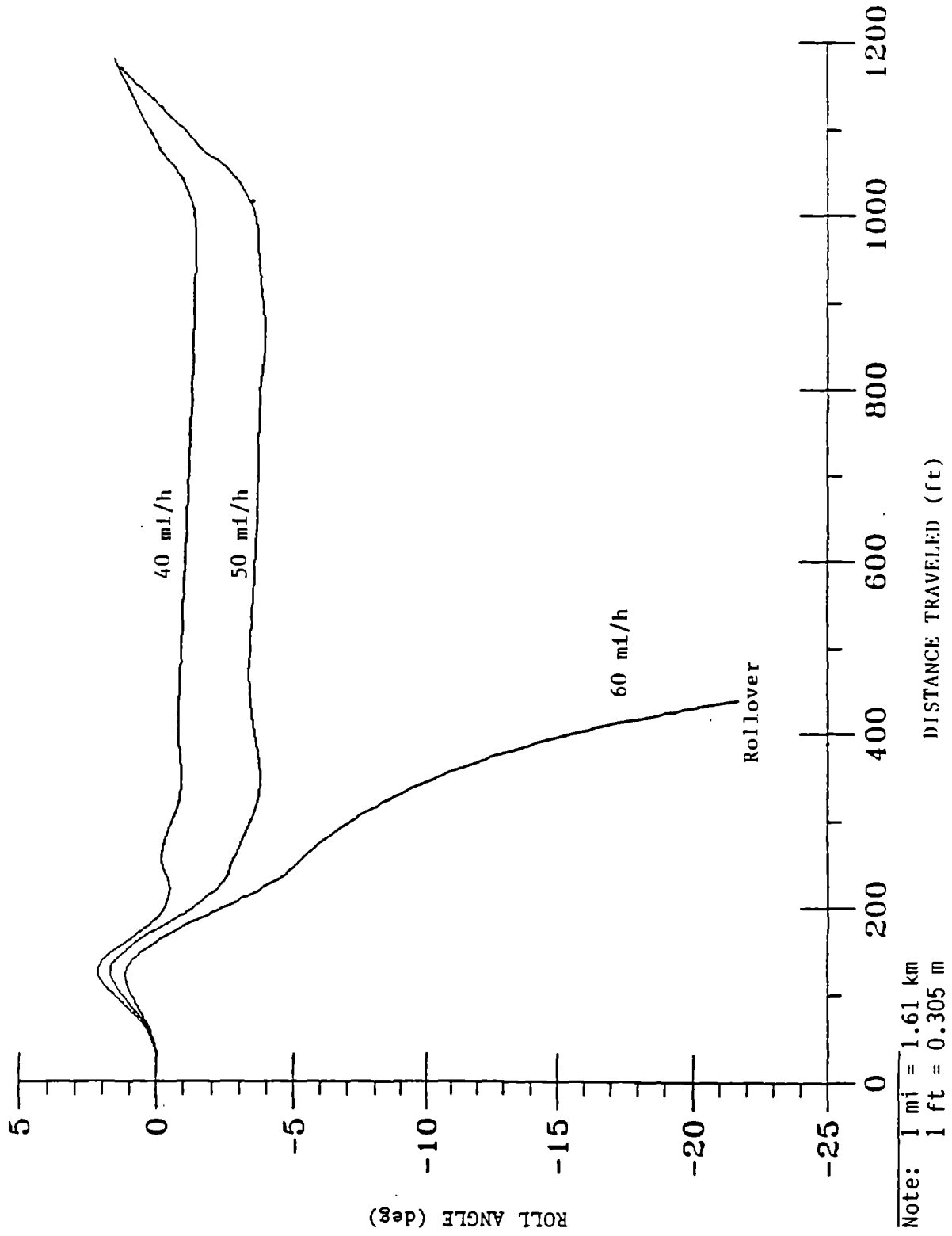


Figure 21. Roll angle versus distance, single-semitrailer truck, case A, Type I transition area.

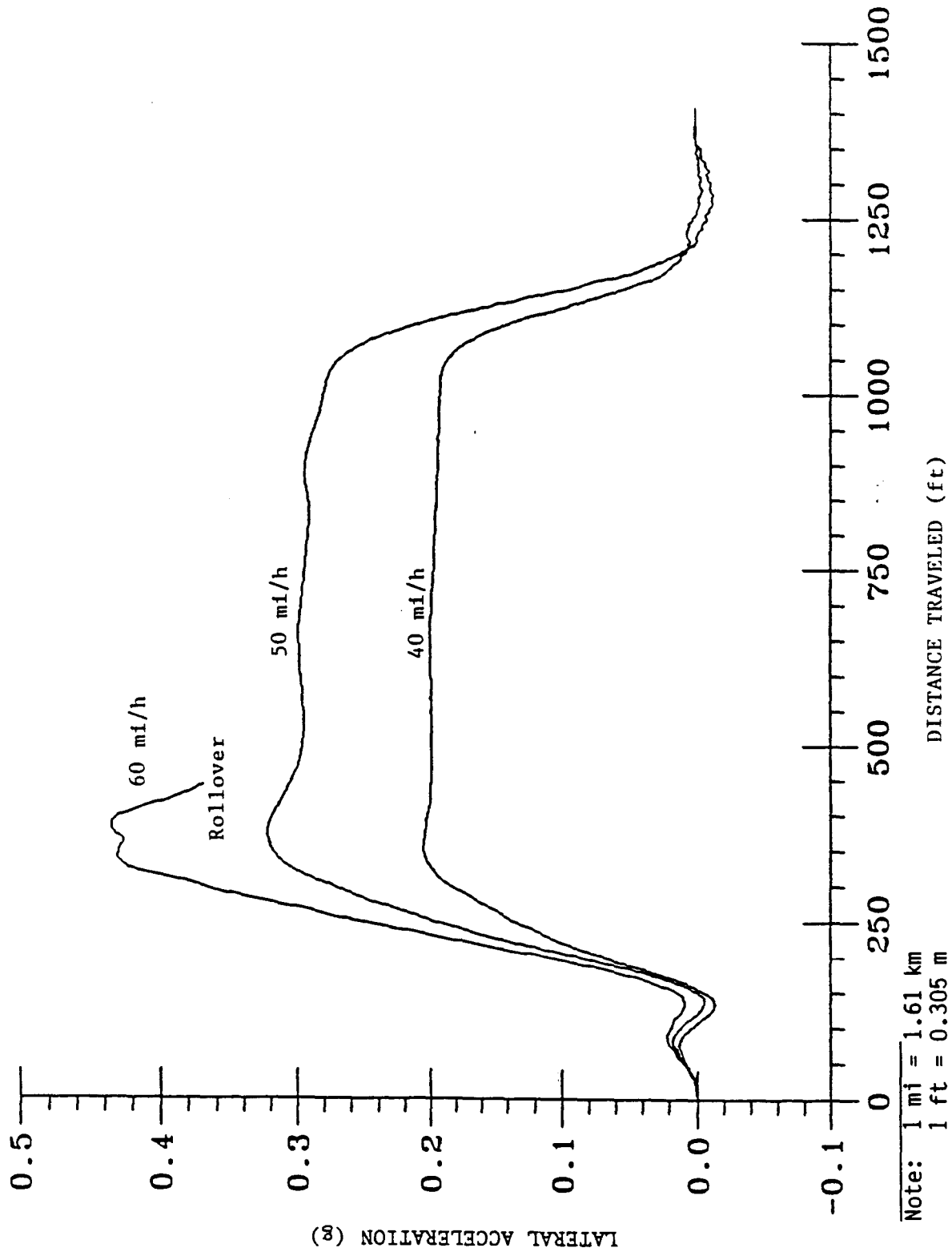


Figure 22. Lateral acceleration versus distance, single-semitrailer truck, case A, Type II transition area.

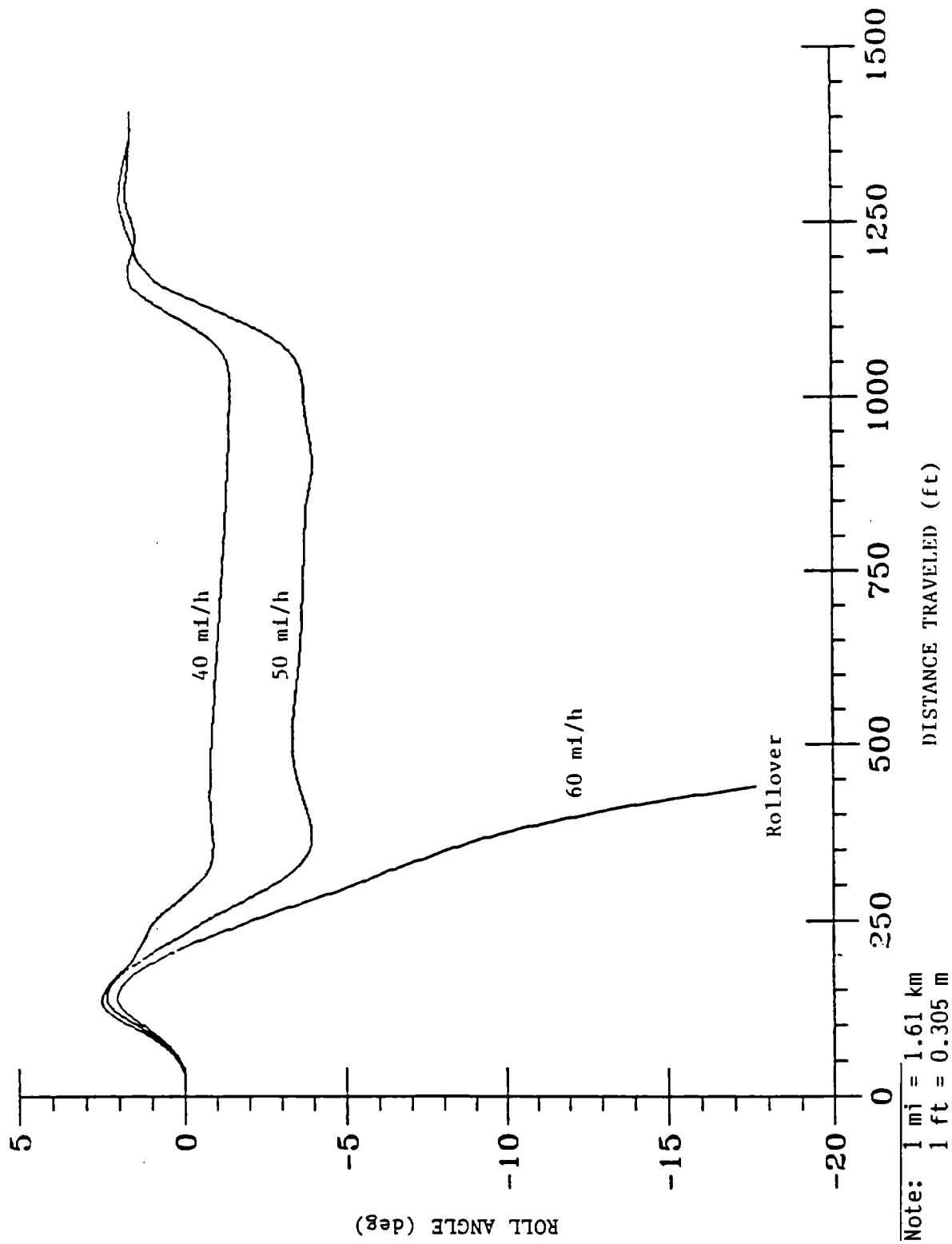


Figure 23. Roll angle versus distance, single-semitrailer truck, case A, Type II transition area.

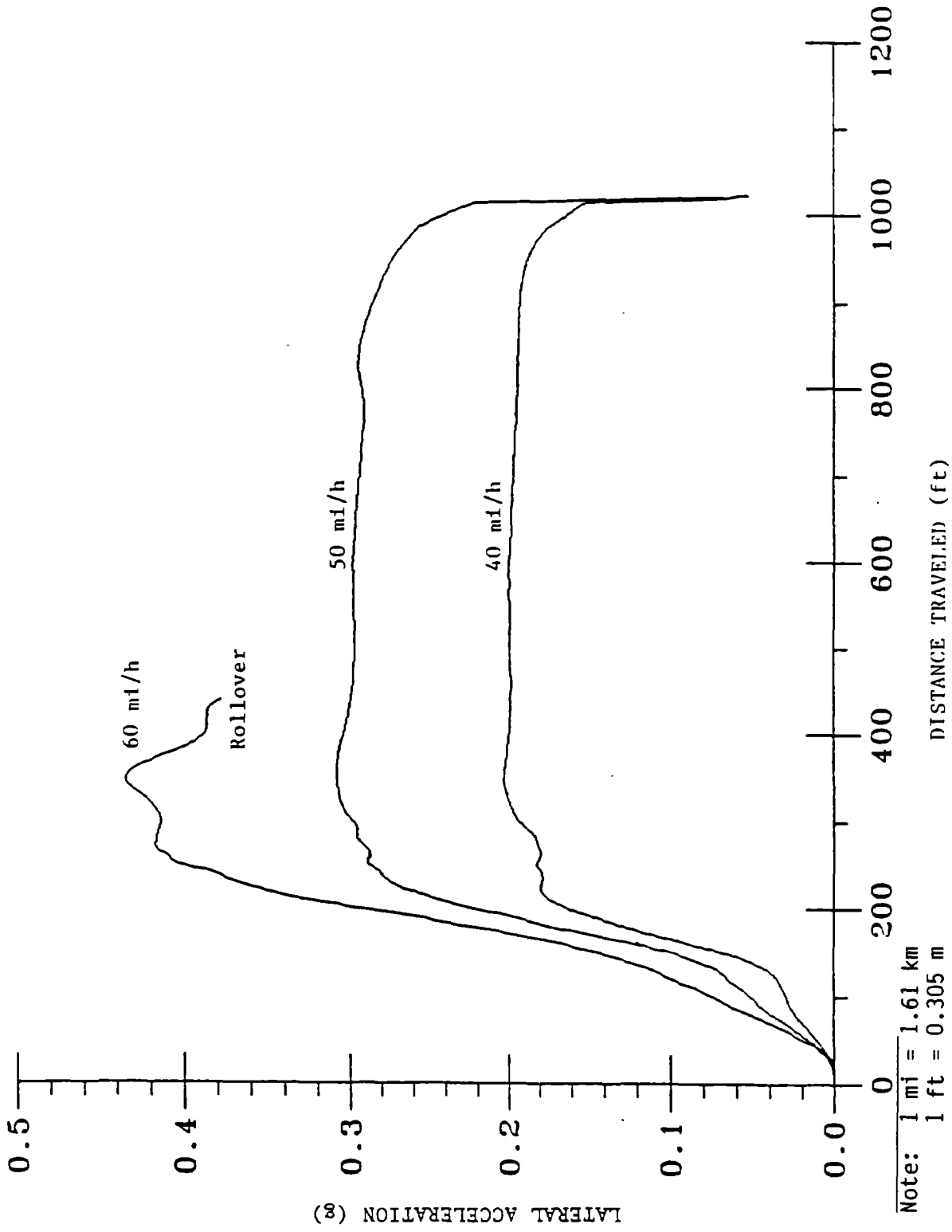


Figure 24. Lateral acceleration versus distance, single-semitrailer truck, case A, Type III transition area.

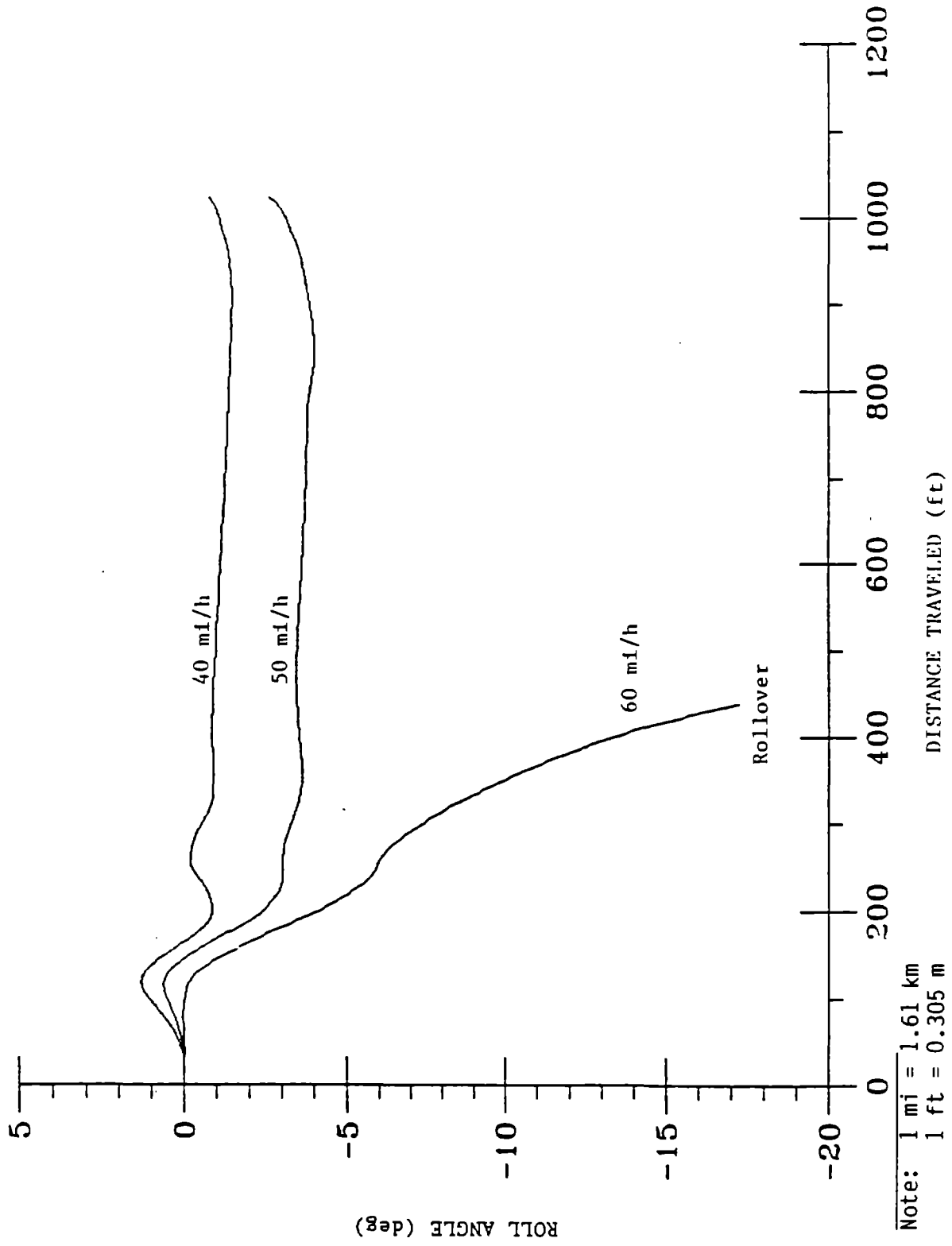


Figure 25. Roll angle versus distance, single-semitrailer truck, case A, Type I transition area.

In an actual turn, the lateral acceleration of the truck reaches a maximum value that exceeds the steady-state lateral acceleration given in equation (17):

$$a_{\max} = M_p a_{ss} \quad (18)$$

where M_p is an overshoot ($M_p \geq 1$). The value of the overshoot, M_p , for a given curve geometry can be calculated from the simulation results using the following equation:

$$M_p - \frac{a_{\max}}{a_{ss}} = \frac{15 R (a_{\max})}{v^2} \quad (19)$$

For linear systems, the value of M_p would be independent of speed. However, since the truck model used in the simulation is nonlinear, M_p varies with speed.

The critical speed formula can now be obtained by combining equations (16), (18), and (19):

$$v_{\text{crit}} = \sqrt{\frac{[p_o + e(x_a)] 15 R}{M_p}} \quad (20)$$

The value of M_p for a given curve geometry was calculated using the simulation results for the highest speed at which rollover did not occur on a given curve.

The values of the critical speed calculated for all cases used in computer simulation are given in table 18. Also listed in table 18 are the values of the AASHTO design speeds. The critical speed exceeds the design speed in all cases. The safety margin is from 11.8 to 33.1 mi/h (19.0 to 53.3 km/h) and is higher for higher design speeds. The values of the acceleration percent overshoot calculated as:

$$M_p \% = \frac{15 R (a_{\max}) - v^2}{v^2} \times 100\% \quad (21)$$

are given in table 19.

Summary of Results: Several key findings are evident from the computer simulation analysis of horizontal curves. These are:

- The simulation results in tables 13 through 15 show that the maximum lateral accelerations experienced at any point on a horizontal curve were only slightly higher than the nominal lateral accelerations indicated by the standard curve formula. The maximum difference in any case was approximately 0.02 g.

Table 18. AASHTO design speed and critical speed values calculated from the computer simulation results.

Case	Critical speed (v_{crit}) (mi/h)			
	AASHTO	Type I	Type II	Type III
A	40	56.3	55.8	57.0
B	50	71.5	70.6	73.0
C	60	90.7	88.9	93.1
D	40	54.5	53.7	54.8
E	50	69.6	68.1	71.0
F	60	88.3	85.5	89.4
G	40	53.7	52.6	53.9
H	50	68.0	66.0	69.3
I	60	85.8	82.5	86.7
J	40	52.9	51.8	53.0
K	50	66.7	64.4	67.6
L	60	84.3	80.3	84.3

Note: 1 mi = 1.61 km

Table 19. Acceleration overshoot values for the simulated cases.

Case	Acceleration overshoot (M_p %)		
	Type I	Type II	Type III
A	8.3	10.4	5.9
B	12.2	15.0	7.4
C	11.4	15.9	5.7
D	8.1	11.2	6.6
E	10.4	15.4	6.2
F	9.0	16.3	6.2
G	7.3	11.5	6.2
H	9.2	15.6	5.1
I	8.0	17.0	6.0
J	6.5	11.2	6.2
K	7.6	15.4	4.7
L	5.9	16.8	5.9
Mean	8.7	14.3	6.0

- The truck in the simulation model rolled over only in those cases where its travel speed exceeded the design speed by 20 mi/h (32 km/h). Rollover would occur at a lower speed if the rollover threshold of the truck were lower than 0.36 g.
- The change in transition geometry from Type I (2/3 - 1/3 rule) to Type II (full superelevation on tangent) increased the maximum lateral acceleration in 20 of the 24 cases. However, the increase was so small--less than 0.02 g in most cases--as to be of little practical significance.
- The Type II transition also generally moved the point of maximum lateral acceleration further into the curve and in most cases increased the negative roll angle of the truck.
- The change in transition geometry from Type I (2/3 - 1/3 rule) to Type III (spiral) reduced the maximum lateral acceleration in 22 of the 24 cases. However, in most cases the benefit of spirals was small--typically less than 0.01 g. The decrease in lateral acceleration due to the presence of a spiral becomes larger as speed increases (except in those cases where the truck rolled over because the speed was too high).
- The spiral transition moved the point of maximum lateral acceleration further into the curve and generally reduced the negative roll angle of the truck.

These results indicate that developing full superelevation on the tangent is not preferable to the use of the 2/3 - 1/3 rule. On the other hand, the use of spiral transitions is desirable. However, because of the small reduction in lateral acceleration, the use of spiral transitions is unlikely to provide a major reduction in rollover accidents.

APPENDIX C

TRUCK OFFTRACKING

When any vehicle is making a turn, its rear wheels do not follow the same path as its front wheels. The magnitude of this difference in paths, known as "offtracking," generally increases with the spacing between the axles of the vehicle and decreases for larger radius turns. Offtracking of passenger cars is minimal because of their relatively short wheelbases; however, many trucks offtrack substantially. The most appropriate descriptor of offtracking for use in highway design is the "swept path width," shown in figure 26 as the difference in paths between the outside front tractor tire and the inside rear trailer tire.

Truck offtracking is addressed in the 1984 AASHTO Green Book through consideration of three design vehicles.¹ The dimensions and turning radii of these design vehicles are given in table 20. The minimum turning radius is defined by the path of the outer front wheel, following a circular arc, at a speed of less than 10 mi/h (16 km/h), and is limited by the vehicle steering mechanism.

Trucks have become longer in recent years as a result of the 1982 Surface Transportation Assistance Act (STAA) and other factors. Table 21 presents the design vehicles recommended in this contract for consideration in highway design. Table 22 presents the detailed axle spacings for those vehicles.

A. Background

The 1984 AASHTO Green Book notes that there are two distinct types of offtracking. Low-speed offtracking is a purely geometrical phenomenon wherein the rear axle(s) of a truck track toward the inside of a horizontal curve, relative to the front axle. Figure 26 illustrates low-speed offtracking. Considerable research has been performed concerning low-speed offtracking, as a function of truck and roadway geometrics, and it is well understood on level surfaces. However, pavement cross-slope, including superelevation on horizontal curves, has an effect on low-speed offtracking that has not been documented in previous research.

High-speed offtracking, on the other hand, is a dynamic, speed-dependent phenomenon. It is caused by the tendency of the rear of the vehicle to move outward due to the lateral acceleration of the vehicle as it negotiates a horizontal curve at higher speeds. High-speed offtracking is less well understood than low-speed offtracking, and it is a function not only of truck and roadway geometrics, but also of the vehicle speed and the suspension, tire, and loading characteristics of the vehicle.

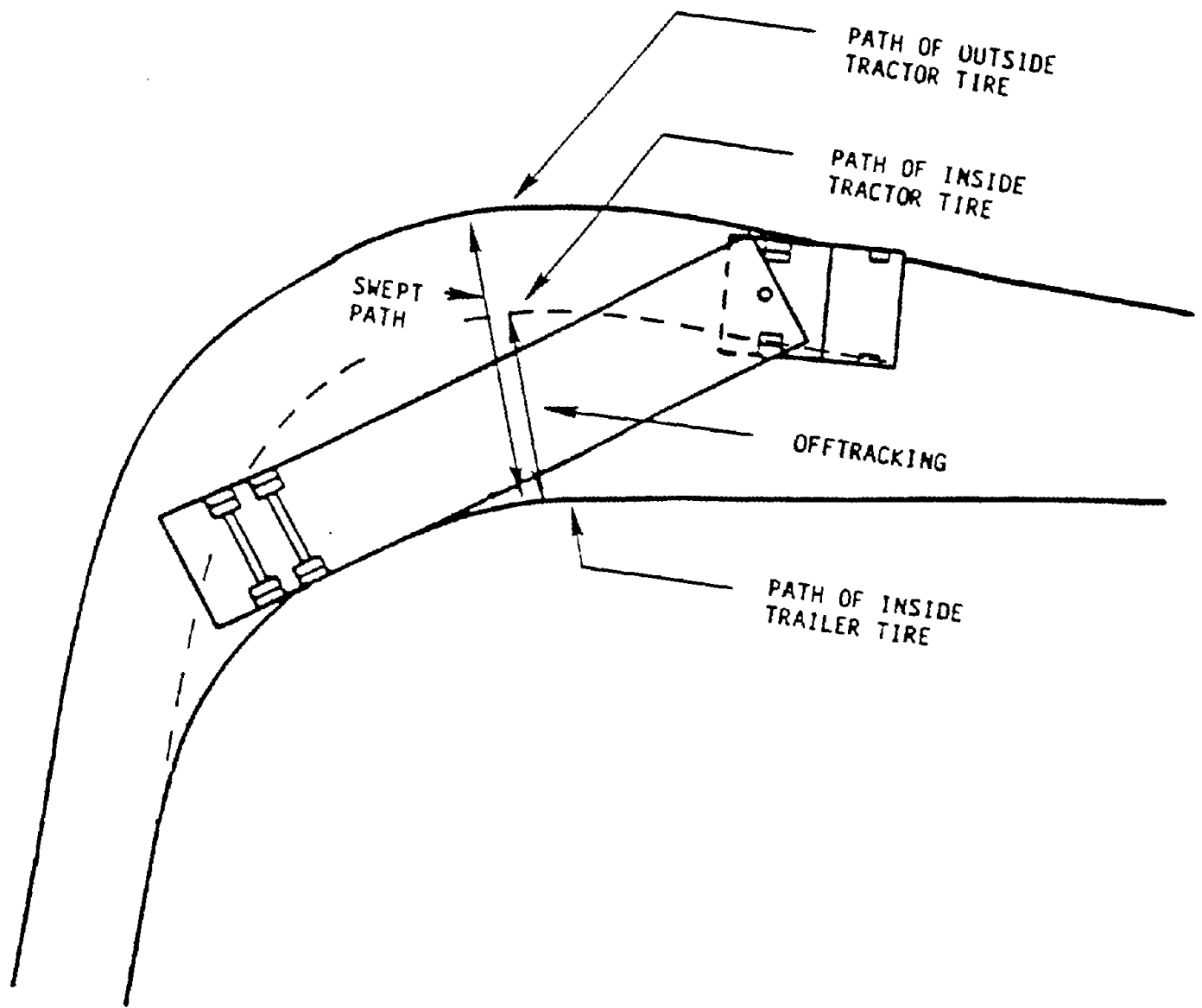


Figure 26. Swept path width and offtracking of a truck negotiating a 90-degree intersection turn.²⁶

Table 20. AASHTO design vehicle dimensions. 1

Design Vehicle Type	Symbol	Height	Dimension (ft)						WB ₁	WB ₂	S	T	WB ₃
			Overall			Overhang							
			Width	Length	Front	Rear	Front	Rear					
Passenger car	P	4.25	7	19	3	5	11						
Single unit truck	SU	13.5	8.5	30	4	6	20						
Single unit bus	BUS	13.5	8.5	40	7	8	25						
Articulated bus	A-BUS	10.5	8.5	60	8.5	9.5	18			4 ^a	20 ^a		
Combination trucks													
Intermediate semitrailer	WB-40	13.5	8.5	50	4	6	13	27					
Large semitrailer	WB-50	13.5	8.5	55	3	2	20	30					
"Double Bottom" semi-trailer - full-trailer	WB-60	13.5	8.5	85	2	3	9.7	20		4 ^b	5.4 ^b	20.9	
Recreation vehicles													
Motor home	MH		8	30	4	6	20						
Car and camper trailer	P/T		8	49	3	10	11	5		18			
Car and boat trailer	P/B		8	42	3	8	11	5		15			

a = Combined dimension 24, split is estimated.

b = Combined dimension 9, 4, split is estimated

WB₁, WB₂, WB₃, are effective vehicle wheelbases.

S is the distance from the rear effective axle to the hitch point.

T is the distance from the hitch point to the lead effective axle of the following unit.

NOTE: 1 ft = 0.305 m

Table 21. Recommended dimensions for longer design vehicles.

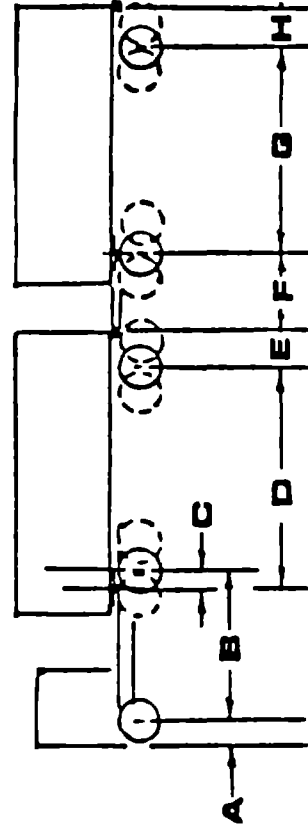
Design vehicle	Dimension (ft)									
	Height	Overall Width	Length	Overhang Front	Overhang Rear	WB ₁	WB ₂	S	T	WB ₃
STAA single with 48-ft trailer and conventional tractor	13.5	8.5	63.5-65.5	2.5	4.5	18.0	38.0-40.0	40.0	-	-
STAA single with 48-ft trailer and long tractor	13.5	8.5	65.5-67.5	2.5	4.5	20.0	38.0-40.0	40.0	-	-
Long single with 53-ft trailer and conventional tractor	13.5	8.5	68.5-70.5	2.5	4.5	18.0	43.0-45.0	45.0	-	-
STAA double with cab-over-engine tractor	13.5	8.5	66.5-68.5	2.5	2.5	10.0	20.5-22.5	22.5	6.0	22.5
STAA double with conventional tractor	13.5	8.5	69.5-71.5	2.5	2.5	13.0	20.5-22.5	22.5	6.0	22.5

Note: WB, WB₁, WB₂, S, T, and WB₃ are defined in table 20.
 1 ft = 0.305 m

Table 22. Detailed axle spacing for longer design vehicles.

Design vehicle	Dimension (ft)								Overall length
	A	B	C	D	E	F	G	H	
STAA single with 48-ft trailer and conventional tractor	2.5	18.0	0.0-2.0	40.5	4.5	-	-	-	63.5-65.5
STAA single with 48-ft trailer and long tractor	2.5	20.0	0.0-2.0	40.5	4.5	-	-	-	65.5-67.5
Long single with 53-ft trailer	2.5	18.0	0.0-2.0	45.5	4.5	-	-	-	68.5-70.5
STAA double with cab-over-engine tractor	2.5	10.0	0.0-2.0	22.5	2.5	6.0	22.5	2.5	66.5-68.5
STAA double with cab-behind-engine tractor	2.5	13.0	0.0-2.0	22.5	2.5	6.0	22.5	2.2	69.5-71.5

Note: Dimensions A through H are defined below.
1 ft = 0.305 m



Current AASHTO criteria for intersection and channelization geometrics and for pavement widening on horizontal curves consider only low-speed off-tracking. The design of intersection and channelization geometrics is properly a function of low-speed offtracking only, because truck operations at intersections generally occur at low speeds. Pavement cross-slope effects on offtracking can generally be ignored in the design of intersection and channelization geometrics, because normal pavement cross-slopes are generally small. Turning roadways at channelized intersections generally operate at low speeds and therefore, do not require much superelevation. However, pavement widening at horizontal curves should consider both low-speed and high-speed offtracking, including superelevation effects.

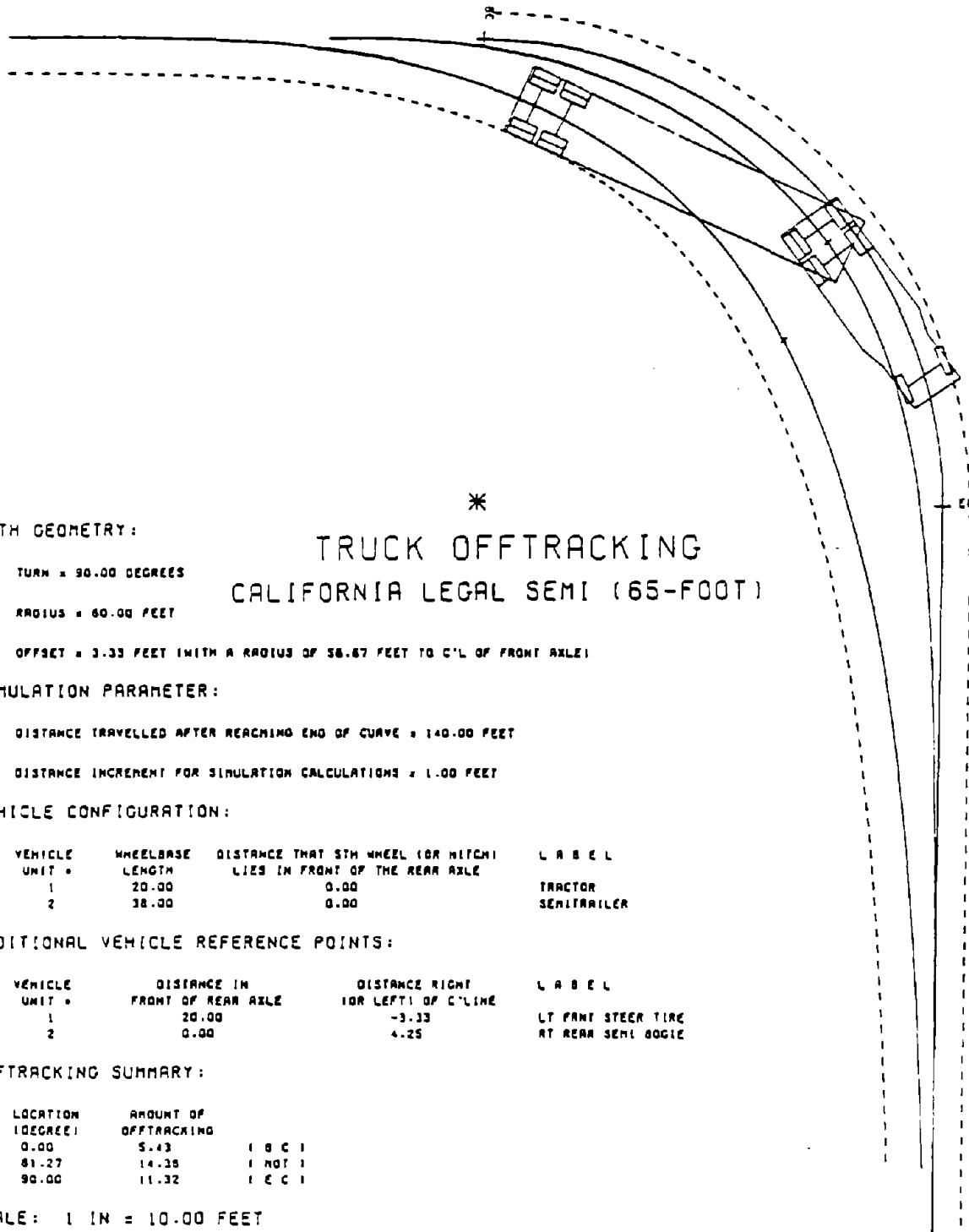
The next section documents the low-speed offtracking characteristics of the recommended design vehicles for use in design of intersection and channelization geometrics. The following section documents the broader consideration of offtracking in pavement widening on horizontal curves.

B. Low-Speed Offtracking

Low-speed offtracking is a well-known phenomenon that has been addressed extensively in past research and is considered in current AASHTO design criteria. The geometrics of low-speed offtracking is addressed by a series of models developed for FHWA and State highway agencies. An offtracking model was developed for FHWA in 1983.²⁷ This model was intended to be run on an Apple microcomputer. An IBM PC version of this model was subsequently developed for FHWA.²⁸ The user specifies the turning path to be followed by the front axles of the truck and the models plot the path of the rear axle and other specified points on the truck. Both the Apple and IBM PC provide plotted output but have no capability for numerical output.

More recently, the IBM PC version of the truck offtracking model was enhanced by the California Department of Transportation (Caltrans) to include numerical output of offtracking and swept pathwidths as well as the turning plot.²⁹ The Caltrans model is intended to run on an IBM mainframe computer. Figure 27 illustrates the output of the Caltrans model.

The Caltrans model was run as part of this study to compare the off-tracking performance of the design vehicles specified in tables 21 and 22 to smaller design vehicles with 37 ft (11.2 m) (WB-50) and 45 ft (13.7 m) trailers.



*
TRUCK OFFTRACKING
CALIFORNIA LEGAL SEMI (65-FOOT)

PATH GEOMETRY:

TURN = 90.00 DEGREES

RADIUS = 60.00 FEET

OFFSET = 3.33 FEET (WITH A RADIUS OF 58.67 FEET TO C/L OF FRONT AXLE)

SIMULATION PARAMETER:

DISTANCE TRAVELLED AFTER REACHING END OF CURVE = 140.00 FEET

DISTANCE INCREMENT FOR SIMULATION CALCULATIONS = 1.00 FEET

VEHICLE CONFIGURATION:

VEHICLE UNIT #	WHEELBASE LENGTH	DISTANCE THAT 5TH WHEEL (OR HITCH) LIES IN FRONT OF THE REAR AXLE	L A B E L
1	20.00	0.00	TRACTOR
2	38.00	0.00	SEMITRAILER

ADDITIONAL VEHICLE REFERENCE POINTS:

VEHICLE UNIT #	DISTANCE IN FRONT OF REAR AXLE	DISTANCE RIGHT OR LEFT OF C/LINE	L A B E L
1	20.00	-3.33	LT FRONT STEER TIRE
2	0.00	4.25	RT REAR SEMI BOGIE

OFFTRACKING SUMMARY:

LOCATION (DEGREE)	AMOUNT OF OFFTRACKING	
0.00	5.43	(B C)
81.27	14.38	(NOT)
90.00	11.32	(C)

SCALE: 1 IN = 10.00 FEET

DATE: 04/19/88

TAPE REEL: 238317

Note: All distances given on this output are in feet (1 ft = 0.305 m).

Figure 27. Example of output provided by Caltrans truck offtracking model.²⁹

Figures 28 through 34 show the maximum offtracking at any point during a turn for specified values of turn radius and turn angle for the following vehicles:

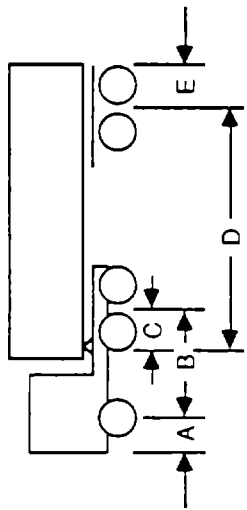
37-ft (11.2-m) semitrailer with conventional tractor (WB-50)	Figure 28
45-ft (23.7-m) semitrailer with conventional tractor	Figure 29
48-ft (14.6-m) STAA semitrailer with conventional tractor	Figure 30
48-ft (14.6-m) STAA semitrailer with long tractor	Figure 31
53-ft (16.2-m) semitrailer with conventional tractor	Figure 32
STAA double-trailer truck with cab-over-engine tractor	Figure 33
STAA double trailer truck with cab-behind-engine tractor	Figure 34

Figures 28 through 34 all represent trucks with a fifth-wheel offset (Dimension C) equal to zero. Fifth-wheel offsets up to 2 ft (0.6 m) are common, but research by Caltrans has shown that moving the fifth-wheel has very little effect on the offtracking performance of the truck.

Swept path widths can be calculated directly by adding 7.58 ft (2.31 m) to the maximum offtracking values shown in figures 28 through 34. Since the Caltrans model calculates offtracking along the truck centerline and the swept path width is the difference in path between front outside axle and the rear inside axle, the difference between offtracking and swept path width is one-half of the tractor axle width plus one-half of the rear trailer axle width. The tractor axle is typically 6.66 ft (2.03 m) wide and the rear trailer axle is typically 8.5 ft (2.59 m) wide, so half their sum is 7.58 ft (2.31 m).

Table 23 compares the maximum offtracking and swept path width for specifying the radii and turn angles for the design vehicles shown in figures 28 through 34 for selected combinations of turn radius and turn angle. The table shows that for the single trailer configurations the amount of offtracking increases nearly linearly with trailer length. For 90° turns the offtracking with a 53-ft (16.2-m) trailer is almost double the offtracking of the WB-50 configuration. The offtracking of doubles is much less than that of STAA singles, and is approximately the same as that of the WB-50.

The results in figures 28 through 34 and table 23 can be used as the basis for design of intersection and channelization geometrics which generally have short radii (up to 300 ft or 110 m). The design of horizontal curves requires consideration of longer radius curves. Figure 35 shows the offtracking on long radius curves for the 48-ft (14.6-m) STAA semitrailer with a long tractor. Thus, figure 35 is simply an extension of figure 31 to longer radii. Comparison of figures 31 and 35 shows that low-speed offtracking exceeds 2 ft (0.6 m) for 48-ft (14.6-m) single-semitrailer truck for horizontal curves with radii up to approximately 500 ft (150 m).



Single 37-ft semitrailer with conventional tractor (WB-50)

A	B	C	D	E
3.0	18.0	0.0	30.0	4.0

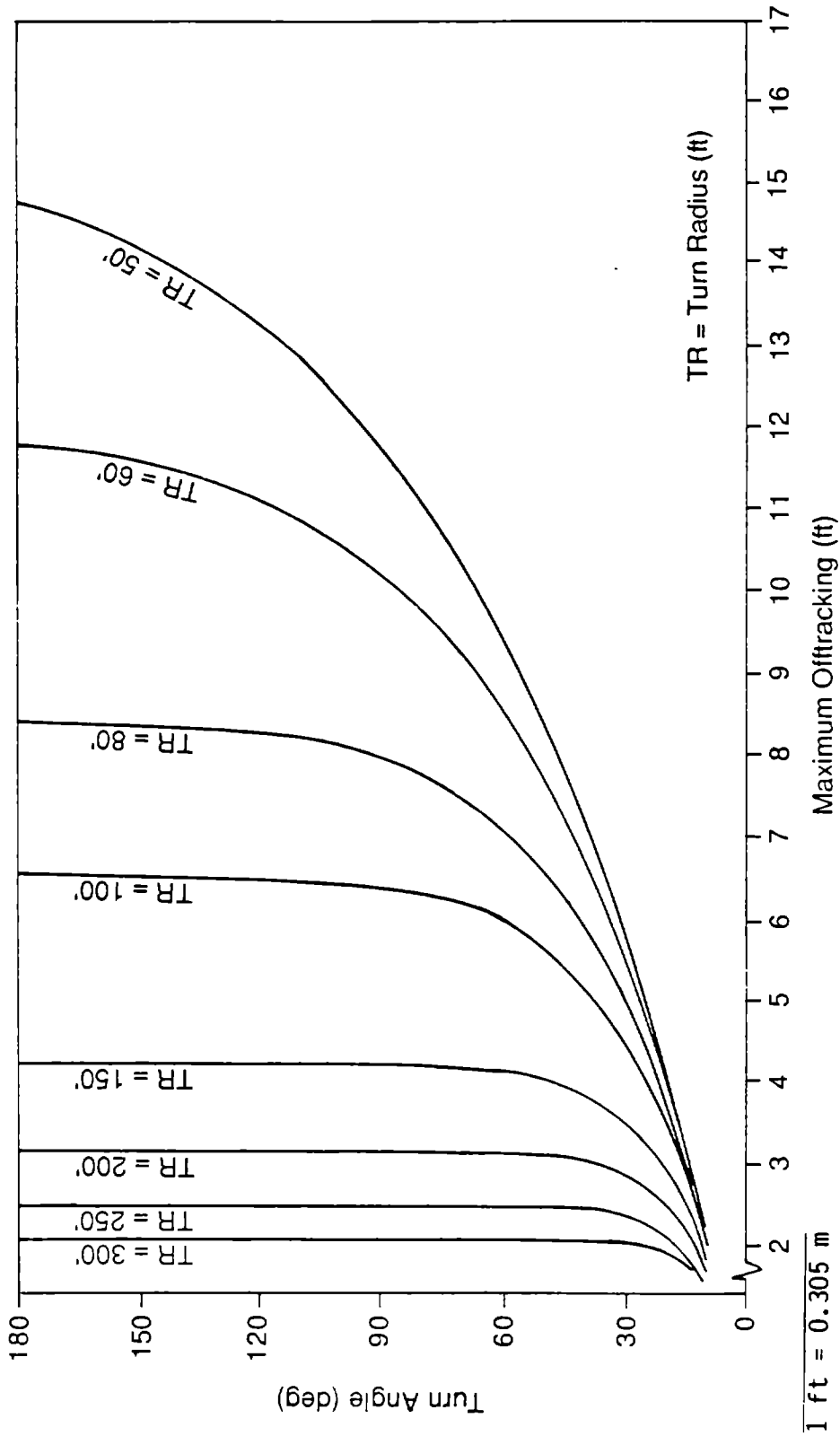
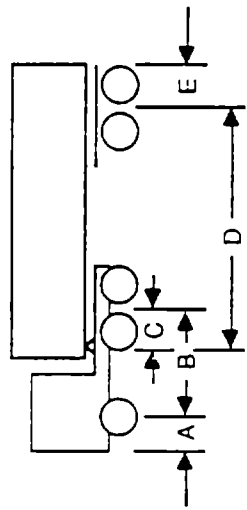


Figure 28. Offtracking plot for single 37-ft (11.2-m) semitrailer truck with conventional tractor (WB-50).



Single 45-ft semitrailer with conventional tractor

A	B	C	D	E
3.0	18.0	0.0	37.5	4.5

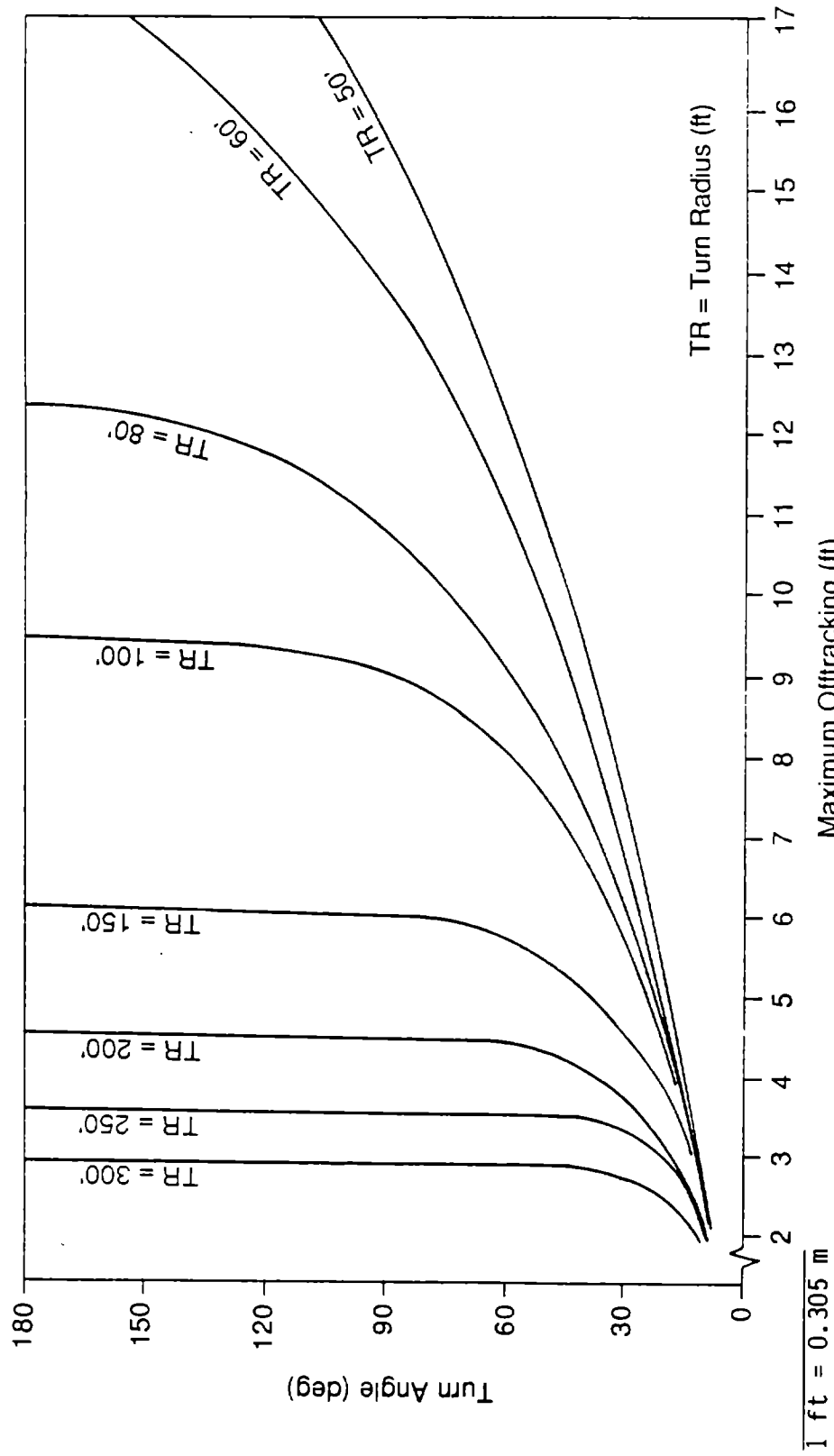
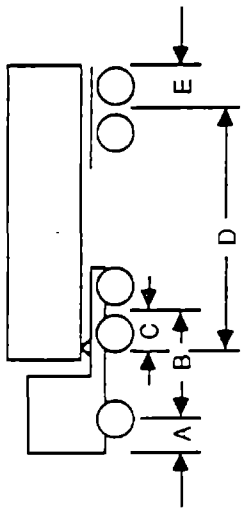


Figure 29. Offtracking plot for single 45-ft (23.7-m) semitrailer truck with conventional tractor.



STAA 48-ft semitrailer with conventional tractor

A	B	C	D	E
3.0	18.0	0.0	40.5	4.5

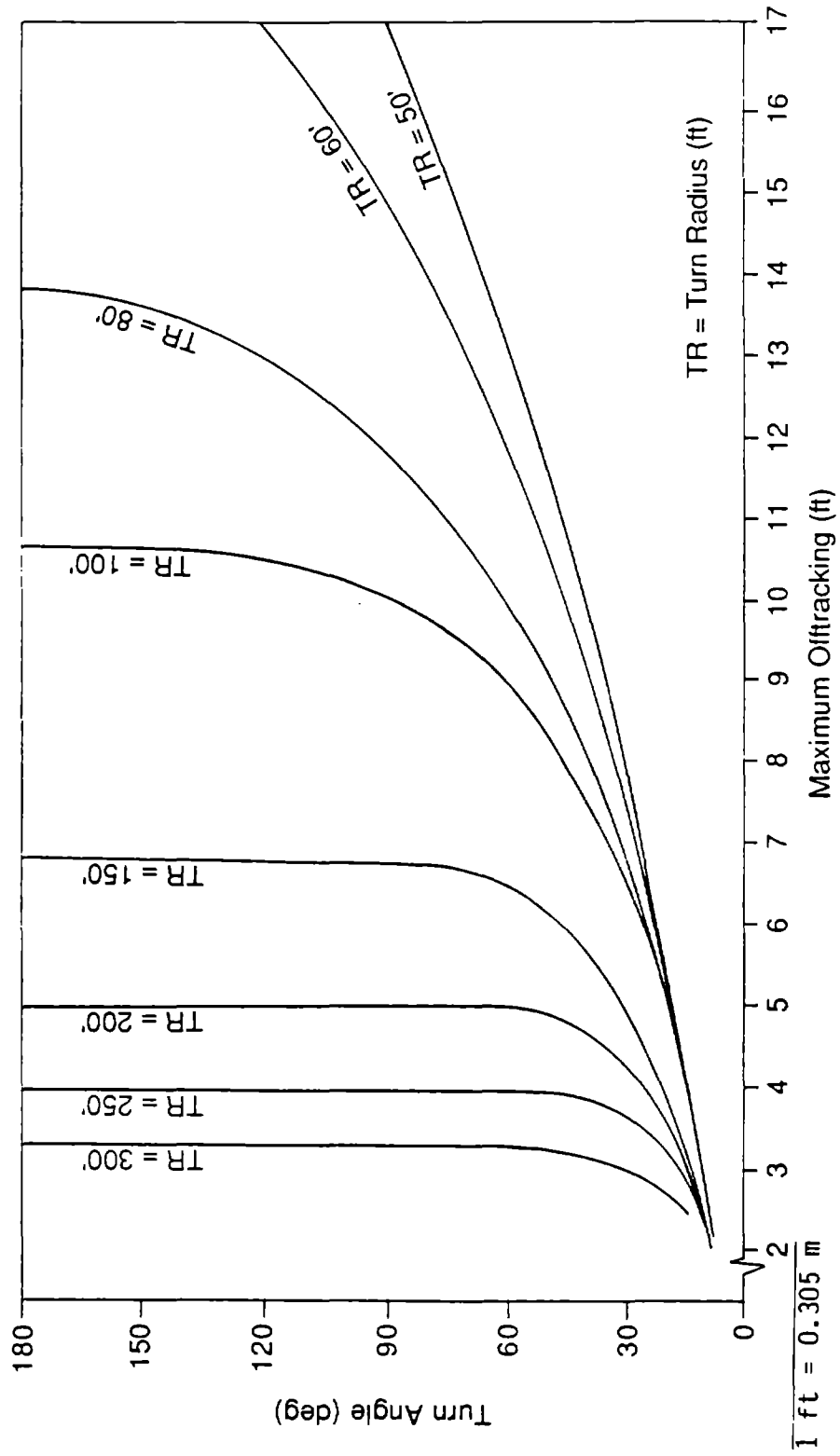
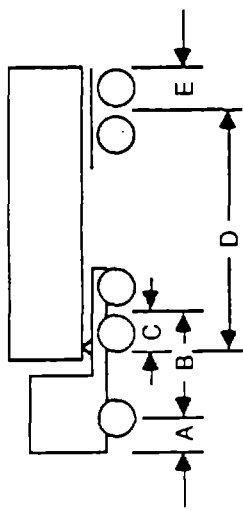


Figure 30. Offtracking plot for STAA single 48-ft (14.6-m) semitrailer truck with conventional tractor.



STAA single 48-ft semitrailer with long tractor

A	B	C	D	E
3.0	20.0	0.0	40.5	4.5

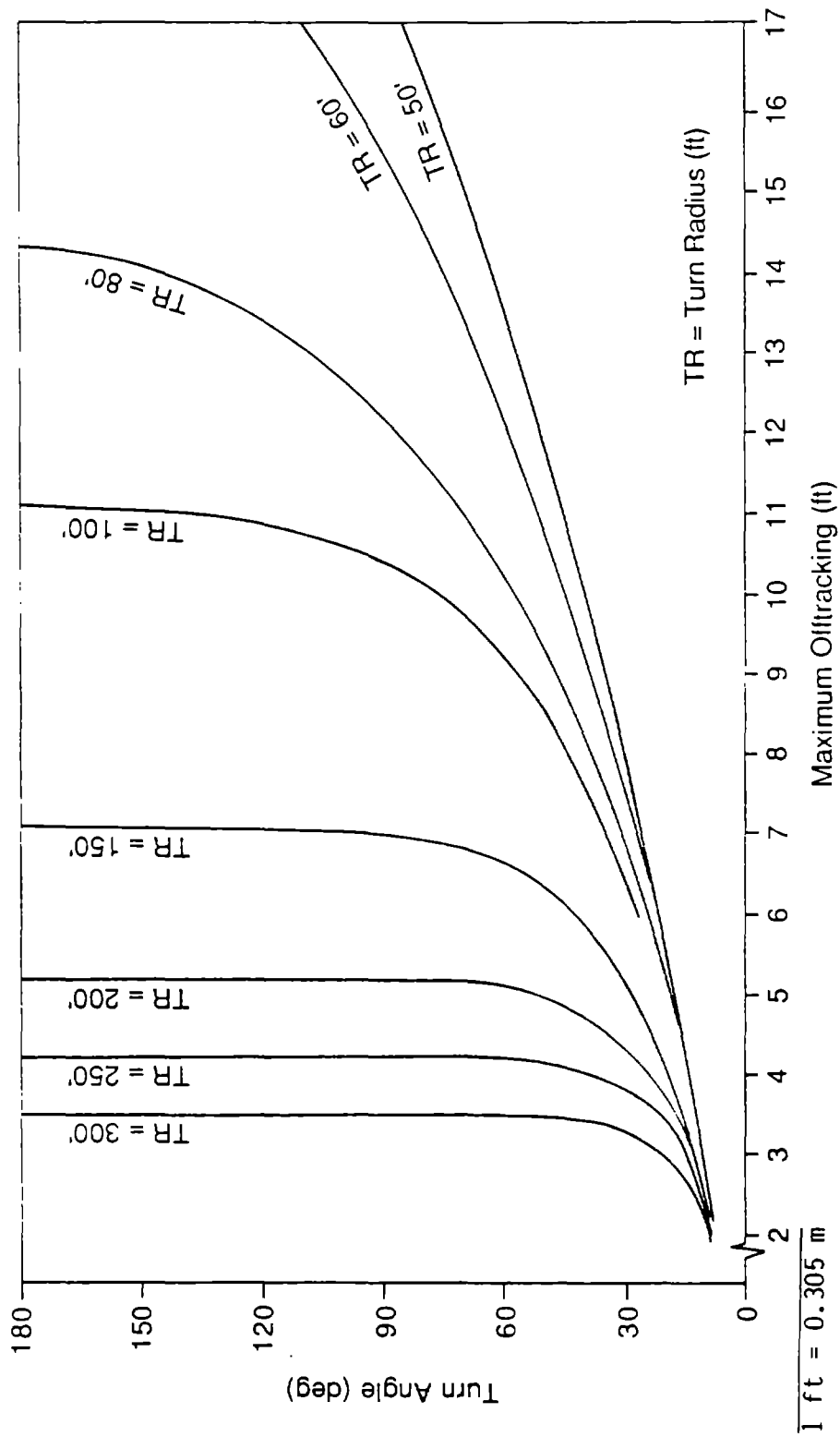
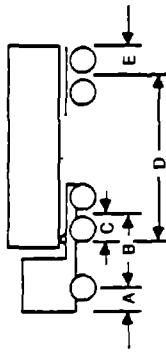


Figure 31. Offtracking plot for STAA single 48-ft (14.6-m) semitrailer truck with long tractor.



Single 53 ft semitrailer with conventional tractor

A	B	C	D	E
3.0	18.0	0.0	45.5	4.5

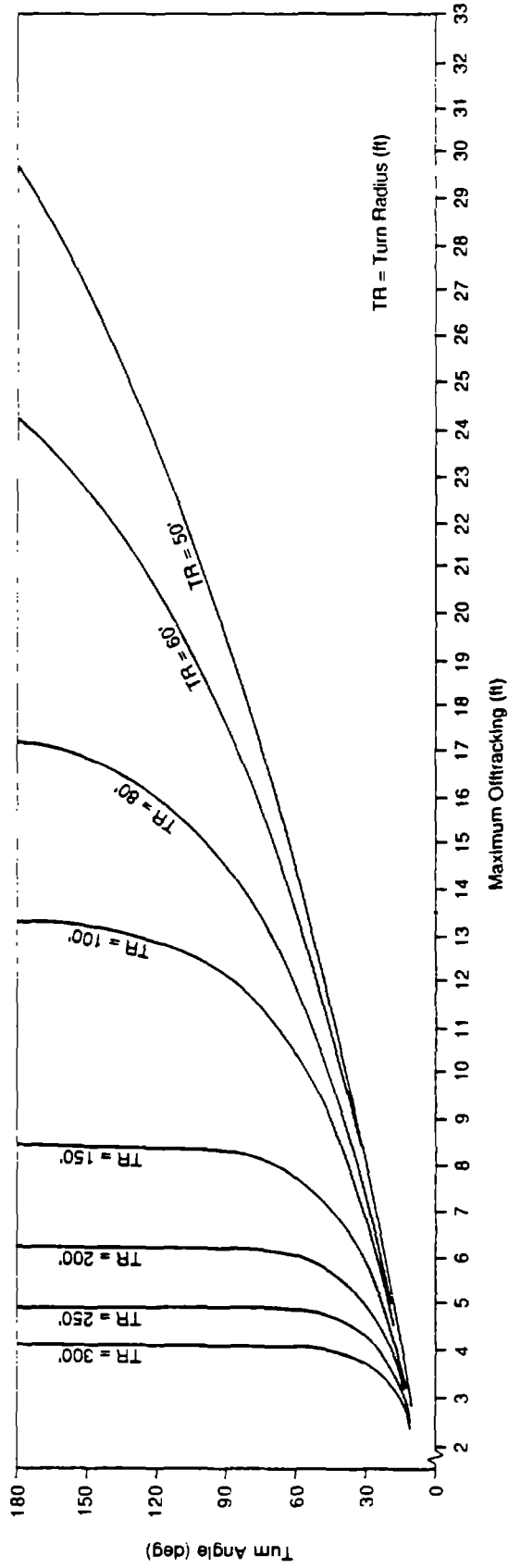


Figure 32. Offtracking plot for long single 53-ft (16.2-m) semitrailer truck with conventional tractor.

$1 \text{ ft} = 0.305 \text{ m}$

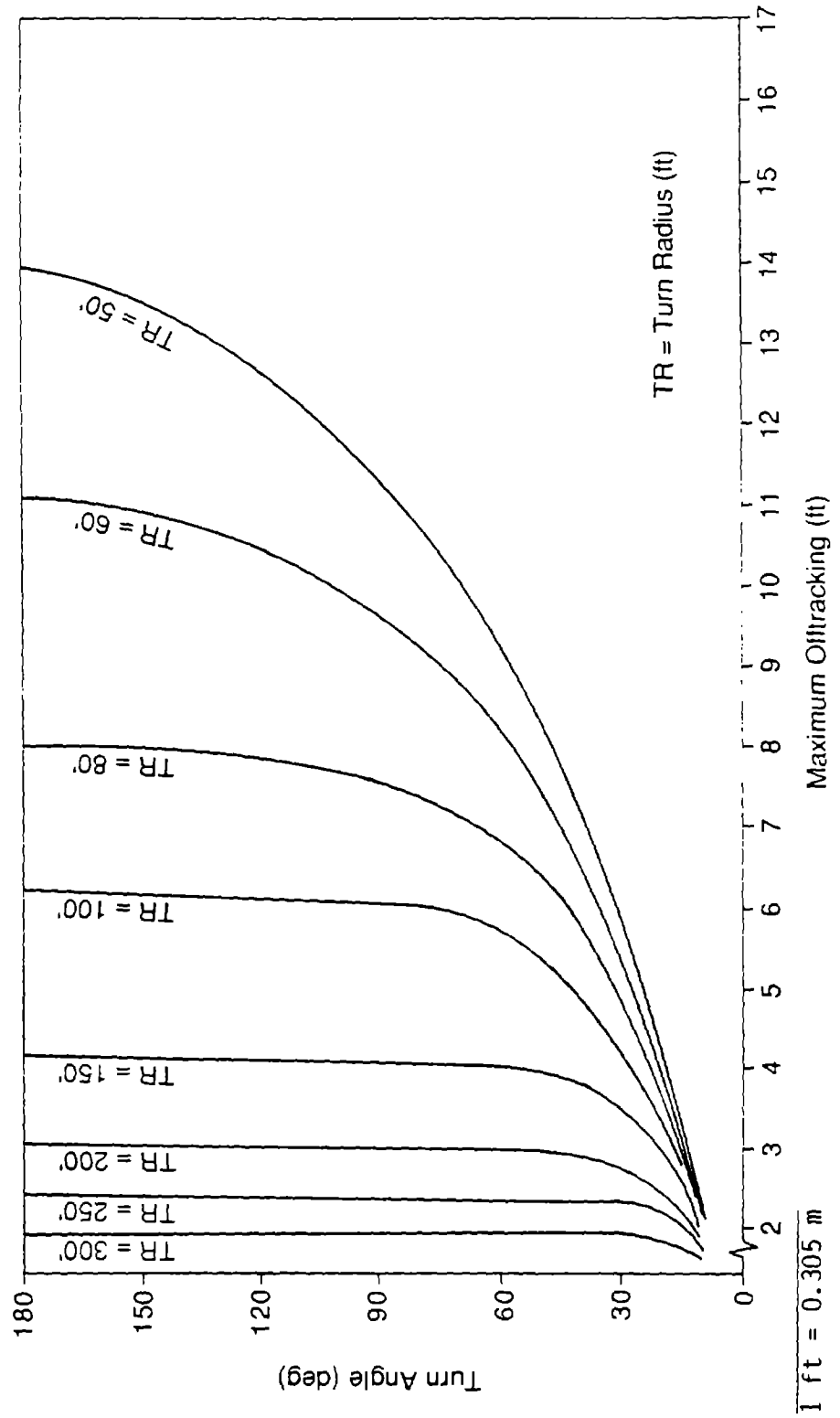
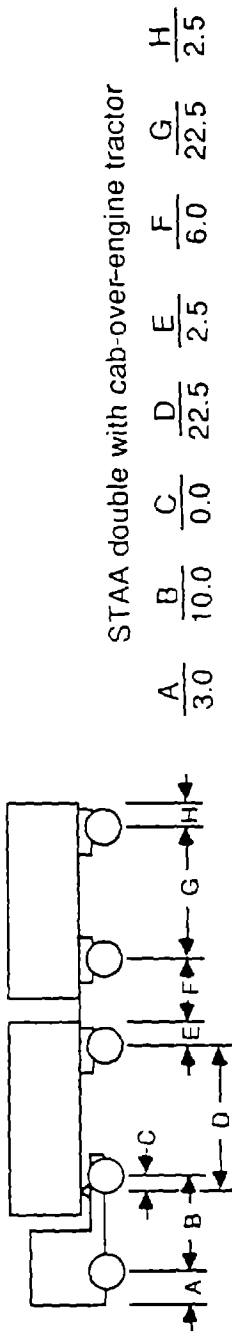


Figure 33. Offtracking plot for STAA double-trailer truck with cab-over-engine tractor.

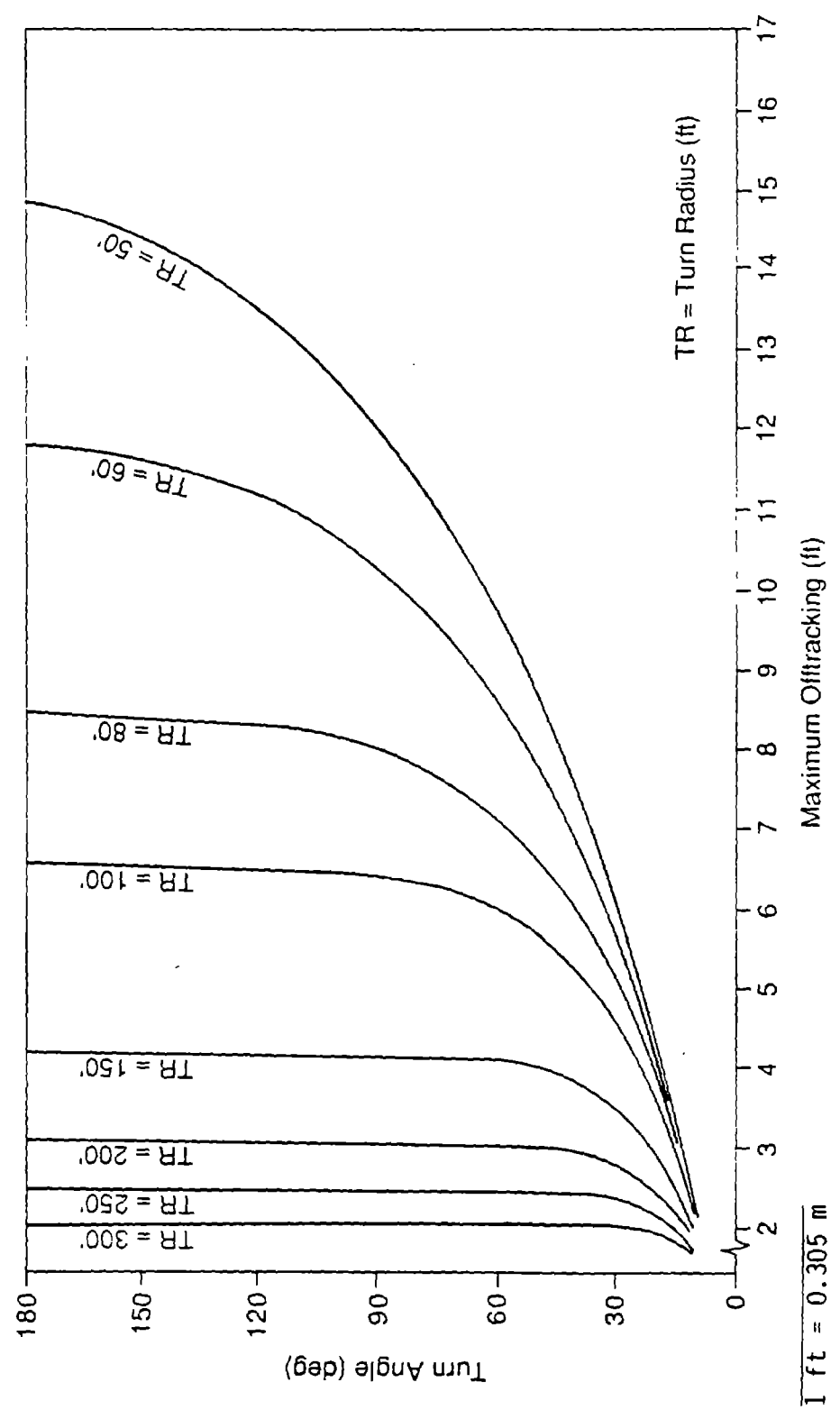
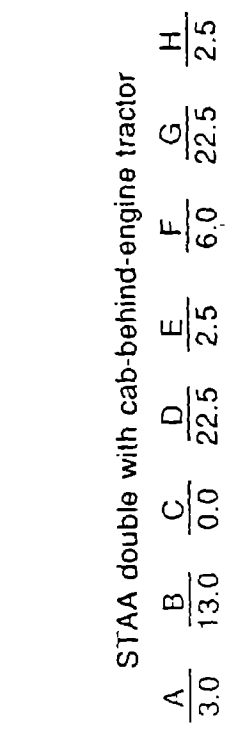


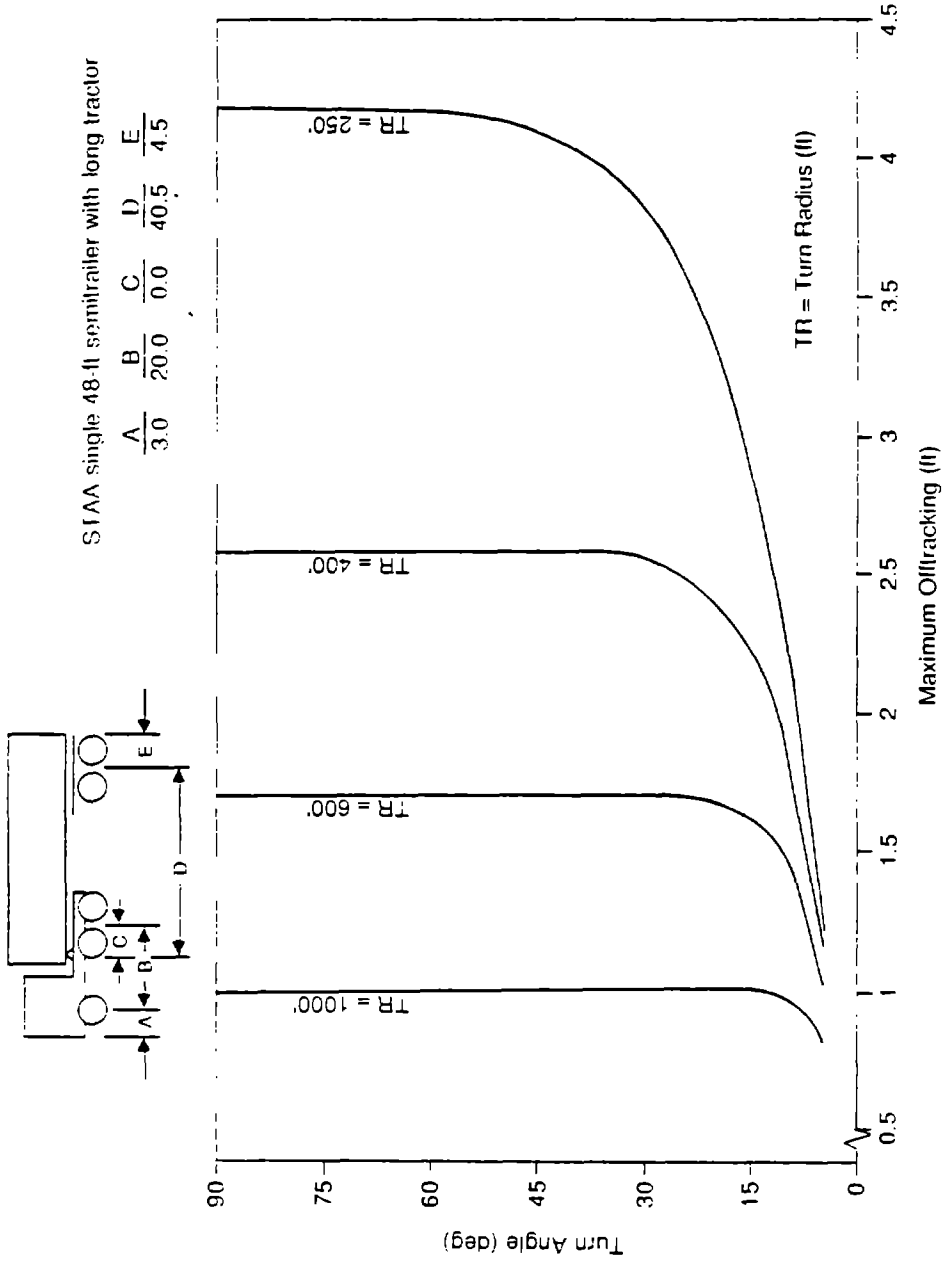
Figure 34. Offtracking plot for STAA double-trailer truck with cab-behind-engine tractor.

Table 23. Offtracking for selected combinations of turn radius and turn angle.

Turn radius (ft) Turn angle:	Maximum offtracking(ft) ^a								
	50			100			300		
	60°	90°	120°	60°	90°	120°	60°	90°	120°
<u>Design vehicle</u>									
Single with 37-ft trailer (WB-50)	9.3	11.8	13.3	6.0	6.5	6.6	2.1	2.1	2.1
Single with 45-ft trailer	12.1	15.5	-	8.0	9.0	9.4	2.9	2.9	2.9
STAA single with 48-ft trailer and conventional tractor	13.0	16.9	-	8.8	10.0	10.5	3.3	3.3	3.3
STAA single with 48-ft trailer and long tractor	13.4	17.4	-	9.1	10.4	10.8	3.4	3.4	3.4
Long single with 53-ft trailer	14.4	19.5	23.4	10.3	12.1	12.8	4.1	4.1	4.1
STAA double with cab-over-engine tractor	9.2	11.3	12.6	5.8	6.1	6.2	1.9	1.9	1.9
STAA double with cab-behind-engine tractor	9.6	11.9	13.4	6.0	6.4	6.4	2.1	2.1	2.1

^a Add 7.58 ft to entries in this table to get maximum swept path width.

Note: 1 ft = 0.305 m.



1 ft = 0.305 m

Figure 35. Offtracking plot for STAA single 48-ft (16.2-m) semitrailer with long tractor on long radius turns.

The implications of the offtracking and swept path width results derived here for design of intersection and channelization geometrics are addressed in volume I.

C. Model for Low-Speed and High-Speed Offtracking Including Superelevation Effects

Various models and formulas have been developed to estimate offtracking by trucks in turns so that turning plots like figure 27 need not be developed for every application. An early example is the Western Highway Institute (WHI) offtracking formula.³⁰ Low-speed offtracking develops gradually as a truck traverses a turn, as is illustrated by figures 28 through 35. The WHI formula estimates the magnitude of fully developed low-speed offtracking, i.e., the maximum offtracking that will occur for any turn angle during a given radius of turn.

In 1981, Bernard and Vanderploeg developed an offtracking model that includes both the low-speed and high-speed contributions to offtracking.³¹ However, their model applies only to vehicles on a level surface. A new model has been developed in this study that extends the Bernard and Vanderploeg model to incorporate the added effect of superelevation on offtracking. Both the Bernard and Vanderploeg model and the new model give values for fully developed offtracking. On shorter curves, the actual offtracking may be less than the fully developed offtracking as indicated by turning templates or computer plotting models, such as the Caltrans model.²⁹

The new model for offtracking of two consecutive axles, axle sets (i.e., tandems or triaxles), or hitch points, is:

$$\begin{aligned}
 OT = & -\frac{\ell^2}{R} \left[0.5 + \frac{\sum (a_i/\ell)^2}{n(1+t/\ell)} \right] \\
 & + \frac{\ell U^2}{R} \left[\frac{1}{\bar{C}_a g(1+t/\ell)} + S \right] \\
 & - \frac{\ell \theta}{\bar{C}_a (1+t/\ell)} - S \ell g \theta
 \end{aligned} \tag{21}$$

- where: OT = fully developed offtracking (ft)
- z = distance between two consecutive axles or centerlines of axle sets or hitch points (ft)
- R = radius of curvature (ft)
- a_i = distance from centerline of axle set to i^{th} axle (ft) (for single axles, $a_1 = 0$; for tandem axles, $a_1 = a_2 = 2$ ft; for triaxles, $a_1 = a_3 = 2$ ft; $a_2 = 0$)
- n = number of axles in set ($n = 1$ for single axle, $n = 2$ for tandem axle, $n = 3$ for triaxle)
- t = pneumatic trail (ft) (for typical values, see page 31 of reference 10)
- U = speed of vehicle (ft/sec)
- g = acceleration of gravity (ft/s²) (equivalent to 32.2 ft/s² or 9.8 m/s²)
- \bar{C}_α = ratio of total cornering stiffness to total normal load (rad⁻¹) (see Equation (22))
- S = roll steer angle (see equation (23))
- θ = superelevation of curve (ft/ft)

The ratio of the total cornering stiffness to total normal load is determined as:

$$\bar{C}_\alpha = \frac{n(C_\alpha/F_{Zr})(F_{Zr})(n_t)(57.296)}{W_a} \quad (22)$$

- where: C_α = cornering stiffness of tires (lb⁻¹ deg⁻¹) (note: page 27 of reference 10 indicates that C_α/F_{Zr} is in the range from 0.1 to 0.2 deg⁻¹)
- F_{Zr} = rated load of tire (lb) (note: typical values are given on page 27 of reference 10)
- n_t = number of tires per axle (usually 4)
- W_a = load (weight) carried by the suspension for axle set (lb)

The roll steer angle is determined as:

$$S = \frac{M_a f s h}{k_r - M_a f g h} \quad (23)$$

where: $M_a f$ = sprung mass supported by axle set (lb-sec²/ft) (= W_a/g)
 s = suspension roll steer coefficient (degrees of steer per degree of roll) (for typical values, see page 66 of reference 10)
 k_r = composite roll stiffness (ft-lb/rad) (for typical values, see page 60 of reference 10)
 h = distance between load center of gravity and suspension roll center, $h_{CG} - h_{RC}$
 h_{CG} = height of center of gravity of load carried by the axle set (ft)
 h_{RC} = height of roll center of suspension system for the axle set (ft) (for typical values, see page 65 of reference 10)

Equation (21) consists of four terms. The first term represents the traditional low-speed offtracking, without superelevation. For a single axle ($a_i = 0$), the first term reduces to:

$$OT = - \frac{0.5 u^2}{R} \quad (24)$$

which is the Western Highway Institute offtracking formula.³⁰

The second term in equation (21) is the speed-dependent term and represents high-speed offtracking. The sign of the second term is positive, indicating that high-speed offtracking tends to offset the low-speed offtracking.

The third and fourth terms represent the effect of superelevation on offtracking. The third term represents the influence of the superelevation itself, and the fourth term represents the influence of roll steer caused by the superelevation.

The sign of offtracking (OT) calculated with equation (21) should be interpreted as follows. For an axle or axle set, negative offtracking indicates that the rear axle tracks inside of the lead axle. Positive offtracking indicates that the rear axle tracks outside of the lead axle. For a hitch point, the sign convention is reversed. Thus, if OT is negative, the hitch point tracks outside of the lead axle. The offtracking for an entire vehicle

is determined as the sum of the individual OT values for all axles or axle sets behind the steering axle and for all hitch points:

$$\text{Total OT} = \sum_j (X_j)(OT_j) \quad (25)$$

where: $X_j = 1$ for an axle or axle set

$X_j = -1$ for a hitch point

$OT_j =$ offtracking for axle, axle set, or hitch point determined from equation (21)

The derivation of this new offtracking model is presented in the next section. Section E examines the sensitivity of the offtracking model to typical ranges of the variables in equations (21), (22), and (23).

D. Derivation of Offtracking Model

Several years ago Bernard and Vanderploeg published a paper describing the mathematics of offtracking, including both the commonly known "low-speed" offtracking as well as the less studied "high-speed" offtracking.³¹ They developed the basic equation of motion for a trailer, as a function of the trailer characteristics and the motion of the hitch point. They then examined in detail the special case of most interest--the motion when the trailer is making a steady turn of radius R at speed U.

The present derivation follows that of Bernard and Vanderploeg, but is limited to the special case of constant R and U. However, it incorporates added features not considered by them. First, it explicitly includes the effects of superelevation. The superelevation directly reduces "high-speed" offtracking, as well as interacts with the roll-steer behavior of the vehicle. Secondly, roll of the body of the trailer relative to the axle(s) also contributes to roll steer. In the following, we use the basic nomenclature and deviation of Vanderploeg, but with the changes just noted.³¹

From figure 36, applying Newton's second law in the direction perpendicular to the trailer centerline gives

$$M(A_y) = H_f + \sum_i F_{ri} \quad (26)$$

where the trailer mass is M, the lateral acceleration is A_y , H_f is the lateral force at the hinge point, and F_{ri} is the lateral force at the tires on axle i.

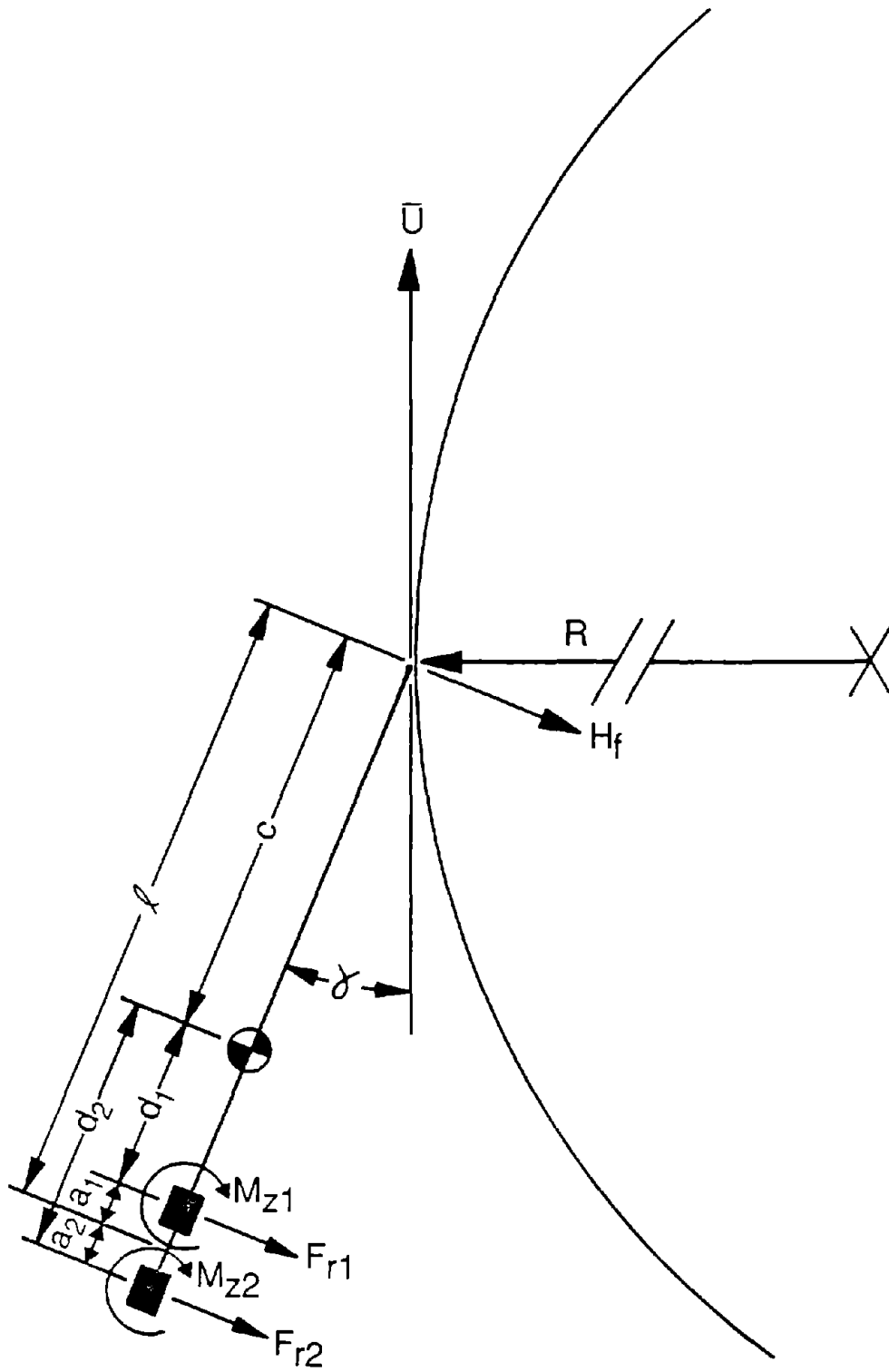


Figure 36. Forces and moments on trailer.

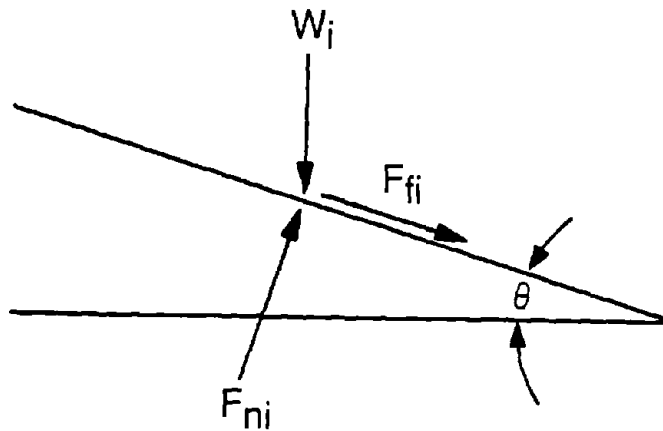


Figure 37. Tire/pavement forces with superelevation.

From figure 37:

$$\sum_i F_{ri} = \sum_i F_{fi} \cos \theta + \sum_i F_{ni} \sin \theta \quad (27)$$

that is, the horizontal component of the tire/pavement forces. The superelevation angle is θ .

Also from figure 37, summing forces in the vertical direction yields:

$$\sum_i F_{ni} \cos \theta = \sum_i W_i + \sum_i F_{fi} \sin \theta \quad (28)$$

where W_i is the portion of the trailer weight on the tires of axle i . Eliminating $\sum_i F_{ni}$ between equations (27) and (28) yields:

$$\sum_i F_{ri} = \sum_i F_{fi} \cos \theta + (\sum_i W_i + \sum_i F_{fi} \sin \theta) \tan \theta \quad (29)$$

Next, consider the sum of moments in the horizontal plane about the trailer CG. From figure 36:

$$I(\ddot{r} + \ddot{\gamma}) = H_f(c) - \sum_i F_{ri}(d_i) + \sum_i M_{zi} \quad (30)$$

where I is the trailer moment of inertia about its CG and r is the rotation rate of the velocity vector, \dot{U} .

The side friction force, F_{fi} , and aligning moment, M_{zi} , are given by:

$$F_{fi} = -C_{\alpha_i} (\alpha_i) \quad (31)$$

$$M_{zi} = K_i (\alpha_i) \quad (32)$$

where C_{α_i} is the combined cornering stiffness for the tires on axle i , K_i is the combined aligning moment for those tires, and α_i is the slip angle (angle between the direction of motion of the trailer $[\dot{U}]$ and the velocity of the tires). This can be shown to be:³¹

$$\tan \alpha_i = -\tan \delta_i - \tan \gamma - \frac{(l+a_i)(r + \dot{\gamma})}{U \cos \gamma} \quad (33)$$

where δ_i is the steer angle of the axle, illustrated by figure 38.

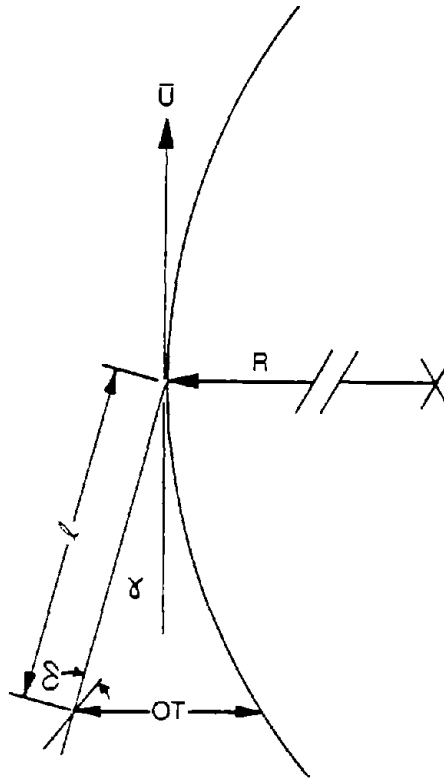


Figure 38. Slip and steer angles.

The lateral acceleration of the trailer CG is:

$$A_y = Ur \cos \gamma - (\dot{r} + \ddot{\gamma}) c \quad (34)$$

When the trailer tends to roll on its suspension, the rolling forces tend to cause the tires to rotate (steer) slightly about a vertical axis. As such, they no longer track in the same direction as the axis of the trailer, as indicated in figure 38. The amount of this steering depends on the rolling moment and the suspension characteristics.

Figure 39 illustrates the roll angle, ϕ , of the trailer negotiating a curve with superelevation, θ .

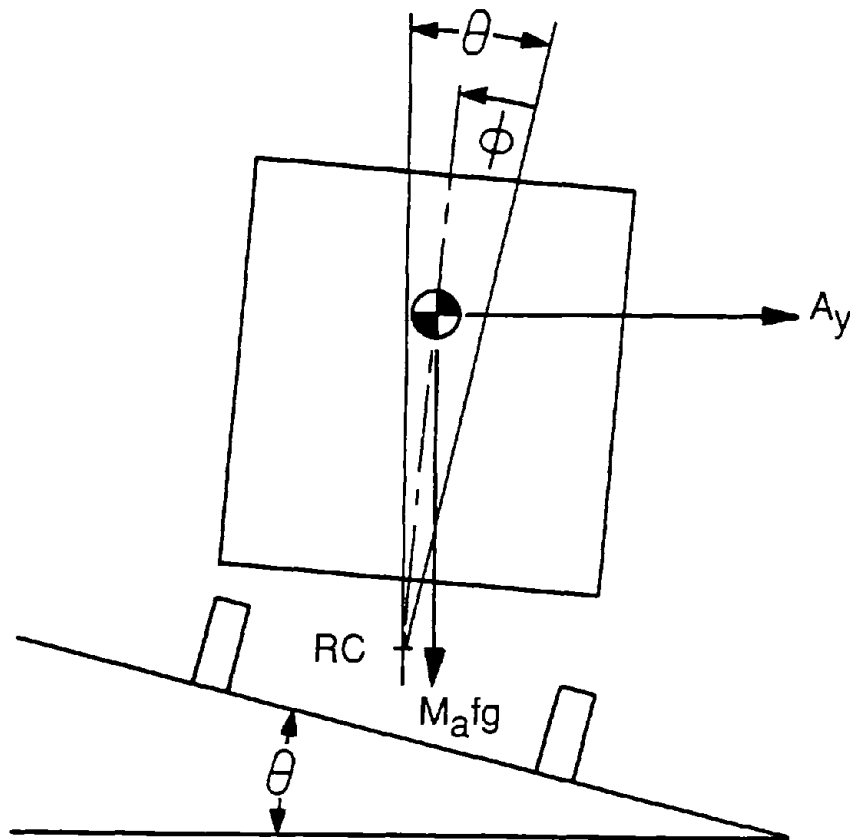


Figure 39. Trailer roll with superelevation.

The roll center, RC in figure 39, is the point in space about which the trailer rolls. It is located a distance, h , below the center of gravity of the portion of the trailer, $M_a f$ supported by the suspension. (M_a is the trailer mass supported by the tires of the axle set; δ is the fraction that is suspended.) Now, summing moments about the roll center gives:

$$M_a f g h \sin(\theta - \phi) + k_r \phi = A_y M_a f h \cos(\theta - \phi) \quad (35)$$

where k_r , the roll stiffness, is a property of the trailer suspension; $k_r \phi$ is the suspension-created restoring moment (clockwise in figure 39). Next, making the usual small angle assumptions for θ and ϕ (e.g., $\sin \theta = \theta$, $\cos \theta = 1$), yields:

$$\phi = M_a f h (A_y - g\theta) / (k_r - M_a f g h) \quad (36)$$

Then, the steer angle, δ_i , is (by definition of s_i):

$$\delta_i = -s_i \phi \quad (37)$$

where s_i is the suspension's roll steer coefficient. If we define:

$$S_i \equiv M_a f s_i h / (k_r - M_a f g h) \quad (38)$$

then:

$$\delta_i = -S_i (A_y - g\theta) \quad (39)$$

This compares with Bernard and Vanderploeg's equation (A-7):

$$\delta_i = -S_i A_y \quad (40)$$

except for the inclusion of the $g\theta$ -term to denote the superelevation, and a more inclusive definition of S_i , to explicitly include the fact that the roll offsets the CG of the trailer, thus negating some of the suspension restoring moment.

Now, using equations (26), (34), and (29) in equation (30), and making the customary small angle assumptions ($\cos \theta \approx 1$, $\sin \theta \approx \tan \theta \approx \theta$) and neglecting θ^2 terms yields:

$$I (\ddot{r} + \ddot{\gamma}) = cM [Ur - c (\dot{r} + \dot{\gamma})] + \sum_i [cC_{\alpha_i} + C_{\alpha_i} d_i + K_i] \alpha_i - \sum_i W_i \theta (c + d_i) \quad (41)$$

Next, for a constant speed and radius turn, $\dot{r} = \dot{\gamma} = \ddot{\gamma} = 0$. Using equation (33) for α_i , and noting from figure 36 that $c + d_i = \ell + a_i$, gives

$$\gamma = \frac{cMUr}{\sum_i [C_{\alpha_i} (\ell + a_i) + K_i]} - \frac{r}{U} \frac{\sum_i [C_{\alpha_i} (\ell + a_i) + K_i] (\ell + a_i)}{\sum_i [C_{\alpha_i} (\ell + a_i) + K_i]} - \frac{\sum_i [C_{\alpha_i} (\ell + a_i) + K_i] \delta_i}{\sum_i [C_{\alpha_i} (\ell + a_i) + K_i]} - \frac{\sum_i W_i (\ell + a_i)}{\sum_i [C_{\alpha_i} (\ell + a_i) + K_i]} \quad (42)$$

At this point we simplify by setting all $K_i = K$, all $C_{\alpha_i} = C_{\alpha}$, and $W_i = W_a/n$ where n is the number of axles in the axle set and W_a is the total load on all tires of the axle set. (Note, however, that $W_a = (c/\ell)Mg$ because some of the weight is carried by the hinge point.) Thus:

$$\sum_i [C_{\alpha_i} (\ell + a_i) + K_i] = n C_{\alpha} \ell + nK \quad (43)$$

since $\sum a_i = 0$. We define the pneumatic trail, t , as K/C_{α} , and \bar{C}_{α} as nC_{α}/W_a . Then, noting that for a steady turn the rotation rate, r , is U/R , equation (42) becomes:

$$\gamma = -\frac{\ell}{R} \left[1 + \frac{\sum_i (a_i/\ell)^2}{n(1+t/\ell)} \right] + \frac{U^2}{R} \left[\frac{1}{\bar{C}_{\alpha} g (1+t/\ell)} + S \right] - S_g \theta - \frac{\theta}{\bar{C}_{\alpha} (1+t/\ell)} \quad (44)$$

where the definition of S_i in equation (38) has also been used, along with setting all $S_i = S$. Finally, defining the offtracking distance, OT, as $e\gamma + e^2/2R$ (see figure 38) gives:

$$\begin{aligned}
 OT = & -\frac{e^2}{R} \left[0.5 + \frac{\sum (a_i/e)^2}{n(1+t/e)} \right] \\
 & + \frac{eU^2}{R} \left[\frac{1}{\bar{C}_a g (1+t/e)} + S \right] \\
 & - \frac{e\theta}{\bar{C}_a (1+t/e)} - S e g \theta
 \end{aligned} \tag{45}$$

which is equation (21).

E. Sensitivity of Offtracking to Truck Characteristics

A sensitivity analysis has been conducted to determine the sensitivity of offtracking to truck characteristics using the new offtracking model. This sensitivity analysis was conducted using a simple computer program to exercise the model given in equations (21), (22), and (23). The truck used for this sensitivity analysis was the STAA single with 48-ft (14.6 m) trailer and conventional tractor given in tables 21 and 22. Both empty and loaded trucks were considered. The typical axle spacings, axle loads, and center of gravity height assumed for empty and loaded trucks are those given in table 24. Table 25 shows both a typical value and a typical range for the other truck parameters in the offtracking model.¹⁰

Vehicle speed and superelevation: Table 26 illustrates the sensitivity of offtracking to vehicle speed and superelevation for the loaded truck documented in table 24 using the typical truck parameters presented in table 25. The values in Table 26 are for a truck on a 500-ft (150-m) radius; shorter radius turns, such as are made at intersections, are not addressed in this sensitivity analysis because speeds are lower and superelevation less common for such turns.

The table shows that the traditional low-speed component of offtracking, as defined, does not vary with either speed or superelevation. It is a function solely of the truck characteristics and the turning path. The negative sign of low-speed offtracking indicates that the rear trailer axle tracks inside of the tractor steering axle. The value of low-speed offtracking, -1.98 ft (-0.60 m), represents the maximum offtracking that could occur on a 500-ft (150-m) radius curve that is long enough for offtracking to fully develop; the Caltrans model could be used to determine the actual offtracking for any curve that is too short to develop that maximum.

Table 24. Assumed characteristics for loaded and empty trucks used in offtracking sensitivity analyses.

<u>Parameter</u>	<u>Tractor drive axle</u>		<u>Rear trailer axle</u>	
	Type of axle set	Tandem (n = 2)		Tandem (n = 2)
Distance from previous axle (x) (ft)	18.0 ^a		40.5 ^a	
	<u>Empty</u>	<u>Loaded</u>	<u>Empty</u>	<u>Loaded</u>
Load (weight) carried by suspension for the axle set (W) (lb)	11,500	30,000	5,000	30,000
Height of center of gravity (in)	51	71.4	60	80

^a Values of dimensions B and D for STAA 48-ft (14.6-m) trailer truck from table 22.

Dimension C (fifth wheel offset) is assumed to be zero.

Note: 1 ft = 1.305 m
 1 lb = 0.454 kg
 1 in = 2.54 cm

Table 25. Typical values of parameters for offtracking model.¹⁰

<u>Parameter</u>	<u>Typical value</u>	<u>Typical range</u>
Cornering coefficient (C_{α}/F_{Zr})	0.15 deg ⁻¹	0.12 to 0.19
Rated load of tire (F_{Zr})	6,040 lb for radial tires 5,150 lb for bias ply tires	
Number of tires per axle	4	2 to 4
Pneumatic trail (t)	0.179 ft	0.15 to 0.23
Suspension roll steer coefficient (s) (degrees of steer per degree of roll)	0.18	-0.04 to 0.213
Composite roll stiffness (k_r) per axle	0.158 x 10 ⁶ in-lb/deg	0.070 to 0.165 x 10 ⁶
Height of roll center (h_{RC})	22 in	21 to 33

Note: 1 lb = 0.454 kg
 1 ft = 0.305 m
 1 in = 2.54 cm

Table 26. Components of total offtracking on a 500-ft (150-m) radius curve.

Truck speed (mi/h)	Superelevation (ft/ft)	Offtracking (ft)			Total
		Low-speed component	High-speed component	Superelevation component	
20	0.00	-1.98	0.28	0.00	-1.70
	0.02	-1.98	0.28	-0.10	-1.80
	0.04	-1.98	0.28	-0.21	-1.91
	0.06	-1.98	0.28	-0.31	-2.02
	0.08	-1.98	0.28	-0.43	-2.12
	0.10	-1.98	0.28	-0.53	-2.23
40	0.00	-1.98	1.13	0.00	-0.85
	0.02	-1.98	1.13	-0.10	-0.96
	0.04	-1.98	1.13	-0.21	-1.07
	0.06	-1.98	1.13	-0.31	-1.17
	0.08	-1.98	1.13	-0.43	-1.28
	0.10	-1.98	1.13	-0.53	-1.38

Note: 1 ft = 0.305 m

Table 26 shows that since the high-speed component of offtracking increases with the square of speed, its value at 40 mi/h (64 km/h) is four times its value at 20 mi/h (32 km/h). The positive sign of the high-speed offtracking turn shows that it is in the opposite sense to the low-speed offtracking term such that the rear trailer axle moves toward the outside rather than the inside of the turn. For the specific truck and the specific radius of curvature shown in table 26, the low-speed and high-speed offtracking terms would completely offset one another on a level surface (i.e., with no superelevation) and with no trailer body roll at 52.9 mi/h (85.1 km/h). At that speed, the rear trailer axle would exactly follow the tractor steering axle and there would be no offtracking. At higher speeds, the rear trailer axle would track outside of the tractor steering axle. The values of the high-speed component of offtracking represent fully developed or steady state offtracking. However, there is no information in the literature about how the high-speed component develops as a truck enters a turn. This issue could be investigated with the Phase-4 model.

Table 26 also shows that the effect of superelevation on offtracking increases linearly with the magnitude of the cross-slope and that this component of offtracking is in the same direction as the low-speed component. In addition, this superelevation effect is independent of speed so that it would contribute to offtracking in low-speed turns at intersections, as well as high speed turns on horizontal curves, whenever there is a pavement cross-slope. The superelevation effect represents the maximum or fully developed offtracking. No information is available about how the superelevation effect develops as a truck enters a turn.

Empty vs. loaded: The loading of a truck has a moderately important effect on offtracking. This effect was investigated in a sensitivity analysis for standard test conditions, including a 500-ft (150-m) radius curve with superelevation of 0.060, a truck travel speed of 40 mi/h (64 km/h), and the typical values of truck parameters given in table 25. The difference in total offtracking between the empty and loaded conditions shown in table 24, including the effects of both the additional spring loads on the axles and the increase in center of gravity height, is 0.63 ft (0.19 m). Total offtracking here represents the sum of the low-speed, high-speed, and superelevation components. The loaded condition has offtracking of -1.17 ft (-0.36 m), as shown in table 26. The empty or unloaded condition has offtracking of -1.80 ft (-0.55 m). Thus, empty trucks have greater negative offtracking than loaded trucks.

Further sensitivity analyses for empty and loaded trucks are presented below using the standard test conditions given above and varying the truck parameters in table 25 one at a time over their typical ranges.

Cornering coefficient: The cornering coefficient [C_{α}/F_{zr} in equation (22)] is the ratio of the cornering stiffness to the rated load of the tire. The offtracking estimates in table 26 have been made using a cornering coefficient of 0.15 deg^{-1} , which represents a typical new radial tire. Cornering coefficients for radial tires typically vary in the range from 0.12 to 0.19 deg^{-1} depending on the tire model and the degree of wear.¹⁰ The cornering coefficient has only a small effect on offtracking. Increasing the cornering coefficient increases negative offtracking. Over the range from 0.12 to 0.19 deg^{-1} , total offtracking varies by only 0.07 ft (0.02 m) for an empty truck and by 0.30 ft (0.09 m) for a loaded truck for the standard test conditions defined above. For all practical purposes, the value of the cornering coefficient could be set to a constant value of 0.15 deg^{-1} in the investigation of offtracking on horizontal curves.

Rated load of tire: Variations over the typical range of rated load of tire have very little effect on offtracking. Bias ply tires have lower rated loads than radial tires and reduce negative offtracking by 0.03 ft (0.01 m) for empty trucks and by 0.11 ft (0.03 m) for loaded trucks. For all practical purposes, the rated load of the tire could be set to a constant value of 6,040 lb (2,750 kg) in the investigation of offtracking on horizontal curves.

Pneumatic trail: The pneumatic trail of the tire determines the magnitude of the steering moment which is applied to the tire during cornering.¹⁹ While the pneumatic trail theoretically has an influence on offtracking [see equation (21)], this influence is so small--less than 0.01 ft (0.003 m) for the standard test conditions--that for all practical purposes the pneumatic trail can be treated as a constant.

Suspension roll steer coefficient: The suspension roll steer coefficient (degrees of roll per degree of steer) has very little effect on offtracking for empty trucks and has a moderately important effect for loaded trucks. An increase in the roll steer coefficient decreases the amount of negative offtracking. For the standard test conditions described above, variation of the roll steer coefficient over its typical range from -0.04 to 0.23 results in a

variation in offtracking of 0.05 ft (0.02 m) for empty trucks and 0.23 ft (0.07 m) for loaded trucks.

Composite roll stiffness: The composite roll stiffness of a truck suspension system represents the relationship between the suspension roll angle and the restoring moment that tends to keep the truck body from rolling further. Increases in the composite roll stiffness result in increases in negative offtracking. For the standard conditions described above, variation of the composite roll stiffness over its typical range from 0.070 to 0.165 million in-lb/deg (8.1 to 19 million g-cm/deg) results in an increase in negative offtracking of 0.05 ft (0.02 m) for empty trucks and 0.27 ft (0.08 m) for loaded trucks. Thus, composite roll stiffness has a very small effect on offtracking for empty trucks and a moderate effect for loaded trucks.

Height of roll center: The height of the roll center has very little effect on offtracking over its typical range of variation. Negative offtracking increases as the roll center is raised. For the standard test conditions given above, variation in the height of the roll center over its typical range from 21 to 33 in (53 to 84 cm), changes offtracking by 0.01 ft (0.003 m) for empty trucks and by 0.04 ft (0.01 m) for loaded trucks. For all practical purposes, the height of the roll center can be set as a constant at its typical value of 22 in (56 cm) in the investigation of offtracking on horizontal curves.

Number of axles: The effect on offtracking of the number of axles can be realistically addressed only by varying several related parameters. If the tractor and trailer have only one rear axle, instead of two, the supported weight must be reduced in accordance with rated tire load and bridge-formula axle loads. The analysis used a maximum load of 20,000 lb (9,080 kg) on these axles. Also, the roll stiffness is generally much less for a single axle suspension; 0.070×10^6 in-lb/deg (8.1×10^6 g-cm/deg) was used here. The negative offtracking is reduced by 0.27 ft (0.08 m) for the single axle tractor and trailer when empty, and by 0.69 ft (0.21 m) when loaded. This truck type will thus generate positive offtracking at lower speeds than tandem axle combinations.

Combined effects: In summary, only five of the truck parameters examined have effects on offtracking that are other than minimal. These are: empty vs. loaded conditions; cornering coefficient; roll steer coefficient; composite roll stiffness; and number of axles. The second, third, and fourth parameters have substantial effects only for loaded trucks, which themselves offtrack less than empty trucks. If these three parameters are set to produce maximum negative offtracking for a loaded truck under the standard test conditions, the resulting offtracking is -1.51 ft (-0.46 m) which is still less negative offtracking than produced by an empty truck. On the other hand, if the two parameters are set to produce minimum negative offtracking, the resulting offtracking is -0.67 ft (-0.20 m). Thus, maximum negative offtracking will typically be obtained for empty trucks and maximum positive offtracking will typically be obtained for loaded trucks. Furthermore, variations in offtracking in excess of a foot (0.3 m) can occur for a given horizontal curve at a given speed, depending upon the truck parameters assumed.

APPENDIX D

TRUCK PERFORMANCE ON GRADES

This appendix presents a detailed review of truck performance on grades to determine the appropriate weight-to-horsepower ratio for use in the analysis of critical length of grade for the current truck population. The appendix focuses on the review of recent work by Gillespie on truck speed loss on grades and includes a reanalysis of the data collected for that study.³²

A. Background

The 1984 AASHTO Green Book presents the current warrant for the addition of a truck climbing lane in terms of a "critical length of grade."³ A climbing lane is not warranted if the grade does not exceed this critical length. If the critical length is exceeded, then a climbing lane is desirable and should be considered. The final decision to install a truck climbing lane may depend on a number of factors, but basically is determined by the reduction in level of service that would occur without the addition. This reduction, in turn, is a function of the traffic volume, the percentage of trucks, the performance capabilities of the trucks, the steepness of the grade, and the length of grade remaining beyond the critical length.

The critical length of grade itself is established by the "gradeability" of trucks. Subjectively, the critical length of grade is the "maximum length of a designated upgrade on which a loaded truck can operate without an unreasonable reduction in speed." The Green Book considers the critical length of grade to be dependent on three factors:

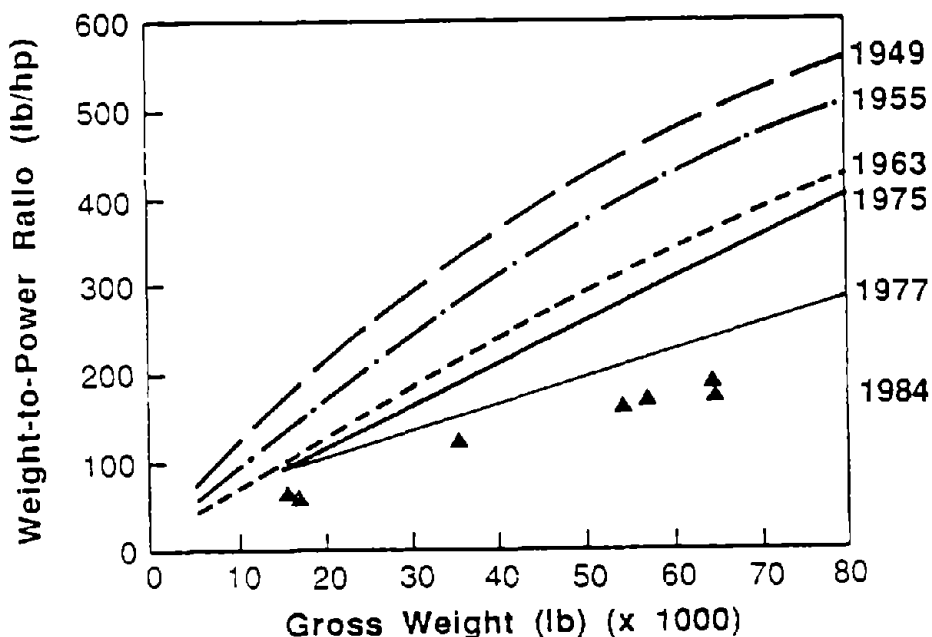
- The weight and power of the representative truck used as the design vehicle, which determine its speed maintenance capabilities on grades.
- The expected speed of the truck as it enters the critical length portion of the grade.
- The minimum speed on the grade below which interference to following vehicles is considered unreasonable.

Based on these factors, the AASHTO Green Book defines the critical length of grade as the length of grade that would produce a speed reduction of 10 mi/h (16 km/h) for a specified design truck.

The 1984 Green Book uses a 300 lb/hp (0.18 kg/W) truck as the design vehicle. This weight-to-power ratio is smaller than that used for the 1965 AASHTO Blue Book; at that time a 400-lb/hp (0.24 kg/W) truck was typical of a heavy truck.³³ The decision to use the more powerful 300 lb/hp (0.18 kg/W) design vehicle was recommended in a 1978 NCHRP study.³⁴ Based on the literature at the time, the NCHRP study concluded that the design vehicle should be

one that a "large" portion of the vehicle population and has poor performance characteristics on grades. These criteria appear reasonable.

Figure 40 illustrates the long-term trends in the weight-to-power ratios of trucks. The figure shows the several lines illustrating trends in average weight-to-power ratio of trucks as a function of gross weight from 1949 to 1975, based on figure III-27 in the AASHTO Green Book. Added to the figure is a line based on the 1977 Truck Inventory and Use Survey (TIUS) performed by the Bureau of the Census and points representing the 1984 Gillespie data.^{32,35} The figure shows that the long-term decrease in weight-to-power ratios of trucks has continued right up to the present. A comparison of the TIUS and Gillespie data demonstrates that the major reason for the reduced weight-to-power ratios of trucks over the last decade is a substantial increase in average engine horsepower. The average tractor power in the 1977 TIUS data was 282 hp (210 kW), in comparison to 350 hp (260 kW) in the Gillespie data.



Note: 1 lb = 0.454 kg
1 hp = 746 W

Figure 40. Trend in weight-power ratios of trucks from 1949 to 1984.^{1,32,35}

The data on which the recommendation to use 300 lb/hp (0.18 kg/W) was based were all obtained in the early to mid 1970's. Thus, they are now about 15 years old. Yet, most available evidence indicates that truck performance

has continued to increase, just as it has since 1949 (see figure 40). The most recently published data, which were obtained in about 1984, show that five-axle, single-semitrailer trucks, the most common heavy trucks, consistently (according to various measures) outperformed the AASHTO 300 lb/hp (0.18 kg/W) design vehicle.³² Therefore, current policy is overly conservative in that it calls for a shorter critical length of grade than is needed for the current heavy truck population.

Double-trailer trucks do have somewhat poorer performance than single-trailer trucks. However, they still perform slightly better than the AASHTO design vehicle. Also, they represent a fairly small fraction of the trucks on the road in most of the United States.

The remainder of this appendix considers the effect of recent changes in truck weight-to-power ratios and the appropriateness of a reduction in the weight-to-power ratio used to determine critical length of grade in the AASHTO Green Book. The elements of the required analysis include review of the Gillespie study, development of a method for estimating weight-to-power ratio from truck performance data, and reanalysis of the Gillespie data to establish a design value of weight-to-power ratio.

B. Literature Review

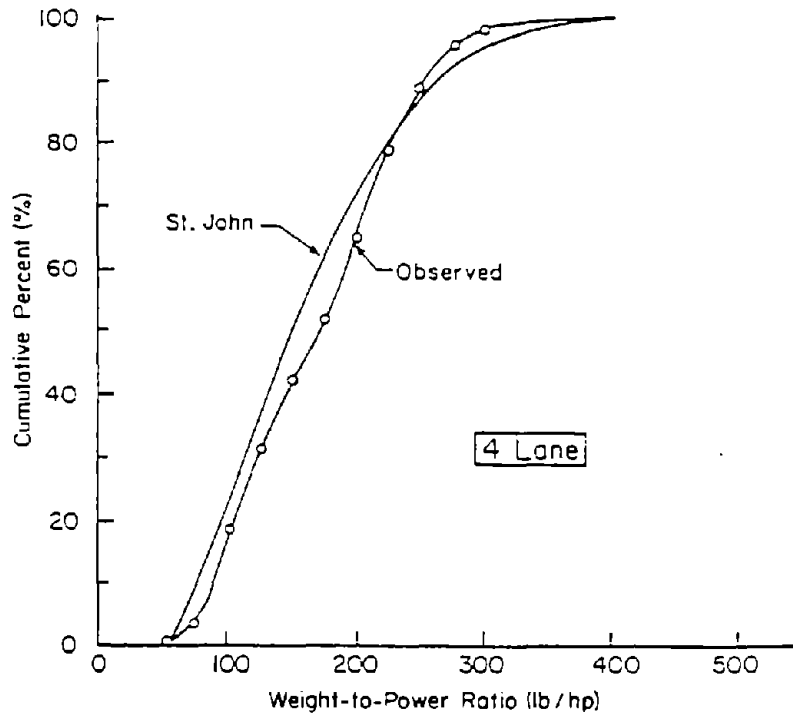
This section of the appendix reviews the literature related to truck performance on grades.

1. Effect of Weight-to-Power Ratio on Final Climbing Speeds

Weight-to-power ratio: The ability of a truck to maintain speed on an upgrade is very sensitive to its weight-to-power ratio. The weight-to-power ratios of trucks have been decreasing steadily for the last 40 years, as tractor engines have become more and more powerful.

A number of studies have addressed recent trends in the weight-to-power ratios of trucks. Figure 41 shows an estimate of the distribution of weight-to-power ratios of trucks made by St. John in 1979 from data collected by the FHWA Bureau of Motor Carrier Safety and the California Department of Transportation.^{36,37} The figure shows that St. John's distribution compares well with field data reported by Messer in a 1983 study.³⁸ The St. John and Messer data are in agreement that the median weight-to-power ratio of trucks is about 160 lb/hp (0.10 kg/W) and the 15th percentile weight-to-power ratio (at the poor end of the performance distribution) is about 240 lb/hp (0.15 kg/W).

Gillespie has reported grade-climbing abilities of trucks as observed in 1984.³² Table 27 presents average values of weight-to-power ratio of trucks obtained from field observations at four sites located in the eastern and western parts of the United States. The table shows the average weight, power, and weight-to-power ratios of trucks by truck type and road class. The weights were obtained at weigh stations; the powers are the driver-reported rated horsepower of the engine. The number of trucks observed for each road class is given in parentheses following the road class.



Note: 1 lb = 0.454 kg
1 hp = 746 W

Figure 41. Comparison of weight-to-power ratios estimated by St. John to those observed by Messer.^{37,38}

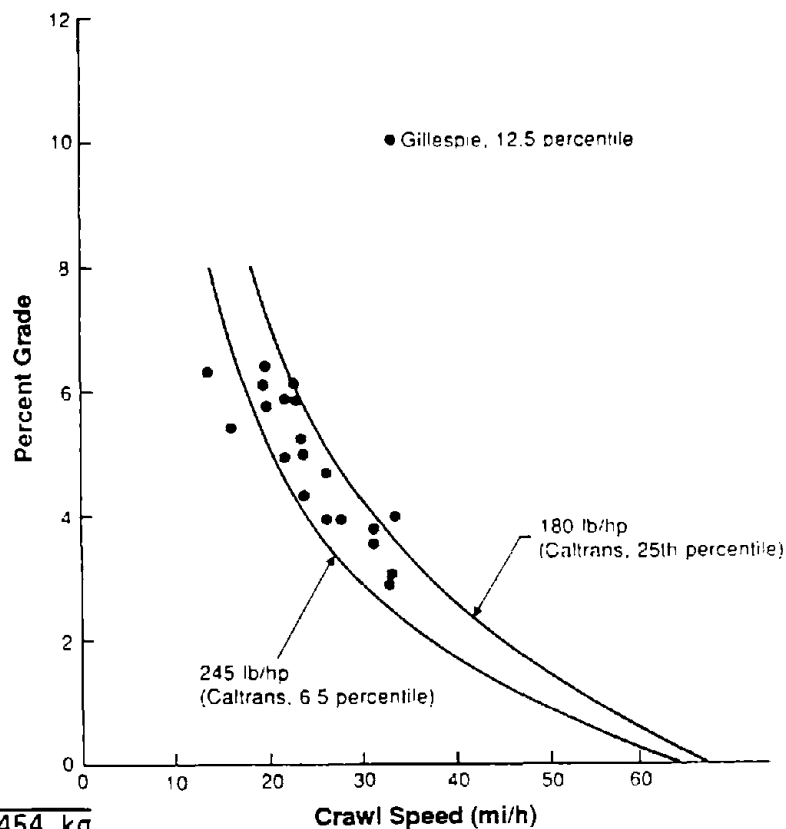
Table 27. Average weights and power values for trucks.³²

	<u>Weight (lb)</u>	<u>Power (hp)</u>	<u>Weight/power</u>
<u>Straight Trucks</u>			
Interstate - East (14)	15,233	219	70
Interstate - West (6)	35,050	267	131
Primary - East (6)	16,575	273	75
<u>Tractor-Trailers</u>			
Interstate - East (157)	54,452	328	166
Interstate - West (233)	64,775	370	175
Primary - East (134)	57,487	330	174
<u>65-ft Doubles</u>			
Interstate - West (19)	64,920	331	196

Note: 1 lb = 0.454 kg
1 hp = 746 W

Of course, extreme values of the distribution of truck weight-to-power ratio are more appropriate than average values in determining design criteria for critical length of grade. Crawl speeds estimated from the results obtained by Gillespie for 12.5 percentile tractor-trailer combinations are shown in figure 42. Gillespie suggested that the 12.5 percentile was a reasonable design value, as it was a relatively poorly performing vehicle, yet one which is reasonably common on the highways. The various points plotted represent results from different classes of highways and different regions of the country.

Data on truck performance, by number of axles, were also collected by the California Department of Transportation in the late 1970's.³⁶ St. John and Kobett analyzed these data and determined that all but the two-axle truck data were similar and could be merged.³⁹ They subsequently used the data in a model to predict detailed truck performance on grade. The same model was applied in the present study with very slight adjustment in the shift delay portion of the model, to updated (1983 to 1984) data from California. The results from this model are also shown in figure 42 for two representative trucks. One is a truck with a weight-to-power ratio of 245 lb/hp (0.15 kg/W), which corresponds to the 6.5 percentile truck from the Caltrans data. The other is the 25th percentile truck, which has a weight-to-power ratio of 180 lb/hp (0.11 kg/W).

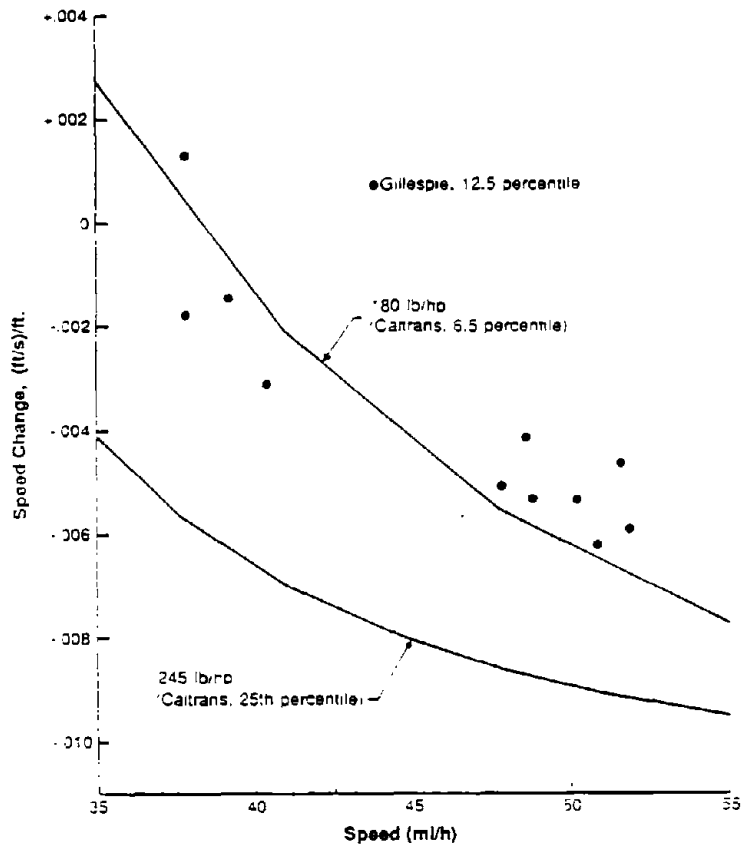


Note: 1 lb = 0.454 kg
1 hp = 746 W

Figure 42. Effect of percent grade on tractor-trailer crawl speeds.^{32,36}

Clearly, these data sources, all derived from field data collected in the early to mid 1980's, are in good agreement. And, they both suggest that a design vehicle, if based on final climbing speed, should have a weight-to-power ratio substantially less than the AASHTO design vehicle value of 300 lb/hp (0.18 kg/W).

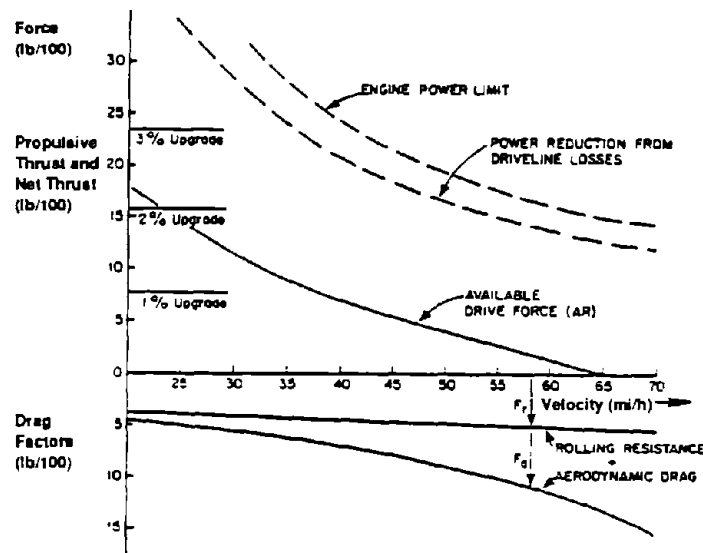
Acceleration capability on grade: The same data described above were also analyzed to determine the ability of the trucks to accelerate (or, alternatively, the forced deceleration) as a function of speed and grade. Figure 43 illustrates some of the results for a 3 percent grade. Here the results from the two data sources are not quite as consistent, but they do both show the same trends. Both show that acceleration performance deteriorates with speed. Also, both show that a 300 lb/hp (0.18 kg/W) design vehicle is overly conservative, and that a design vehicle with a lower weight-to-power ratio is more appropriate.



Note: 1 ft = 0.305 m
 1 mi = 1.61 km
 1 lb = 0.454 kg
 1 hp = 746 W

Figure 43. Truck speed change per unit distance as a function of speed.^{32,36}

Effect of aerodynamic losses on power available to maintain speed on grades: Gillespie provides insight into the quantitative nature of the various power losses in a truck. Figure 44, from Gillespie, illustrates that at speeds less than 25 to 30 mi/h (40 to 48 km/h), the aerodynamic losses are minimal, compared to other losses. But, at speeds of 55 mi/h (88 km/h) and greater, they are the dominant losses. For the truck illustrated, the maximum speed possible on level terrain is about 65 mi/h (105 km/h). Even though the truck engine still produces power at that speed, it is all consumed in overcoming the various losses, the greatest of which is the aerodynamic loss, so no power is available to produce acceleration.



Note: 1 lb = 0.454 kg
1 mi = 1.61 km

Figure 44. Forces acting on a vehicle as a function of speed.³²

C. Computation of Weight-to-Power Ratio From Observed Speeds of Trucks

This section of the appendix provides a brief critique of the Gillespie study together with a rationale for reanalysis of his data.

Gillespie obtained data on truck performances on grades for over 4,000 trucks at 20 sites in the United States in 1984 (apparently). These are the most recent data of this type, and certainly of this magnitude, so it would not be cost effective to repeat that data collection effort at this time. However, Gillespie's analysis views the data in such a way that his results shed little light on weight-to-horsepower or aerodynamics, other than to indicate that the trucks have improved performance capabilities over those used by AASHTO for the Green Book.

The author begins his report by reviewing the equations governing truck performance on a grade. The fundamental equation is:

$$W(1 + e)A_x = F_d - F_r - F_a - W(G_r) \quad (46)$$

where:

W = gross weight of truck
 e = effective weight of truck's rotating components, divided by W
 A_x = forward acceleration, in g's
 F_d = engine drive force at the wheels
 F_r = rolling resistance of the wheels
 F_a = aerodynamic drag force
 G_r = grade, expressed as percent/100

The value of e is small compared to 1, especially at highway speeds, so is neglected. Dividing equation (46) by W, and rearranging, yields:

$$AR = A_x + G_r = F_d/W - (F_r + F_a)/W \quad (47)$$

where AR is termed the acceleration reserve--the force available, per unit of gross weight, to accelerate the vehicle and/or to climb a grade. Equation (47) assumes that the truck driver is applying all available power to maintaining speed, so that any reduction in speed is solely the effect of the grade or the rolling and aerodynamic losses.

Figure 44, taken from the Gillespie study, illustrates how these various terms vary with speed.⁴⁸ F_d varies inversely with speed, because the engine power (= force times speed) is essentially constant with speed, given the large number of gear ratios available to a truck driver. F_r is nearly constant with speed, and F_a increases (negatively) as the square of the speed. The available force, corresponding to AR, is shown as the available drive force. Unfortunately, it is inaccurately drawn, in that it does not reflect the quadratic nature of F_a. At low speeds the aerodynamic force is nil, so the available force should approach the lower of the dashed curves in the figure, differing only by the essentially constant rolling resistance.

The author simplified equation (47) by assuming AR to satisfy a linear relation of the form:

$$AR = C_1 + C_2V \quad (48)$$

where:

V is the truck speed
 C₁ and C₂ are constants to be determined for each truck

The authors of the present report are not in agreement with this assumption for several reasons. First, it is not apparent to us that the available drive force in figure 44 is a straight line, but is instead very curvilinear. (This is especially important in view of the fact that the constants were evaluated at speeds ranging from highway speeds [55 mi/h or 88.5 km/h] down to crawl speeds [15 mi/h or 24.1 km/h] on grades exceeding 6 percent.) Second, by using the linear approximation, there is no way to estimate the effect of aerodynamic drag, which varies as the square of the speed. Third, this form also loses the effect of the weight-to-horsepower ratio, which is contained in the F_d term that is proportional to $1/V$.

The reader should be cautioned that Gillespie does introduce a "weight-to-horsepower" term, defined by:

$$W/P_3 = 550/(AR V) \quad (49)$$

This is a weight-to-power expression only in terms of its units. It would correspond to the truck's weight-to-power ratio if there were no rolling or aerodynamic losses. Moreover, W/P_3 has the disconcerting feature that it is a function of speed. Tabulated values of this quantity should not be confused with real weight-to-horsepower ratios.

Instead of equation (48), a more accurate representation could be used, such as:

$$AR V = P/W - AV - BV^2 - CV^3 \quad (50)$$

where:

P/W is the effective power-to-weight ratio, corresponding to the lower dashed curve of figure 44.

A , B , and C are constants to be determined, corresponding to the rolling and aerodynamic losses.

Ideally, the author's field data could be applied to determine, directly, P/W and the constants, A , B , and C . Unfortunately, this cannot be done because of limitations in the data, as discussed next.

The data were collected by measuring speeds at four locations on each grade, for each truck. The first location was 500 to 1,000 ft (150 to 300 m) after the beginning of the grade; thus, no initial entry speed is available. The next two locations were each 900 to 1,000 ft (270 to 300 m) further up the grade, respectively, and the final location was at a point further up the grade where the trucks were using their final crawl speeds.

To use these data with equation (50), or its equivalent, note that:

$$A_x g = dV/dt = dV/dx(dx/dt) = VdV/dx,$$

so, from equation (45),

$$dV/dx = (AR - G_r)g/V \quad (51)$$

One can estimate from the speed reduction between the first and second locations a value of dV/dx ; G_r and V (average) are known, so AR can be calculated. A second value of AR is obtained for the speed reduction between the second and third locations. Finally, at the last location $dV/dx = 0$ so $AR = G_r$ at that location.

The above provides three relationships, but there are four unknowns (P/W , A , B , and C). Therefore, additional information is needed. We attempted to solve these equations by estimating one of the unknowns, B . B is the speed-dependent portion of the rolling friction loss. The value of 0.00044 was used, as recommended by SAE, but sensitivity analyses showed that the results were relatively insensitive to this value.⁴⁰

Unreasonable results were obtained, which were found to result from inconsistent speed values at the first two locations on the lower portion of the grade. In some cases the truck speed was found to be higher at the second location than at the first, which violates the assumption that the truck is always using maximum power or else the truck just entered the highway and was still accelerating up to speed. Because of these inconsistencies, it was decided to not use these data, but instead to derive a method for estimating weight-to-power ratio solely from the final crawl speeds of the trucks.

At steady crawl speed, $dV/dx = 0$, so $AR = G_r$. Using this fact and equation (50), solving for W/P gives

$$W/P = \frac{550 g (1-0.04 h)}{1.47 V_f (gG_r + A + 1.47 B V_f + 1.47 C V_f^2)} \quad (52)$$

where, in this representation:

W/P = weight-to-power ratio (lb/hp)

g = acceleration of gravity (ft/s²)

h = altitude (thousands of ft)

V_f = crawl speed (mi/h)

This incorporation of h in the numerator reflects the loss in horsepower of the engine at altitude, due to reduced atmospheric pressure (oxygen) in accordance with SAE practice.⁴⁰

The rolling resistance terms (A and B) are recommended by St. John and Kobett to be:³⁹

$$A = 0.2445$$

$$B = 0.00044$$

These values, based on mid-1970's data, represent less friction than recommended by SAE as early as 1951, which have not been revised as of 1987, although technology improvements have undoubtedly reduced rolling friction losses during this period.^{40,41} We are not aware of any more current data than was used by St. John and Kobett, however.

The aerodynamic term, corresponding to C, is given by:

$$C = 1/2 \frac{0.002384 C_D g (1-0.006887h)^{4.255}}{W/Area} \quad (53)$$

where:

C_D = drag coefficient

Area = truck frontal area (ft²)

The h-term is an altitude correction to the nominal sea-level air density of 0.002384 lb/ft³ (0.03816 kg/m³). The drag coefficient, C_D , recommended by SAE in 1951 and henceforth, ranges from 0.63 to 0.83.⁴¹ The Western Highway Institute suggested that 0.52 to 0.68 was a more modern (1969) range.⁴² Current values are undoubtedly lower; we used $C_D = 0.6$ in our calculations. Also, the projected area, Area, was taken to be 102 ft² (9.5 m²).

Of the four terms in the summation in the denominator of equation (52), the dominant term on the grades used by Gillespie is gG_r , which accounted for 80 to 90 percent of the total. The constant part of the rolling resistance (A) accounted for an additional 10 percent, whereas the C-term added from a few to 10 percent (at higher crawl speeds) and the B-term added only a percent or less.

Thus, successive appropriations can be made to calculate values of W/P, depending on the assumptions (and hence, number of terms) included in equation (52). The crudest (and highest) estimate of W/P uses only gG_r , effectively assuming there are no rolling or aerodynamic losses. A better estimate is made by including an assumed value (0.2445) for A. The C-term can also be added, but only if W is known (which is the case for only a portion of four sites in the Gillespie study).

Finally, for those sites where both P and W are known, the nominal weight-to-horsepower ratio can be calculated directly as:

$$W/P_N = \frac{W}{0.94 P} \quad (54)$$

where the factor, 0.94, is introduced, based on the assumption that only about 94 percent of the engine rated horsepower is actually delivered to the drive axles.

D. Reanalysis of Gillespie Data

A reanalysis of the Gillespie data was undertaken using equations (52), (53), and (54). This analysis determined weight-to-power ratios only for tractor-trailer combination trucks; single-unit or straight trucks were excluded. The weight-to-power ratios obtained would have been lower still if single-weight trucks had been included. Equation (52), using just the gG_r and A-terms, provides the best available estimate of weight-to-power ratio (W/P_2) when only the final climbing speed of the truck is known. Equation (52) provides a more accurate estimate of weight-to-power ratio (W/P_4) when the gross weight of the truck is known as well and all four terms in the denominator are included. The gross weight is known only for four data collection sites where surveys were conducted at weigh scales. Finally, equation (54) provides an estimate of weight-to-power ratio (W/P_N) where both the gross weight of the truck and the rated engine horsepower are known, as they are at the four weigh scale sites.

Table 28 summarizes the results of the analysis, showing several key parameters of the distributions of W/P_2 , W/P_4 , and W/P_N derived from the Gillespie data. As shown in the table, the 12.5th percentile value for both W/P_2 and W/P_N is approximately 250 lb/hp (0.15 kg/W), and W/P_4 is somewhat lower.

Based on these results, 250 lb/hp (0.15 kg/W) appears to be an appropriate, yet conservative, up-to-date value to replace 300 lb/hp (0.18 kg/W) in the design criteria for critical length of grade.

Table 28. Distributions of weight-to-power ratios (lb/hp) from reanalysis of Gillespie data

<u>Measure</u>	<u>Number of trucks observed</u>	<u>Mean</u>	<u>Standard deviation</u>	<u>Median (50th %ile)</u>	<u>87.5th %ile</u>
W/P_2	3,037	180	56.5	173	248
W/P_4	496	155	46.7	148	214
W/P_N	496	186	61.5	193.6	260

APPENDIX E

INTERSECTION SIGHT DISTANCE

This appendix reports the results of pilot field studies to test a data collection methodology for the evaluation of case III-B and -C intersection sight distance (ISD) requirements for trucks at STOP-controlled "T" intersections. Sensitivity analyses early in the research showed that application of the AASHTO ISD model to trucks can result in required sight distances exceeding 3,000 ft (900 m). It is unlikely that such long sight distances are practical and would actually be required by truck drivers. Therefore the form and basic assumptions of the AASHTO model itself need to be reconsidered, which in turn requires field data on interactions between vehicles at intersections.

Data collected at three intersections were compared to the AASHTO Green Book criteria for acceleration, deceleration, and minimum separation between vehicles.¹ This would allow assumed values in the current AASHTO ISD model to be replaced, if necessary. An alternative approach to the AASHTO ISD criteria is to modify the ISD model with criteria based upon gap acceptance. This pilot study identified gaps that truck drivers accepted in making right or left turns. These data could be used as the basis for sight distance criteria to assure that truck drivers on the minor road have sight distance equal to or greater than their acceptable time gap.

The objectives of this study were to:

- Develop a data collection methodology to determine acceleration, deceleration, speed reduction, minimum separation, and gap acceptance characteristics of trucks making left and right turns from a STOP-controlled minor road onto a through road.
- Perform a pilot test of the methodology through data collection at three intersections.
- Compare the field data with Green Book values.
- Recommend a work plan for a comprehensive field study of ISD requirements for trucks.

This study's scope was adequate to conduct a pilot test of data collection techniques to guide future efforts. A larger study would be needed to fully develop the gap acceptance concept for a broader range of vehicle types, driver types, intersection geometrics, and approach speeds. Such a study would also provide the information necessary to improve practical application of the Green Book ISD criteria.

The following specific results were sought in this study:

- A preliminary estimate for the gaps (time and/or distance) that minor road trucks accept during a turn maneuver onto a two-lane roadway.
- An estimate of the average acceleration rate for a minor road truck turn maneuver.
- An estimate of the average deceleration rate of major road vehicles during a minor road truck's turn maneuver. Also, an estimate of the speed reduction by a major road vehicle during the truck's turn maneuver.
- An estimate of the minimum separation distance between the turning vehicle and an oncoming vehicle.

A. Overall Study Methodology

Three intersections with similar geometric characteristics were selected. In all cases, the minor road approach contained a high volume of truck traffic. One intersection was an asphalt and aggregate plant driveway, the second was a truck stop exit, and the third was located near an industrial park.

The data collection plan used a combination of three traffic observation techniques: video recording, human observers, and portable traffic data collectors. The video and traffic data collectors were synchronized to a common time base.

Between three and five video cameras were used at the intersections. The cameras were positioned to record turning movements at the intersection and approaching vehicles along the major roadway. The major roadway cameras recorded between 300 and 500 ft (90 and 150 m) depending on the camera quality and the number of cameras located along the approach. Each video camera contained an internal clock that superimposed the time on the video recording so that the times of specific events could be identified during the data reduction process.

Traffic data collectors were utilized before and during the study. They aided in the initial screening of intersections by providing information such as traffic volumes, axle classifications (percent trucks), and speed data. During the actual study, the traffic data collectors were used to obtain approaching and departing vehicle speeds.

In the data reduction phase, the time data needed for the analyses were obtained from the videotapes. An initial step was to locate in the video picture the centerline of the minor road approach (hereafter referred to as the reference line) and 100-ft (30-m) increments from the reference line along the major roadway. These points were measured during the set up of the field equipment and documented by having a member of the project team wave a flag as each of several vehicles passed that point. During the data reduction, the

flagged locations were represented by lines drawn on sheets of clear acetate that were overlaid on a video monitor establishing a scale for data reduction. The lines were used to determine (1) the approximate location of major road vehicles when a minor road truck came to a stop at the intersection, (2) the time or distance gaps that minor road trucks accepted or rejected, (3) the acceleration profile of minor road trucks, (4) the deceleration of major road vehicles, (5) the speed reduction of major road vehicles, and (6) the minimum separation between major road vehicles and turning trucks. The data reduced from the videotape were entered directly into a microcomputer spreadsheet for subsequent analysis. Figure 45 illustrates the distance gap, time gap, and minimum separation definitions.

A critical gap value (in seconds) was calculated from the overall distribution of gaps for each movement (left or right turn) and each vehicle type (five-axle truck or less-than-five-axle truck) at each intersection. Acceleration rates were estimated for the minor road trucks, and deceleration rates and speed reductions were estimated for the major road vehicles that were impeded by turning minor road trucks. The results were compared to vehicle characteristics described in the Green Book and other related literature.

B. Data Collection

1. Intersection Selection

Potential intersections were identified through phone contacts with trucking associations, planning commissions, municipalities, police, and State departments of transportation. Candidate intersections satisfied the following conditions or criteria:

- Unobstructed sight distance (preferably at least 1,000 ft [300 m]).
- Between 5 and 10 percent truck traffic on major road.
- Minor road associated with a truck generator or with a high percentage of truck traffic.
- Two-lane roadways for both the major and minor roads, meeting as a "T" intersection (preferably without turn lanes).
- Minor road controlled by a STOP sign.
- Posted speed limit for the major road greater than or equal to 40 mi/h (64 km/h).
- Intersection located at least 1,000 ft (300 m) from a signalized intersection.
- Good geometrics, i.e., intersecting at approximately a 90° angle with relatively flat grades.

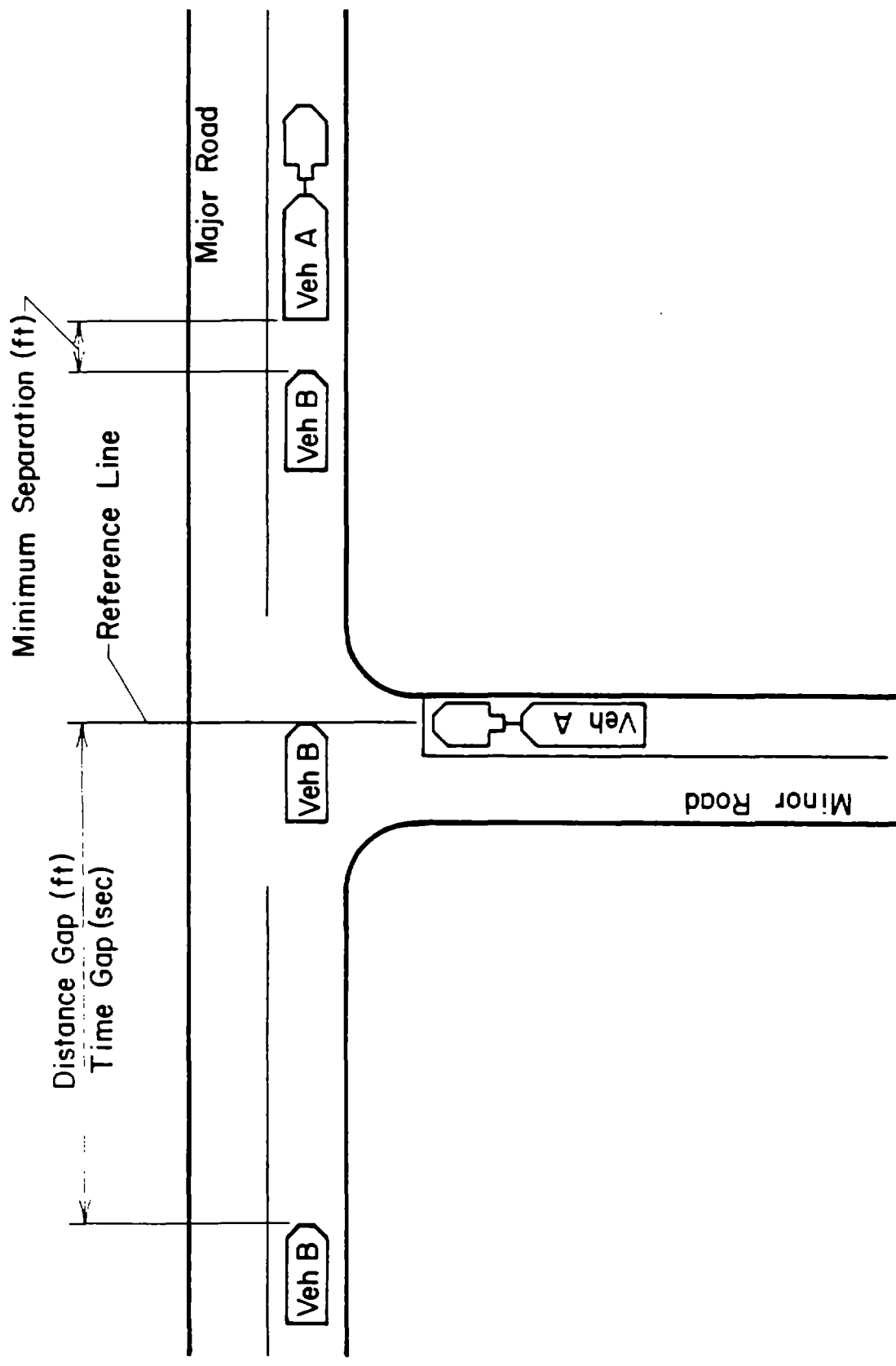


Figure 45. Gap and minimum separation dimensions considered in intersection sight distance criteria.

Visits were made to candidate intersections identified during the initial contacts. Photographs were taken, sketches drawn, and the following preliminary descriptive data were obtained during the initial visits: location of intersection (municipality; county; responsible governmental agency); intersection type; estimated volume; apparent percent trucks; truck type on minor; sight distance; speed limit; distance to nearest signal or major intersection; geometry (line, grade, cross section); approach grades; potential equipment placement; advantages; and disadvantages.

Intersections with acceleration lanes, left turn lanes, low truck volume on the minor road, or low total volume on the major road (large gaps) were eliminated. Arrangements were then made with the agencies responsible for the remaining intersections (typically the State department of transportation, the local municipality, State police, and local police) for the placement of traffic data collectors to record traffic volume and percent trucks on the major and minor roads. Counts were made for a minimum of 24 hours.

Based on the information from the site visits and the traffic counts, three study intersections were chosen. Table 29 summarizes the characteristics of each intersection.

2. Data Collection Plan

The primary objective of this pilot study was to develop, test, and recommend an effective data collection approach. The same data collection procedure was to be employed at each study site. Two plans were developed: a video camera plan, used at each intersection, and a tapeswitch plan, which was tried and subsequently abandoned as discussed later in this section.

The initial task in preparing for data collection was to inform the responsible agencies of anticipated collection days and to ask permission to place traffic data collector tubes on the roads. This step was required to satisfy the agency's concern over liability issues. Difficulties arose when adverse weather conditions prevented data collection on the selected days; agencies then had to be contacted again with the new dates. The need to contact agencies prior to collecting the data severely limited the flexibility of choosing the site for the day's data collection.

a. Video Data Collection Plan

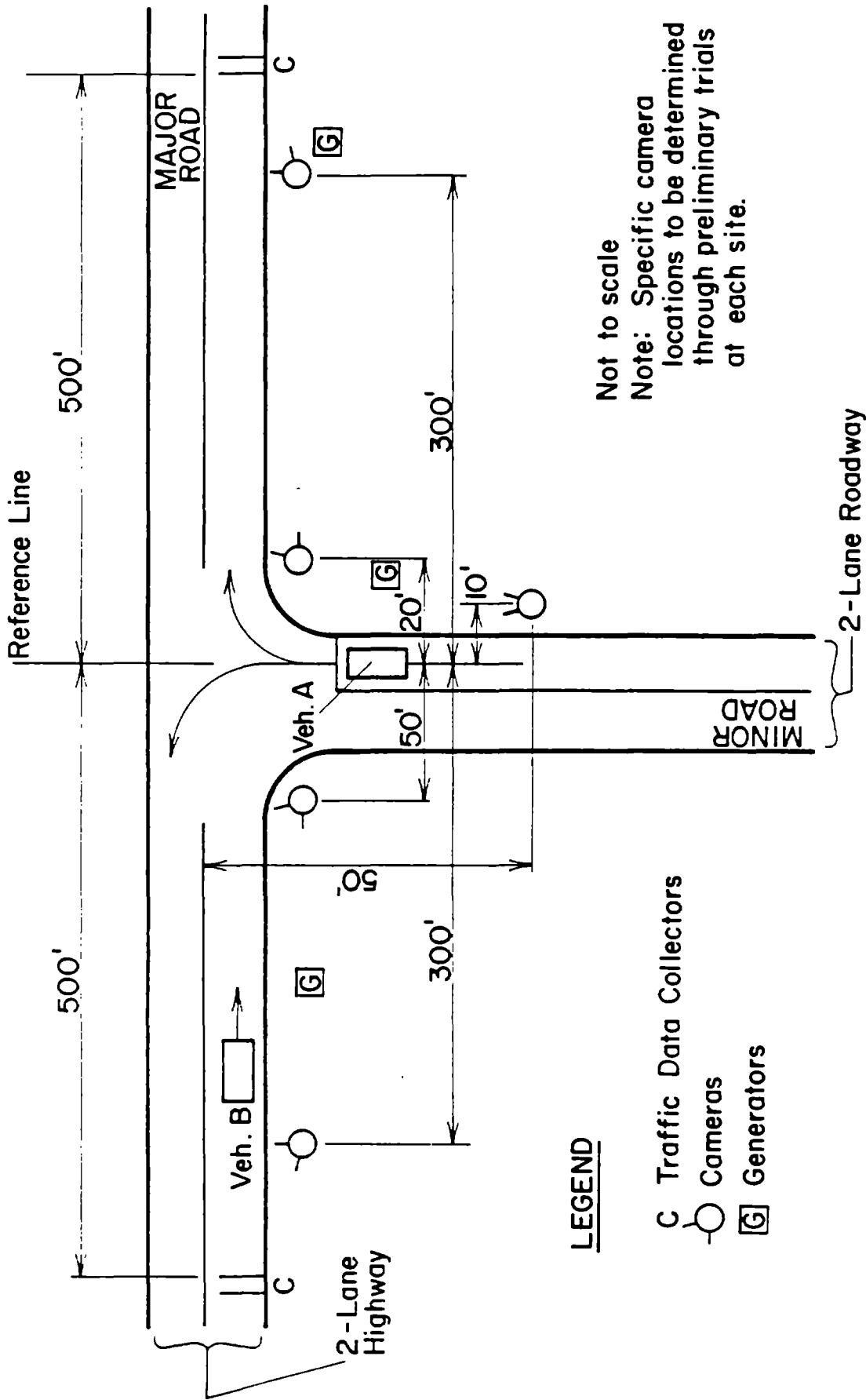
Under this plan, video equipment was used to record the movement of the vehicles at each intersection. All data needed for the evaluation could be collected using videotape. Automated traffic data recorders were used to obtain supplementary data on the speed distribution on the major road and spot speeds for decelerating or accelerating vehicle, as well as traffic volumes during the study. Human observers assessed the frequency of "unsafe" maneuvers. Figure 46 presents the typical equipment layout for data collection.

Table 29. Selected intersection characteristics for ISD study sites.

No.	Intersection		Volume (veh/day) ^a		% Trucks ^a		Speed limit ^b (mi/h)	85th percentile speed (mi/h)	Descriptive profile	
	Major road	Minor road	Major	Minor	Major	Minor			Major	Minor
1	RT 26	Central Valley Asphalt Plant	14,000	175	15	90	45	47	level	level
2	RT 64	Truck Stop 64	7,000	500	20	95	40	51	level	level
3	Trindle	Railroad	20,000	2,000	20	25	40	40	level	level

^a Values are unadjusted count volumes obtained in September 1988 during site selection.
^b Major-roadway approach.

Note: 1 mi = 1.61 km



Not to scale
 Note: Specific camera locations to be determined through preliminary trials at each site.

LEGEND

- C Traffic Data Collectors
- Camera
- ⊠ Generator

Note: 1 ft = 0.305 m

Figure 46. Typical setup for video collection plan.

Data collection began by properly orienting the video cameras. The cameras were positioned to maximize the length of road filmed without jeopardizing the resolution of the vehicles on the film. Typically, one camera recorded the overall operations at the intersection (100 ft [30 m] on either side of the center of the minor road approach); several other cameras recorded the major roadway approaches. Approximately 300 ft (90 m) of road was discernible for each approach leg camera.

Once videotaping commenced, an internal clock was started. Each internal clock was synchronized with a master clock. A lap-top portable computer, with continuous time display, provided coordination of the counters and video cameras.

Two roadway traffic counters recorded major roadway approach or departure speeds for individual vehicles. The counters were generally located 500 ft (150 m) from the intersection. Since the counters could display and store individual vehicle speeds, an observer was not needed to manually record the speed of each approaching or departing vehicle.

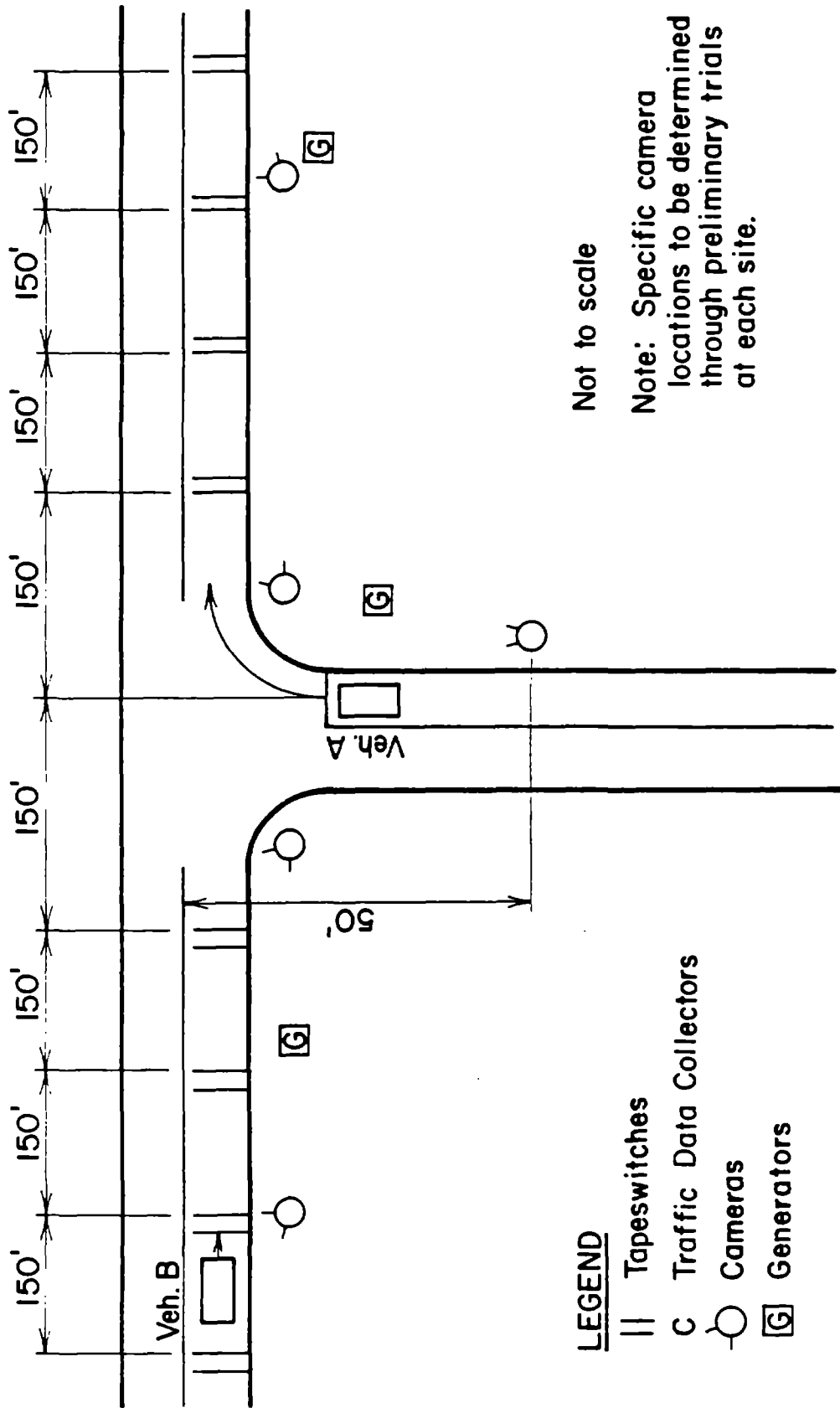
b. Tapeswitch Data Collection Plan

Another data collection plan was developed using traffic data recorders that can store data by individual vehicles, 16 tapeswitches, a lap-top portable microcomputer, and a software program to record the time that each vehicle arrives and departs from the minor road approach. A sketch of the intended collection plan is shown in figure 47.

A set of four groups of tapeswitch pairs was used to measure the major road vehicle deceleration; another set was used to measure the minor road vehicle acceleration. Each pair of tapeswitches measure the speed and the number of axles of individual vehicles. The pairs were spaced at 150-ft (46-m) increments. The sets of four pairs generated the speed profile of a vehicle as it approached or departed from the intersection for 450 ft (137 m).

A computer subroutine was acquired that could insert a mark into the data file at the time (to the nearest second) that specific computer keys were pushed. Over 20 different types of marks were available in the program. The marks that were programmed for the first installation included minor road vehicle type (PC, 2, 3, 4, etc. axles), turning maneuver (left, right, or through), arrival time, and departure time.

This method of collection was intended to produce more accurate data and to save time during data reduction since all the required data would be directly available in computer files and would not need to be reduced from the videotape. The speed data collected would be spot speeds at four locations 150 ft (46 m) apart. The video cameras would be installed as described in the previous section but would serve as a backup to the data in the traffic data collectors.



LEGEND

- || Tapeswitches
- C Traffic Data Collectors
- Camera
- Ⓜ Generators

Note: 1 ft = 0.305 m

Figure 47. Typical setup for tapeswitch data collection plan.

Inclement weather (rain and freezing temperatures) prevented this data collection technique from being deployed successfully. Because of pavement and were frequently dislodged by passing traffic. In order to stay on schedule, the tapeswitch data collection approach was abandoned and all data were collected using the video collection plan.

3. Equipment

Selection of equipment was based on the development of a traffic data collection system that would be flexible yet capable of recording vehicle performance at various intersections for several hours. Some of the requirements that were met by the selected equipment included:

- Portable.
- Capable of temporary installation.
- Flexible (able to accommodate different intersections with varied geometric characteristics).
- Capable of classifying all vehicles that enter the study area.
- Capable of having a time associated with the recorded data.
- Capable of recording vehicle positions.
- Capable of recording gap data in terms of either time or distance.
- Unobtrusive, so that visibility of the equipment could be minimized to avoid modification of driver behavior.

The following equipment was selected for data collection:

- Five portable video cameras with the capability of superimposing a continuous stopwatch on the screen.
- Five heavy-duty tripods.
- Two portable traffic counters capable of storing traffic data for individual vehicles (data not stored in bins).
- One portable lap-top computer.
- Two 1,000-W, portable, gasoline-powered generators.
- One DC-AC inverter (to operate a camera from a car battery).
- Miscellaneous--extension cords, power strips, measuring wheel, paint, vests and flags (traffic control), videotapes, traffic counter road tubes, nails, etc.

4. Site-Specific Data Collection Plans

A summary of the data collection and the number of trucks recorded at each site is provided in table 30.

a. Route 26 and Central Valley Asphalt Intersection

The data collection at this rural site was hampered by adverse weather (rain and freezing temperatures). Few trucks exited from the plant, and the video cameras would not operate under very low temperatures. Five attempts to collect data resulted in only 9.75 hours of usable data. Figure 48 depicts the layout of the final data collection plan at this site.

b. Route 64 and Truck Stop 64 Intersection

The second site is a truck stop near a rural Interstate highway. Figure 49 illustrates the placement of the equipment.

c. Trindle Road and Railroad Avenue

The third site was located near an industrial park in an urbanized area. Figure 50 shows the schematic of the intersection and the placement of the equipment on the first day of taping. The major road at this site has a relatively high traffic volume (20,000 veh/day).

C. Data Reduction

The data reduction from the videotape was based on the 100-ft (30-m) reference lines on a sheet of clear acetate taped to a television screen that provided a measurement scale. The process of reducing data for a particular vehicle began by reviewing the videotape frame by frame to determine the exact location of a vehicle crossing each 100-ft (30-m) increment line. A video operator used the slow motion and stop-frame features of the video playback unit to stop the tape just as the vehicle's bumper crossed the line on the acetate sheet and then recorded the time shown by the clock superimposed on the screen. Separate acetate sheets were required for each intersection, each camera, and in most cases for each direction of travel. Reference marks aligned with stationary objects in the video picture allowed the acetate sheets to be realigned after being removed.

1. Equipment

The data reduction, although relatively simple, was time-consuming because to reduce the required information (gap, acceleration, deceleration, and minimum separation), the operator had to view several different videotapes simultaneously.

Table 30. Amount of data collected.

<u>Study</u>	<u>Hours of videotaping</u>	<u>Number of trucks recorded</u>	
		<u>Right</u>	<u>Left</u>
Route 26 and Central Valley Asphalt			
10/12/88, Wednesday	0.00	a	a
10/19/88, Wednesday	1.75	6	14
10/21/88, Friday	2.00	3	32
10/24/88, Monday	0.00	b	b
10/27/88, Thursday	6.00	40	31
Subtotal	9.75	49	7
Route 64 and Truck Stop 64			
10/17/88, Monday	6.00	c	c
10/26/88, Wednesday	6.10	273	8
Subtotal	12.10	273	8
Trindle and Railroad			
10/31/88, Monday	5.50	62	14
11/1/88, Tuesday	8.00	87	14
Subtotal	<u>13.50</u>	<u>149</u>	<u>28</u>
TOTAL	35.35	471	113

-
- a Cold weather.
 - b Rain began during setup.
 - c Unusable data due to battery failures.

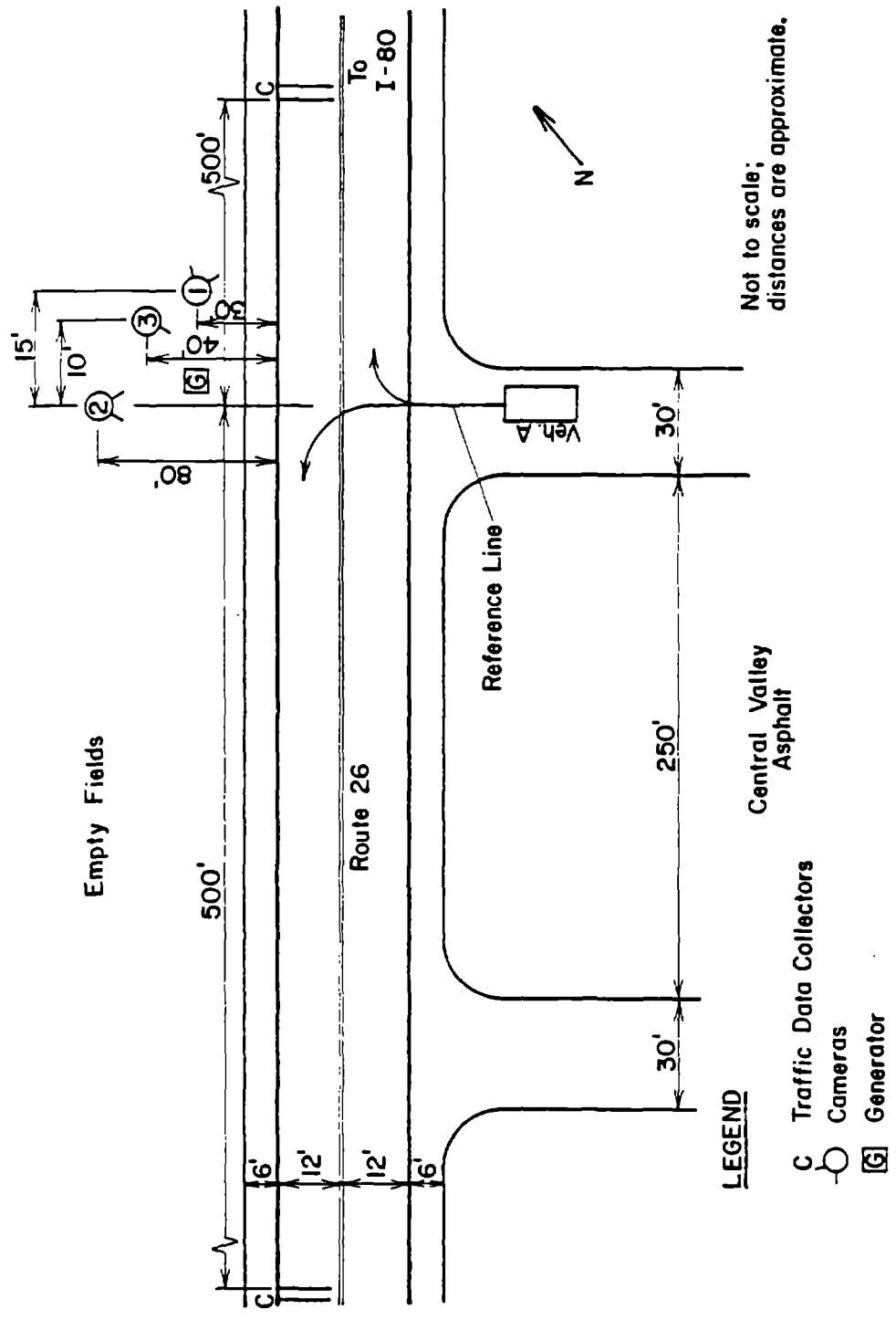
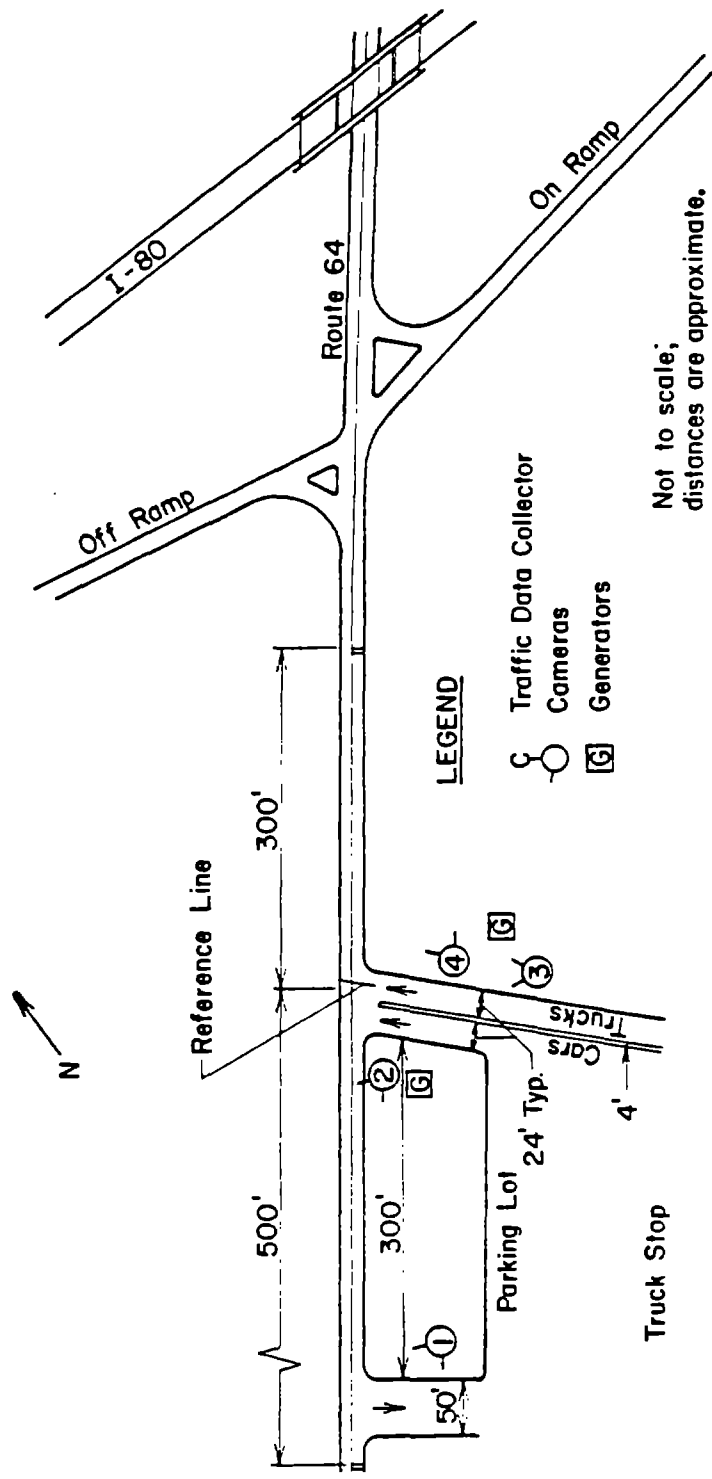


Figure 48. Site plan for Route 26 and Central Valley Asphalt intersection.



Note: 1 ft = 0.305 m

Figure 49. Site plan for Route 64 and Truck Stop 64 intersection.

This was accomplished with side-by-side video playback monitors and video playback equipment that had the following capabilities: slow motion, freeze frame, and frame-by-frame advancement. The following equipment was used during the video reduction:

- Two full-function videocassette recorders.
- One four-head videocassette recorder.
- Three 19-in (48-mm) video monitors.
- One microcomputer with a spreadsheet program for data entry and calculations.

2. Gap Acceptance

Gap acceptance data were reduced to document the length and duration of gaps that were accepted and rejected by trucks on the minor road approach. The videotape with the direct view along the reference line on the minor road (e.g., camera 3 in figure 50) was used to reduce the gap information. The operator used the following procedure to obtain the necessary gap data:

1. Consecutively number each minor road truck that approached the intersection.
2. Classify each vehicle according to number of axles.
3. Record the type of maneuver (right or left turn).
4. Record the arrival time (time at which the vehicle came to a complete stop). If the vehicle did not come to a complete stop, record the words "did not stop" under the departure time column and do not record any additional information.
5. Record the time the first vehicle, traveling on the major road, passed the reference line (center of the minor approach).
6. Record the time at which each subsequent major-road vehicle passed the reference line until the minor-road vehicle departed. For left turns, vehicles traveling in both directions on the major road were documented. For right turns, data were recorded for one direction only unless the driver on the minor road was waiting for an adequate gap in both directions (in order to use the far lane to complete the turn). In the latter case, data for both directions of major-road vehicles were recorded.
7. Record the departure time of the minor-road vehicle.
8. Record the time the next vehicle on the major road crossed the reference line.

9. Review the other tapes covering the major-road approaches to determine which gaps to eliminate from the data set. Data were eliminated if the minor-road vehicle did not stop, if a turning vehicle caused the gap, or if the gap-causing vehicle turned onto the major road from a nearby driveway.
10. Calculate the gap lengths rejected and accepted.

The videotapes were reviewed several times to collect and check the required data. Table 31 presents the number of vehicles for which data were reduced in the analysis. The number of deleted vehicles is shown in the "Data Deleted" column. Approximately 35, 47, and 20 percent of the vehicle data at the Central Valley Asphalt, Truck Stop 64, and Trindle and Railroad, intersections, respectively, were deleted. Failure of the minor-road trucks to stop completely was the primary reason for deleting data.

Table 31. Number of vehicles reduced for gap analysis.

<u>Intersection</u>	<u>Left turn</u>			<u>Right turn</u>		
	<u>Data reduced</u>		<u>Data deleted</u>	<u>Data reduced</u>		<u>Data deleted</u>
	<u>5-Axle</u>	<u>< 5-Axle</u>		<u>5-Axle</u>	<u>< 5-Axle</u>	
Central Valley Asphalt	1	58	18	0	23	26
Truck Stop 64	5	2	1	134	7	132
Trindle and Railroad	16	8	4	91	26	32

3. Acceleration

Acceleration data were reduced to determine the acceleration rates of trucks as they turned right or left from the minor road approach onto the major road. The trucks were divided into the following groups for each intersection:

- Right turns accepting gaps greater than 20 s.
- Right turns accepting gaps less than 20 s.
- Left turns accepting gaps greater than 20 s in both directions.
- Left turns accepting gaps less than 20 s in at least one direction.

The data reduction procedure for right and left turns required the use of a different series of tapes. Due to the limited amount of reduction equipment and the complexity of the setup, right and left turns were reduced separately.

The equipment setup required to reduce acceleration data was more complex than the setup required for gap data. For most sites, three tapes were reviewed simultaneously to obtain complete acceleration information for a particular truck. Acetate sheets were marked in 100-ft (30-m) increments using the flagging procedure described earlier. The operator used the monitors to follow the truck from screen to screen as the turn maneuver was accomplished. The departure time and the times at which a truck passed the 100-ft (30-m) increment lines were read from the video screen and recorded in a computer spreadsheet.

The operator's major difficulty was synchronizing the three videotapes initially and keeping them near synchronization throughout the data reduction process. The videotapes could not be run simultaneously for an acceleration maneuver and were played independently of each other. The operator found a particular vehicle on the reference line tape using the gap data, and then determined the physical characteristics of the vehicle and recorded any available acceleration data. The reference line tape was paused when the accelerating vehicle began to move out of view. The operator then moved to the next screen in sequence and found the vehicle as it accelerated through the camera's field of view, and so on until the truck completely traversed the study area.

When a truck was near the limits of the field of view of a particular camera, it became difficult to determine when it crossed a 100-ft (30-m) increment line. This problem was caused in part by poor picture clarity when vehicles were farther than 300 ft (90 m) from the camera. The problem was compounded by the recording angles (see figures 48 to 50). Due to roadside development that limited the maximum distance from the roadway at which cameras could be placed, it was impossible to place the cameras perpendicular to the road and still get more than 200 ft (60 m) of roadway in the field of view. Therefore, the cameras had to be placed so that their field of view was along the roadway rather than across it.

Table 32 presents the number of accelerating vehicles available for analysis. Data for some vehicles were eliminated if (1) the vehicle did not stop completely at the intersection, (2) particular 100-ft (30-m) data points were missing because that particular camera had not yet been started, (3) the vehicle slowed to make a turn within the study area, or (4) other miscellaneous reasons.

Table 32. Number of vehicles for acceleration analysis.

Intersection	Left turn			Right turn		
	Data reduced		Data deleted	Data reduced		Data deleted
	5-Axle	< 5-Axle		5-Axle	< 5-Axle	
Central Valley Asphalt	0	59	18	0	18	31
Truck Stop 64	5	0	3	50	0	223
Trindle and Railroad	13	0	15	117	0	32

4. Deceleration

Deceleration data were reduced to determine the deceleration rates and speed reductions of major-road vehicles that were impeded by a truck turning right or left out of the minor road. Minor-road vehicles identified from the gap data that did not stop at the intersection or accepted gaps greater than 20 s were eliminated from the potential deceleration data set. The potential deceleration data were then divided into the following groups:

- Right turns accepting gaps less than 20 s.
- Left turns accepting gaps less than 20 s in the near lane.
- Left turns accepting gaps less than 20 s in the far lane.

The equipment setup required to reduce the deceleration data was similar to the setup to reduce acceleration data. The operator traced the movement of the major road vehicle as it approached the intersection across several monitors using video data for several cameras. The departure time of the minor road vehicle and the time the major-road vehicle crossed the 100-ft (30-m) increment lines were recorded in a computer spreadsheet.

The deceleration data reduction process had problems similar to those for the acceleration data reduction. A stopped minor-road vehicle blocking the view of the reference line caused a major problem. Again, due to camera angle and picture quality, it was difficult for the operator to track the movement of a vehicle when it was at the edge of the camera's field of view.

Table 33 presents the number of decelerating vehicles available for analysis. Data were eliminated if (1) the minor-road vehicle did not come to a complete stop at the intersection, (2) the minor-road vehicle accepted a gap over 20 s (representing a gap of more than 1,000 ft [300 m]), (3) particular 100-ft (30-m) data points were missing because that particular camera had not yet been started, (4) the vehicle slowed to make a turn within the study area, or (5) other miscellaneous reasons.

Table 33. Number of vehicles for deceleration analysis.

<u>Intersection</u>	<u>Left turn</u>			<u>Right turn</u>		
	<u>Data reduced</u>		<u>Data deleted</u>	<u>Data reduced</u>		<u>Data deleted</u>
	<u>5-Axle</u>	<u>< 5-Axle</u>		<u>5-Axle</u>	<u>< 5-Axle</u>	
Central Valley Asphalt	0	7	70	0	0	49
Truck Stop 64	0	0	8	14	0	259
Trindle and Railroad	14	9	14	29	11	109

5. Minimum Separation

Minimum separation (referred to as "tailgate distance" in the AASHTO Green Book) is the distance between the rear bumper of a truck turning onto the major road and the front bumper of a following vehicle on the major roadway (see figure 45). Minimum separation was determined by comparing the acceleration data for the minor-road truck with the deceleration data for the following vehicle on the major roadway. The minimum time (or distance) separation between the estimated acceleration and deceleration curves can be scaled from a plot of their respective time vs. distance profiles. This procedure is explained in greater detail in a later section.

A sample of turning maneuvers for which both acceleration and deceleration data were available was selected for the minimum separation evaluation. The problems associated with reducing those data sets, discussed above, also apply to the minimum separation data set.

D. Data Analysis

1. Gap Acceptance Behavior

a. Background

The initial goal was to have gap acceptance data for at least 50 minor-road vehicles for each combination of maneuver type (left or right turns) and vehicle types (five-axle trucks or less-than-five-axle trucks). However, several vehicle/maneuver type combinations at the intersections had less data available. An analysis was conducted for each combination for which at least 15 minor-road truck turning maneuvers were available. Table 31, presented earlier, identifies the number of usable vehicle data sets and the number of vehicles eliminated during the data phase.

The objective of the gap acceptance analysis was to determine the critical gap; i.e., the smallest gap that is likely to be accepted by most drivers. A gap was defined as the time interval between the arrival of one vehicle and the next on the major road. The critical gap cannot be determined

from observation of a single driver, but only from the distribution of gaps accepted and rejected by many drivers. Three alternative methods of determining the critical gap were selected for this study: the Greenshield method; the Raff method; and the logit model.^{43,44,45} Figure 51 illustrates a typical gap acceptance plot for each method.

The Greenshield method uses histograms to represent the time gaps accepted and rejected by minor road drivers. The vertical axis in the upper portion of figure 51 represents the number of gaps accepted or rejected for each gap length (shown on the horizontal axis). Greenshield defined the "average minimum acceptable time gap" as the shortest time gap that will be accepted by more than 50 percent of the drivers.⁴³

The Raff method is graphical and consists of drawing two cumulative distribution curves as shown in the middle portion of figure 51. As originally developed, the Raff method dealt with lags rather than gaps. A lag is the time interval between the arrival of a minor-road vehicle at the intersection and the arrival of the next major-road vehicle. One curve relates the lag length, L , to the number of accepted lags less than or equal to L , and the other relates L to the number of rejected lags greater than L . The intersection of these two curves yields the "critical lag" value, which Raff defined as the lag length for which the number of shorter lags accepted is the same as the number of longer lags rejected.⁴⁴ The Raff study addressed only lags and not gaps, because of concern that gap acceptance or rejection would be a function of the point in time during the gap at which the minor road vehicle arrived. However, studies since Raff's work have indicated that the acceptance of lags is not significantly different from the acceptance of gaps, and that the lag and gap data can be combined.^{46,47} Therefore, the lag and gap data for each vehicle/maneuver type combination were merged and analyzed together in the present study.

When the dependent variable is a variable that indicates a choice (i.e., either the acceptance or rejection of a gap), the shape of the response function will frequently be curvilinear and can be approximated using a logistic function. A property of the logistic function is that it can easily be linearized through a single transformation. This transformation is called the logistic or logit transformation. The lower portion of figure 51 depicts a sample logistic curve which relates the length of a gap to the probability of acceptance.

b. Determination of Gap Acceptance Values

Greenshield Method: Figure 52 presents an example of the Greenshield method applied to five-axle trucks turning right at the Trindle and Railroad intersection.⁴³ The average minimum acceptable time gap (i.e., the minimum time gap accepted by more than 50 percent of the driver) occurs at 8.25 s (three drivers accepted and three drivers rejected the gaps between 8.0 and 8.5 s). A similar approach was used to apply the Greenshield method to the remaining vehicle/maneuver type combinations.

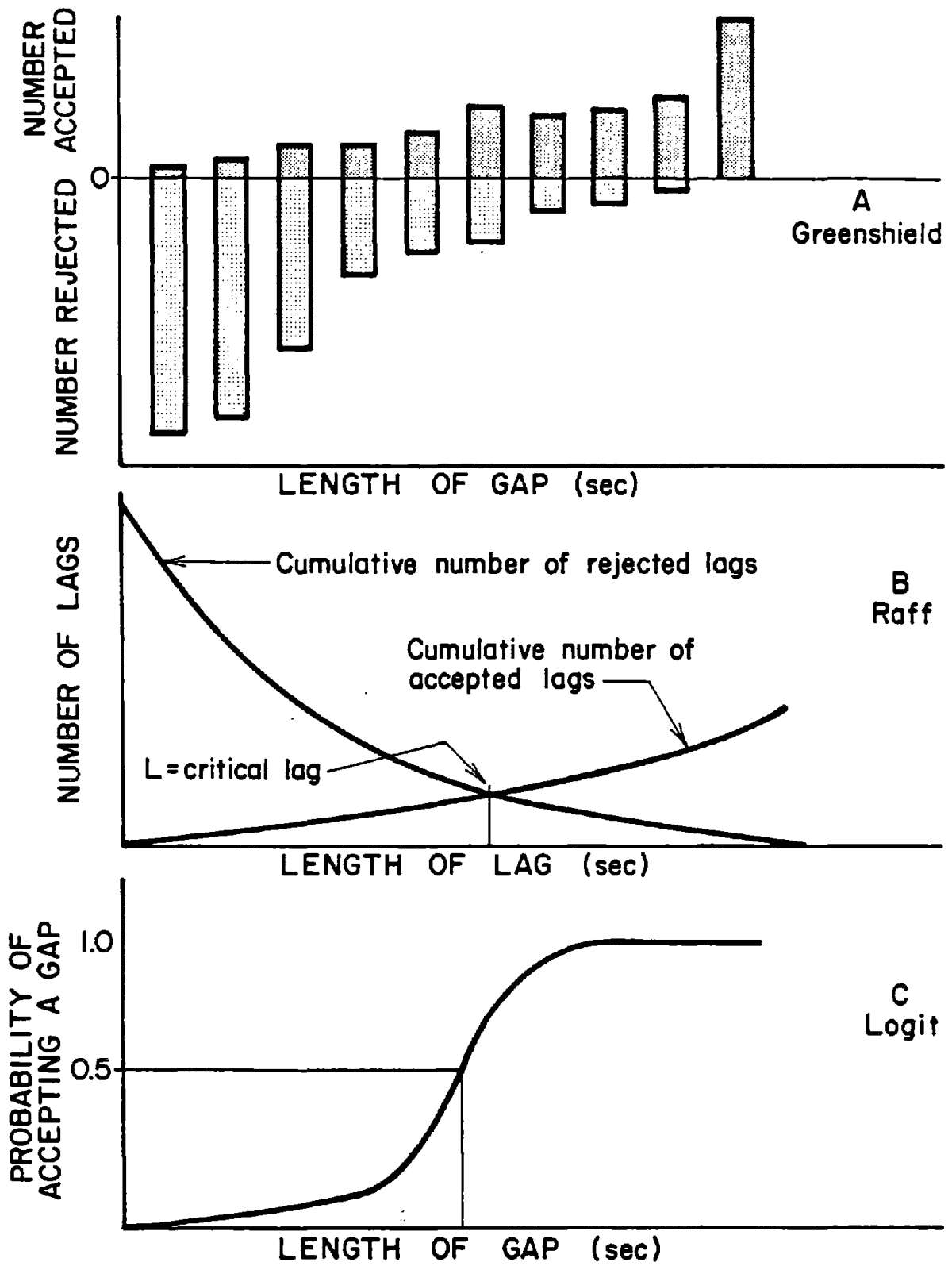


Figure 51. Typical gap acceptance plots for Greenshield, Raff, and logit methods.

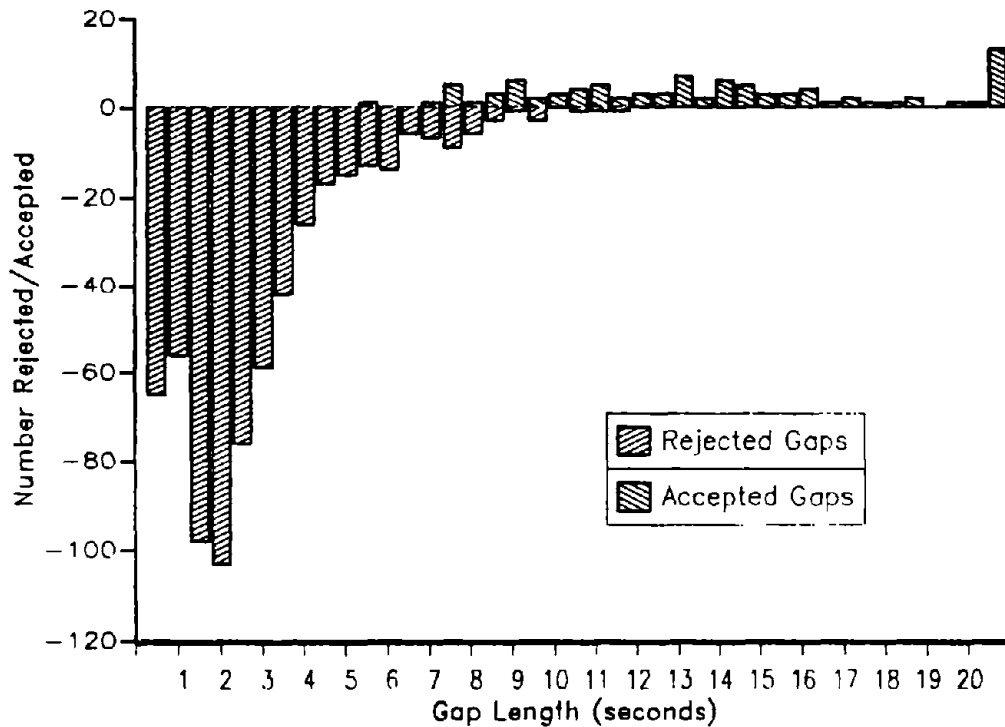


Figure 52. Gap acceptance analysis by Greenshield method for a typical data set.

The Greenshield method was selected for the gap acceptance analyses because of its simplicity. However, the results from some of the analyses must be interpreted with caution due to small sample sizes. An extremely small accepted gap length could become the average minimum acceptable time gap if a few drivers accepted that gap length and none or only one of the drivers rejected it.

Raff Method: An example of the results from the Raff graphical method is illustrated in figure 53 for five-axle trucks turning right at the Trindle and Railroad intersection.⁴⁴ One curve relates the gap length, t , with the number of accepted gaps less than t and the other relates t with the number of rejected gaps greater than t . The intersection of these two curves at 8.5 s is the critical gap value. A similar approach was used to apply the Raff graphical method to the remaining vehicle/maneuver type combinations.

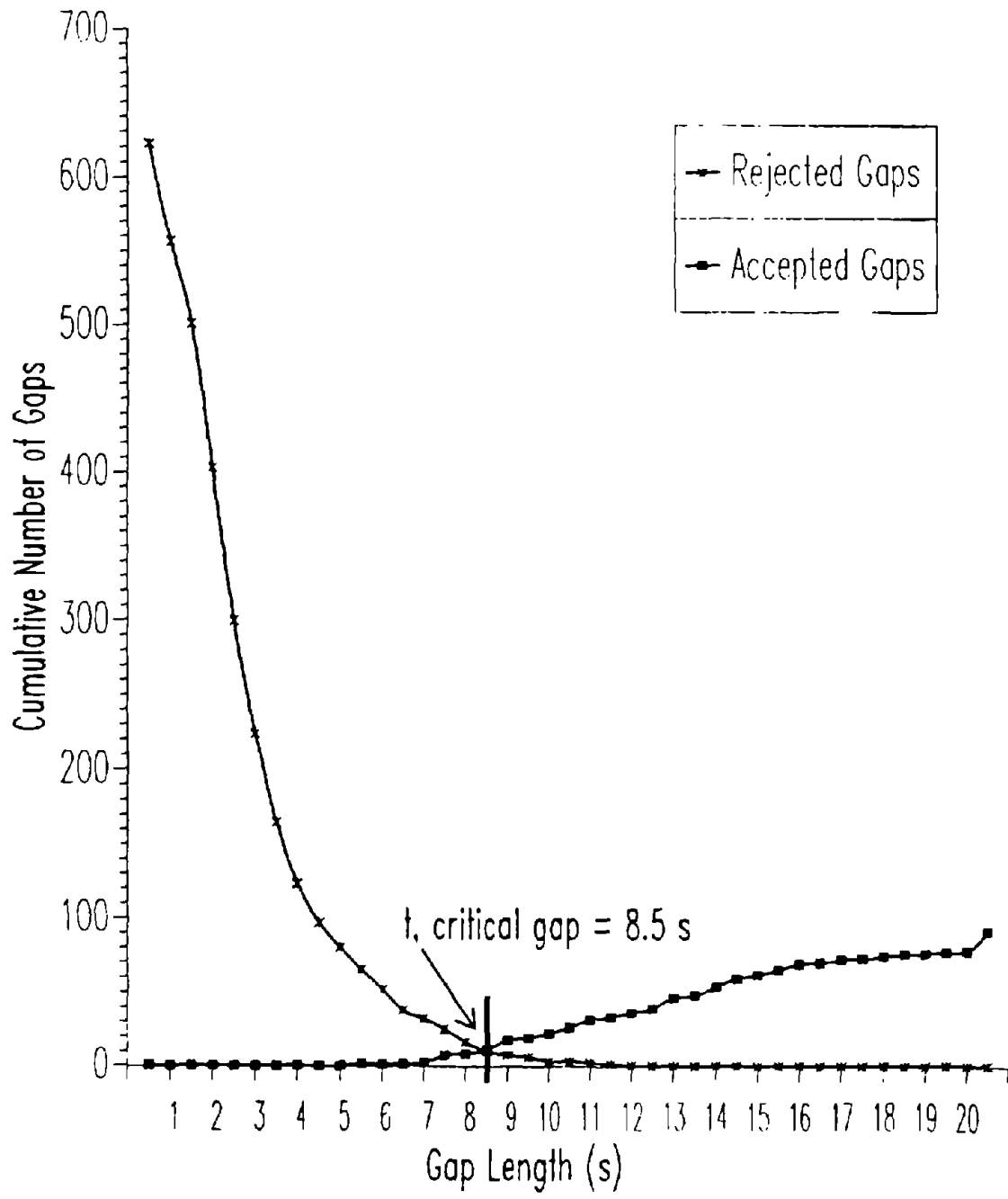


Figure 53. Gap acceptance analysis by Raff method for a typical data set.

Logit Model: Choice modeling (such as whether to accept a gap) may be done by using a logistic growth model to determine the probability of taking a certain action.⁴⁵ Logistic or logit models have been used in previous studies to model the probability of accepting gaps of varying lengths.^{46,48} The simple, dichotomous-choice logistic function is:

$$P = \frac{1}{1 + e^{-(\beta_0 + \beta_1 X)}} \quad (55)$$

where: P = probability of accepting a gap
 X = variable related to gap acceptance decision (i.e., gap length)
 β_0, β_1 = Coefficients to be determined

When the dependent variable is a 0,1 (accept or reject) indicator variable, the mean response represented by equation (55) is a probability. The logistic function can be easily linearized with the following transformation:

$$P' = \log_e \left(\frac{P}{1-P} \right) = \beta_0 + \beta_1 X \quad (56)$$

where: P' = transformed probability.

A sample logistic curve and its corresponding equation for right turns by five-axle trucks at the Trindle and Railroad intersection are shown on figure 54. The probability of accepting a gap of specified length is found by reading from the curve in the figure or by solving equation (56) for a particular gap length. The gap length that will be accepted with a 50 percent probability can be found by substituting 0.5 for P as shown below:

$$\log_e \frac{0.5}{1-0.5} = -9.58 + 1.12 X \quad (57)$$

$$X_{50\%} = 8.52 \text{ s}$$

Fifty percent of the five-axle truck drivers making right turns at the Trindle and Railroad intersection accepted a gap of 8.52 s and 85 percent accepted a gap of 10.06 s. A similar approach was used to apply the logit model to the remaining vehicle/maneuver type combinations.

Findings: Tables 34 and 35 contain the results from the above methods. The alternative methods generally yielded critical gap values within a 2-s range of each other.

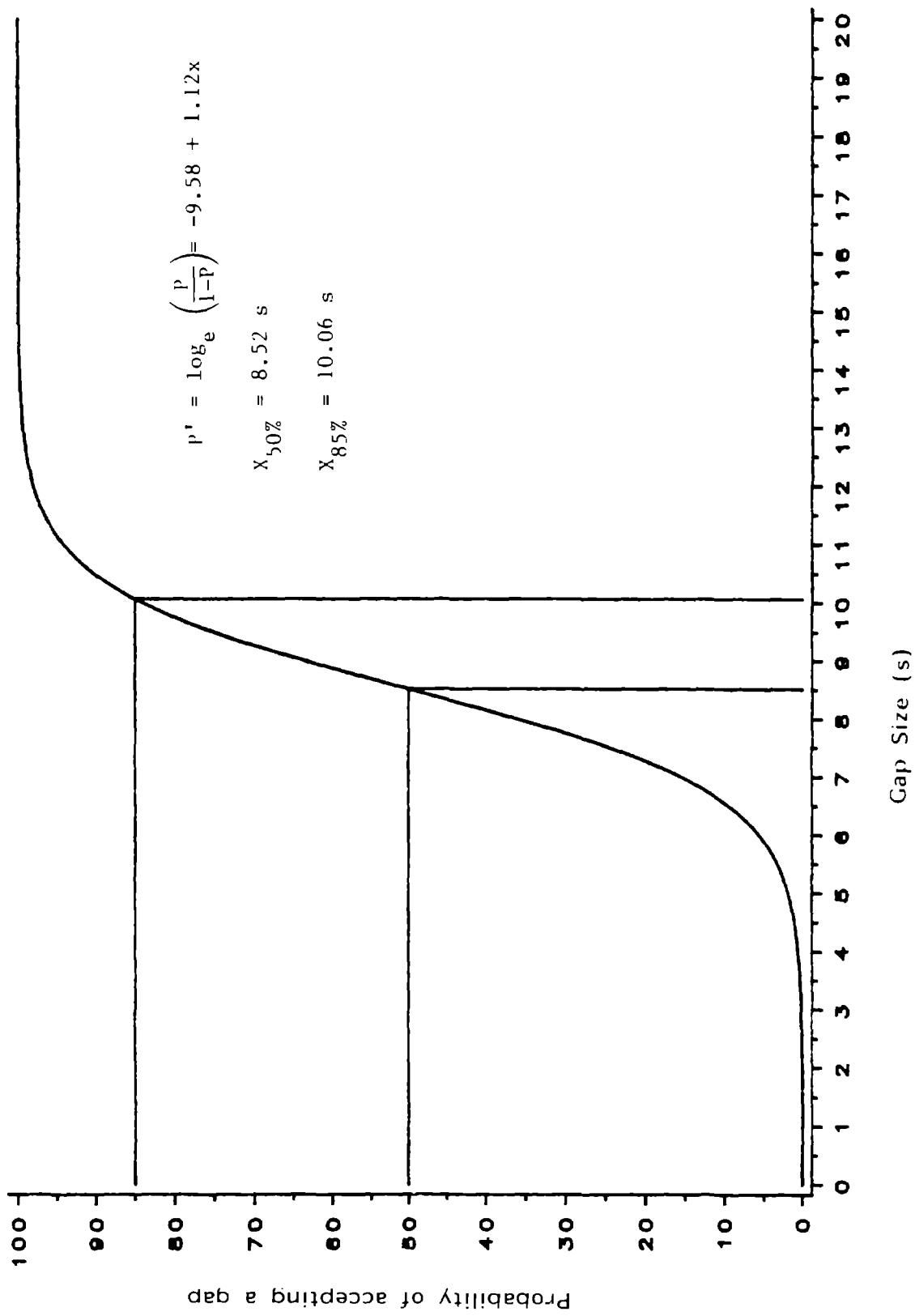


Figure 54. Gap acceptance analysis using logit model for a typical data set.

Table 34. Results of gap acceptance analysis, critical gap (s) for left-turn maneuvers.

Intersection	Data sets	Five-axle trucks				Data sets	Less-than-five-axle trucks			
		G ^a	R	L-50	L-85		G	R	L-50	L-85
1 Central Valley Asphalt	1	Insufficient data				58	10.25	10.50	11.16	13.89
2 Truck Stop 64	5	Insufficient data				2	Insufficient data			
3 Trindle & Railroad	16	7.25	8.25	8.27	9.84	8	Insufficient data			

Analyses were not performed for data sets containing less than 15 accepted gaps (i.e., 15 minor-road vehicles).

^a where

- G = Greenshield method
- R = Raff method
- L-50 = Logit model at 50% probability of accepting a gap
- L-85 = Logit model at 85% probability of accepting a gap

Table 35. Results of gap acceptance analysis, critical gap (s) for right-turn maneuvers.

Intersection	Data sets	Five-axle trucks				Data sets	Less-than-five-axle trucks			
		G ^a	R	L-50	L-85		G	R	L-50	L-85
1 Central Valley Asphalt	0	Insufficient data				23	10.75	12.50	13.17	15.86
2 Truck Stop 64	134	10.75	12.50	12.43	14.78	7	Insufficient data			
3 Trindle & Railroad	91	8.25	8.50	8.52	10.06	26	6.25	6.50	7.25	8.87

Analyses were not performed for data sets containing less than 15 accepted gaps (i.e., 15 minor-road vehicles).

^a where

- G = Greenshield method
- R = Raff method
- L-50 = Logit model at 50% probability of accepting a gap
- L-85 = Logit model at 85% probability of accepting a gap

c. Discussion of Results

The results obtained for several of the vehicle/maneuver type combinations were questionable due to limited data. For example only 3 of the 23 less-than-five-axle trucks turning right at the Central Valley Asphalt intersection accepted gaps less than 20 s. A 20-s gap represents over 1,000 ft (300 m) of sight distance. The smallest gap accepted (10.75 s) became the minimum accepted gap according to Greenshield's method since only one rejected gap occurred at the same time value. The Raff and logit methods produced higher critical gap values of 12.5 and 13.1 s, respectively, for the same data set.

The analysis at the Truck Stop 64 intersection produced similar results. The Greenshield method had a smaller critical gap than either Raff or logit methods. Because the Greenshield method involves the assessment of gap acceptance behavior for each particular gap length without considering the rest of the data, it does not consider the distribution of gaps accepted or rejected at other gap lengths. Since the Raff method considers cumulative distributions and the logit method considers the probability of accepting different size gaps, the results are influenced by the several larger-than-30-s gaps accepted.

The three alternative methods produced very consistent results for all vehicle/maneuver type combinations at the Trindle and Railroad intersection and left turns by less-than-five-axle trucks, and the Central Valley Asphalt intersection.

Table 36 summarizes findings from similar studies for trucks and passenger cars and results reported in the 1985 Highway Capacity Manual for passenger cars.^{46,49,50} A 1981 British study measured the "median accepted gap" for cars, vans, and trucks in a crossing and merging operation.⁵⁰ The United Kingdom's crossing maneuver is similar to the United States' left-turn-from-the-major-road maneuver, and the merging operation is similar to the United States' right-turn maneuver. The data for the vans and trucks were combined into an "all goods" category when the data were "sparse". This study determined the median accepted gap (i.e., the gap length that had a 50 percent probability of acceptance) using the probit transformation. Gap lengths found in this study for passenger cars are more than 1 s less than the critical gaps found in other studies and the Highway Capacity Manual.^{46,47}

An Indiana study included field studies to estimate gap acceptance distribution for minor road drivers when crossing or merging with major road traffic at STOP-controlled intersections.⁴⁶ Truck data for all maneuvers were combined since the number of trucks observed (34, 75, and 43 right-turn, through, and left-turn maneuvers, respectively) was small. The critical gap was determined using the logit model. The findings of the present study at the high-volume Trindle and Railroad intersection are similar to the findings of the Indiana study for all truck maneuvers.

Table 36. Findings from similar studies.

<u>Study</u>	<u>Measured</u>	<u>Critical gap (s)</u>		
		<u>Site</u>	<u>Passenger Cars</u>	<u>Trucks</u>
United Kingdom ⁵⁰	Left turns (UK conditions)	1	3.91	4.63
		3	3.66	5.33
		4	4.31	4.99
		5	4.41	4.91
Indiana, 1980 multilane, divided highways ⁴⁶	PC, right turns Trucks, all possible maneuvers		6.73	
			8.40	
Highway Capacity Manual, 1985 ⁴⁹		<u>Running speed (major road)</u>		
			<u>30 mi/h</u>	<u>55 mi/h</u>
		Right turn from stop, 2 lanes	5.5	6.5
		Left turn from stop, 2 lanes	6.5	8.0

Note: 1 mi = 1.61 km

The critical gap lengths found at the Central Valley Asphalt intersection appear large when compared to other high volume intersections. Since the major road at this intersection has an ADT of 14,000 veh/day, one would suspect the critical gap acceptance value to fall between the findings at the Trindle and Railroad intersection (20,000 veh/day) and the Truck Stop 64 intersection (7,000 veh/day). However, the critical gap lengths at the Central Valley Asphalt intersection are higher than those at the Truck Stop 64 intersection for right turns and more than 2 s higher than those at the Trindle and Railroad intersection. Also, drivers turning right were found to wait for larger gaps than drivers turning left, which is the opposite of the expected behavior.

The Central Valley Asphalt intersection has some unique characteristics that may explain the observed findings. The intersection is located approximately 2,000 ft (600 m) north of a signalized intersection. Drivers turning right noticeably wait for the end of platoons of approaching vehicles formed by the upstream signal to pass. Also, the vehicle leaving the plant were fully loaded three- or four-axle aggregate or concrete trucks with low acceleration capabilities, which might be expected to wait for longer gaps.

The ADT on the major road at the Truck Stop 64 intersection is 7,000 veh/day. Very large gaps are available at this low volume. Several truck drivers waited for large gaps (defined in this study as gap length

greater than 20 s). Accepted gaps at this intersection were larger than those at the Trindle and Railroad intersection.

Almost all trucks turning right at the Truck Stop 64 intersection entered the I-80 entrance ramps located approximately 500 ft and 1,000 ft (150 and 300 m) downstream from the truck exit. Truck drivers may have waited for larger gaps than usual at this location since they would only accelerate for a short distance before slowing to make the turn onto the entrance ramps.

By contrast, truck drivers at the Trindle and Railroad intersection were pressured by traffic conditions to accept smaller gaps than those accepted at the other sites. The frequency of gaps greater than 20 s was small; long queues occasionally formed on the minor road behind the truck. The five-axle trucks typically encroached into the far lane of the major road to complete the turn maneuver. Several truck drivers forced the far-lane vehicles onto the shoulder during right-turn maneuvers.

d. Distance Gaps

The distance gap is the distance between successive vehicles on the major road measured when the lead vehicle is passing the minor-road intersection. Distance gaps are potentially preferable to time gaps for intersection sight distance studies since the distance gap is the sight distance that the minor road vehicle must have to see the next oncoming vehicle when the previous vehicle on the major road passes the intersection. Distance gaps are more difficult to measure than time gaps but are more reliable because the apparent time gaps can increase greatly if the gap is accepted and the following major-road vehicle is forced to decelerate.

Data concerning the distance gaps accepted were obtained at the Trindle and Railroad intersection for situations in which the approaching major road vehicle was within the camera field of view (i.e., within 500 ft [150 m] of the intersection) and this vehicle was not eliminated for some other reason (decelerating to make a turn, entering the major road from a driveway with the study area, etc.). Only 22 percent of the major-road vehicles at the Trindle and Railroad intersection were within the camera field of view at the time the preceding vehicle passed the minor road intersection. The distance gaps were obtained using the deceleration data reduction setup. The major-road vehicle that followed the turning vehicle was identified using the reference line videotape. The tapes were rewound to determine where this vehicle was at the time when the previous vehicle crossed the reference line. The distance gaps were estimated to the nearest of 25 ft (8 m). The available data on distance gaps accepted are listed in table 37. The distance gaps required several cameras and were only available when the major road vehicle was within 500 ft (150 m) of the intersection.

Table 37 also shows the calculated average speed of the major-road vehicles. This calculated speed is based on the assumption that a driver maintains a constant speed for the entire length of the distance gaps. This assumption, however, is not supported by the field data, because the drivers on the major road were observed to reduce their speed when a minor-road vehicle entered the major road traffic stream. The calculated average speed for

Table 37. Distance gaps for trucks at the Trindle and Railroad intersection.

<u>Vehicle no.</u>	<u>Axle</u>	<u>Time gap (s)</u>	<u>Distance gap (ft)</u>	<u>Direction</u>	<u>Average speed (mi/h)</u>
RIGHT TURNS					
E 50	2	6.31	200	Eastbound	21.6
F 44	5	8.64	200	Eastbound	15.8
F 48	5	8.96	200	Eastbound	15.2
F 46	5	9.05	200	Eastbound	15.1
F 98	3	9.56	200	Eastbound	14.3
E 66	2	6.14	300	Eastbound	33.3
E 46	5	6.97	300	Eastbound	29.3
E 69	5	7.44	300	Eastbound	27.5
F 21	5	8.91	300	Eastbound	23.0
E 10	5	7.01	350	Eastbound	34.0
F 47	5	8.64	350	Eastbound	27.6
E 13	5	8.11	375	Eastbound	31.5
E 8	5	11.58	400	Eastbound	23.6
E 9	2	6.36	500	Eastbound	53.6
F 52	3	7.24	500	Eastbound	47.1
E 32	2	7.84	500	Eastbound	43.5
F 64	5	8.68	500	Eastbound	39.3
E 65	5	10.34	500	Eastbound	33.0
F 16	4	8.74	375	Westbound	29.3
F 57	5	9.48	400	Westbound	28.8
F 58	5	11.71	400	Westbound	23.3
F 74	5	7.95	400	Westbound	34.3
F 84	5	11.88	400	Westbound	23.0
F 87	5	8.35	300	Westbound	24.5
F 97	5	7.17	300	Westbound	28.5
Average Speed:					28.8
LEFT TURNS					
E 56	5	8.34	300	Eastbound	24.5
E 67	2	11.55	300	Westbound	17.7
F 43	5	11.67	400	Westbound	23.4
F 60	5	12.13	400	Westbound	22.5
Average Speed:					22.0

Note: 1 ft = 0.305 m
1 mi = 1.61 km

major-road vehicles involved in right- or left-turn maneuvers is 29 and 22 mi/h (47 and 35 km/h), respectively, substantially lower than the 85th percentile speed of 40 mi/h (64 km/h) at this site. However, informal checks on the actual speeds of these vehicles in the range from 400 to 500 ft (120 to 150 m) from the intersection found that they were consistently higher than the calculated values. This indicates that the major-road vehicles were, in fact, decelerating during the maneuver.

The distance gap accepted by a minor-road vehicle is a preferable measure compared to the time gap. Unfortunately, measuring distance gaps is much more difficult than measuring time gaps, because the camera field of view must extend further from the intersection. Sight distance requirements calculated from critical time gaps and 85th percentile speeds are greater than the field observed distance gaps. For example, if the critical gap is 8.5 s and the major-roadway speed is 40 mi/h (64 km/h), the calculated sight distance is 500 ft (150 m). The predicted distance gap from table 37 for a 8.5-s accepted gap would be between 300 and 400 ft (90 and 120 m).

2. Acceleration Rates

a. Determination of Average Acceleration Rates

Average accelerations were calculated using average speeds and average time required to traverse a given distance. Since the speed data collected was based on measured travel time for 100-ft (30-m) increments, average velocity was calculated for each 100-ft (30-m) segment. Table 38 presents an example of the acceleration rate calculations for a specific five-axle vehicle at the Trindle and Railroad intersection.

Table 38. Example calculation for acceleration rate.

<u>Adjusted distance (ft)</u>	<u>Adjusted time (s)</u>	<u>Average time (s)</u>	<u>Average distance (ft)</u>	<u>Average velocity (mi/h)</u>	<u>Average acceleration 0 to 510 ft (mi/h/s)</u>
0	0.00				
160	9.25	4.63	80	11.76	
260	12.36	10.81	210	21.87	
360	14.63	13.50	310	29.97	
460	16.81	15.72	410	31.13	
560	18.91	17.86	510	32.39	1.81

Note: 1 ft = 0.305 m
1 mi = 1.61 km

The average acceleration for the vehicle in table 38 was calculated as follows:

$$A = \frac{V_2 - V_1}{T_2 - T_1} = \frac{32.39 - 0}{17.86 - 0} = 1.81 \text{ mi/h/sec} \quad (58)$$

where: $V_1 = 0$

$$V_2 = \left(\frac{100}{18.91 - 16.81} \right) \left(\frac{3600}{5280} \right) = 32.39 \text{ mi/h} \quad (52.15 \text{ km/h})$$

$T_1 = 0$

$$T_2 = \frac{18.91 + 16.81}{2} = 17.86 \text{ s}$$

The results of the average acceleration calculations were used to generate cumulative distribution plots for four sets that are presented in figures 55 through 58. From these plots, the 50th and the 85th percentile acceleration rates were determined. Table 39 provides a summary of the findings.

For comparative purposes, table 40 presents the average acceleration rates determined from distance-versus-time plots reported by Hutton, who measured the acceleration of trucks with weight-to-power ratios of 100, 200, 300, and 400 lb/hp (0.06, 0.12, 0.18, and 0.24 kg/W) on a level and straight roadway.⁵¹ Table 40 also includes average acceleration rates calculated from the data in figure IX-22 in the Green Book assuming an initial speed of zero.

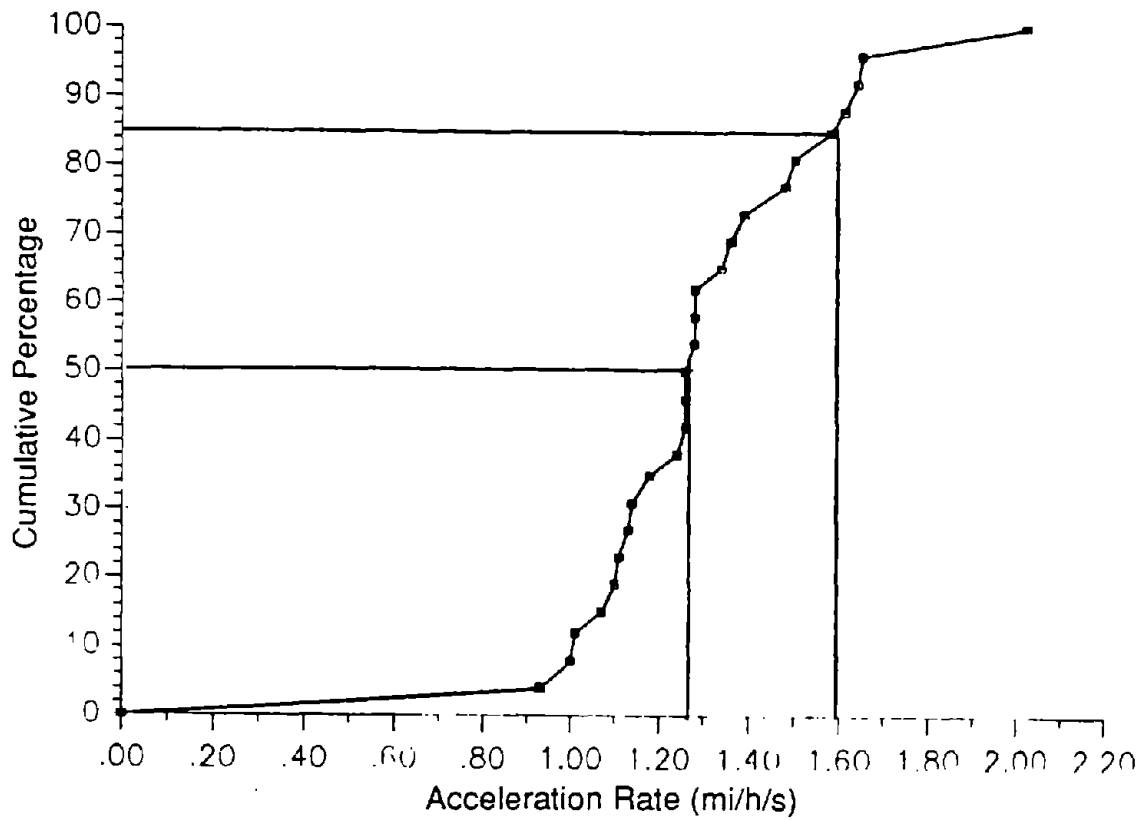


Figure 55. Cumulative distribution of average acceleration rate for left turns by four-axle trucks at the Central Valley Asphalt intersection.

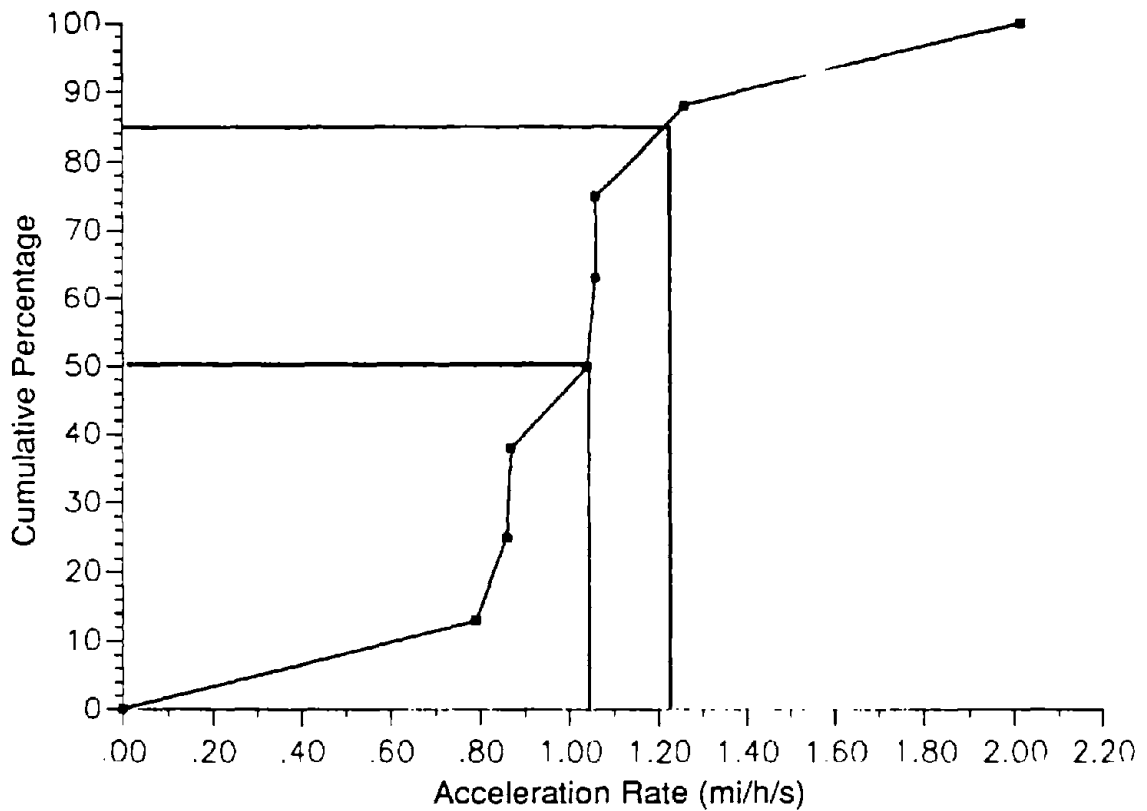


Figure 56. Cumulative distribution of average acceleration rate for right turns by four-axle trucks at the Central Valley Asphalt intersection.

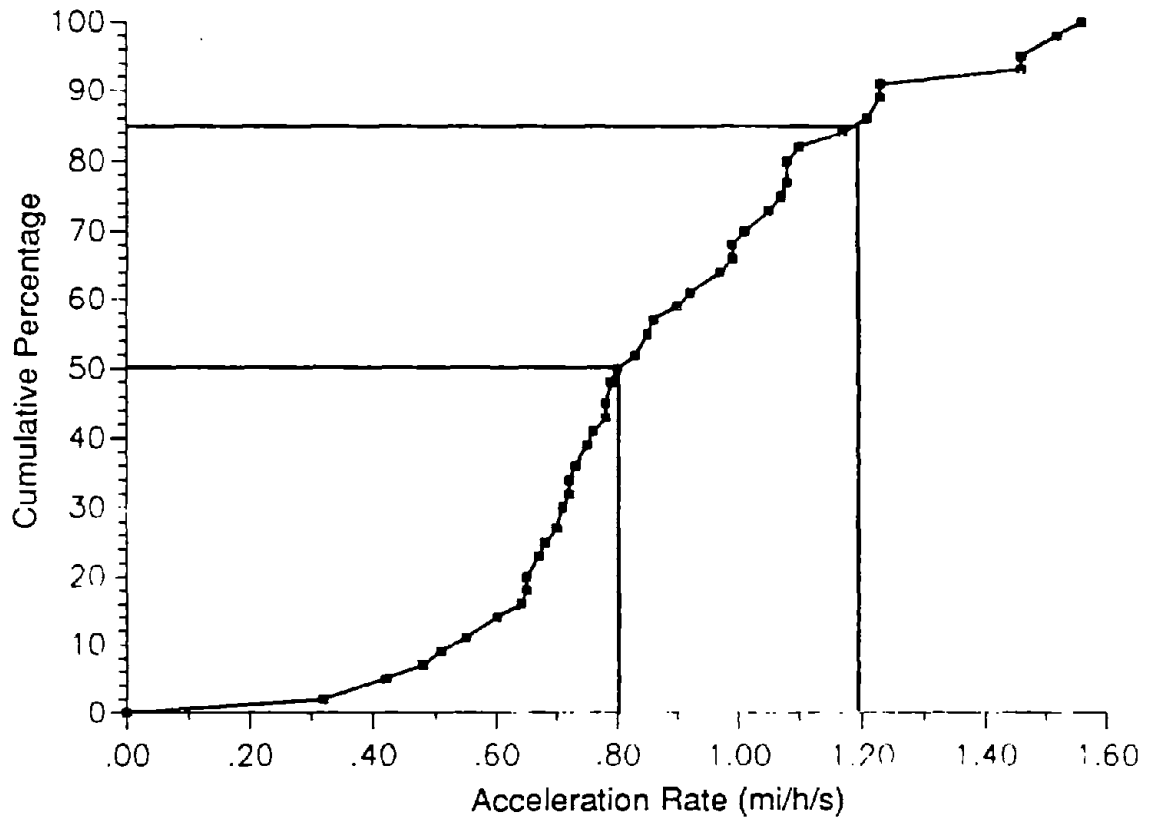


Figure 57. Cumulative distribution of average acceleration rate for right turns by five-axle trucks at the Truck Stop 64 intersection.

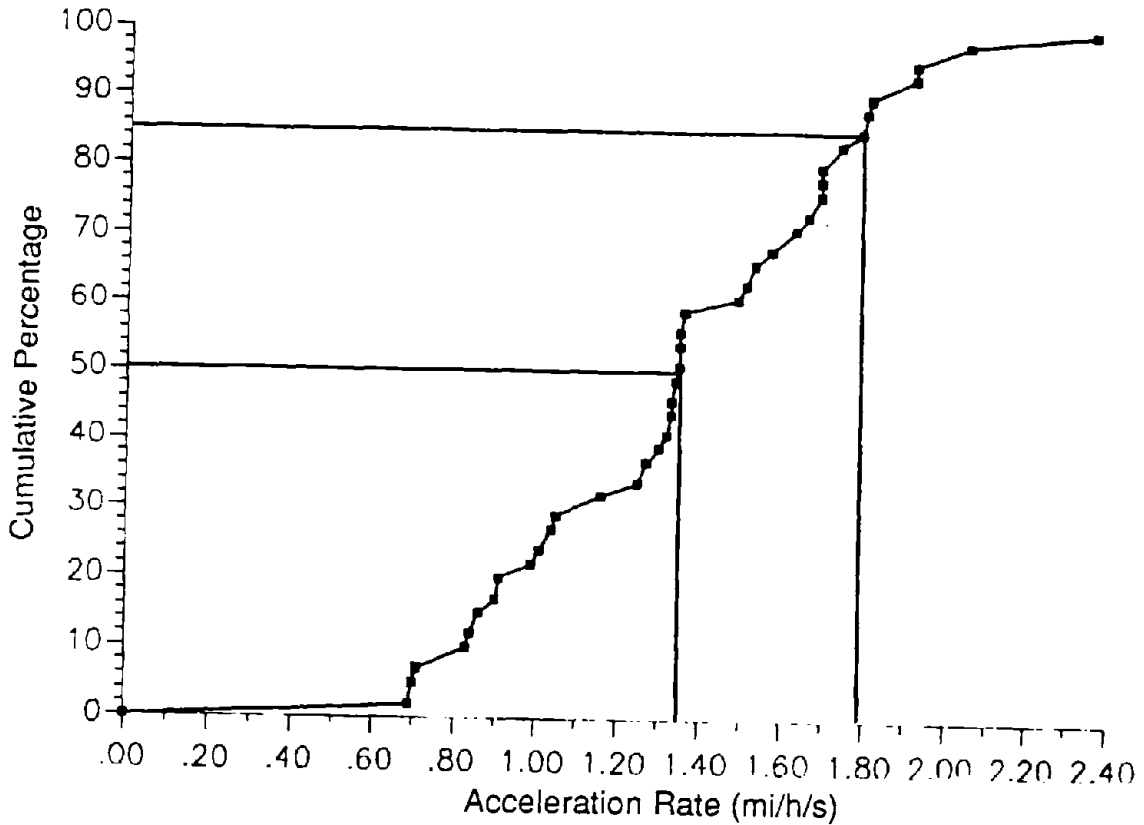


Figure 58. Cumulative distribution of average acceleration rate for right turns by five-axle trucks at the Trindle and Railroad intersection.

Table 39. Acceleration rates calculated from field data.

<u>Intersection</u>	<u>Maneuver</u>	<u>No. of axles</u>	<u>Distance (ft)</u>	<u>No. of vehicles</u>	<u>Acceleration rate (mi/h/s)</u>	
					<u>50th percentile</u>	<u>85th percentile</u>
Central Valley Asphalt	Left turn	3 & 4	0-290	25	1.27	1.58
Central Valley Asphalt	Right turn	3 & 4	0-490	8	1.04	1.21
Truck Stop 64	Right turn	5	0-350	43	0.80	1.20
Trindle and Railroad	Right turn	5	0-510	41	1.37	1.74

Note: 1 ft = 0.305 m
1 mi = 1.61 km

Table 40. Acceleration rates reported in the literature.

<u>Distance (ft)</u>	<u>Hutton⁵¹</u>				<u>AASHTO^a</u>
	<u>100 lb/hp</u>	<u>200 lb/hp</u>	<u>300 lb/hp</u>	<u>400 lb/hp</u>	
0-290	1.57	1.14	1.03	1.01	0.75
0-350	1.53	1.13	1.03	1.01	0.76
0-490	1.38	1.11	1.01	0.90	0.78
0-510	b	b	b	b	0.79

^a Values based on Green Book figure IX-22.¹

^b Data not available, curves terminate at 500 ft.

Note: 1 lb = 0.454 kg
1 hp = 746 W

b. Discussion of Results

The intersection approaches at the study sites were located on tangent sections and intersected at nearly 90° angles. All approaches had a maximum grade of 1 percent. Because of this, no adjustments for the effect of grade were made in the calculation of acceleration rates.

A signalized intersection is located approximately 2,000 ft (600 m) south of the Central Valley Asphalt intersection. The presence of this intersection did not appear to affect the acceleration behavior of the turning vehicles. The calculated average acceleration rates were within the range represented by the Hutton curves. The median acceleration rate for trucks turning left is between the Hutton value for 100 and 200 lb/hp (0.06 to 0.12 kg/W) trucks. The median right turn acceleration rate is near the Hutton value for a truck with a weight-to-power ratio of 300 lb/hp (0.18 kg/W), but the sample size for this determination is small (9 trucks).

The acceleration rates at the Truck Stop 64 intersection were lower than at the other study sites. This intersection had unique characteristics that affected the acceleration behavior of the trucks making a right turn. Since freeway entrance ramps were located approximately 500 and 1,000 ft (150 to 300 m) downstream of the intersection, the majority of the trucks turning right from the truck stop eventually turned into one of these ramps. Thus, these trucks did not accelerate to the average running speed of the roadway. This hypothesis is supported by the calculated acceleration rates. The median acceleration rate is significantly lower than that determined at other study sites. The rate is also lower than the rate determined by Hutton for a truck with a weight-to-power ratio of 400 lb/hp (0.24 kg/W) but compares well with the rate calculated from AASHTO (which represents an older truck fleet with higher weight-to-power ratios).⁵¹

The Trindle and Railroad intersection has a signalized intersection located approximately 2,000 ft (600 m) east of the intersection. Queues from this signal did not extend into the study area. The median acceleration rate at the Trindle and Railroad intersection is near the Hutton value for a truck with a weight-to-power ratio of 100 lb/hp (0.06 kg/W) for the 0 to 490 ft (0 to 150 m) distances.⁵¹ The urbanized setting and high traffic volume on the major road influence the acceleration rates at this site.

The acceleration rates calculated using Green Book figure IX-22 are considerably lower than the truck with the highest weight-to-power ratio evaluated by Hutton and most of the rates calculated at the three study intersections.^{1,51} As shown in table 40, the AASHTO acceleration rates are relatively constant (approximately 0.77 mi/h/s or 1.23 km/h/s) for the specific distances.

3. Deceleration Rates and Speed Reductions

An analysis of deceleration rates and speed reductions was conducted for data sets segregated by intersection and by vehicle/maneuver type, as in the case of the acceleration rate data. Because of the limited number of data points, the data associated with right turns by five-axle trucks at the Truck

Stop 64 and Trindle and Railroad intersections were combined into a single data set. Because the number of data points for left-turning trucks was small, only a limited analysis of these data was conducted.

a. Determination of Deceleration Rates and Speed Reductions

Deceleration rates and speed reductions for vehicles on the major road that were impeded by a turning vehicle were calculated from the average speeds of these vehicles for each 100-ft (30-m) increment. These average speeds were then examined to identify where a maximum deceleration rate or speed reduction occurred. Major-road vehicles that reduced speed by less than 5 mi/h (8 km/h) through the observation area or displayed erratic or extreme speed variations were eliminated from the analysis.

Figure 59 presents the cumulative distribution of the maximum deceleration rate occurring prior to the intersection for major-road vehicles impeded by five-axle trucks turning onto the major road. Typically these deceleration rates occurred over a 200- to 400-ft (60- to 120-m) total distance ending 50 to 150 ft (15 to 45 m) prior to the intersection. Fifty percent of the major-road vehicles impeded by five-axle trucks turning onto the highway had deceleration rates of 3.67 mi/h/s (5.91 km/h/s) or less. Eighty-five percent of the major-road vehicles had deceleration rates of 5.85 mi/h/s (9.41 km/h/s) or less.

Table 41 presents the speed reduction for each major road vehicle grouped by initial speed. The cumulative distribution for the speed reduction by vehicle on the major road is shown in figure 60. Fifty percent of the major road vehicles had a speed reduction of 21 mi/h (34 km/h) or less when impeded by five-axle trucks. Eighty-five percent had speed reduction of 38 mi/h (61 km/h) or less. The estimated speed reduction for each 5-mi/h (8-km/h) initial speed group is also shown in table 41. These speed reductions ranged from 40 mi/h (64 km/h) for trucks with a 70-mi/h (113 km/h) initial speed to 15 mi/h (24 km/h) for trucks with initial speeds of 35 and 40 mi/h (56 to 64 km/h).

Only a limited amount of data was available for left turns. The calculated speed reduction and deceleration rate for each major road vehicle impeded by a left-turning truck vehicle are presented in table 42. A review of the data did not indicate any noticeable difference between the speed reductions or deceleration rates of vehicles in the far lane and vehicles in the near lane during a left-turn maneuver. More data would be required to reach a conclusion on whether drivers in the far lane respond differently to left-turning trucks than drivers in the near lane.

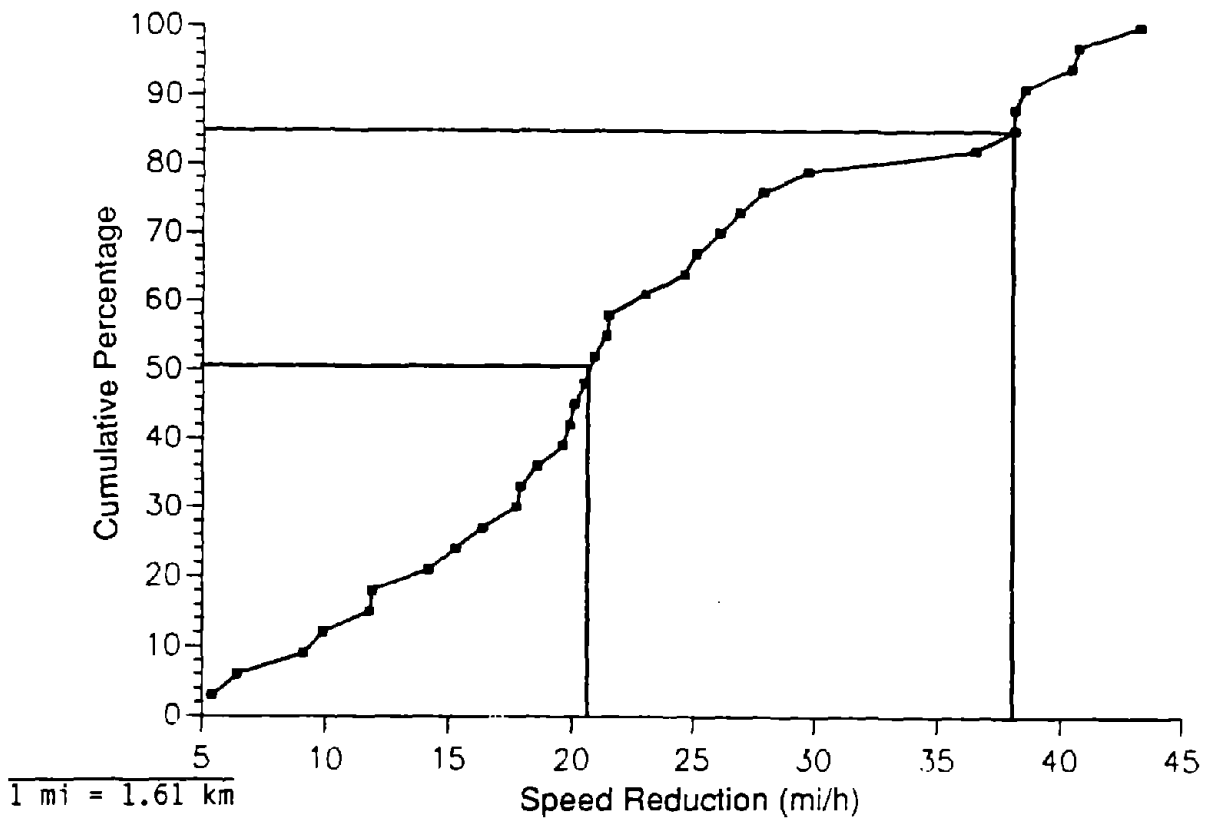


Figure 59. Cumulative distribution of deceleration rates for major road vehicles impeded by turning maneuvers by five-axle trucks.

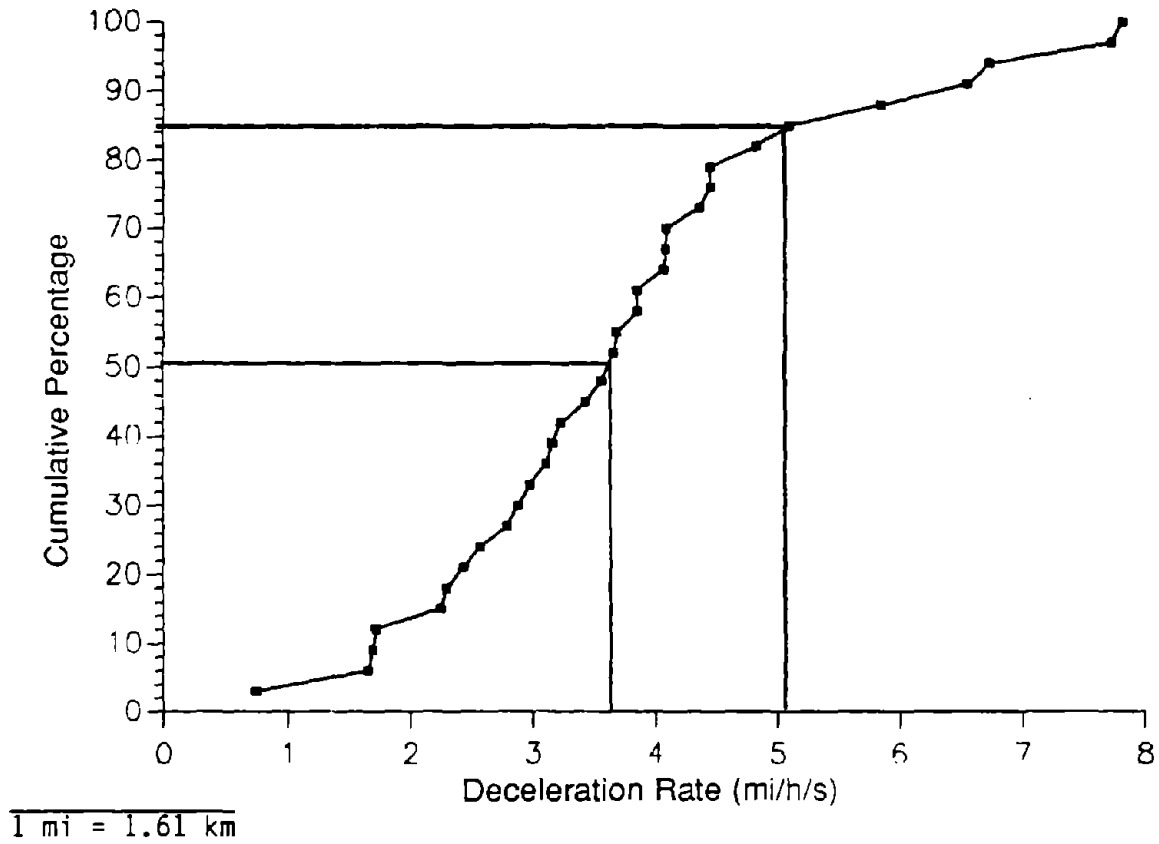


Figure 60. Cumulative distribution of speed reductions for major road vehicles impeded by turning maneuvers by five-axle trucks.

Table 41. Speed reductions for major road vehicles impeded by five-axle trucks turning right.

Vehicle ID no.	Gap accepted (s)	Initial speed (mi/h)	Speed reduction (mi/h)	Deceleration rate (mi/h)	Rounded initial speed (mi/h)	Estimated speed reduction (mi/h)
76 F	10.78	68	40.4	7.83	70	40
116 C	18.95	64	43.2	4.46	65	35
147 C	18.45	63	29.7	6.56		
99 C	13.12	62	40.7	5.85	60	35
47 F	8.64	62	38.5	7.74		
261 C	14.65	60	36.5	3.68		
49 F	12.81	57	27.9	5.10	55	30
46 F	9.05	52	38.1	4.84	50	25
78 F	10.55	52	26.9	6.75		
84 F	11.88	52	26.1	4.37		
130 C	16.92	52	5.4	0.74		
97 F	7.17	51	17.7	2.79		
48 F	8.96	49	38.1	4.46		
57 F	9.48	49	25.1	3.85		
18 F	14.85	49	20.9	3.85		
41 F	15.90	48	21.4	3.66		
176 C	19.35	47	24.6	2.30		
17 F	13.22	46	23.0	3.56	45	20
117 C	18.55	46	17.9	2.57		
232 C	15.95	46	9.1	1.72		
201 C	14.75	45	21.5	2.25		
27 F	12.56	45	19.6	3.11		
65 E	10.34	45	18.6	4.09		
24 E	19.45	43	20.1	2.98	40	15
209 C	12.97	43	16.4	1.69		
28 E	10.81	43	15.3	4.09		
25 F	9.88	41	20.5	4.07		
30 E	15.35	41	11.9	3.23		
22 E	13.74	41	11.8	3.16		
36 F	12.98	40	14.2	2.88		
38 E	14.14	37	9.9	2.43	35	15
48 E	12.27	36	6.4	1.65		
49 E	15.61	35	19.9	3.43		

Note: 1 mi = 1.61 km

Table 42. Deceleration rates and maximum speed reductions for left turns.

<u>Vehicle no.</u>	<u>No. axles</u>	<u>Gap accepted (s)</u>	<u>Vehicle type</u>	<u>Speed reduction (mi/h)</u>	<u>Deceleration rate (mi/h/s)</u>
TRINDLE AND RAILROAD, EASTBOUND					
36 E	3	7.78	PC	18.2	6.33
45 F	3	11.21	PC	6.3	1.94
53 F	5	9.03	PC	15.8	2.79
55 F	5	12.32	PC	18.1	2.86
56 E	5	8.34	PC	29.4	2.80
58 E	5	7.27	PC	12.6	3.25
61 E	3	11.51	PICKUP	15.2	5.37
TRINDLE AND RAILROAD, WESTBOUND					
22 F	5	15.48	PC	13.0	3.83
23 F	5	17.75	PC	15.9	4.56
31 F	5	16.59	PC	12.4	3.15
43 F	5	11.67	PC	10.7	2.18
45 F	3	11.21	PC	18.7	5.83
53 F	5	9.03	PC	13.9	3.28
56 F	5	8.24	PC	27.1	6.24
58 E	5	7.27	PC	27.7	2.53
60 F	5	12.13	PC	12.8	2.76
61 E	3	11.51	PC	21.3	3.46
CENTRAL VALLEY ASPHALT, SOUTHBOUND					
3 D	2	16.35	5-AX	13.6	3.18
7 D	3	11.35	PC	14.0	3.51
27 D	3	11.85	2-AX	26.2	5.47
30 D	2	7.81	PC	20.9	5.20

Note: 1 mi = 1.61 km

b. Discussion of Results

Figure II-13 of the Green Book illustrates the deceleration distances for passenger vehicles approaching intersections. These distances, which are based on comfortable deceleration rates, are determined from the initial speed when brakes are applied and the speed reached. Curves are provided for the following final speeds: 50, 40, 30, 20, and 0 mi/h (80, 64, 48, 32, and 0 km/h). Deceleration rates calculated for several combinations of initial speed and speed reached are presented in table 43.

Table 43. Deceleration rates (mi/h/s) from the Green Book.¹

Initial speed (mi/h)	Speed reached (mi/h)				
	50	40	30	20	0
70	6.08	6.47	6.19	6.30	6.25
60	5.78	5.88	5.67	5.74	5.57
50		5.29	5.11	5.15	5.10
40			4.12	4.64	4.70
30				4.08	3.78
20					3.92

Note: Deceleration rates are based on information from Green Book figure II-13.¹ The rates were calculated with the following equation:

$$\text{deceleration rate} = \frac{V_f^2 - V_i^2}{2 * \text{distance}}$$

$$1 \text{ mi} = 1.61 \text{ km}$$

Table 44 contains the observed normal deceleration rates for passenger cars on dry pavement from the Transportation and Traffic Engineering Handbook.⁵² The handbook states that deceleration rates up to 5.5 mi/h/s (8.9 km/h/s) are reasonably comfortable for passenger car occupants.

The majority of the deceleration rates observed in the field are within the comfortable rates from both the Green Book and the handbook. Vehicles with deceleration rates greater than those given in the Green Book had initial speeds higher than 62 mi/h (100 km/h). These high-speed vehicles made speed reductions between 25 and 41 mi/h (40 and 66 km/h) when a truck entered the traffic stream. A 25-mi/h (40-km) speed reduction by these vehicles reduced their speed to approximately the posted speed limit which was 40 mi/h (64 km/h) at both the Truck Stop 64 and Trindle and Railroad intersections.

Table 44. Deceleration rates from the Transportation and Traffic Engineering Handbook.⁵²

Speed change (mi/h)	Deceleration rate (mi/h/s)
15 - 0	5.3
30 - 0	4.6
40 - 30	3.3
40 - 50	3.3
50 - 60	3.3
60 - 70	3.3

Note: Rates are observed normal deceleration rates for passenger cars on dry pavements. Deceleration rates up to 5.5 mi/h/s are reasonably comfortable for car occupants.⁵²

1 mi = 1.61 km

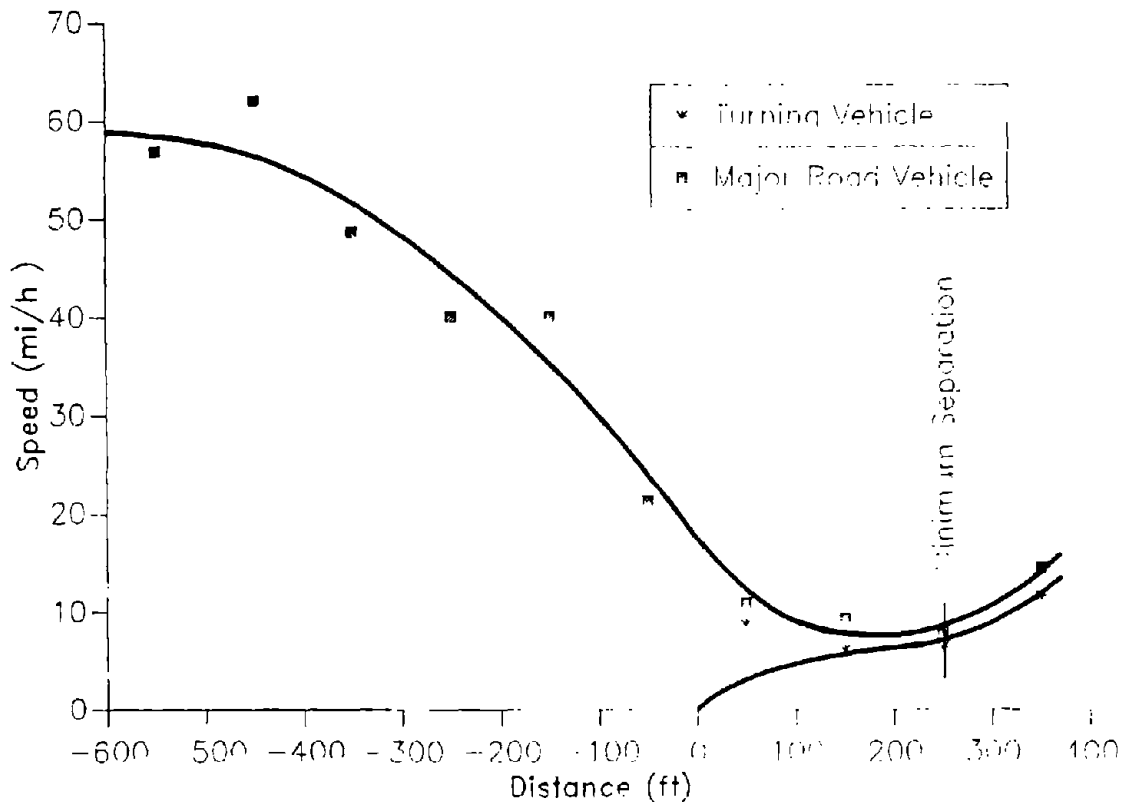
4. Minimum Separation Between Vehicles

The minimum separation analysis determined the minimum distance between the turning truck and the following major-road vehicle at any point during the maneuver (see figure 45). Minimum separation is referred to as "tailgate distance" in the Green Book. This analysis was based on the speed/distance profiles of both the accelerating truck and the decelerating major-road vehicle. Only right-turning trucks were considered. Seven data sets from the Truck Stop 64 intersection and six sets from the Trindle and Railroad intersection in which the minimum separation occurred within the camera field of view were available. Although the size of the available sample was very limited, these data were analyzed to provide some preliminary estimates of field-observed minimum separation. These results serve primarily to illustrate the method that could be used to determine minimum separation in a future effort on a larger scale than this pilot study.

a. Determination of Minimum Separation Between Vehicles

As stated above, minimum separation was determined from plots of speed versus distance to estimate the separation distance and the location at which it occurred. A sample data set for one turning vehicle (Vehicle 99) at the Truck Stop 64 intersection is shown in figure 61.

Minimum separation occurs when both the accelerating truck and the major road vehicle are at approximately the same speed. The major-road vehicle in figure 61 reached its minimum speed at approximately 250 ft (76 m) beyond the intersection. Its speed was 11 mi/h (18 km/h) and the accelerating truck's speed was at 10 mi/h (16 km/h). The headway time, t , between the vehicles was estimated by finding the difference between each vehicle's arrival time at the



Note: 1 ft = 0.305 m

Figure 61. Speed vs. distance plot to determine minimum separation for a typical vehicle.

apparent minimum separation point (250 ft [76 m] beyond the intersection). For the example presented in the figure, the time headway was 0.63 s. The minimum separation distance was then estimated using the following equation:

$$MS = (1.47 Vt) - L \quad (59)$$

where: MS = Minimum separation distance (ft)
V = Velocity of turning vehicle (mi/h)
t = Time headway between vehicles (s)
L = Length of turning vehicle (ft)

The calculated minimum separation distances and headway for each data set are shown in table 45. Minimum separation between vehicles typically occurred between 200 and 400 ft (60 to 120 m) beyond the intersection. The speeds of the vehicles at minimum separation were between 10 and

Table 45. Minimum separation times and distances for right turns by five-axle trucks.

Vehicle no.	Axle	Gap accepted (s)	Headway time (s)	Minimum separation distance (ft)	Minimum separation time (s)	Speed at minimum separation (mi/h)		Distance beyond intersection (ft)
						Major	Minor	
TRUCK STOP								
94	5	11.18	1.00	25	1.55	12	11	250
99	5	13.12	0.63	25	1.89	10	9	250
116	5	18.95	2.17	25	1.89	10	9	300
130	5	16.92	1.33	25	0.81	20	21	350
147	5	18.45	1.07	25	0.74	24	23	300
176	5	19.35	2.38	25	0.81	20	21	350
209	5	12.97	0.86	25	0.71	24	24	350
TRINDLE AND RAILROAD								
22	5	13.74	5.01	109	3.22	23	23	300
24	5	19.45	4.38	91	2.69	24	23	500
28	5	10.81	4.13	143	2.95	34	33	500
38	5	14.14	4.80	88	2.85	21	21	250
45	5	10.31	4.53	57	2.15	17	18	200
59	5	8.88	5.24	75	3.00	18	17	250

Note: 1 ft = 0.305 m
1 mi = 1.61 km

24 mi/h (16 and 39 km/h) at the Truck Stop 64 intersection and between 17 and 34 mi/h (27 and 55 km/h) at the Trindle and Railroad intersection. The speeds at minimum separation are much lower than the observed 85th percentile approach speeds of 51 mi/h (82 km/h) at the Truck Stop 64 intersection and 40 mi/h (64 km/h) at the Trindle and Railroad intersection.

The time headway between the major-road vehicles and the turning trucks at the Truck Stop 64 intersection was 2.4 s or less corresponding to a minimum separation distance of approximately 25 ft (8 m). Larger minimum separations were maintained by the major-road drivers at the Trindle and Railroad intersection, which is in an urban rather than a rural setting. These drivers typically maintained 4- to 7-s minimum headways and 50- to 150-ft (15- to 45-m) minimum separations.

b. Comparison of Results

The minimum separation distances at urban intersections would be expected to be smaller than the minimum separation at low-volume rural intersections. However, the observed minimum separations at the Truck Stop 64 intersection were lower than at the Trindle and Railroad intersection. The truck drivers at the Truck Stop 64 intersection did not accelerate as fast as the truck drivers at the urban intersection, and the running speed on the major road was also higher at the rural intersection. As a result, the major-road drivers "closed the gap" on the trucks turning from the Truck Stop 64 intersection faster than at the Trindle and Railroad intersection. This observation is supported by the location of minimum separation between at these intersections. Several of the minimum separation locations at Trindle and Railroad occurred more than 300 ft (90 m) beyond the intersection.

The Green Book does not provide any specific guidance on the values to use for minimum separation or "tailgate distance." When the curve labeled B-2a and Ca in Green Book figure IX-27 is reproduced using distance and time values approximated from Green Book figure IX-22, the resulting minimum separation distance, measured between the rear bumper of the turning vehicle and the front bumper of the major-road vehicle, is approximately 1 s multiplied by the major road speed. A 1-s minimum separation headway represents minimum separation distance of 15 ft (5 m) at 10 mi/h (16 km/h) and 30 ft (9 m) at 20 mi/h (32 km/h).

The general findings from this very limited analysis are that drivers accepted minimum separation times of approximately 1 s at the Truck Stop 64 intersection but generally used higher separations at the Trindle and Railroad intersection. Drivers appear to prefer larger separations between their vehicle and a turning vehicle if possible, but will accept 1 s or less in some situations.

E. Summary of Findings

The findings of this pilot study are summarized in tables 46 through 49 which present the 50th and 85th percentile probabilities of accepting a gap; the 50th and 85th percentile acceleration rates, deceleration rates, and speed

Table 46. Time gaps accepted from field data.

<u>Intersection</u>	<u>Turn maneuver</u>	<u>Truck type</u>	<u>Time gap (s)</u>	
			<u>50th percentile</u>	<u>85th percentile</u>
Central Valley Asphalt	Left	Less-than-five-axle	11.16	13.89
Central Valley Asphalt	Right	Less-than-five-axle	13.17	15.86
Truck Stop 64	Right	Five-axle	12.43	14.78
Trindle and Railroad	Left	Five-axle	8.27	9.84
Trindle and Railroad	Right	Five-axle	8.52	10.06
Trindle and Railroad	Right	Less-than-five-axle	7.25	8.87

Table 47. Acceleration rates from field data.

<u>Intersection</u>	<u>Turn maneuver</u>	<u>Truck type (no. of axles)</u>	<u>Distance (ft)</u>	<u>Acceleration rate (mi/h/s)</u>	
				<u>50th percentile</u>	<u>85th percentile</u>
Central Valley Asphalt	Left	4	0-290	1.27	1.58
Central Valley Asphalt	Right	4	0-490	1.04	1.21
Truck Stop 64	Right	5	0-350	0.80	1.20
Trindle and Railroad	Right	5	0-510	1.37	1.74

Note: 1 mi = 1.61 km

Table 48. Deceleration rates and speed reductions for major-road vehicles impeded by right turns by five-axle trucks.

	<u>50th percentile</u>	<u>85th percentile</u>
Deceleration rate	3.67 mi/h/s	5.85 mi/h/s
Speed reduction	21.2 mi/h	38.1 mi/h

Note: 1 mi = 1.61 km

Table 49. Minimum separation times and distances.

<u>Intersection</u>	<u>Headway time (s)</u>	<u>Minimum separation distance (ft)</u>
Truck Stop 64	1.00	25
	0.63	25
	2.17	25
	1.33	25
	1.07	25
	2.38	25
	0.86	25
Trindle and Railroad	5.01	109
	4.38	91
	4.13	143
	4.80	88
	4.53	57
	5.24	75

Note: 1 ft = 0.305 m

reduction; and the minimum separation times and distances. Each table is briefly described below:

Table 46--time gaps accepted (s) at 50th and 85th percentile probability. These gaps were determined using the logit model. The table is arranged by intersection, maneuver type, and truck type.

Table 47--acceleration rate (mi/h/s) for the predominant truck type for left and right turns at the Central Valley Asphalt intersection and for right turns for the other two intersections.

Table 48--deceleration rates (mi/h/s) and speed reductions (mi/h) for major-road vehicles at the Trindle and Railroad and Truck Stop 64 intersections that were impeded by 5-axle trucks making right turns.

Table 49--minimum separations in terms of time and distance for the Truck Stop 64 and Trindle and Railroad intersections. These findings are very limited due to small sample sizes.

F. Alternative Intersection Sight Distance Criteria

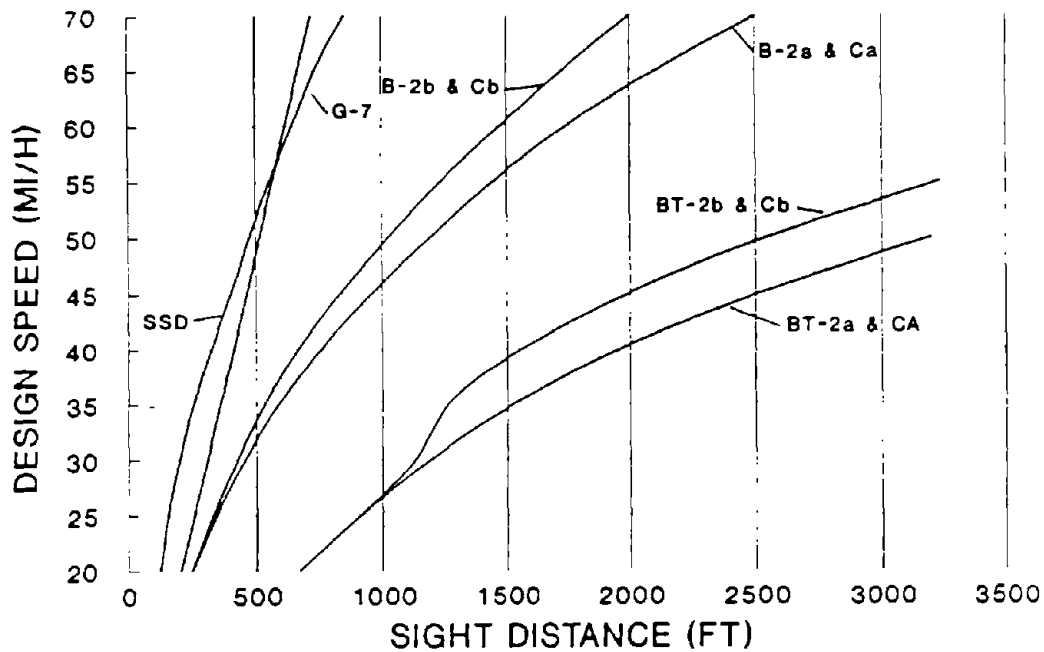
An objective of the intersection sight distance (ISD) study was to compare the resulting field data with the existing AASHTO Green Book criteria. It should be kept in mind that the current field study was a pilot study and a larger study would be required if existing criteria were to be revised. Figures 62 and 63 contain the curves developed from the following sources:

- AASHTO ISD criteria for passenger cars (B-2a & Ca and B-2b & Cb curves).
- ISD criteria for trucks (BT-2a & Ca and BT-2b & Cb curves) based on AASHTO model and Green Book estimates of truck acceleration rates.
- AASHTO stopping sight distance for passenger cars (SSD curve).
- ISD and SSD criteria for trucks based on AASHTO model and truck performance data from the literature (SSD-TW, SSD-TB, CS-T70, CS-T75, RS-T70, RS-T75 curves).
- ISD criteria for trucks based on AASHTO model and truck performance data from the pilot field studies.
- ISD criteria based on gap acceptance (G-7, G-10, and G-15 curves).

Table 50 summarizes the basic sight distance model and the parameter values used to derive each intersection sight distance curve identified above. Table 51 provides comparable information for the stopping sight distance curves. The following sections describe the basis for each curve in more detail.

1. AASHTO ISD Criteria for Passenger Cars

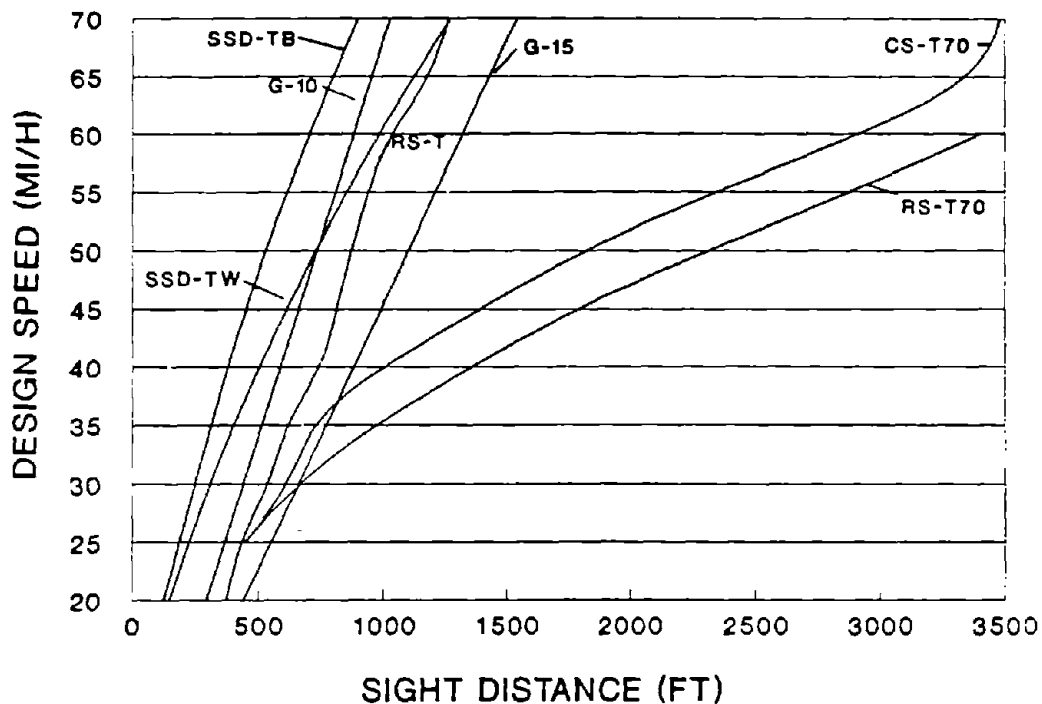
These curves are reproduced from figure IX-27 of the Green Book. Curve B-2a & Ca in figure 62 represents the required sight distance for a passenger car to turn left or right onto a two-lane highway and accelerate to the design speed without being overtaken by a vehicle approaching from the right and traveling at the design speed. Curve B-2b & Cb represents the safe sight distance for a passenger vehicle to turn left or right onto a two-lane highway and accelerate to the average running speed without being overtaken by vehicle approaching from the right and reducing speed from design speed to average running speed.



<u>Sight distance curve</u>	<u>Description</u>
G-7	Sight distance from gap acceptance procedure for 7-s gap
SSD	Stopping sight distance for a passenger car (from Green Book table III-1)
B-2a & Ca	Sight distance for a passenger car to turn and attain design speed (from Green Book figure IX-27)
BT-2a & Ca	Sight distance for a truck to turn and attain design speed (using Green Book truck characteristics in AASHTO procedure)
B-2b & Cb	Sight distance for a passenger car to turn and attain average running speed (from Green Book figure IX-27)
BT-2b & Cb	Sight distance for a truck to turn and attain average running speed (using Green Book truck characteristics in AASHTO procedure)

Note: 1 mi = 1.61 km
1 ft = 0.305 m

Figure 62. Intersection sight distance curves from Green Book.



<u>Sight distance curve</u>	<u>Description</u>
G-10	Sight distance from gap acceptance procedure for 10-s gap
G-15	Sight distance from gap acceptance procedure for 15-s gap
SSD-TB	Stopping sight distance for a truck with a conventional brakes system and best-performance truck driver (from table 23 in volume I)
SSD-TW	Stopping sight distance for a truck with a conventional brakes system and worst-performance truck driver (from table 23 in volume I)
RS-T	Sight distance for a truck from this field study to turn and attain the reduced speed that the major-road vehicle is traveling (using findings from field data in AASHTO procedure)
CS-T70	Sight distance for a 70-ft (21-m) truck to turn and attain the constant speed that the major-road vehicle is traveling (using findings from field data in AASHTO procedure)
RS-T70	Sight distance for a 70-ft (21-m) truck to turn and attain the reduced speed that the major road vehicle is traveling (using truck characteristics from the literature in AASHTO procedure)

Note: 1 mi = 1.61 km
1 ft = 0.305 m

Figure 63. Intersection sight distance curves for present study.

Table 50. Basic sight distance model and parameter values used to derive each intersection sight distance curve.

Sight distance curve	Basic sight distance model	Minor road vehicle acceleration performance	Lowest speed reached by major road vehicle	Vehicle length (ft)	Critical acceptable gap
B-2a & Ca	AASHTO Green Book figure IX-27	AASHTO Green Book figure IX-27	Design speed	19	N/A
B-2b & Cb	AASHTO Green Book figure IX-27	AASHTO Green Book figure IX-27	Average running speed	19	N/A
BT-2a & Ca	AASHTO Green Book figure IX-27	AASHTO Green Book figure IX-22	Design speed	55	N/A
BT-2b & Cb	AASHTO Green Book figure IX-27	AASHTO Green Book figure IX-22	Average running speed	55	N/A
CS-T70	AASHTO Green Book figure IX-27	Hutton, 200 lb/hp truck	Design speed	70	N/A
CS-T75	AASHTO Green Book figure IX-27	Hutton, 300 lb/hp truck	Design speed	75	N/A
RS-T70	AASHTO Green Book figure IX-27	Hutton, 200 lb/hp truck	Average running speed	70	N/A
RS-T75	AASHTO Green Book figure IX-27	Hutton, 300 lb/hp truck	Average running speed	75	N/A
RS-T	AASHTO Green Book figure IX-27	Field data (figure 63)	Average running speed	55	N/A
G-7	Gap acceptance procedure	-	-	-	7 s
G-10	Gap acceptance procedure	-	-	-	10 s
G-15	Gap acceptance procedure	-	-	-	15 s

Table 51. Basic sight distance model and parameter values used to derive each stopping sight distance curve.

<u>Sight distance curve</u>	<u>Basic sight distance model</u>	<u>Initial speed</u>	<u>Braking performance</u>	<u>Vehicle type</u>
SSD	AASHTO Green Book table III-1	Design speed	AASHTO Green Book	Passenger car
SSD-TW	AASHTO Green Book table III-1	Design speed	Worst-performance driver (table 5)	Truck
SSD-TB	AASHTO Green Book table III-1	Design speed	Best-performance driver (table 5)	Truck

2. ISD Criteria Based on AASHTO Model and AASHTO Truck Acceleration Rates

The Green Book indicates that sight distance for trucks will be considerably longer than for passenger vehicles but does not provide criteria or a clearly defined method to determine the actual sight distance needed by a truck. In the absence of any estimates of truck acceleration rates in the ISD discussion in the Green Book, the truck acceleration curves in Green Book figure IX-22 were used to replace the passenger car acceleration rates used in curve B-2a & Ca and curve B-2b & Cb. The resulting model is illustrated by curves BT-2a & Ca and BT-2b & Cb shown in the upper portion of figure 62. The derivation of this curve is discussed in more detail in volume I of this report.

3. AASHTO Stopping Sight Distance for Passenger Cars

The curve labeled SSD in figure 62 represents the AASHTO criteria for stopping sight distance for a passenger car on a wet pavement. The values are derived from table III-1 in the Green Book.

4. ISD and SSD Criteria Based on AASHTO Model and Truck Performance Data from the Literature

ISD and SSD criteria based on the AASHTO models and estimates of truck performance data from the literature are presented in figure 63.⁴⁸ The stopping sight distance values represent controlled braking by an empty truck on a poor, wet road with relatively good radial tires for a worst-performance driver (SSD-TW) and a best-performance driver (SSD-TB). The constant speed (CS) curves represent the case in which the major road vehicle travels at a constant speed equal to the design speed, while the reduced speed (RS) curves represent the case in which the major-road driver reduces speed from the

design speed to the average running speed of the highway. A complete discussion of the derivation of these curves can be found in volume I of this report.

5. ISD Criteria Based on AASHTO Model and Truck Performance
Data from Pilot Field Studies

The results of the pilot study can be used to demonstrate the implications of the collected field data when used in the AASHTO ISD model. These results must be used with caution since the field findings were limited. The RS-T curve in figure 63 is based only on the data for right turns by five-axle trucks. The data that were used to determine this curve are:

- Speed reduction for major road vehicles.
- Time and distance for acceleration by five-axle truck making right turns.
- Deceleration rate for major-road vehicles.
- Minimum separation time.

Speed reduction values were based on observations made at the Trindle and Railroad and Truck Stop 64 intersections. The assumed values are listed in table 52.

Table 52. Speed reductions from pilot field study used to derive ISD criteria.

<u>Initial speed</u> (mi/h)	<u>Speed reduction</u> (mi/h)
20	5
25	10
30	10
35	15
40	15
45	20
50	25
55	30
60	35
65	35
70	40

Note: 1 mi = 1.61 km

Truck acceleration time and distance values used in modifying the Green Book B-2b & Cb curve were determined from Green Book figure IX-22, which is a speed-versus-distance plot. Figure 64 is a speed-versus-distance plot of vehicle trajectories at the Trindle and Railroad intersection. An "average curve" was estimated between the limits of the data shown in figure 64. Truck acceleration time and distance values for use in this analysis were determined from this average curve by the same method used with the Green Book figure IX-22.

The distance and time for deceleration by the major-road vehicle were determined using the 50th percentile deceleration rate for major road vehicles impeded by five-axle trucks. The 3.67 mi/h/s (5.91 km/h/s) deceleration rate is well within comfortable rates specified in the Green Book and the Transportation and Traffic Engineering Handbook.^{1,52} Also, the resulting distances agree with deceleration distances observed in the field.

The minimum separation time between the rear bumper of the turning vehicle and the front bumper of the major road vehicle was assumed to be 1.0 s. Minimum separation distance is the product of the average running speed and 1.0 s.

Other assumptions made for the analysis include:

- Perception-reaction time = 2.0 s.
- Turning vehicle radius = 60 ft (18 m)
- Length of vehicle = 55 ft (17 m).

Table 53 and figure 63 present the analytical results. Also presented in Table 53 are the ISDs based on truck acceleration time, t_t , and distance, P , values determined from Green Book figure IX-22. The results based on the field data are between 44 and 71 percent lower than the results based on Green Book figure IX-22.

A sample calculation for 55 mi/h (88 km/h) design speed is shown below. Figure 65 illustrates the distances considered in these calculations.

Step 1--Determine the Distance Traveled by the Major Road Vehicle

$$Q = 1.47 V_{ds} t_{ds} + D_{dec} + 1.47 V_{rs} t_{rs} \quad (60)$$

$$t_{rs} = t - t_{ds} - t_{dec} \quad (61)$$

$$t = t_t + J \quad (62)$$

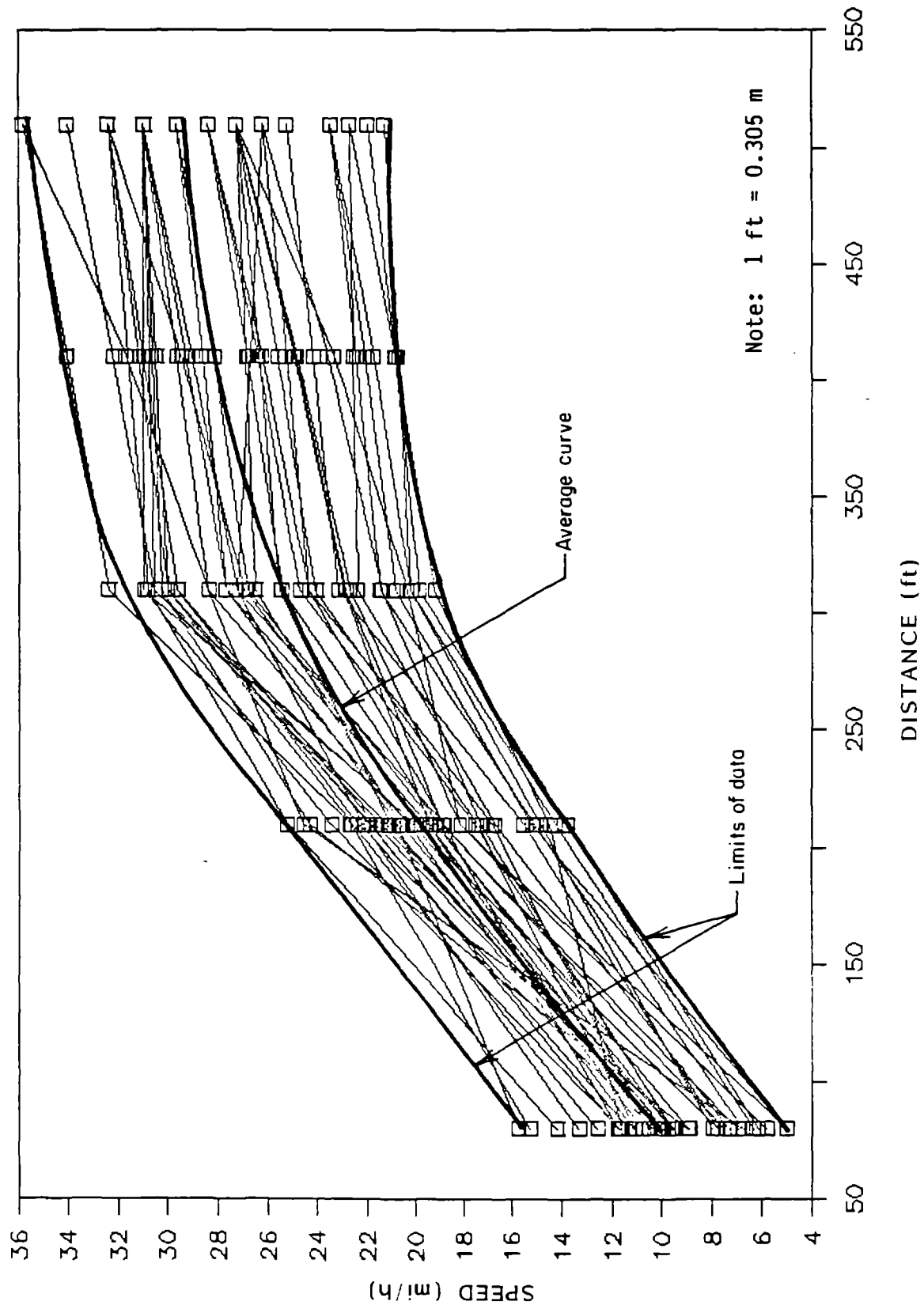


Figure 64. Speed vs. distance curves for right turns by five-axle trucks at the Trindle and Railroad intersections.

Table 53. ISD criteria for reduced speeds by major-road vehicles (ISD-RS-T) from field data.

Design speed V_d (mi/h)	Speed reduction (mi/h)	Running speed V_{rs} (mi/h)	Acceleration		Deceleration		Running speed time t_{rs} (s)	Intersection sight distance	
			Time t_t (s)	Distance P (ft)	Distance D_{def} (ft)	Time t_{def} (s)		ISD-RS-T (ft)	AASHTO ISD-B-2b&Cb (ft)
20	5	15	14.60	135	24	0.93	11.67	375	670
25	10	15	14.60	135	54	1.85	10.75	415	903
30	10	20	17.52	210	68	1.85	13.67	555	1,179
35	15	20	17.52	210	112	2.78	12.74	601	1,213
40	15	25	19.48	275	133	2.78	14.70	759	1,549
45	20	25	19.48	275	191	3.71	13.77	812	1,971
50	25	25	19.48	275	255	4.63	12.85	872	2,516
55	30	25	19.48	275	327	5.56	11.92	939	3,232
60	35	25	19.48	275	405	6.49	10.99	1,013	a
65	35	30	27.52	600	453	6.49	19.03	1,208	a
70	40	30	27.52	600	545	7.41	18.11	1,268	a

^a Acceleration time and distance values not available.

Note: 1 mi = 1.61 km
1 ft = 0.305 m

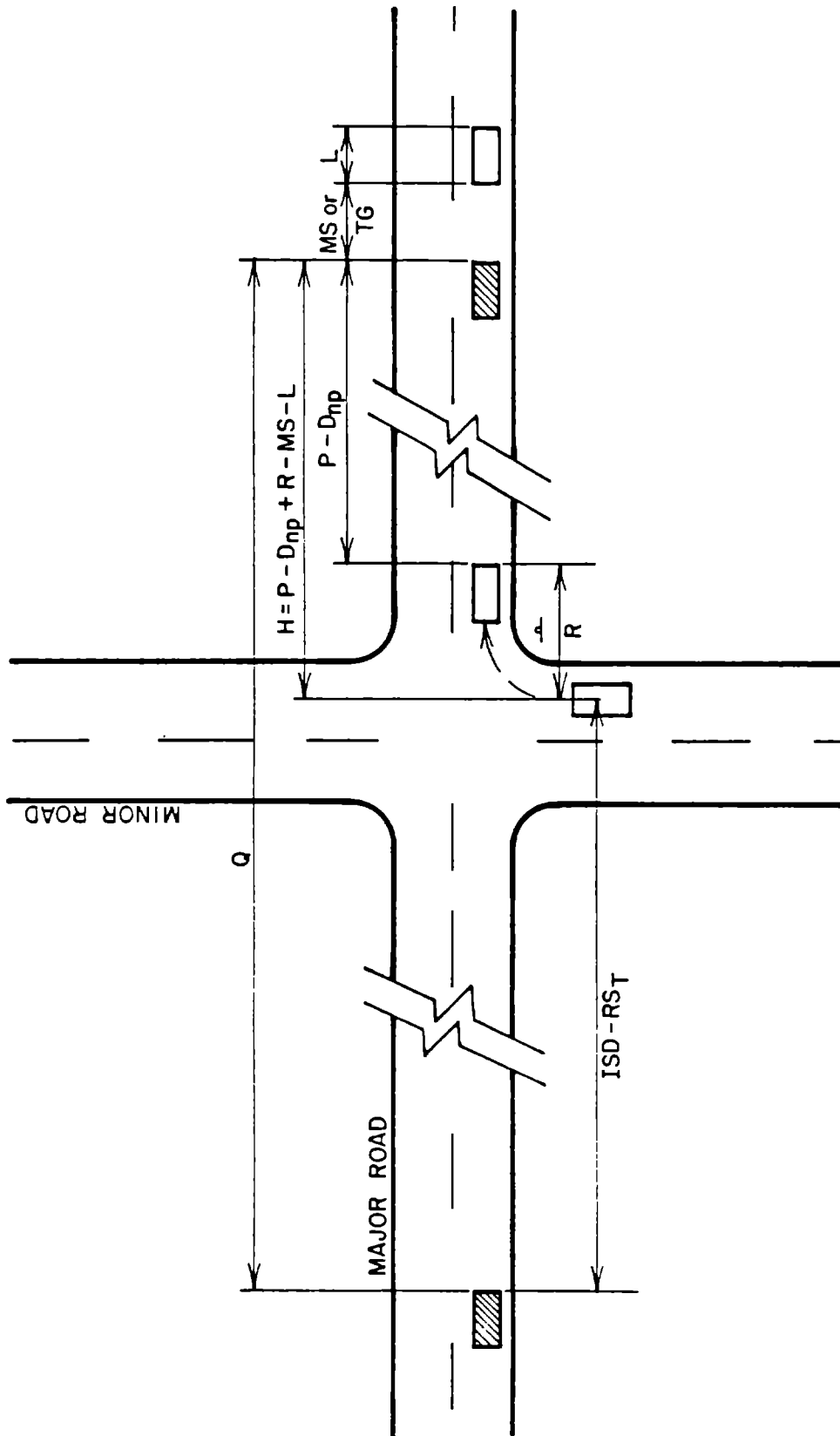


Figure 65. Distances considered in case III-C criteria for intersection sight distance.

$$t_{ds} = J + t_{pr} \quad (63)$$

$$D_{dec} = (V_{rs}^2 - V_{ds}^2) / 2d \quad (64)$$

$$t_{dec} = (2 D_{dec}) / (V_{ds} + V_{rs}) \quad (65)$$

where:

Q = distance traveled by the major-road vehicle during the minor-road truck's turning maneuver (ft); (see Figure 65)

V_{ds} = design speed of major road (mi/h)

t_{ds} = time major-road vehicle is traveling at design speed during turning maneuver (s)

D_{dec} = distance traversed by major-road vehicle during deceleration (ft)

t_{dec} = time major-road vehicle is decelerating (s)

V_{rs} = running speed of major-road vehicle (mi/h)

t_{rs} = time major-road vehicle is traveling at its running speed (V_{rs}) during the turning maneuver (s)

t = time for a stopped minor-road truck to move into the traffic stream and accelerate to the design speed (s)

J = sum of the perception time and the time required to actuate the clutch or actuate an automatic shift (s); (assumed: J = 2.0 s)

t_t = acceleration time for the minor-road truck to complete the turning maneuver (s)

t_{pr} = perception-reaction time for the major-road driver (s); (assumed: $t_{pr} = 2.0$ s)

d = deceleration rate (mi/h/s)

With a design speed, V_{ds} , of 55 mi/h (89 km/h) and an assumed speed reduction of 30 mi/h (48 km/h) (see table 52), the running speed, V_{rs} , is 25 mi/h (40 km/h). The deceleration distance, D_{dec} , is calculated from equation (64) using a deceleration rate, d, of -3.67 mi/h/s (0-5.91 km/h/s) and

the time to decelerate, t_{dec} , is calculated using equation (65). For this example, D_{dec} is equal to 327 ft (100 m) and t_{dec} is equal to 5.56 s.

The sum of the perception time and the time required to actuate the clutch or actuate an automatic shift, J , is assumed to be 2.0 s. Perception-reaction time, t_{pr} , is also assumed to be 2.0 s. Therefore, the time the major road vehicle is traveling at the design speed, t_{ds} , is 4.0 s.

Figure 64 is used to establish the values of the distance traveled, P , and acceleration time, t_t , for five-axle trucks making right turns. For example, when an average five-axle truck reaches 25 mi/h (40 km/h), it has traveled a distance of 275 ft (84 m). The acceleration time, t_t , given in table 53 was calculated based on 5 mi/h (84 m) speed increments as demonstrated in table 54.

Table 54. Acceleration distance and time for right turns by five-axle trucks at the Trindle and Railroad intersections.

Speed reached (mi/h)	Distance traveled, P (ft)	Incremental		Acceleration time, t_t (s)
		Distance (ft)	Time (s)	
5	25 ^a	25	6.80	6.80
10	75	50	4.54	11.34
15	135	60	3.27	14.60
20	210	75	2.92	17.52
25	275	65	1.97	19.48
30	600 ^a	325	8.04	27.52
35-70	Data not available			

^a Values approximated.

Note: Incremental time = $\frac{2 * \text{incremental distance}}{V_o + V_f}$

1 mi = 1.61 km

1 ft = 0.305 m

The distance traveled by a major-road vehicle during the minor-road truck-turning maneuver is calculated using the data given above. The calculation is performed as follows:

$$Q = 1.47 (55) (4) + 327 + 1.47 (55 - 30) (19.48 + 2 - 5.56 - 4)$$

$$= 1,088 \text{ ft}$$

Step 2--Determine the Distance Traveled by the Turning Vehicle

$$H = P - D_{np} + R - MS - L \quad (66)$$

$$D_{np} = \pi * R/2 \quad (67)$$

$$MS = 1.47 V_{rs} t_{MS} \quad (68)$$

where:

H = major-road vehicle's distance from the intersection when it is at the assumed minimum separation distance from minor-road truck (ft)

P = total distance traveled by minor-road truck from the stopped position to location where it reaches the design speed (ft)

D_{np} = distance minor-road truck traveled during the turning maneuver that is not parallel to major highway (ft)

R = radius of turn for minor-road truck (ft)

MS = minimum separation distance (ft)

L = length of minor-road vehicle (ft)

V_{rs} = running speed of major-road vehicle (mi/h)

t_{MS} = minimum separation time (s); (assumed: $t_{MS} = 1.0$ s)

The minimum separation time, t_{MS} , is assumed to be 1.0 s. The radius, R, and vehicle length, L, were assumed to be 60 and 55 ft (18.3 and 16.8 m), respectively. These values are based on Green Book tables IX-20 and II-1. The distance traveled by the turning truck, P, is based on figure 64. The value for this example is 275 ft (84 m). The calculation for the distance traveled by the turning truck is shown below:

$$\begin{aligned} H &= 275 - (\pi*(60/2)) + 60 - 1.47 (55-30) (1) - 55 \\ &= 149 \text{ ft} \end{aligned}$$

Step 3--Determine Intersection Sight Distance

The intersection sight distance required under the reduced speed assumption, ISD-RS-T, is calculated as:

$$\text{ISD-RS-T} = Q - H = 1088 - 149 = 939 \text{ ft}$$

where: ISD-RS-T = sight distance along the major roadway's far lane (to the left for right turns) assuming that the major-road vehicle reduces speed from design speed to running speed during minor-road truck's turning maneuver (ft); (see figure 65)

Q = distance traveled by the major-road vehicle during the minor-road truck's turning maneuver (ft)

H = major-road vehicle's distance from the intersection when at assumed minimum separation distance from the minor-road truck (ft)

6. ISD Criteria Based on Gap Acceptance

Sight distance values were calculated based on design speed and critical gap lengths of 7, 10, and 15 s. The 7-s criterion was used because the Green Book states (1) that a "minimum of 7 s should be available to the driver of a passenger vehicle crossing the through lanes" on a local road or street; and (2) that the resulting "sight distance should be sufficient to permit a vehicle on the minor leg of the intersection to cross the travelway without requiring the approaching through-traffic to slow down."¹

The 10- and 15-s gaps were selected as the 85th percentile probabilities of a five-axle truck accepting a gap at a high-volume location (Trindle and Railroad) and a low-volume location (Truck Stop 64), respectively.

7. Comparison of ISD Curves

When the curves derived directly from ISD criteria and vehicle characteristics given in the Green Book are compared (see figure 62), three general groupings result: (1) ISD criteria based on the AASHTO model and truck acceleration values from Green Book figure IX-22 (curves BT-2a & Ca and BT-2b & Cb); (2) AASHTO ISD criteria for passenger cars as given in the Green Book (B-2a & Ca and B-2b & Cb), and (3) the curves for AASHTO SSD and the ISD criteria based on acceptance of a 7-s gap.

The ISD curves from this present study fall into two groups (see figures 62 and 63). One group consists of the ISD criterion based on the AASHTO model and truck performance acceleration values from the literature. The group includes both the major-road vehicle at CS and RS conditions. The

other group consists of the remaining curves (G-10, G-15, SSD-TW, SSD-TB, and RS-T). The curve based on findings from the field data collection (RS-T) is between the 10-s gap curve and the 15-s gap curve. The SSD values for both best and worst performance truck drivers (SSD-TB and SSD-TW) are less than the values based on the field studies.

G. Recommended Data Collection for Future Intersection Sight Distance Studies

The pilot study reported in this appendix was intended primarily to test a data collection approach that could establish reasonable estimates for the following parameters:

- Acceleration rates (time versus distance curves) of trucks starting from a completely stopped position and negotiating a right- or left-turn maneuver.
- Deceleration rates (time versus distance curves) of vehicles approaching from either direction along a two-lane roadway.
- Speed reduction of vehicles approaching from either direction along a two-lane roadway.
- Minimum separation between the rear of the turning truck and the front of a vehicle approaching along the major roadway.
- Time and distance gaps accepted by the turning trucks.

The remainder of this appendix evaluates the overall work plan and the particular tasks accomplished in this study. Recommendations are provided for improving the data collection, data reduction, and numerical analysis procedures to perform a comprehensive field study and valid statistical analysis to establish ISD requirements.

A few specific videotaping problems were encountered. These included: camera time drift, equipment failure due to extremely low ambient temperatures at the study sites, and limited viewing distance due to at-grade camera setup. The cold, damp, inclement weather conditions also curtailed the effective use of tapeswitches with automated traffic data recorders.

Nonetheless, with a combination of videotaping, traffic data collection equipment, and human observations, this study provided a feasible field data collection plan for both urban and rural intersections. A minimum field crew size of four individuals is preferred, considering the numerous logistic tasks and observation points that must be under constant surveillance.

Each step of the pilot work plan is reviewed below:

1. Identify Candidate Intersections

The preliminary selection of intersections in this study was limited by the intended scope and project schedule. A comprehensive investigation would justify a detailed stratified sampling plan including:

- Various functional classes of roadway intersections.
- Urban and rural locations.
- Ranges of appropriate traffic volumes.
- Distribution of different vehicle types (trucks and automobiles).
- Variations in horizontal and vertical alignment.
- Alternative major-roadway cross section.
- Ranges of available sight distance.
- 4-leg and T-intersections.

Several months should be devoted to preliminary site visits and gathering sample traffic characteristic information. A detailed checklist of site criteria should be developed to assist in the final selection of intersections.

2. Establish the Field Data Collection Procedures

Two plans were prepared for the pilot study: (1) an at-grade video camera approach, and (2) a collection scheme based primarily on the use of tapeswitches and traffic data collection equipment that records individual vehicle speeds, number of axles, volumes, vehicle classification, and time of event. Future studies should test the tapeswitch plan and should consider elevating (and concealing) the video cameras. Elevated camera locations are not available at all sites but, where available, could greatly extend the camera field of view.

The five-camera at-grade setup was adequate for obtaining deceleration, minimum separation, and time gap data. As discussed earlier, the video cameras recorded the traffic operations at the intersection and approximately 500 ft (150 m) along each approach leg of the major roadway. Additional cameras may be necessary if acceleration or distance gap information is desired occur beyond 500 ft (150 m). Driveways and other roadside access features in urbanized areas limit the range of viewing and create undesirable interactions with the turning or approaching vehicles, and should be avoided where possible.

Reliable and durable video equipment is necessary in order to minimize later adjustments to timing operations and camera coordination. Each camera's field of view should overlap the next and each pair of cameras should include a distinguishable common reference point.

The 100-ft (30-m) increments along the approach legs were established using a flagging technique. The reliability of this method decreases as the distance from the camera increases. With elevated camera locations, the accuracy of distance measurement should improve. An alternative approach is to place black or white tape on the road, shoulder, or curb so that reference markings are always visible on the videotape. Control sections may be

necessary to determine if such markings affect driver behavior. The marking technique would be most effective in an elevated situation.

Before actual field data collection begins, several specific items should be considered:

- Video cameras should be positioned so that the front end of each vehicle is clearly within the camera field of view. This will minimize the need to make adjustments for varying vehicle lengths during the data reduction phase and will simplify later numerical analysis.
- Tapeswitches should be considered as an alternate means to record the necessary field data if driveways along the major roadway within the study segment do not restrict their installation.
- Elevated video viewing could limit the number of camera setups; reduce field setup time; improve data reduction reliability; mitigate some of the effects of field data collection activities; and improve overall field operations.
- Depending on the study design, special attention may be required regarding the need for additional cameras and tapeswitches in areas of horizontal and vertical alignment restrictions. The related effects of limited available sight distance should also be recognized.

Video cameras are sensitive to moisture and extreme ambient temperatures. It is strongly recommended that special consideration be given to careful scheduling of the primary field activities to avoid adverse weather conditions. Due to the significant consequences of lost field efforts, a contingency field management strategy would need to be developed for a comprehensive data collection.

3. Data Reduction

A full-function videocassette recorder with the following primary features improves the efficiency and reliability of the final results:

- Slow motion control.
- Freeze frame.
- Individual frame advance.

Each turning vehicle should be assigned an identification number that remains with that vehicle throughout the data reduction. This facilitates examination of the data as individual events as well as retrieval of specific information after the data has been combined for overall comparisons. It is also more efficient initially to reduce the various data types (gap acceptance, acceleration, and deceleration) as independent data sets. Otherwise, three or more video monitors may be needed to simultaneously track the turning vehicle and the vehicles traveling along the major roadway.

4. Anticipated Results

The overall methodology conducted in the pilot work provides a practical and reasonable means for establishing estimates of the intended parameters. Weaknesses lie in the limited data set and the loss of accuracy in viewing trucks and other vehicles farther than 500 ft (150 m) downstream of the study intersection. It was demonstrated that the data needed to formulate ISD criteria using either the existing AASHTO model or the gap acceptance approach can be established from actual field investigation.

A more comprehensive study would provide the basis to:

- Modify existing ISD criteria.
- Provide guidance for quantifying appropriate ISD parameters where no values are presently available (e.g., minimum separation, deceleration rate, and speed reduction).
- Critically evaluate the implications of adopting ISD criteria based on gap acceptance knowledge.

Additionally, the anticipated results would improve the general design and operational characteristics of STOP-controlled intersections. Future research would also yield specific information over a range of vehicle types and driver characteristics at intersections with known geometrics and actual approach and departure speeds.

APPENDIX F

COST-EFFECTIVENESS METHODOLOGY

This appendix describes the cost-effectiveness methodology used to assess the economic justification for changes in highway design and operational criteria to accommodate trucks. Candidate revisions in highway design and operational criteria to accommodate trucks were identified during the research and are discussed in volume I of this report. However, these candidate revisions are not being recommended for implementation unless a cost-effectiveness analysis indicates that the reduction in accidents resulting from the revised criteria would be sufficient to offset the resulting increase in highway construction and/or maintenance costs. The cost-effectiveness methodology is illustrated by an example that addresses revised stopping sight distance criteria for trucks.

A. Overview of Cost-Effectiveness Methodology

Cost-effectiveness analysis is typically employed to determine whether the benefits of proposed action outweigh its costs and, therefore, whether that action is economically justified. The action under consideration could be a specific proposed project or a general change in highway design and operational criteria. Cost-effectiveness analysis requires quantitative estimates of both the costs and benefits of the proposed action. The costs are nearly always expressed in monetary terms. The benefits may be expressed either in monetary terms (e.g., savings in dollars) or in nonmonetary terms (e.g., number of accidents reduced). Accident cost estimates have been developed to allow analysts to convert the number of accidents reduced at different severity levels into dollar cost savings.

In the case of the revised highway design and operational criteria to accommodate trucks that are under consideration in this study, the costs of implementing the revised criteria can be estimated but no safety measures of effectiveness are available to estimate their benefits. Therefore, the cost-effectiveness analysis was structured to determine the percent reduction in accidents that would be needed at various ADT and truck volume levels to make a specific change in highway design or operational criteria economically justified. Engineering judgment must then be applied to determine whether the calculated percent reduction in accidents could reasonably be expected to be achieved.

The percent reduction in accidents that would be needed to make a specific revision in highway design and operational criteria cost-effective was generally determined as:

$$\text{Percent Reduction} = \frac{(\text{CC} - \text{RV} \times \text{PW}) \times 100}{\text{AR} \times \text{TA} \times \text{ADT} \times \text{N} \times \text{L} \times 10^{-6} \times \text{AC} \times \text{SPW}} \quad (69)$$

- where:
- CC = Construction cost (\$) to implement revised criteria at one typical site
 - RV = Residual value of construction cost (\$) at end of analysis period
 - AR = Expected accident rate (accidents per million veh-mi) for specified highway type and traffic conditions
 - TA = Expected proportion of accidents involving trucks (see equation 70)
 - ADT = Average daily traffic volume (veh/day)
 - N = Number of days per year = 365
 - L = Length (mi) of improved site
 - AC = Cost savings (\$) per accident reduced
 - SPW = Uniform series present worth factor
 - PW = Single amount present worth factor

This formulation for the cost-effectiveness analysis in equation (69) is based on the general approach to economic analyses presented in the AASHTO Manual on User Benefit Analysis for Highway and Bus-Transit Improvements.⁵³ The formulation has been modified from the net return analysis approach used in the AASHTO manual, where the costs and benefits are known, to the form shown in equation (69) where the percent accident reduction that would be required to make the revised criteria cost effective is calculated. A formulation similar to equation (69) is used to address intersection improvements; for intersections, the accident rate (AR) is expressed per million entering vehicles, the ADT is expressed in entering vehicles per day, and the site length (L) is omitted. Each element of the cost-effectiveness expression is discussed below. The following discussion documents all of the assumed values of construction cost, accident cost savings, etc. used to develop the cost effectiveness analysis results presented in volume I. Some, but not all, of these data are used in the stopping sight distance examples that follow in this appendix.

1. Construction Costs

Construction costs for revised criteria were computed from estimates of the construction quantities and unit construction costs that would be required to implement the revised criteria for trucks. Unit costs for construction bid items were estimated from national estimates compiled by FHWA and from estimates obtained from the Pennsylvania Department of Transportation.⁵⁴ The unit construction costs used in the cost-effectiveness analysis included:

General excavation	\$2.99/yd ³ (\$3.91/m ³)
Removal and replacement of rigid pavement	4.78/ft ² (51.43/m ²)
Removal and replacement of rigid shoulder	4.25/ft ² (45.72/m ²)
Removal and replacement of flexible pavement	4.05/ft ² (43.57/m ²)
Removal and replacement of flexible shoulder	3.51/ft ² (37.76/m ²)

All of the unit construction costs include a 10 percent allowance for contingencies (miscellaneous, unbudgeted items). The pavement and shoulder costs include an additional 10 percent allowance for engineering costs.

Quantities for the construction items were calculated in a manner similar to the method that would be used in design of an improvement project. For example, the additional earthwork required to provide vertical curves with increased stopping sight distance was calculated by determining the roadway centerline profile elevations and cross sections at 100-ft (30-m) stations for both AASHTO and revised stopping sight distance criteria. Several costing scenarios were typically examined. In the case of the stopping sight distance analysis, the following four construction cost scenarios were evaluated:

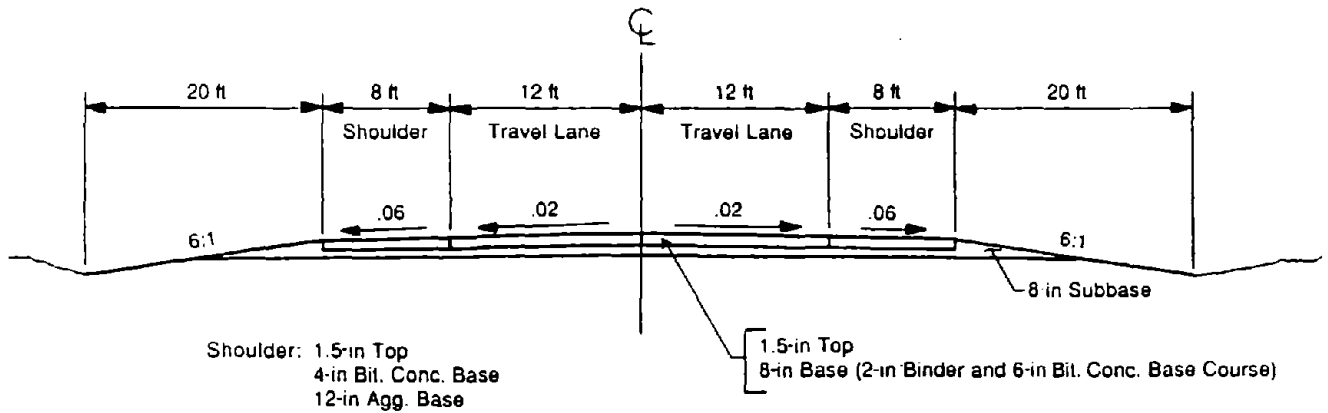
- Rural two-lane highway--new construction or major reconstruction.
- Rural two-lane highway--rehabilitation.
- Rural freeway--new construction or major reconstruction.
- Rural freeway--rehabilitation.

Figure 66 illustrates the assumed cross sections for the typical two-lane highway and freeway assumed in the analyses.

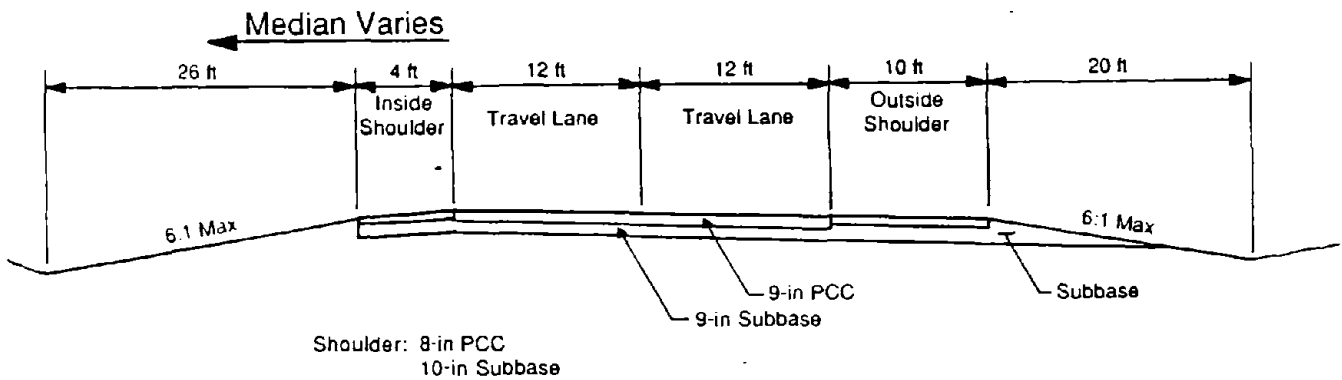
The scenario involving new construction or major reconstruction involved only additional earthwork costs to provide longer stopping sight distance. In the case of new construction, pavement and shoulder construction costs would be unaffected by the decision to provide longer stopping sight distance. In the case of major reconstruction, it is assumed that the pavement and shoulders would need to be replaced as part of the project, so the decision to provide additional stopping sight distance would have no effect on pavement and shoulder costs. However, the rehabilitation scenario includes the cost of replacing the pavement and shoulder which would not be necessary if the stopping sight distance were not being improved.

In some cases, where construction costs were dependent on site-specific conditions, multiple estimates of construction cost were made. For example, in the case of longer vertical curves needed to implement increased stopping sight distances for trucks, the cost of constructing the increased vertical curves was estimated separately for a range of algebraic differences in grade from 1 to 10 percent. Then, estimates of the relative frequency of each algebraic difference in grade were used to combine the earthwork costs into a single average for all algebraic differences in grade. The data in table 55 were obtained for rural two-lane highways in Texas and for both rural two-lane highways and rural freeways in the State of Washington. The Texas data represent selected two-lane highways in rolling terrain in east Texas, and are not necessarily representative of the flatter terrain in west Texas. The Washington data represent all rural two-lane highways and all rural Interstate freeways in the State. The table shows the relative distribution of crest vertical curves by algebraic difference in grade. The distribution for two-lane highways is based on the average of the Texas and Washington data, giving equal weight to the data from each State. Equal weights were used because the data from Washington, which represent the entire State, would otherwise far outweigh the data from Texas, which represent a small sample of roadways. The distribution for freeways is based on the Washington data alone.

RURAL TWO LANE HIGHWAY



RURAL FREEWAY



Note: 1 ft = 0.305 m
1 in = 2.54 cm

Figure 66. Typical cross sections for cost-effectiveness analysis.

Table 55. Distribution of crest vertical curves by algebraic difference in grade.

Algebraic difference in grade (%)	Rural two-lane highways			Rural freeways	
	Number of crest vertical curves		Proportion of crest vertical curves ^c	Number of crest vertical curves (Washington) ^d	Proportion of crest vertical curve
	Texas ^a	Washington ^b			
1	194	2,965	0.345	253	0.558
2	131	1,465	0.197	89	0.196
3	100	995	0.142	50	0.110
4	83	689	0.109	26	0.057
5	53	521	0.075	16	0.035
6	43	333	0.055	12	0.026
7	20	225	0.030	3	0.007
8	11	141	0.018	4	0.009
9	11	141	0.018	0	0.000
10	7	90	0.011	0	0.000
	653	7,565		453	

^a Selected sites in rolling terrain (192.2 mi [309.3 km] of highway).

^b Statewide (5,082.9 mi [8,178.3 km] of highway).

^c Average with equal weight given to each State.

^d Statewide (501.6 mi [807.1 km] of highway).

The recommendations of the AASHTO User Benefit Analysis Manual concerning the residual value of the improvement at the end of the 20-year analysis period were followed.⁵³ The construction items related to pavements, shoulders, and signs have service lives less than or equal to 20 years, so they have no residual value at the end of the analysis period. Earthwork is generally considered to have a service life substantially longer than the analysis period (typically, 40 to 50 years). This longer service life can be accounted for properly in the economic analysis by assigning a residual value to the earthwork at the end of the analysis period. In this case, the residual value for earthwork is estimated as 50 percent of its initial cost.

2. Expected Accident Rate

The expected accident rates for rural two-lane highways, freeways, and intersections, as a function of average daily traffic volume were estimated from 1987 data provided by the California Department of Transportation (Caltrans).⁵⁵ Data on the typical severity distributions of accidents were obtained from the same source. Table 56 shows these estimates which are based on statewide data for California State highways and were developed by Caltrans for use as expected values in their accident surveillance system.

Table 56. Expected accident rates and severity distributions based on California data.⁵⁵

Area type	Roadway or inter-section type	Design speed (mi/h)	Terrain	Average daily traffic volume (veh/day)	Accident rate (accidents per million veh-mi)	Proportion of accidents by severity level		
						Fatal	Injury	PDO ^a
<u>Highway Segments</u>								
Rural	Two-lane	> 55	Rolling	All	1.35 + 450/ADT	0.039	0.487	0.474
Rural	Freeway (4-lane)	> 65	All	≤ 15,000	0.40 + 650/ADT	0.047	0.473	0.480
Rural	Freeway (4-lane)	> 65	All	> 15,000	0.35 + 0.000004*ADT	0.032	0.446	0.522
<u>Intersections</u>								
Rural	Four-leg or multileg (STOP or YIELD control)	-	-	All	0.40 ^b	0.024	0.449	0.473

^a PDO = property-damage-only.

^b Accidents per million entering vehicles.

Note: 1 mi = 1.61 km

3. Expected Proportion of Accidents Involving Trucks

A change in stopping sight distance criteria is being considered primarily to benefit trucks. Therefore, the cost-benefit analysis has been structured to determine the required percentage reduction in truck accidents. Because most accidents involve more than one vehicle, the percentage of accidents that involve trucks is higher than the percentage of trucks in the traffic stream, as follows:

$$TA = T \times (1 - MV) + 2 \times T \times (1-T) \times MV + T^2 \times MV \quad (70)$$

where: TA = expected proportion of accidents involving trucks
T = proportion of trucks in traffic stream
MV = proportion of multiple-vehicle accidents

Equation (70) is based on the assumption that accident rates for passenger cars and trucks are essentially equal and that all multiple-vehicle accidents involve only two vehicles.

4. Average Daily Traffic Volume

Cost-effectiveness calculations were performed for a range of average daily traffic volumes (ADTs) for each facility type. ADT affected the outcome of the cost-effectiveness analysis in two ways. First, the exposure in vehicle-miles of travel or number of entering vehicles at intersections increased with increasing ADT. Second, the accident rate was assumed to vary with ADT following the relationships shown in table 56. For rural two-lane highways, the analysis considered an ADT range from 1,000 to 15,000 veh/day. For rural freeways, the ADT range considered was 2,000 to 50,000 veh/day. For intersections, the ADT range considered was 2,000 to 30,000 entering vehicles/day.

5. Length of Improved Site

An appropriate length of highway to represent a typical improved site was chosen for each analysis. For example, in the case of the stopping sight distance analysis, the length used in the analysis was the average length of the improved vertical curves to be constructed. This was estimated from the vertical curve lengths for each algebraic difference in grade and the relative frequency of each algebraic difference in grade based on actual road profiles from Texas and Washington.

6. Accident Cost Savings

The cost savings for each accident reduced were based on estimates from a recent FHWA technical advisory.⁵⁶ These estimates are:

- Fatal accident \$1,700,000
- Injury accident 14,000
- Property-damage-only
 accident 3,000

These accident cost savings are not based on out-of-pocket losses to accident victims but rather are based on a "willingness to pay" concept developed by FHWA research. In other words, the accident cost savings represent the amount that potential accident victims would be willing to pay to avoid involvement in the accident.

7. Present Worth Factors

The principles of economic analysis require that comparisons between costs and benefits of improvement projects must be made at the same point in time. In this case, for consistency with the AASHTO Manual on User Benefit Analysis for Highway and Bus Transit Improvements, all costs and benefits were reduced to their present worth (i.e., their value at the time when the improvement is constructed).⁵³

The appropriate factor to reduce the accident reduction benefits, represented as a uniform series of annual cash flows over the entire analysis period to their present worth is called the uniform series present worth factor. This factor is:

$$SPW = \frac{(1 + i)^n - 1}{i(1 + i)^n} \quad (71)$$

where: SPW = uniform series present worth factor
 i = minimum attractive rate of return (or discount rate) represented as a decimal = i%/100
 n = duration of analysis period (yr)

The appropriate factor to reduce the residual value to its present worth before subtracting it from the construction cost is the single amount present worth factor, defined as:

$$PW = \frac{1}{(1 + i)^n} \quad (72)$$

where: PW = single amount present worth factor

The single amount present worth factor is entirely analogous to the uniform series present worth factor discussed above except that it is applied to determine the present worth of a single amount on a specified future date rather than a series of annual amounts over a specified period.

The minimum attractive rate of return (or discount rate) represents the time value of money. This rate should equal the return on alternative investments that must be foregone if the improvement is constructed. The AASHTO user benefit analysis manual emphasizes that this rate should represent the real long-term cost of capital, over and above the inflation rate.⁵³ If a higher minimum attractive rate of return--representing current market interest rates--were used, it would also be necessary to increase the accident cost

each year to keep pace with inflation. The minimum attractive rate of return was estimated as 5 percent ($i = 0.05$) based on the rate cited in the recent FHWA bulletin on accident costs.⁵⁶

The analysis period was 20 years in all cases except for signing analyses, in which case a 5-year analysis period was used.

B. Examples of Cost-Effectiveness Analysis for Stopping Sight Distance

The sensitivity analyses presented in volume I of this report concluded that current AASHTO stopping sight distance criteria do not completely accommodate trucks. Table 57 compares the current AASHTO criteria with the candidate revisions to those criteria developed in volume I. The following discussion illustrates the cost-effectiveness analysis that was conducted to determine how likely it is that the additional construction costs to provide improved stopping sight distance for trucks would be economically justified by reduced accidents.

Table 57. Candidate stopping sight distance criteria for trucks in comparison to AASHTO criteria.

Design speed (mi/h)	Minimum stopping sight distance (ft)	
	AASHTO	Truck
20	125	150
30	200	275
40	325	475
50	475	675
60	650	900
70	850	1,175

Note: 1 mi = 1.61 km
1 ft = 0.305 m

1. Example 1--Rural Two-Lane Highway--New Construction or Major Reconstruction

Example 1 addresses the cost-effectiveness of providing increased stopping sight distance for trucks on rural two-lane highways. Table 58 shows the assumed conditions for this example. The previous sections have documented these assumptions.

Table 58. Assumed condition--example 1.

Highway type	Rural two-lane
Design speed	60 mi/h
Cross-section width	84 ft
Costing scenario	New construction or major reconstruction (earthwork only)
Earthwork cost	\$2.99/yd ³
Residual value	50% of earthwork cost
Fatal accident cost	\$1,700,000
Injury accident cost	\$14,000
PDO accident cost	\$3,000
Analysis period	20 yr
Minimum attractive rate of return	5%

Note: 1 mi = 1.61 km
 1 ft = 0.305 m
 1 yd = 0.914 m

Table 59 documents the calculation of the additional construction costs necessary to provide improved stopping sight distance for trucks on a rural two-lane highway being newly constructed or undergoing major reconstruction. For example 1, these costs consist entirely of increased expenditures for earthwork, since it is assumed that the pavement and shoulders are either not built yet or will need to be completely replaced as part of the reconstruction. Since the additional stopping sight distance will be provided at crest vertical curves, all of the required earthwork is cut rather than fill. The table shows the cost of the additional cut required to improve one vertical curve for each algebraic difference in grade. The overall average cost to provide improved stopping sight distance is estimated to be about \$18,000 per vertical curve. This estimate was determined as a weighted average using as weights the relative frequencies of each algebraic difference in grade from table 55.

Table 60 presents the results of the cost-effectiveness analysis, expressed in terms of the accident reductions that would be required to make the improvement cost effective. The cost-effectiveness analysis in table 60 has been performed for a range of ADT from 1,000 to 15,000 veh/day.

Column 1 in the table presents the specific values of ADT that were used.

Column 2 presents the expected accident rate, based on the data for rural two-lane highways in table 56. Columns 3 and 4 present the expected proportion of fatal and injury accidents, also based on table 56. Column 5 indicates the expected percentage of multiple-vehicle accidents.

Table 59. Computation of average construction cost per vertical curve--example 1.

(1)	(2)	(3)	(4)	(5)	(6)	(7)
Algebraic difference in grade (%)	Vertical curve length (ft) (AASHTO)	Vertical curve length (ft) (truck)	Earthwork ^a (yd ³)	Construction ^b cost (\$)	Relative ^c proportion of algebraic difference in grade	Weighted ^d average cost
1	310	394	93	279	0.345	96
2	620	788	622	1,862	0.197	367
3	930	1,181	2,084	6,237	0.142	888
4	1,240	1,575	4,884	14,614	0.109	1,594
5	1,550	1,969	9,551	28,577	0.075	2,144
6	1,860	2,363	16,489	49,335	0.055	2,170
7	2,170	2,756	26,227	78,470	0.030	2,369
8	2,480	3,150	39,138	117,100	0.018	2,078
9	2,790	3,544	55,720	166,714	0.018	2,958
10	3,100	3,938	76,409	228,615	0.011	2,585
Avg. length	909	1,155				Average cost per vertical curve = \$17,788

^a Computed as sum of vertical profile differences at 100-ft (30-m) stations along the vertical curve times 100 ft (30 m) times cross-section width of 84 ft (26 m).

^b Computed using unit cost data in table 58.

^c From table 55.

^d Weighted average construction cost per vertical curve computed as the sum over all algebraic differences in grade of column (5) times column (6).

Note: 1 ft = 0.305 m

1 yd = 0.914 m

Table 60. Computation of minimum percent accident reduction required for cost effectiveness--example 1.

(1)	(2)	(3)	(4)	(5)	(6)	(7)	(8)	(9)	(10)	(11)	(12)
Average daily traffic (veh/day)	Accident rate (accidents per million veh-mi)	Proportion of fatal accidents	Proportion of injury accidents	Proportion of multiple vehicle accidents	Number of accidents per mi per yr	Average accident cost (\$)	Minimum percent reduction in truck accidents on vertical curves				
							1%	5%	10%	20%	30%
1,000	1.80	0.039	0.487	0.726	0.66	74,500	629.1	128.0	65.4	34.2	23.9
2,000	1.58	0.039	0.487	0.726	1.15	74,500	359.5	73.1	37.4	19.5	13.7
3,000	1.50	0.039	0.487	0.726	1.64	74,500	251.7	51.2	26.2	13.7	9.6
4,000	1.46	0.039	0.487	0.726	2.14	74,500	193.6	39.4	20.1	10.5	7.4
5,000	1.44	0.039	0.487	0.726	2.63	74,500	157.3	32.0	16.3	8.6	6.0
6,000	1.43	0.039	0.487	0.726	3.12	74,500	132.4	26.9	13.8	7.2	5.0
7,000	1.41	0.039	0.487	0.726	3.61	74,500	114.4	23.3	11.9	6.2	4.3
8,000	1.41	0.039	0.487	0.726	4.11	74,500	100.7	20.5	10.5	5.5	3.8
9,000	1.40	0.039	0.487	0.726	4.60	74,500	89.9	18.3	9.3	4.9	3.4
10,000	1.40	0.039	0.487	0.726	5.09	74,500	81.2	16.5	8.4	4.4	3.1
11,000	1.39	0.039	0.487	0.726	5.58	74,500	74.0	15.1	7.7	4.0	2.8
12,000	1.39	0.039	0.487	0.726	6.08	74,500	68.0	13.8	7.1	3.7	2.6
13,000	1.38	0.039	0.487	0.726	6.57	74,500	62.9	12.8	6.5	3.4	2.4
14,000	1.38	0.039	0.487	0.726	7.06	74,500	58.5	11.9	6.1	3.2	2.2
15,000	1.38	0.039	0.487	0.726	7.56	74,500	54.7	11.1	5.7	3.0	2.1

Note: 1 mi = 1.61 Km

Column 6 presents the expected number of accidents per mile per year, computed as $(1) \times (2) \times 365 \times 10^{-6}$. Column 7 presents the average cost per accidents based on the accident severity distribution shown in the table and the FHWA accident costs given above.

Columns 8 through 12 present the minimum percentage reduction in truck accidents that would be required to make the improvement cost effective for various specified percentages of trucks in the traffic stream, computed from equation (69). These percentage reductions apply to the expected number of truck accidents for a length of highway equal to the average length of vertical curve shown in table 59. For example, the first row of the table indicates that the improvement in stopping sight distance would be cost effective if 30 percent of the vehicles in the traffic stream were trucks and the improvement reduced truck accidents by 23.9 percent.

Columns 8 through 12 are best interpreted by an engineering judgment as to whether the specified percentage reduction in truck accidents is likely from an improvement in stopping sight distance on a vertical curve. Accident reductions greater than 100 percent are impossible, and indicate clearly that a stopping sight distance improvement would not be cost effective. Accident reductions approaching 100 percent are very unlikely and indicate that the stopping sight distance improvement is probably not cost effective. On the other hand, small values of accident reduction may be very achievable and indicate that a stopping sight distance improvement is very likely to be cost-effective. The author's judgment is that reductions in truck accidents up to 10 or 20 percent are possible, but higher accident reductions are highly unlikely. Therefore, the results of each example are interpreted below in relation to reductions in truck accidents of 10 and 20 percent.

The data in columns 8 through 12 suggest that stopping sight distance improvements for trucks are cost effective in new construction or major reconstruction on rural two-lane highways at higher ADTs and higher truck percentages. For example, if a change in stopping sight distance criteria for trucks could produce a 10-percent reduction in truck accidents, the improvement will be cost effective for rural two-lane highways with truck volumes over about 800 trucks/day. If a 20-percent reduction in truck accidents could be achieved, stopping sight distance improvements for trucks would be cost effective at volumes of about 400 trucks/day.

Example calculation: An example calculation is presented to illustrate how the minimum percent reduction in truck accidents (columns 8 through 12 in table 60) was determined. For illustrative purposes, the minimum percent reduction will be computed for the case in example 1 with average daily traffic volume of 5,000 veh/day and 10 percent trucks in the traffic stream. The basic assumptions for this example are summarized in table 58.

The minimum percent reduction in truck accidents required for cost effectiveness is calculated from equation (69). This example will show how the value of each of the variables in equation (69) was determined. This same computational procedure is also used in the other examples presented in the remainder of this appendix.

The construction costs and residual value in equation (69) are determined from the data in table 59. The construction cost (CC) is the average cost per vertical curve to perform additional earthwork for improving the sight distance, or \$17,788 per vertical curve. As shown in the table, \$17,788 is the average cost over the full range of algebraic difference in grade weighted by the relative proportion of each algebraic difference in grade on a sample of highways in Texas and Washington. CC is computed as the sum of the products of columns 5 and 6 in table 59.

The residual value (RV) is the remaining value of the improvement at the end of the 20-year analysis period. As shown in table 58, RV is estimated as 50 percent of the earthwork cost or \$8,894. The residual value is based only on earthwork costs, and no residual value is assumed for items with shorter service lives such as pavement and shoulder costs.

The uniform series present worth factor (SPW) was calculated from equation (71) as:

$$SPW = \frac{(1 + 0.05)^{20} - 1}{0.05(1 + 0.05)^{20}} = 12.46$$

The single amount present worth factor (PW) was calculated from equation (72) as:

$$PW = \frac{1}{(1 + 0.05)^{20}} = 0.377$$

The estimated values of accident rate (AR) presented in column 2 of table 60 are based on Caltrans estimates of accident rate as a function of ADT given in table 56. For the case in question, the value of AR is 1.44 accidents per million veh-mi (2.31 accidents per million veh-km).

The expected proportion of accidents involving trucks (TA) is computed from the assumed proportion of trucks in the traffic stream (0.10) and the estimated proportion of multiple vehicle accidents on two-lane highways (0.726, based on Caltrans data). Using equation (70):

$$TA = 0.01(1 - 0.726) + 2(0.10)(1 - 0.10)(0.726) + (0.10)(0.10)(0.726) = 0.165$$

In other words, if trucks constitute 10 percent of the traffic stream, then approximately 16.5 percent of accidents would be expected to involve one or more trucks.

The value of the average daily traffic volume (ADT) term is assumed to be 5,000 veh/day.

The number of days per year (N) is 365.

The length of the improved sites will vary from 394 to 3,938 ft (120 to 1,201 m) as a function of algebraic difference in grade as shown in table 59. If a substantial length of highway is improved, the average length of the improved sites (L) can be calculated by the same weighting procedure used to determine construction costs. Thus, the estimates for L and CC from table 59 show that the average improved vertical curve will be 1,155 ft (352 m) long and it will cost \$17,788 to improve that curve.

The average cost savings per accident reduced (AC) is computed from the accident severity distribution given in table 60 and the FHWA estimates of accident costs by severity level given in table 58. AC is computed as:

$$AC = 0.039(\$1,700,000) + 0.487(\$14,000) + 0.474(\$3,000) = \$74,500$$

Based on equation (69), the minimum percent reduction in truck accidents can then be calculated as:

$$\text{Percent Reduction} = \frac{[17,788 - (8,894)(0.377)] 100}{(1.44)(0.165)(5,000)(365)(0.219)(10^{-6})(74,500)(12.46)} = 16.3\%$$

In other words, a sight distance improvement for trucks would be cost effective for new construction on a rural two-lane highway with an ADT of 5,000 veh/day and 10 percent trucks if it reduced truck accidents by 16.3 percent. Engineering judgment is the only available basis for deciding whether a sight distance improvement would be likely to reduce that many accidents.

2. Example 2--Rural Two-Lane Highway--Rehabilitation

Example 2 addresses rehabilitation of rural two-lane highways, as opposed to new construction or major reconstruction, which were addressed in example 1. The assumed conditions for example 2 are presented in table 61. The computational approach for example 2 is entirely analogous to example 1 except that the construction costs for rehabilitation include earthwork, pavement removal and replacement, and shoulder removal and replacement. The pavement and shoulder costs are included in this case because it is assumed that these costs are being incurred only because the sight distance is being improved.

Table 62 is analogous to table 59, but includes the added pavement and shoulder costs, which increase the expected improvement cost substantially from about \$18,000 to about \$182,000 per vertical curve.

Table 63 presents the results of the cost-effectiveness analysis and is entirely analogous to table 60. The results in table 63 demonstrate that it is almost never cost effective to improve stopping sight distance on a rural two-lane highway in a rehabilitation project, if the improvement requires replacement of the pavement and shoulder where this would not otherwise be necessary.

Table 61. Assumed conditions--example 2.

Highway type	Rural two-lane
Design speed	60 mi/h
Cross-section width	84 ft
Costing scenario	Rehabilitation (earthwork, pavement, and shoulder)
Earthwork cost	\$2.99/yd ³
Residual value	50% of earthwork cost
Pavement type	Flexible
Pavement removal and replacement cost	\$4.05/ft ²
Shoulder type	Flexible
Shoulder removal and replacement cost	\$3.51/ft ²
Fatal accident cost	\$1,700,000
Injury accident cost	\$14,000
PDO accident cost	\$3,000
Analysis period	20 yr
Minimum attractive rate of return	5%

Note: 1 mi = 1.61 km
 1 ft = 0.305 m
 1 yd = 0.914 m

Table 62. Computation of average construction cost per vertical curve--example 2.

(1) Algebraic difference in grade (%)	(2) Vertical curve length (ft) (AASHTO)	(3) Vertical curve length (ft) (truck)	(4)		(5)		(6) Shoulder ^c (ft ²)	(7) Earthwork cost (\$)	(8) Pavement ^d and shoulder cost (\$)	(9) Construction ^e Cost (\$)	(10) Relative ^f proportion of algebraic difference in grade	(11) Weighted ^g average cost
			Earthwork ^a (yd ²)	Pavement ^b (ft ²)	Pavement ^b (ft ²)	Shoulder ^c (ft ²)						
1	310	394	93	7,200	4,800	279	46,008	46,287	0.345	15,947		
2	620	788	622	16,800	11,200	1,862	107,352	109,214	0.197	21,530		
3	930	1,181	2,084	26,400	17,600	6,237	168,696	174,933	0.142	24,899		
4	1,240	1,575	4,884	36,000	24,000	14,661	230,040	244,654	0.109	26,690		
5	1,550	1,969	9,551	45,600	30,400	28,577	291,384	319,384	0.075	24,002		
6	1,860	2,363	16,489	55,200	36,800	49,335	352,728	402,063	0.055	22,087		
7	2,170	2,756	26,227	64,800	43,200	78,470	414,072	492,542	0.030	14,867		
8	2,480	3,150	39,138	74,400	49,600	117,100	475,416	592,516	0.018	10,512		
9	2,790	3,544	55,720	84,000	56,000	166,714	536,760	703,474	0.018	12,481		
10	3,100	3,938	76,409	93,600	62,400	228,615	598,104	826,719	0.011	9,349		
Avg. length = 909										1,155	Average cost per VC = \$182,364	

a Computer as sum of vertical profile differences at 100-ft (30-m) stations along the vertical curve times 100 ft (30 m) times cross-section width of 84 ft (26 m)

b Computer as pavement width of 24 ft (7.3 m) times length of vertical curve.

c Computer as shoulder width of 16 ft (4.9 m) times length of vertical curve.

d Computer using unit cost data in table 61.

e Sum of columns (7) and (8).

f From table 55.

g Weighted average construction cost per vertical curve computed as the sum over all algebraic differences in grade of column (9) times column (10).

Note: 1 ft = 0.305 m
1 yd = 0.914 m

Table 63. Computation of minimum percent accident reduction required for cost effectiveness--example 2.

(1)	(2)	(3)	(4)	(5)	(6)	(7)	(8)	(9)	(10)	(11)	(12)
Average daily traffic (veh/day)	Accident rate (accidents per million veh-mi)	Proportion of fatal accidents	Proportion of injury accidents	Proportion of multiple vehicle accidents	Number of accidents per mi per yr	Average accident cost (\$)	Minimum percent reduction in truck accidents on vertical curves	Percent trucks	Percent trucks	Percent trucks	Percent trucks
1,000	1.80	0.039	0.487	0.726	0.66	74,500	7,813.4	1,589.5	812.2	424.7	296.8
2,000	1.58	0.039	0.487	0.726	1.15	74,500	4,464.7	908.3	464.1	242.7	169.6
3,000	1.50	0.039	0.487	0.726	1.64	74,500	3,125.3	635.8	324.9	169.9	118.7
4,000	1.46	0.039	0.487	0.726	2.14	74,500	2,404.1	489.1	249.9	130.7	91.3
5,000	1.44	0.039	0.487	0.726	2.63	74,500	1,953.3	397.4	203.0	106.2	74.2
6,000	1.43	0.039	0.487	0.726	3.12	74,500	1,644.9	334.6	171.0	89.4	62.5
7,000	1.41	0.039	0.487	0.726	3.61	74,500	1,420.6	289.0	147.7	77.2	54.0
8,000	1.41	0.039	0.487	0.726	4.11	74,500	1,250.1	254.3	130.0	68.0	47.5
9,000	1.40	0.039	0.487	0.726	4.60	74,500	1,116.2	227.1	116.0	60.7	42.4
10,000	1.40	0.039	0.487	0.726	5.09	74,500	1,008.2	205.1	104.8	54.8	38.3
11,000	1.39	0.039	0.487	0.726	5.58	74,500	919.2	187.0	95.6	50.0	34.9
12,000	1.39	0.039	0.487	0.726	6.08	74,500	844.7	171.8	87.8	45.9	32.1
13,000	1.38	0.039	0.487	0.726	6.57	74,500	781.3	158.9	81.2	42.5	29.7
14,000	1.38	0.039	0.487	0.726	7.06	74,500	726.8	147.9	75.6	39.5	27.6
15,000	1.38	0.039	0.487	0.726	7.56	74,500	679.4	138.2	70.6	36.9	25.8

Note: 1 mi = 1.61 km

For example, even at the extremely high volume of 15,000 veh/day and 30 percent trucks in the traffic stream (i.e., 4,500 trucks/day), a stopping sight distance improvement would have to reduce truck accidents by more than 20 percent to be cost effective. Substantially greater percentage reductions in accidents would be required for cost effectiveness at lower volume levels.

3. Example 3--Rural Freeway--New Construction or Major Reconstruction

Example 3 is a cost-effectiveness analysis of improvement of stopping sight distance for trucks for new construction or major reconstruction on a rural freeway. The assumed conditions for example 3 are presented in table 64. The assumed cross section for a rural freeway differs from that of a two-lane highway, as shown in figure 66. The freeway case uses a highway design speed of 70 mi/h (113 km/h), as opposed to 60 mi/h (97 km/h) in the two-lane case, resulting in longer vertical curves.

Table 64. Assumed conditions--example 3.

Highway type	Rural freeway
Design speed	70 mi/h
Cross-section width	168 ft (84 ft for each roadway)
Costing scenario	New construction or major reconstruction (earthwork only)
Earthwork cost	\$2.99/yd ³
Residual value	50% of earthwork cost
Fatal accident cost	\$1,700,000
Injury accident cost	\$14,000
PDO accident cost	\$3,000
Analysis period	20 yr
Minimum attractive rate of return	5%

Note: 1 mi = 1.61 km
 1 ft = 0.305 m
 1 yd = 0.914 m

Table 65 presents the added earthwork cost to improve the stopping sight distance for trucks on crest vertical curves for each individual algebraic difference in grade, and averaged over all algebraic differences in grade based on the freeway data in table 55. The additional earthwork to improve stopping sight distance on a rural freeway would be about \$32,000 per crest vertical curve for both directions of travel combined.

Table 66 presents the results of the cost-effectiveness analysis for freeway ADTs from 2,000 to 50,000 veh/day. The analysis results show that the additional expenditures to improve stopping sight distance would be cost effective only on higher volume rural freeways. For example, if the stopping

Table 65. Computation of average construction cost per vertical curve--example 3.

(1)	(2)	(3)	(4)	(5)	(6)	(7)
Algebraic difference in grade (%)	Vertical curve length (ft) (AASHTO)	Vertical curve length (ft) (truck)	Earthwork ^a (yd ³)	Construction ^b cost (\$)	Relative ^c proportion of algebraic difference in grade	Weighted ^d average cost
1	540	671	373	1,117	0.558	624
2	1,080	1,342	3,298	9,867	0.196	1,939
3	1,620	2,014	11,138	33,324	0.110	3,678
4	2,160	2,685	26,382	78,936	0.057	4,531
5	2,700	3,365	51,520	154,148	0.035	5,445
6	3,240	4,027	88,978	266,222	0.026	7,052
7	3,780	4,698	141,307	422,790	0.007	2,800
8	4,320	5,369	210,933	631,113	0.009	5,573
9	4,860	6,041	300,284	898,451	0.000	0
10	5,400	6,712	411,911	1,232,438	0.000	0
Avg. length = 1,061				Average cost per vertical curve =		\$31,640

^a Computed as sum of vertical profile differences at 100-ft (30-m) stations along the vertical curve times 100 ft (30 m) times cross-section width of 168 ft (51 m)

^b Computed using unit cost data in table 64.

^c From table 55.

^d Weighted average construction cost per vertical curve computed as the sum over all algebraic differences in grade of column (5) times column (6).

Note: 1 ft = 0.305 m

1 yd = 0.914 m

Table 66. Computation of minimum percent accident reduction required for cost effectiveness--example 3.

(1)	(2)	(3)	(4)	(5)	(6)	(7)	(8)	(9)	(10)	(11)	(12)
Average daily traffic (veh/day)	Accident rate (accidents per million veh-mi)	Proportion of fatal accidents	Proportion of injury accidents	Proportion of multiple vehicle accidents	Number of accidents per mi per yr	Average accident cost (\$)	1%	5%	10%	20%	30%
2,000	0.73	0.047	0.473	0.730	0.53	88,000	1,030.8	209.7	107.2	56.0	39.2
3,000	0.62	0.947	0.473	0.730	0.68	88,000	807.9	164.4	84.0	43.9	30.7
4,000	0.56	0.047	0.473	0.730	0.82	88,000	664.3	135.1	69.1	36.1	25.2
5,000	0.53	0.047	0.473	0.730	0.97	88,000	564.0	114.7	58.6	30.7	21.4
10,000	0.47	0.047	0.473	0.730	1.70	88,000	321.4	65.4	33.4	17.5	12.2
15,000	0.44	0.047	0.473	0.730	2.43	88,000	224.8	45.7	23.4	12.2	8.5
20,000	0.43	0.032	0.446	0.730	3.14	62,200	245.7	50.0	25.5	13.4	9.3
25,000	0.45	0.032	0.446	0.730	4.11	62,200	187.9	38.2	19.5	10.2	7.1
30,000	0.47	0.032	0.446	0.730	5.15	62,200	149.9	30.5	15.6	8.1	5.7
35,000	0.49	0.032	0.446	0.730	6.26	62,200	123.2	25.1	12.8	6.7	4.7
40,000	0.51	0.032	0.446	0.730	7.45	62,200	103.6	21.1	10.8	5.6	3.9
45,000	0.53	0.032	0.446	0.730	8.71	62,200	88.6	18.0	9.2	4.8	3.4
50,000	0.55	0.032	0.446	0.730	10.04	62,200	76.9	15.6	8.0	4.2	2.9

Note: 1 mi = 1.61 km

sight distance improvement reduced truck accidents by 10 percent, the improvement would be cost effective on rural freeways with truck volumes over about 4,000 trucks/day. If the stopping sight distance improvements reduced truck accidents by 20 percent, the improvement would be cost effective on rural freeways with truck volumes over about 2,000 trucks/day.

4. Example 4--Rural Freeway--Rehabilitation

Example 4 is similar to example 3 except that it represents a rehabilitation case for a rural freeway, rather than a new construction or major reconstruction case. Table 67 summarizes the assumed conditions for example 4. As in the two-lane highway rehabilitation case, the freeway rehabilitation example considers costs for earthwork, pavement removal and replacement, and shoulder removal and replacement.

Table 67. Assumed conditions--example 4.

Highway type	Rural freeway
Design speed	70 mi/h
Cross-section width	168 ft (84 ft for each roadway)
Costing scenario	Rehabilitation (earthwork, pavement, and shoulder)
Earthwork cost	\$2.99/yd ³
Residual value	50% of earthwork cost
Pavement type	Rigid
Pavement removal and replacement cost	\$4.78/ft ²
Shoulder type	Rigid
Shoulder removal and replacement cost	\$4.25/ft ²
Fatal accident cost	\$1,700,000
Injury accident cost	\$14,000
PDO accident cost	\$3,000
Analysis period	20 yr
Minimum attractive rate of return	5%

Note: 1 mi = 1.61 km
 1 ft = 0.305 m
 1 yd = 0.914 m

Table 68 presents construction cost estimates which indicate that improvement of stopping sight distance in a freeway rehabilitation project would cost about \$491,000 per crest vertical curve, including both directions of travel. Table 69 presents the results of the cost-effectiveness analysis, which indicate that it is highly unlikely that any stopping sight distance improvement on a freeway would reduce enough accidents to make the improvement

Table 68. Computation of average construction cost per vertical curve--example 4.

(1)	(2)	(3)	(4)	(5)	(6)	(7)	(8)	(9)	(10)	(11)
Algebraic difference in grade (%)	Vertical curve length (ft) (AASHTO)	Vertical curve length (ft) (truck)	Construction quantities		Shoulder ^c (ft)	Earthwork cost (\$)	Pavement ^d and shoulder cost (\$)	Construction ^e Cost (\$)	Relative proportion of algebraic difference in grade	Weighted average cost ^g
			Earthwork ^a (yd ³)	Pavement ^b (ft ²)						
1	540	671	373	32,208	18,788	1,117	233,803	234,920	0.558	131,203
2	1,080	1,342	3,298	64,416	37,576	9,867	467,606	477,473	0.196	93,808
3	1,620	2,014	11,138	96,672	56,392	33,324	701,758	735,082	0.110	81,135
4	2,160	2,685	26,382	128,880	75,180	78,936	935,561	1,014,497	0.057	58,227
5	2,700	3,356	51,520	161,088	93,968	154,148	1,169,365	1,323,512	0.035	46,747
6	3,240	4,027	88,978	193,296	112,756	266,222	1,403,168	1,669,389	0.026	44,222
7	3,780	4,698	141,307	225,504	141,544	422,790	1,636,971	2,059,761	0.007	13,641
8	4,320	5,369	210,933	257,712	150,332	631,113	1,870,774	2,501,887	0.009	22,092
9	4,860	6,041	300,284	289,968	169,148	898,451	2,104,926	3,003,377	0.000	0
10	5,400	6,712	411,911	322,176	187,936	1,232,438	2,338,729	3,571,167	0.000	0
Avg. length = 1,061									Average cost per VC =	\$491,074

a Computer as sum of vertical profile differences at 100-ft (30-m) stations along the vertical curve times 100 ft (30 m) times cross-section width of 168 ft (51 m).
 b Computed as total pavement width of 48 ft (15 m) times length of vertical curve.
 c Computed as total shoulder width of 28 ft (8.5 m) (10 ft [3.1 m] outside shoulders plus 4 ft [1.2 m] inside shoulders) times length of vertical curve.
 d Computed using unit cost data in table 67.
 e Sum of columns (7) and (8).
 f From table 55.
 g Weighted average construction cost per vertical curve computed as the sum over all algebraic differences in grade of column (9) times column (10).

Note: 1 ft = 0.305 m
 1 yd = 0.914 m

Table 69. Computation of minimum percent accident reduction required for cost effectiveness--example 4.

(1)	(2)	(3)	(4)	(5)	(6)	(7)	(8)	(9)	(10)	(11)	(12)
Average daily traffic (veh/day)	Accident rate (accidents per million veh-mi)	Proportion of fatal accidents	Proportion of injury accidents	Proportion of multiple vehicle accidents	Number of accidents per mi per yr	Average accident cost (\$)	Minimum percent reduction in truck accidents on vertical curves				
							1%	5%	10%	20%	30%
2,000	0.73	0.047	0.473	0.730	0.53	88,000	19,474.6	3,961.9	2,024.4	1,058.7	739.8
3,000	0.62	9.947	0.473	0.730	0.68	88,000	15,263.9	3,105.2	1,586.7	829.8	579.8
4,000	0.56	0.047	0.473	0.730	0.82	88,000	12,550.3	2,553.2	1,304.6	682.3	476.7
5,000	0.53	0.047	0.473	0.730	0.97	88,000	10,655.9	2,167.8	1,102.7	579.3	404.8
10,000	0.47	0.047	0.473	0.730	1.70	88,000	6,072.7	1,235.4	631.3	330.1	230.7
15,000	0.44	0.047	0.473	0.730	2.43	88,000	4,246.4	863.9	441.4	230.8	161.3
20,000	0.43	0.032	0.446	0.730	3.14	62,200	4,642.7	944.5	482.6	252.4	176.4
25,000	0.45	0.032	0.446	0.730	4.11	62,200	3,549.1	722.0	368.9	192.9	134.8
30,000	0.47	0.032	0.446	0.730	5.15	62,200	2,831.7	576.1	294.4	153.9	107.6
35,000	0.49	0.032	0.446	0.730	6.26	62,200	2,328.1	473.6	242.0	126.6	88.4
40,000	0.51	0.032	0.446	0.730	7.45	62,200	1,957.2	398.2	203.5	106.4	74.3
45,000	0.53	0.032	0.446	0.730	8.71	62,200	1,674.1	340.6	174.0	91.0	63.6
50,000	0.55	0.032	0.446	0.730	10.04	62,200	1,451.9	295.4	150.9	78.6	55.2

Note: 1 mi = 1.61 km

cost effective if the improvement required replacement of the pavement and shoulders. Even in the highest volume case with 30 percent trucks on a freeway that carries 50,000 veh/day (i.e., 15,000 trucks/day), the stopping sight distance improvement would need to reduce nearly 50 percent of truck accidents to be cost effective.

5. Summary

The four examples presented above indicate that stopping sight distance improvements for trucks are probably cost effective in new construction or major reconstruction only on very high volume two-lane highways and freeways. If the stopping sight distance improvement is assumed to reduce 10 percent of truck accidents on vertical curves, the improvement would be cost effective for rural two-lane highways with trucks volumes over 800 trucks/day and rural freeways with truck volumes over 4,000 trucks/day. If the stopping sight distance improvement is assumed to reduce 20 percent of truck accidents, the corresponding truck volumes required for cost effectiveness would be 400 trucks/day on rural two-lane highways and 2,000 trucks/day on rural freeways.

In rehabilitation projects, where the pavement and shoulder would not otherwise need to be replaced, the improvement of stopping sight distance for trucks is virtually never cost effective on either two-lane highways or freeways.

REFERENCES

1. American Association of State Highway and Transportation Officials, A Policy on Geometric Design of Highways and Streets" (Washington, D.C.: 1984).
2. R. M. Clarke, W. A. Leasure, R. W. Radlinski, and M. Smith, Heavy Truck Safety Study, DOT HS 807 109 (Washington, D.C.: National Highway Traffic Safety Administration, March 1987).
3. P. L. Olson, D. E. Cleveland, P. S. Fancher, L. P. Kostyniuk, and L. W. Schneider, Parameters Affecting Stopping Sight Distance, NCHRP Report 270 (Washington, D.C.: Transportation Research Board, June 1984).
4. K. Saito, J. J. Henry, and R. R. Blackburn, "Development and Application of Predictor Models for Seasonal Variations in Skid Resistance," Proceedings of Australian Road Research Board, Vol. 13, 1986.
5. J. C. Wambold, "Obtaining Skid Number at Any Speed from a Test at a Single Speed," Presented at the 67th Annual Meeting of the Transportation Research Board, January 1988.
6. P. F. Bohn and H. D. Dunkle, Computer Simulation of the Effect of Road Roughness on Tire-Pavement Forces in Braking and Cornering, FHWA-RD-77-124 (Washington, D.C.: Federal Highway Administration, 1977).
7. A. Dijks, "Influence of Tread Depth on Wet Skid Resistance of Tires," Transportation Research Record 621 (Washington, D.C.: Transportation Research Board, 1977).
8. G. F. Hayhoe and C. G. Shapley, Factors Affecting the Skidding Performance of Trucks, (University Park, Pennsylvania: Pennsylvania Transportation Institute).
9. R. D. Ervin and R. E. Wild, The Noise and Traction Characteristics of Bias Ply Truck Tires, UM-HSRI-PF-76-2-1, Highway Safety Research Institute (Ann Arbor: University of Michigan, 1976).
10. P. S. Fancher, R. D. Ervin, C. B. Winkler, and T. D. Gillespie, A Factbook of the Mechanical Properties of the Components of Single-Unit and Articulated Heavy Vehicles, DOT HS 807 125 (Washington, D.C.: National Highway Traffic Safety Administration, December 1986).
11. I. Gusakov, R. Rice, S. Pugliese, and R. Galganski, An Evaluation of Methods to Investigate Truck Tire Wet Traction, DOT HS 806 577 (Washington, D.C.: National Highway Traffic Safety Administration, 1984).

12. P. S. Fancher, "Sight Distance Problems Related to Large Trucks," Transportation Research Record 1052 (Washington, D.C.: Transportation Research Board, 1986).
13. R. W. Radlinski, S. F. Williams, and J. M. Machey, "The Importance of Maintaining Air Brake Adjustments," Paper No. 821263, Society of Automotive Engineers, 1982.
14. R. W. Radlinski and S. F. Williams, NHTSA Heavy Duty Brake Research Program -- Report No. 2: The Effect of Adjustment on Air Brake Performance, DOT HS 806 740 (Washington, D.C.: National Highway Traffic Safety Administration, April 1985).
15. R. W. Radlinski and M. A. Flick, "Benefits of Front Brakes on Heavy Trucks," Paper No. 870493, Society of Automotive Engineers, 1987.
16. R. W. Radlinski and S. C. Bell, NHTSA's Heavy Vehicle Brake Research Program -- Report No. 6: Performance Evaluation of a Production Anti-Lock System Installed on a Two-Axle Straight Truck, DOT HS 807 046 (Washington, D.C.: National Highway Traffic Safety Administration, August 1, 1986).
17. R. W. Radlinski and M. A. Flick, "A Vehicle Test Procedure for Determining Adhesion Utilization Properties," Paper No. 840334, Society of Automotive Engineers, 1984.
18. R. W. Radlinski and S. F. Williams, NHTSA Heavy Duty Vehicle Brake Research Program -- Report No. 1: Stopping Capability of Air Braked Vehicles, DOT HS 806 738 and 739 (Washington, D.C.: National Highway Traffic Safety Administration, April 1985).
19. R. W. Radlinski and M. A. Flick, "Tractor and Trailer Brake System Compatibility," Paper No. 861942, Society of Automotive Engineers, 1986.
20. R. W. Radlinski, "Braking Performance of Heavy U.S. Vehicles," Paper No. 870492, Society of Automotive Engineers, 1987.
21. R. D. Ervin, M. Barnes, C. C. MacAdam, and R. Scott, Impact of Specific Geometric Features on Truck Operations and Safety at Interchanges, FHWA/RD-86/057 (Washington, D.C.: Federal Highway Administration, 1986).
22. C. C. MacAdam, P. S. Fancher, G. T. Hu, and T. D. Gillespie, A Computerized Dynamics Model of Trucks, Tractor-Semitrailers, Doubles, and Triples Combinations, UM-HSRI-80-58, Highway Safety Research Institute (Ann Arbor: University of Michigan, September 1980).
23. M. El-Gindy and J. Y. Wong, "A Comparison of Various Computer Simulation Models for Predicting the Directional Response of Articulated Vehicles," Vehicle System Dynamics, Vol. 16, No. 5-5, 1987.

24. R. D. Ervin, "Influence of Size and Weight Variables on the Roll Stability of Heavy Duty Trucks," SAE Paper No. 831163, Society of Automotive Engineers, August 1983.
25. C. C. MacAdam, "A Computer-Based Study of the Yaw/Roll Stability of Heavy Trucks Characterized by High Centers of Gravity," SAE Technical Paper Series (Society of Automotive Engineers, November 1982).
26. D. B. Fambro, J. M. Mason, and N. S. Cline, "Intersection Channelization Guidelines for Longer and Wider Trucks," Presented at the 67th Annual Meeting of the Transportation Research Board, January 1988.
27. M. Sayers, FHWA/UMTRI Vehicle Offtracking Model and Computer Simulation -- User's Guide, Version 1.00 (Ann Arbor: University of Michigan Transportation Research Institute, June 1984).
28. Analysis Group, Inc., "FHWA Vehicle Offtracking Model -- IBM PC Version 1.0: Program Documentation and User's Guide," July 20, 1986.
29. California Department of Transportation, "Truck Offtracking Model (TOM), Program Documentation and Users Guide," Division of Transportation Planning (Sacramento, 1985).
30. Western Highway Institute, "Offtracking Characteristics of Trucks and Truck Combinations," Research Committee Report No. 3 (San Francisco: February 1970).
31. J. E. Bernard and M. Vanderploeg, "Static and Dynamic Offtracking of Articulated Vehicles," SAE Paper No. 800151, Society of Automotive Engineers, 1981.
32. T. D. Gillespie, Methods for Predicting Truck Speed Loss on Grades, FHWA/RD-86/059 (Washington, D.C.: Federal Highway Administration, November 1985).
33. American Association of State Highway Officials, A Policy on Geometric Design of Rural Highways (Washington, D.C.: 1965).
34. G. F. Hayhoe and J. G. Grundman, "Review of Vehicle Weight/Horsepower Ratio as Related to Passing Lane Criteria," Final Report to NCHRP Project 20-7, Task 10 (Washington, D.C.: Transportation Research Board, October 1978).
35. Bureau of the Census, "Truck Inventory and Use Survey - 1977," Census of Transportation (Washington, D.C.: U.S. Department of Commerce, 1979).
36. P. Y. Ching and F. D. Rooney, Truck Speeds on Grades in California, FHWA-CA-T0-79-1 (Sacramento: California Department of Transportation, June 1979).

37. A. D. St. John, "The Truck Population on High Type Rural Highways" (Kansas City, Missouri: Midwest Research Institute, unpublished paper, August 1979).
38. C. J. Messer, "Two-Lane Two-Way Highway Capacity," Final Report of NCHRP Project 3-28A (Washington, D.C.: Transportation Research Board: February 1983).
39. A. D. St. John and D. R. Kobett, Grade Effects on Traffic Flow Stability and Capacity, NCHRP Report 185 (Washington, D.C.: Transportation Research Board, 1978).
40. Society of Automotive Engineers, "Truck Ability Prediction Procedure," Recommended Practice J688, August 1987.
41. C. Sall, "Truck Road Performance -- Actual Versus Computed," SAE Quarterly Transactions, Vol. 5, No. 1, Society of Automotive Engineers, January 1951.
42. Western Highway Institute, "Horsepower Consideration for Trucks and Truck Combinations" (San Francisco: 1978).
43. B. D. Greenshield, D. Schapiro, and E. L. Ericksen, "Traffic Performance at Urban Intersections," Technical Report No. 1, Yale Bureau of Highway Traffic, Eno Foundation for Highway Traffic Control, 1977.
44. M. S. Raff and J. W. Hart, "A Volume Warrant for Urban Stop Signs" (Eno Foundation for Highway Traffic Control, 1950).
45. J. Neter, W. Wasserman, and M. Kutner, Applied Linear Statistical Models, Second Edition (Homewood, Illinois: Irwin, 1985).
46. A. E. Radwan, K. C. Sinha, and H. L. Michael, Development and Use of a Computer Simulation Model for the Evaluation of Design and Control Alternatives for Intersections of Minor Roads with Multi-Lane Rural Highways: Selection of the Simulation Model, FHWA-IN-79-8 (Washington, D.C.: Federal Highway Administration, July 1979).
47. F. A. Wagner, "An Evaluation of Fundamental Driver Decision and Reaction at an Intersection," Highway Research Record 118 (Washington, D.C.: Highway Research Board, 1966).
48. T. H. Maze, "A Probabilistic Model of Gap Acceptance Behavior," Transportation Research Record 795 (Washington, D.C.: Transportation Research Board, 1981).
49. Transportation Research Board, Highway Capacity Manual, Special Report 209 (1985).
50. J. Wennell and D. F. Cooper, "Vehicle and Driver Effects on Junction Gap Acceptance," Traffic Engineering and Control, Vol. 22, No. 12, December 1981.

51. T. D. Hutton, "Acceleration Performance of Highway Diesel Trucks," Paper No. 70664, Society of Automotive Engineers, 1970.
52. W. S. Homburger, ed., Transportation and Traffic Engineering Handbook, Second Edition, Institute of Transportation Engineers (Englewood Cliffs, New Jersey: Prentice-Hall, 1982).
53. American Association of State Highway and Transportation Officials, A Manual on User Benefit Analysis for Highway and Bus Transit Improvements - 1977 (Washington, D.C.: 1978).
54. Federal Highway Administration, "Price Trends for Federal-Aid Highway Construction," Fourth Quarter 1988 (Washington, D.C.: 1989).
55. California Department of Transportation, "1987 Accident Data on California State Highways, (Road Miles, Travel, Accidents, Accident Rates)" (Sacramento: 1988).
56. Federal Highway Administration, "Motor Vehicle Accident Costs," Technical Advisory, Classification Code T 7570.1 (Washington, D.C.: June 30, 1988).

